SMS 2026
SMART MATERIALS AND SURFACES

NanoMed 2026

SENSORS 2026

EGF 2026
European Graphene Forum

JOINT INTERNATIONAL CONFERENCES

SMS 2026 · NanoMed 2026 · Sensors 2026 · EGF 2026

Book of Abstracts

21 – 23 October 2026

SEVILLE · SPAIN

ORGANIZED BY

SETCOR
Conferences & Exhibitions

SMS / NanoMed / Sensors / EGF 2026
Joint International Conferences Program

21 - 23 October 2026, Seville – Spain

Wed. 21 Oct. 2026		
08:00 - 12:00	**Conference Registration**	
09:00 - 10:00	**Welcome Coffee Break – Foyer**	
SMS 2026 / EGF 2026 / Sensors 2026 / NanoMed 2026 Joint Plenary Session I		
Conference Room Santa Cruz		
Session Chairs: **Prof. Arcady Zhukov, Univ. of Basque Country, Spain** **Prof. Li Lu, National Univ. of Singapore Research Institute, Singapore**		
10:00 - 10:30	Functional Materials: From Self-Cleaning Surfaces to Radiative Cooling Coatings **I.P Parkin**	**Prof. Ivan Parkin**, Univ. College London, **UK**
10:30 - 11:00	High-performance, heteroepitaxial, device layers for wide-ranging electrical and electronic applications. **A.Goyal**	**Prof. Amit Goyal**, Oak Ridge & Univ. at Buffalo, **USA**
11:00 - 11:30	Ultraclean van der Waals interfaces for novel materials and twistronics **R. Gorbachev**	**Prof. Roman Gorbachev**, Univ. of Manchester, **UK**
11:30 - 12:00	Coherent propagation of Laser Induced Periodic Surface Structures by doping in ZnO films G. Gomez-Munoz, R. Ariza, J.F. Ramos-Justicia, F. Cabello-Pardos, A. Pablo Perez1, J. Gonzalo, B. Sotillo, C. Lopez-Santos, P. Fernandez and **J. Solis**	**Prof. Javier Solis**, Instituto de Optica-CSIC, **Spain**
12:00 - 14:00	**Lunch Break – Restaurant**	
SMS 2026 Session I. A: **Multifunctional Materials & Surfaces / Nano-Systems / Adaptive Materials and Structures**		
Conference Room Santa Cruz		
Session Chairs: **Prof. Javier Solis, Instituto de Optica-CSIC, Spain** **Prof. Ivan Parkin, Univ. College London, UK** **Prof. Claire Carmalt, Univ. College London, UK**		
14:00 - 14:30	Functional thermomechanical properties of NiTi shape memory alloy coatings fabricated by thermal plasma HVAF method **P. Sittner**, S. Samal and S. Joshi	**Dr. Petr Sittner**, Czech Academy of Sciences, **Czech Rep.**
14:30 - 15:00	Self-stratifying coatings and vitrimers: a path toward multifunctional, repairable and recyclable surface systems **M. Jimenez**, A. Kerrache, A. Lebeau, M. Casetta, F. Samyn and J.F. Gohy	**Prof. Maude Jimenez**, Univ. Lille, **France**
14:45 - 15:00	A pre-ceramic sol-gel coating for thermal protection **M. Busquet** and J. Garcia	**Mrs. Marie Busquet**, Institut de Recherche St Exupéry, Toulouse, **France**
15:00 - 15:15	One-step RF sputtering deposition of strained epitaxial NiZnAl spinel ferrite thin films C. Granados-Miralles, A. Gonzalo, J. Soler-Morala, A.M. Friedel, E. García-Tabarés, A. Gudín, J. Rubio-Zuazo, P. Perna and **I. Arnay**	**Dr. Iciar Arnay Ortigosa**, Univ. Carlos III de Madrid, **Spain**
15:15 - 15:30	Surface Plasmon Resonance Imaging of Meta surfaces Patterned Via Pyramidial Interference Lithography **R.G. Sabat**	**Prof. Ribal Georges Sabat**, Royal Military College of Canada, **Canada**
15:30 - 15:45	Generation of structural colors in Ag-based plasmonic nanostructures by direct fs-laser irradiation	**Dr. Jose Gonzalo**, IO-CSIC, Madrid, **Spain**

	A. Philip, A. P. Pérez-Marín, J. Siegel, **J. Gonzalo**, M. Garcia-Lechuga	
15:45 - 16:00	Hydrophobicity Recovery Mechanisms in Silicone and Epoxy Out-door Insulating Materials Under Contamination and Corona Stress **A. Milionis**, J. Goerlich, A. Leal-Ayala, P. Meier, D. K. Hohl and S. Kornhuber	**Dr. Athanasios Milionis**, ABB Switzerland Ltd., **Switzerland**
16:00 - 16:30	**Posters session / Afternoon Coffee Break – Foyer**	
Session Chairs: **Prof. Maude Jimenez, Univ. Lille, France** **Dr. Petr Sittner, Czech Academy of Sciences, Czech Rep**		
16:30 - 17:00	Scalable Routes to Functional Materials: Photocatalytic, TCO and Anti-Soiling Coatings **C. J. Carmalt**	**Prof. Claire Carmalt**, Univ. College London, **UK**
17:00 - 17:15	The role of casting skin and section thickness in zinc coating formation on cast iron with added Ni **K. Bracka-Kęsek**, J. Marosz, M. Górny and B. Cygan	**Dr. Karolina Bracka-Kęsek**, AGH Univ. of Krakow, **Poland**
17:15 - 17:30	Cyclic Behavior of Hybrid SMA-Steel Rings as Smart Dampers and the Effect of Diametric Difference on Interface Interference **E. Choi**, S. Park and M-K. Jang	**Prof. Eunsoo Choi**, Hongik Univ., **Rep. Korea**
17:30 - 17:45	Surface Coating Engineering to Enhance Safety of High-Energy Lithium-Ion Batteries **N. L. Wu** and S, J. Chang	**Prof. Nae-Lih Wu**, National Taiwan Univ., **Taiwan**
17:45 - 18:00	Integrating Safe and Sustainable by Design into the Development of Bio-Based Functional Textile Coatings: The SSbD4CheM Textile Case Study **P.Tovillas**	**Dr. Pablo Tovillas Greca**, NOVEX, **Spain**
18:00 - 18:15	Origami-Inspired Foldable Textile Structures for Programmable Shape Morphing **D. Zhang**, C. Harnett, J. Schulte, C. Heyen and T. Gries	**Ms. Danchen Zhang**, RWTH Aachen Univ., **Germany**
18:15 - 18:30	Water Drops Sliding Over Arrays of Janus Micropillars With Hydrophilic Tops: A New Mechanism of Drop Charging **F.Darvish**, M.Isaacs, S.Shumaly, L. Delance and H..Butt	**Dr. Fahimeh Darvish**, Max Planck Institute for Polymer Research, **Germany**

Wed. 21 Oct. 2026		
Sensors 2026 / EGF 2026- Session I. B: Graphene and 2D Materials / Sensor Materials		
Conference Room Arenal		
Session Chairs: Prof. Roman Gorbachev, Univ. of Manchester, UK Prof. Paul Motzki, Saarland Univ., Germany		
14:00 - 14:30	Clean Interfaces in van der Waals Materials: From Adhesion to Transparent Point Contacts **P. Ares**	**Dr. Pablo Ares,** Univ. Autónoma de Madrid, **Spain**
14:30 - 15:00	From Process Integration to Functional Graphene Photonic Devices **M. Lukosius**	**Dr. Mindaugas Lukosius,** IHP-Institute for High Performance Microelectronics**, Germany**
15:00 - 15:30	EMI shielding by horizontally- aligned MWCNTs polymer nanocomposites **R. Checchetto**, G. Fredi and B. L. Wardle	**Prof. Riccardo Checchetto**, Univ. of Trento, **Italy**
15:30 - 15:45	Influence of Directly Deposited Hexagonal Boron Nitride Interlayers on the Interface Properties and Photo response of Graphene/Si Heterostructures **Š. Meškinis**, A. Vasiliauskas, A. Guobienė, Š. Jankauskas, V. Stankus, M. Andrulevičius and R. Gudaitis	**Dr. Šarūnas Meškinis**, Kaunas Univ. of Technology, **Lithuania**
15:45 - 16:00	Overview of Core-Shell Nanowires with 2D Layered Shell **B. Polyakov**, E. Butanovs, A. Kuzmin, L. Dipane and S. Piskunov	**Dr. Boris Polyakov**, Univ. of Latvia, **Latvia**
16:00 - 16:30	**Posters session / Afternoon Coffee Break – Foyer**	
Session Chairs: Prof. Ana Primo Arnau, Instituto de Tecnología Química (UPV-CSIC) Velencia, Spain Dr. Mindaugas Lukosius, IHP-Institute for High Performance Microelectronics, Germany Dr. Pablo Ares, Univ. Autónoma de Madrid, Spain		
16:30 - 17:00	Intelligent Actuator(-Sensor) Systems based on Shape Memory Alloys and Dielectric Elastomers **P. Motzki**	**Prof. Paul Motzki**, Saarland Univ., **Germany**
17:00 - 17:15	Wearable Sensors and Flexible Electrodes from Laser-Induced Graphene and MXene **M. Spasenović**, T. Vićentić, A. Gavran, K. Tošić, V. Vojnović, I. Rašljić-Rafajilović and M.V. Pergal	**Dr. Marko Spasenovic**, Univ. of Belgrade, **Serbia**
17:15 - 17:30	Development of printed temperature sensors based on antenna patterns **J. Escobar**, F. Bourhim, Y. Cervantes and C. Laporte	**Dr. Julien Escobar**, IRT Saint Exupery, **France**
17:30 - 17:45	Flexible Screen-Printed Gold Electrode Arrays as Platforms for Hybrid-Nanomaterial-Enhanced Electrochemical Sensing **N. Godja**, S. Assadollahi, M. Hütter, P. Mehrabi, N. Khajehmeymandi, T. Schalkhammer and F-D. Munteanu	**Mrs. Norica-Carmen Godja** Attophotonics Biosciences GmbH, **Austria**
17:45 - 18:00	Eco-friendly electrospun PEDOT-based nonwovens for wearable touch sensors E. A. Slejko, G. Carraro, D. Cavallo, R. Spotorno, C. Gambardella, V. Piazza, M. Pantano and **M. Smerieri**	**Dr. Marco Smerieri**, IMEM-CNR, **Italy**
18:00 - 18:15	Design, Electrochemical Characterization, and Analytical Applications of Innovative Bi-Band Microelectrodes **K. Jedlińska** and B. Baś	**Dr. Katarzyna Jedlinska**, AGH Univ. of Krakow, **Poland**
18:15 - 18:30	Development of a novel voltammetric sensor based on MWCNT-juglone paste electrode for high sensitive melatonin measurement in pharmaceutical formulations and dietary supplements **J. Smajdor-Baran**	**Dr. Joanna Smajdor-Baran**, AGH Univ. of Krakow, **Poland**
18:30 - 18:45	Effect of Plasma Treatment on Laccase-Based Electrochemical Biointerfaces **S. Baluta**, W. Tylus, P. Jamróz, M. Czok, K. Malecha and J. Cabaj	**Dr. Sylwia Baluta**, Wroclaw Univ. of Science and Technology, **Poland**

Wed. 21 Oct. 2026		
SMS 2026 / NanoMed 2026 - Session I. C: Bio-Medical Materials & Living Surfaces/ Bio-Nanofabrication & Engineering		
Conference Room Nervion		
Session Chairs: Prof. Luisa Fiandra, University of Milano Bicocca, Italy Prof. Isabel Izquierdo Barba, Complutense Univ. of Madrid, Spain		
14:00 - 14:30	Enginnering the Nano-Biointerface- From understanding to measuring and controlling biological function. **P. Rivera Gil**	**Prof. Pilar Rivera Gil,** Univ. Pompeu Fabra, Barcelona, **Spain**
14:30 - 14:45	Rational Design of Stable and Biocompatible CuS Plasmonic Nanocrystals with Tunable NIR-II Photo-responsive Properties for Biomedical Applications **F. Barbero**, S. Shanmugam, D. Maccarrone, G. Perrone, K. Mareschi, I. Kokalari, A.M. Ferretti and I. Fenoglio	**Dr. Francesco Barbero**, Univ. of Torino, **Italy**
14:45 - 15:00	Adsorption and desorption of bioactive organic molecules in the con-fined interlayer space of clay minerals for potential drug delivery systems. Experimental and molecular modeling approaches. **C.I. Sainz-Díaz**, A. Hernández-Laguna, S. Kanwal, C. Viseras-Iborra and A. Borrego-Sánchez	**Dr. C. Ignacio Sainz-Díaz**, IACT_CSIC- Granada, **Spain**
15:00 - 15:15	Advanced Synthetic Polymer-Based Blockers: A Superior Pathogen-Free Alternative to BSA for IVD Surface Coating **L. Kostka**, V. Šubr, M. Tůmová, P. Dráber, J. Plicka and T. Etrych	**Dr. Libor Kostka**, Institute of Macromolecular Chemistry, **Czech Rep.**
15:15 - 15:30	HPMA Copolymer–Gemcitabine Conjugates: Impact of Drug Release Kinetics on Antitumor Efficacy **R. Pola**, K. Běhalová, N. Adamcová, M. Ivančík, M. Šírová, I.B. Kilic, P. Procházková, P. Kašpárek, A. Bulková, P. Lukac, L. Vannucci, B. Říhová, M. Kovář and T. Etrych	**Dr. Robert Pola,** Institute of Macromolecular Chemistry, **Czech Rep**.
15:30 - 15:45	Tribocorrosion Behaviour of Ti6Al7Nb Orthopaedic Alloy: Comparison Between New and Clinically Retrieved Femoral Stem Surfaces **M. Jenko**, B. Kocjančič, T. Kosec, Š. Tadel Kocjančič and M. Debeljak	**Prof. Monika Jenko**, MD-RI Institute for Materials Research in Medicine, **Slovenia**
15:45 - 16:00	Persistent Micro and Nanoscale Corundum Residues on Grit Blasted Titanium Alloy Hip Implants: Biological and Clinical Implications **B. Kocjancic**, M. Jenko and M. Debeljak	**Dr. Bostjan Kocjancic**, Univ. Medical Centre Ljubljana, **Slovenia**
16:00 - 16:30	**Posters session / Afternoon Coffee Break – Foyer**	
Session Chairs: Prof. Monika Jenko, MD-RI Institute for Materials Research in Medicine, Slovenia		
16:30 - 16:45	Surface Degradation and Thrombotic Deposition on Blood-Contacting Polymeric Components of ECMO Systems **Š. Tadel Kocjancic**, M. Debeljak, M. Jenko and B. Kocjancic	**Dr. Spela Tadel Kocjancic**, Univ. Medical Centre Ljubljana, **Slovenia**
16:45 - 17:00	Abdominal PP meshes coated with functional biodegradable nanofibers for the simultaneous prevention of postoperative adhesions and infections **S. Degoutin**, M. Dufay, M. Jimenez, M. Casetta, M. Maton, F. Cazaux, S. Bellayer, F. Chai, N. Blanchemain	**Dr. Stéphanie Degoutin**, Univ. of Lille, **France**
17:00 - 17:15	Evaluation of the Protective Performance and Electrochemical Stability of Nitradine Commercial Formulation **C.A. Freiria de Oliveira**, V.C. Oliveira, A.P. Macedo, E. Watanabe, R. Galo and V.O. Pagnano	**Ms. Carolina A. Freiria de Oliveira**, Univ. of São Paulo, **Brazil**
17:15 - 17:30	Defect-Engineered Hexagonal Boron Nitride as a Dual-Action Orthopedic Biomaterial for Simultaneous Osteogenesis and Osteosarcoma Therapy L. Souyris, I. Charodin, F. Salmeron, **Z. Saleh**, H. Belaid, D. Cornu, P-Y. Collart-Dutilleul, M. Bechelany and V. Cavaillès	**Ms. Zahraa Saleh**, Univ Montpellier, **France**

17:30 - 17:45	Nanocellulose as a Cosmetic Ingredient through an SSbD Lens **O. Panák**, U. Novak, A. Assis, D. Barak, D. Kohen, A. Blinderman, M. Velimirovic Fanfani, B. Hardy, P. D. Kolokathis, Y. Kohl, W. A. Gebbink and F. Pérez Sánchez	**Dr. Ondrej Panak**, National Institute of Chemistry, **Slovenia**
17:45 - 18:00	Multifunctional algae-based treatment combining colouration and antibacterial activity in knitted cotton textiles **A. Björkquist** and N-K. Persson	**Mrs. Anna Bjorkquist**, University of Borås, **Sweden**

Thu. 22 Oct. 2026		
SMS 2026 / EGF 2026 / Sensors 2026 / NanoMed 2026 Joint Plenary Session II		
Conference Room Santa Cruz		
Session Chairs: **Prof. Ivan Parkin, Univ. College London, UK** **Prof. Elisa Michelini, Univ. of Bologna, Italy** **Dr. Raul Arenal, Univ. of Zaragoza, Spain**		
09:00 - 09:30	Ultrafast domain wall propagation in amorphous magnetic microwires. **A. Zhukov,** P. Corte-Leon, A. Gonzalez, P. A. Rodríguez Jiménez and V. Zhukova	**Prof. Arcady Zhukov,** Univ. of Basque Country**, Spain**
09:30 - 10:00	Crystal Growth and Chemical Engineering of Two-Dimensional Magnets, Semiconductors and Dielectrics **Z. Sofer**	**Prof. Zdeněk Sofer**, UCT Prague, **Czech Rep.**
10:00 - 10:30	**Posters session/ Morning Coffee Break – Foyer**	
Session Chairs: **Prof. Ivan Parkin, Univ. College London, UK** **Prof. Elisa Michelini, Univ. of Bologna, Italy** **Prof. Zdeněk Sofer, UCT Prague, Czech Rep**		
10;30 - 11:00	How to get from nano to active surface in energy storage materials: A long and winding road. **P. Gomez-Romero**	**Prof. Pedro Gomez-Romero,** ICN2 (CSIC-BIST)-Barcelona, **Spain**
11:00 - 11:30	From Ensemble Binding to Single-Molecule Statistics in pH-conditioned biosensing **L. Torsi**	**Prof. Luisa Torsi**, Univ. of Bari, **Italy**
11:30 - 12:00	Clinical Validation of Wearable Piezoelectric Sensor & MicroLEDs for Skin Phototherapy and Cardiovascular Monitoring **K. Jae Lee**	**Prof. Keon Jae Lee**, Korea Advanced Institute of Science and Tech. (KAIST), **Rep. of Korea**
12:00 - 14:00	**Lunch Break – Restaurant**	
Group Photo – 13:45		
SMS 2026 / EGF 2026 joint Session II. A: **Functional Electronics and Energy Materials**		
Conference Room Santa Cruz		
Session Chairs: **Prof. Claire Carmalt, Univ. College London, UK** **Prof. Lluís Mañosa Carrera, Univ. of Barcelona, Spain** **Prof. Hermenegildo García Gómez, Univ. Polytech Valencia,Spain**		
14:00 - 14:30	Unveiling the Atomic Configuration and Physical Properties of Low-Dimensional (2D) Materials via Advanced TEM **R. Arenal**	**Dr. Raul Arenal**, Univ. of Zaragoza, **Spain**
14:30 - 15:00	Ion transportation in organic/inorganic composite electrolyte and its full battery Y. Wang and **L. Lu**	**Prof. Li Lu**, National Univ. of Singapore Research Institute, **Singapore**
15:00 - 15:30	Building a Coordinated European Ecosystem for Advanced Materials: Lessons from the InnoMatSyn CSA **A. Irazustabarrena**	**Ms. Ane Irazustabarrena Murgiondo**, TECNALIA, **Spain**
15:30 - 15:45	Graphene-based formulations for high-definition capillary printing of electrolyte-gated field-effect transistors **H. Mahi**, M. Pascual and N. Battaglilni	**Ms. Hassina Mahi**, Univ. Paris Cité, **France**
15:45 - 16:00	Modulating The Resonance Response Of Monolayer Graphene Nanodrums: A Molecular Dynamics Study **J. Varillas** and M. Kalbáč	**Dr. Javier Varillas**, Heyrovsky Institute, **Czech Rep.**

16:00 - 16:30	**Posters session/ Afternoon Coffee Break – Foyer**	
16:30 - 17:00	Halide perovskites for next generation optoelectronics **M. Anaya**	**Dr. Miguel Anaya**, Institute of Materials Science of Seville, **Spain**
17:00 - 17:15	Unlocking Robust 2D Hybrid Perovskite Optoelectronics **K.J. Riisnaes**, R. Mastria, A. Bacon, I. Lieontis, O. Lam, L. De Marco, M. Craciun and S. Russo	**Dr. Karl Jonas Riisnaes**, University Exeter, **UK**
17:15 - 17:30	Tailoring structured multifunctional carbon nanotube supported catalysts for the valorization of glycerol to 1,2-propanediol D. Lumpp, M. Mohammadi and **J. Albert**	**Prof. Jakob Albert**, Univ. of Hamburg, **Germany**

Conference Dinner
22 Oct. 2026, from 19:30

Thu. 22 Oct. 2026		
Sensors 2026 / NanoMed 2026 Joint Session II.B: Nanotechnology in Diagnostics, Imaging & Bio-Sensing / Biomedical sensors		
Conference Room Arenal		
Session Chairs: Prof. Luisa Torsi, Univ. of Bari, Italy Prof. Riccarda Antiochia, Univ. of Rome "La Sapienza", Italy		
14:00 - 14:30	Plasmon-Driven In Situ Synthesis of Chiral Polymer Thin Films for Enantioselective Sensing **O. Soppera**	**Prof. Olivier Soppera**, Univ. Haute-Alsace, **France**
14:30 - 15:00	Bioinspired nanobiosensors for portable and wearable diagnostics **E. Michelini**	**Prof. Elisa Michelini**, Univ. of Bologna, **Italy**
15:00 - 15:30	Calorimetric Lateral Flow Immunoassays: Next-Generation Point-of-Care Biosensors Targeting Tumor Related Extracellular Vesicles and their miRNA Content **J. M. de La Fuente**	**Prof. Jesus M de la Fuente,** ICMA, CSIC /Univ de Zaragoza and CIBER-BBN, **Spain**
15:30 - 15:45	Matrix-Activated Sensors for Human Serum Analysis **A. Barbaroux,** B. Chovelon, E. Fiore, S. Vezirian, M. Henry, M. Zoubeidi, M. C. DeRosa, C. Ravelet and E. Peyrin	**Ms. Amandine Barbaroux**, Univ. Grenoble Alpes, **France**
15:45 - 16:00	Modulating Agglutination for Quantitative Paper Diagnostics **A. Tripathi**, R. More, S. Corrie and G. Garnier	**Mr. Anuragmani Tripathi**, Monash Univ., **Australia**
16:00 - 16:30	**Posters session/ Afternoon Coffee Break – Foyer**	
Session Chairs: Prof. Jesus M de la Fuente, ICMA, CSIC /Univ de Zaragoza and CIBER-BBN, Spain Dr. Marco Smerieri, IMEM-CNR, Italy		
16:30 -17:00	C-peptide Immunosensor as a novel tool for Diabetes Management **R. Antiochia**, C. Tortolini and F. Dotta	**Prof. Riccarda Antiochia**, Univ. of Rome "La Sapienza", **Italy**
17:00 - 17:15	Rapid handheld graphene FET platform for dual acute myocardial infarction biomarker detection **J.P. Ramoso**, L. Ranatunge and W. Balachandran	**Mr. John Paolo Ramoso**, Brunel Univ. of London, **UK**
17:15 - 17:30	Graphenic DCDR/GERS Platforms for Ultrasensitive and Selective Raman Detection of Human Interleukin-6 E. de la O-Cuevas and **J.M. Saniger**	**Dr. Jose Manuel Saniger,** Univ. Nacional Autónoma de México, **Mexico.**
17:30 - 17:45	A Novel Lab On-A-Chip For Biomarkers Monitoring On In Vitro Barriers Models S. Marasso, **M. Cicolini**, J. Babic, R. Cue López, A. Ballesio, M. Cocuzza, F. Frascella and L. Napione	**Dr. Martina Cicolini**, Politecnico di Torino, **Italy**
17:45 - 18:00	From bilayer to multilayer BGO/ZnO heterostructures for fast-timing ToF-PET detectors **M. Konefał**, N. Babayevska, A. Padmanaban, I. Yakymenko, I. Iatsunskyi, M. Jancelewicz and O. Sidletskiy	**Dr. Magdalena Konefał**, Adam Mickiewicz Univ., **Poland**

Conference Dinner
22 Oct. 2026, from 19:30

Thu. 22 Oct. 2026		
NanoMed 2026 Session II. C: Nanotechnology in Drug Delivery, Oncology & Theranostics / Safety & Future Frontiers		
Conference Room Nervion		
Session Chairs: Prof. Pilar Rivera Gil, Univ. Pompeu Fabra - Barcelona, Spain Prof. Rosaria Rinaldi, Univ. of Salento, Italy		
14:00 - 14:30	From erythrocyte-based cardiovascular risk assessment to the development of synthetic erythrocytes **N.C. Santos**	**Prof. Nuno C. Santos**, iMM Lisboa, **Portugal**
14:30 - 15:00	Nanoengineering the Bone Regenerative Microenvironment **I. Izquierdo Barba**	**Prof. Isabel Izquierdo Barba,** Complutense Univ. of Madrid, **Spain**
15:00 - 15:15	Engineering Nano-emulsions: How Lipid Composition Controls Cellular Outcomes **AB. Dávila Ibáñez**, L. Funtes Varela, S. Bravo, C. Costa, A. Cabezas and R. López López	**Dr. Ana Belen Davila Ibanez**, Oncomet- Health Research Institute of Santiago, **Spain**
15:15 - 15:30	Biofunctionalized ZnO nanoflowers as a non-viral mechanoporation platform for gene delivery in epidermolysis bullosa **G. Mandriota**, G. Leccese, C. De Stradis, R. Maria Percoco, C. Baldari, S. Schirinzi, S. D'Amone, G. Maiorano, G. Gigli and I. Elenà Palamà	**Dr. Giacomo Mandriota**, CNR Nanotec, **Italy**
15:30 - 15:45	Reactivating the STING pathway in PTK7-positive acute leukemia cells using DNA-based theranostic nanodevices **E. Ottalagana**, A. Marranci, A. Moscardini, F. Olimpico, L. Tedeschi, F. Rea, T. Salvatori, I. Squiccimarro, P. Mastella, F. Beltram, S. Luin and A.G. Luserna di Rorà	**Mrs. Elisa Ottalagana**, Scuola Normale Superiore & CNR- Pisa, **Italy**
15:45 - 16:00	Magnetic liposomal drug delivery systems in ovarian cancer therapy: new opportunities to overcome drug resistance **J. Nowak-Niedźwiecka**, A. Mamczur, B. Machnicka, A. Czogalla, M. Cano, V. Garcia-Caballero and J. J. Giner-Casares	**Dr. Julia Nowak-Niedźwiecka**, Univ. of Zielona Góra, **Poland**
16:00 - 16:30	**Posters session / Afternoon Coffee Break – Foyer**	
Session Chairs: Prof. Nuno C. Santos, iMM Lisboa, Portugal Prof. Isabel Izquierdo Barba, Complutense Univ. of Madrid, Spain Dr. Francesco Barbero, Univ. of Torino, Italy		
16:30 - 17:00	Harnessing Nature Driven Nanotechnology: Polyphenol Based Platforms to Enhance Immune and Cancer Therapy. M. Cascione, V. De Matteis and **R. Rinaldi**	**Prof. Rosaria Rinaldi**, Univ. of Salento, **Italy**
17:00 - 17:30	Novel Cancer NanoMedicines: From Therapy of poorly vascularized tumors to protection from radiotherapy induced damage in the skin **B. Godin**	**Prof. Biana Godin**, Houston Methodist Research Institute, **USA**
17:30 - 17:45	Reprogramming the Pancreatic Adenocarcinoma Microenvironment integrating mutSEMA3A mRNA-Lipid Nanoparticles with a Vascularized Organ-on-Chip Model **G.Tomaino**, L.Salvioni, L.Fiandra, E.Giraudo, M.Innocenti and D.Prosperi	**Dr. Giulia Tomaino,** Univ. of Milan Bicocca, **Italy**
17:45 - 18:00	Dual-Targeting Strategy to Repurpose Cetuximab with HFn Nanocon-jugates for Immunotherapy of Triple-Negative Breast Cancer **L. Barbieri**, A. Banfi, L. Salvioni, M. Innocenti, D. Prosperi and L. Fiandra	**Dr. Linda Barbieri**, Univ. of Milano-Bicocca, **Italy**
18:00 - 18:15	Circulating Tumor Cells and Their Secretome Drive Pre-Metastatic Niche Formation in the Liver of Pancreatic Ductal Adenocarcinoma Patients.	**Dr. Maria Principia Scavo**, IRCCS de Bellis, **Italy**

	M. Principia Scavo, G. Panzetta, R. Palieri, M. De Luca, F. Balestra, F. Rizzi, C. Perrone, N. Depalo and G. Giannelli	

Conference Dinner
22 Oct. 2026, from 19:30

Fri. 23 Oct. 2026		
SMS 2026 / EGF 2026 Session III.A: Environment & Sustainable Materials/Surfaces properties & applications		
Conference Room Arenal		
Session Chairs: Prof. Ana Primo Arnau, Instituto de Tecnología Química (UPV-CSIC) Valencia, Spain Dr. Raul Arenal, Univ. of Zaragoza, Spain		
08:30 - 09:00	Solid-State Caloric Cooling: A Clean Path to the Future of Refrigeration **L. Mañosa**	**Prof. Lluís Mañosa Carrera**, Univ. of Barcelona, **Spain**
09:00 - 09:30	Low-Carbon 3D Construction Printing: Materials, Modelling and Autonomous Construction **K. M. Liew**	**Prof. Kim Meow Liew**, City Univ. of Hong Kong, **China**
09:30 - 09:45	Manganese-Modified Co- and Cu- Based Mixed Oxides for Enhanced Catalytic Oxidation of Toluene and CO C.E. Bounoukta, E. Genty, C. Poupin, F. Cazier, G. Leyssens and V. Tschamber, J.P. Dacquin, S. Royer, Balay, F. Robic, **S. Siffert** and R. Cousin	**Prof. Stephane Siffert**, Univ. du Littoral Côté d'Opale, **France**
09:45 - 10:00	Effect of A-Site Substitution on the Catalytic Performance of $LaMnO_3$ Perovskites for Complete Oxidation of pollutants C.E. Bounoukta, E. Genty, C. Poupin, C. Ciotonea, F. Cazier, G. Leyssens, V. Tschamber, J.P. Dacquin, S. Royer, Balay, F. Robic, S. Siffert and R. Cousin	**Prof. Renaud Cousin**, Univ. du Littoral Côté d'Opale, **France**
10:00 - 10:30	**Morning Coffee Break – Foyer**	
10:30 - 11:00	MXenes as versatile 2D materials for next-generation catalysis **A. Primo**	**Prof. Ana Primo Arnau,** Instituto de Tecnología Química (UPV-CSIC) Velencia, **Spain**
11:00 - 11:15	Efficient Transformation of Glucose into 5-Hydroxymethylfurfural using PO4-terminated Nb2C MXene as Catalyst **A. Raya-Barón**, E. Romero-Salicio, L. Tian, B. Cojocaru, V. Parvulescu, A. Primo and H. García	**Dr. Alvaro Raya Baron**, Instituto de Tecnología Química (UPV-CSIC) Velencia, **Spain**
11:15 - 11:30	Effect of Graphene on the Consolidation and Tribological Performance of PEEK Composites Processed by Rapid Sinter Pressing I. C. Vladu, C. Arévalo, E. M. Perez-Soriano, A. J. Dudau, E. Neubauer and **I. Montealegre-Meléndez**	**Prof. Isabel Montealegre Meléndez**, Univ. Sevilla, **Spain**
11:30 - 11:45	Valorization of aggregate-washing sludge and cork residues for porous ceramics with tailored physical and thermal properties **B.G. Silva-García**, J. M. Terrones-Saeta, L. Segovia-Guerrero, N. Baladés and D. L. Sales	**Mrs. Blanca Gema Silva Garcia**, Univ. de Cádiz, **Spain**

Fri. 23 Oct. 2026		
NanoMed / Sensors 2026 joint Session III.B: Nanotechnology in Drug Delivery / Environmental Sensors / Smart Sensor Networks		
Conference Room Nervion		
Session Chairs: Prof. Olivier Soppera, Univ. Haute-Alsace, France Prof. Luisa Fiandra, University of Milano Bicocca, Italy Dr. Marco Smerieri, IMEM-CNR, Italy		
09:00 - 09:15	Catalytically propelled Janus pectin micromotors for enhanced tumour penetration and active drug delivery **T. Raj**, S. Ariraman, S. Chakraborty, V. Selvaraj, B. Roy, H. Kress, E. Mani and S. Sudhakar	**Mr. Thilak Raj**, Indian Institute of Technology Madras, **India**
09:15 - 09:30	Functional Materials for Non-Enzymatic Electrochemical Detection of Metabolites **M. Kuznowicz**, A. Jędrzak and T. Jesionowski	**Dr. Maria Kuznowicz**, Poznan University of Technology, **Poland**
09:30 - 09:45	Recent advances in optical materials and smart fibers to combat counterfeiting M.S. Abdelrahman, Z.E. Ahmed, Y.A. Attia, C. Falldorf, R.B. Bergmann and **T. A. Khattab**	**Prof. Tawfik A. Khattab**, Textile Research & Tech. Institute, **Egypt**
10:00 - 10:30	**Morning Coffee Break – Foyer**	
10:30 - 10:45	Humidity-Assisted Machine Learning Calibration of PdAu Resistive Hydrogen Sensors Under Aerobic Conditions **J. Herbeck-Tazibt**, H. I. Turan, M. A. Djeziri, T. Fiorido and H. T. Hayvaci	**Mr. Jordan Herbeck-Tazibt**, Aix-Marseille Univ, **France**
10:45 - 11:00	Challenges on dual-output rectifier-based power management circuits for triboelectric nanogenerators **F. Reverter**, O. López, J. O. Casas and M. Gasulla	**Dr. Ferran Reverter**, Univ. Politècnica de Catalunya, **Spain**
11:00 - 11:15	Self-Powered Non-Contact PP/PVDF Triboelectric Sensor Enhanced by Low-Permittivity Supporting Layers **P. Slobodian** and B. Hausnerova	**Prof. Petr Slobodian**, Tomas Bata University- Zlin, **Czech Rep.**
11:15 -11:30	Assessing olive oil adulteration by comparing the discerning performances of nanostructured gas sensors and human olfaction **M. Astolfi**, M. Masin, M. Barbieri, I. Donelli, L. Montesi,,S. Gherardi, C. Malagù, A. Pignatelli and G. Rispoli	**Dr. Michele Astolfi**, Univ. of Ferrara, **Italy**
11:30 - 11:45	Damage Detection Sensitivity of Sensor Technologies Under Varying Operational Conditions **M. Dziendzikowski**, K. Kowalczyk and Z. Dworakowski	**Dr. Michal Dziendzikowski**, Warsaw University of Technology, **Poland**

SMS / Sensors / NanoMed / EGF 2026 Joint International Conferences

Posters Sessions

All Posters are to be displayed for 21 and 22 Oct. 2026

N.	Poster Title	Author, Affiliation, Country
1.	Multidirectional Mechanical Stability and Seam Efficiency of Woven Reinforced Laminated Composites **I. Schwarz**	**Prof. Ivana Schwarz**, Univ. of Zagreb, **Croatia**
2.	Plasmon-Enhanced Photocatalysis in Microflow: Synthesis and Application of surface-modified Au/PDMS nanocomposite **M. Rašljić Rafajilović**, M. V. Bošković, K. Radulović, M. Obradov and D. Vasiljević-Radović	**Dr. Milena Rašljić Rafajilović**, Univ. of Belgrade, **Serbia**
3.	Optimization of RF-Sputtered TiO2 on Dewetted Au Nanoparticles for Plasmonic Photocatalysis **M. V. Bošković**, O. Živković, M. Obradov, M. Rašljić Rafajilović and D. Vasiljević Radović	**Mr. Marko Bošković**, Univ. of Belgrade, **Serbia**
4.	Safe and Sustainable Bio-Based Functional Coatings for Textiles by Atmospheric Pressure Plasma Polymerization P.Tovillas, **M. Martínez-Falcón**. M. Iñiguez and M. Martínez-Vergara	**Dr. María Martínez Falcon**, NOVEX, **Spain**
5.	Durability assessment of UV-cured functional SiOxNy thin films using climate chamber **E. Shmagina**, J. Küpersep, V.Shirokova and S. Bereznev	**Ms. Elizaveta Shmagina**, Tallinn Univ. of Technology, **Estonia**
6.	Core–Shell Engineering of Ge Quantum Dots for Enhanced Photodetector Response: Experiment and Electromagnetic Simulations I. Periša, **T.Car**, K.V. Kripesh, K. Salamon and M. Mičetić	**Dr. Tihomir Car**, Rudjer Boskovic Institute, **Croatia**
7.	Real-Time Plantar Pressure Monitoring and Personalized Offloading Feedback Using a Graphene/PVDF Fabric Sensor **N. Faramarzi**, D. Boodaghian Asl, N. Pesce, H. Cheraghi Bidsorkhi, A. G. D'Aloia and M. S. Sarto	**Ms. Negin Faramarzi**, Sapienza Univ. of Rome, **Italy**
8.	Atmospheric-Pressure Plasma-Engineered LTCC Gold Electrodes for Dopamine Biosensing **J. Cabaj**, W. Tylus, P. Jamróz, M. Czok, K. Malecha and S. Baluta	**Prof. Joanna Cabaj**, Wroclaw Univ. of Science and Technology, **Poland**
9.	Comparative study of the effects of Er:YAG, Cold Plasma and UV treatments on the surface wettability of titanium alloy and zirconium dioxide surfaces. An in vitro study **Z. Afradi**, M. Laky, B. Laky, A. Moritz and H.A. Shokoohi Tabrizi1	**Dr. Zohreh Afradi**. Medical Univ. of Vienna, **Austria.**
10.	From Catecholamines to Nanohybrids: New Materials for Point-of-Care Biosensing **A. Jędrzak**, M. Kuznowicz and T. Jesionowski	**Mr. Artur Jędrzak**, Poznan Univ. of Technology, **Poland**
11.	Atomic-scale characterization of Ti-based alloy biomaterials for hip and knee endoprostheses **E. A. Gonzalez**, M. G. Sandoval, P. V. Jasen, M. J. Jiménez, G.P. Brizuela, A. Hernández-Laguna, A. Juan and C. I. Sainz-Díaz	**Ms. Estela Andrea Gonzalez**, UNS- Bahía, **Argentina**
12.	Grading of magnetic anisotropy and engineering of domain wall dynamics in Fe-rich microwires by stress- annealing. A.Zhukov, P. Corte-Leon, J. M. Blanco and **V. Zhukova**	**Dr. Valentina Zhukova**, Univ. of Basque Country, **Spain**
13.	Temperature-Guided Formation of Functional Silico-Alumino-Phosphate Binders Revealed by Multinuclear Solid-State NMR **J. Brus**, M. Urbanova, I. Sedenkova and M. Keppert	**Dr. Jiri Brus**, Institute of Macromolecular Chemistry CAS, **Czech. Rep**
14.	Fast-charging Lithium-ions Batteries via Easy Interfacial Modifications **Y-T Weng** and N-L Wu	**Dr. Yu-Ting Weng**, National Taiwan Univ., **Taiwan**
15.	Recycling Potential of Conductive Ink Printed Substrates **K.I. Ivanda**, M.V. Bezjak, T. Cigula and R. Kulčar	**Prof. Katarina I. Ivanda**, Univ. of Zagreb, **Croatia**
16.	From ceramic powders to 3D printed bio-inspired scaffolds based on baghdadite **Ș. Caramarin**, R-R. Piticescu and A. Okos	**Mrs. Stefania Caramarin**, National R&D Institute for Non-Ferrous & Rare Metals, **Romania**
17.	Green Synthesis of Gold Nanoparticles Using Silybum marianum Extracts and Silybin for Future Tissue Regeneration Applications **B. Strojny-Cieślak**, M. Pruchniewski, Z. Nowak and A. Ostrowska	**Dr. Barbara Strojny-Cieślak,** Warsaw Univ. of Life Sciences, **Poland**

18.	Advanced Biomaterial Platforms for Tissue Regeneration: Thickness-Tunable PBAT Nanofibrous Scaffolds and Injectable Silk Fibroin Microcarriers S.O. Akbulut, S. Ekicier Acar, E. Konuk Tokak, D. Çakır, A.S. Çakmak, T. Gültan and **M. Gümüşderelioğlu**	**Prof. Menemşe Gümüşderelioğlu**, Hacettepe Univ., **Turkiye**
19.	Biomimetic Poly-(L-lactide) Scaffold Nanostructured with Graphene Oxide and Gold Nanoparticles for Enhanced Skin Regeneration **M. Pruchniewski**, B. Strojny-Cieślak, R. Kasprzak, P. Nakielski, A. Ostrowska and E. Sawosz	**Mr Michał Pruchniewski,** Warsaw Univ. of Life Sciences, **Poland**
20.	Distinct Thermomechanical Profiles of Conventional and Shape-Memory Polymers for Clear Orthodontic Aligners **J. Oblak**, M. Jenko and M. Ovsenik	**Dr. Jan Oblak,** University of Ljubljana, **Slovenia**
21.	In Vitro Cytotoxicity Assessment of Thermoformed and 3D-Printed Clear Aligner Materials: A Pilot Study of Artificial Ageing and Extraction Time R. Ovsenik, M. Ovsenik, M. Bitenc, M. Jenko and **L. Kolenc**	**Dr. Lea Kolenc**, University of Ljubljana, **Slovenia**
22.	pH-Controlled Ionotropic Crosslinking of Alginate–Pectin Microbeads: Multiscale NMR Insights into Ion-Specific Network Formation **M. Urbanova**, I. Sedenkova, M. Pavelkova, K. Kubova and J. Brus	**Dr. Martina Urbanova**, Institute of Macromolecular Chemistry, **Czech Rep.**
23.	Development and Characterization of Curcumin Nanoparticle-Loaded Hydrogel for Skin Regeneration Applications R.D. Pavaloiu, M. Eremia, D. Miu, M. Vladu, A. Albulescu, G. Neagu, R. Albulescu, M. Petrescu and **F. Shaat**	**Dr. Fawzia Shaat**, INCDCF-ICCF Bucharest, **Romania**
24.	Nanoparticle-Based Luminescent Approaches in Biomedical Research: Assessing Cellular Internalization **A.I. Becerro**, E. Arroyo, B. Torres-Herrero, J.M. de la Fuente and M. Ocaña	**Dr. Ana Isabel Becerro**, CSIC-US- Seville, **Spain**
25.	Light-driven organic microrobots as efficient agents for photodynamic treatment of bacterial lung infections. **A. Lancézeux**, R. de Pedro-Jove, I. Ratera, J. Vila and P. Mayorga-Burrezo	**Mr. Allan Lancézeux**, ICMAB-CSIC, Univ. Autónoma Barcelona, **Spain**
26.	Pancreatic Ductal Adenocarcinoma-Derived Small Extracellular Vesicles Remodel the Hepatic Pre-Metastatic Niche through Hybrid Epithelial–Mesenchymal Transition States **F. Balestra**, G. Panzetta, M. De Luca, F. Rizzi, R. Comparelli, M. L. Curri, G. Giannelli, N. Depalo and M. P. Scavo	**Dr. Francesco Balestra**, IRCCS. de Bellis, **Italy**
27.	Extracellular Vesicles from Colorectal Cancer Models for Targeted Drug Delivery **M. De Luca**, F. Balestra, R. Palieri, G. Panzetta, F. Rizzi, C. Perrone, M. Lucia Curri, G. Giannelli, N. Depalo and M. Principia Scavo	**Dr. Maria De Luca**, IRCCS. de Bellis, **Italy**
28.	Verteporfin-loaded nanoemulsions as a promising platform for ovarian cancer photodynamic therapy **L. Fuentes**, A. E. Arias, C. Abuín, M. Abal, C. Costa, R. López and A. B. Dávila	**Ms. Laura Fuentes Varela**, Oncomet- Health Research Institute of Santiago (IDIS), **Spain**
29.	Engineered Saccharomyces cerevisiae biosensor for detection of Candida albicans virulence-associated pheromone signalling: design, construction, and low-cost smartphone fluorescence readout **L. Gogianu**, M. Simion and M. Popescu	**Ms. Larisa Gogianu,** the National Institute for Research in Development in Microtechnologies, **Romania**
30.	Multilayered BGO@CsPbBr3 Heterostructures as Potential Scintilla-tors for TOF-PET **N. Babayevska**, M. Konefał, M. Jancelewicz, M. Jarek, A. Padmanaban, I. Yakymenko and O. Sidletskiy	**Prof. Nataliya Babayevska**, Adam Mickiewicz Univ., **Poland**
31.	Treatment of Contaminated Water in Cuba Using Heterogeneous Solar Photocatalysis with Zeolite Minerals **S. Ramírez**, M. Rodrigo Moya, A.R. Ruiz-Salvador, A. Jimenez, I. Canosa, A. Flores, L. Riesgo, K. Borrego, T. Farías and M. Ballesteros	**Prof. Surey Ramírez González**, Univ. Central Marta Abreu de las Villas, **Cuba**
32.	Surface chemistry of Mg–Fe oxide spinels governing selective arsenic and phosphate removal **S. Delibaltova**, B. Dojčinović, Ž. Jaćimović, H. Kolev, I. Yordanova, M. Ognjanović, I. Spasojević, M. Milić, V. Girman, M. Fabián and B. Antić	**Mrs. Simona Delibaltova**, Institute of Catalysis, **Bulgaria**
33.	Effect of Mg Incorporation on the Structure and Groundwater Purification Performance of Mg–Fe Oxide Spinels **A. Vasileva**, B. Dojčinović, Ž. Jaćimović, H. Kolev, I. Yordanova, M. Ognjanović, I. Spasojević, M. Milić, V. Girman, M. Fabián and B. Antić	**Ms. Anna Vasileva**, Institute of Catalysis, **Bulgaria**

34.	Synergy in contact electrification mechanisms of polyvinyl acetate nanogenerators **B. Hausnerova** and P. Slobodian	**Prof. Berenika Hausnerova**, Tomas Bata Univ. in Zlin, **Czech Rep**.
35.	Potentiometric determination of anionic and cationic surfactants using an imidazolium–tetrakis(perfluorophenyl)borate ion-pair sensor **H. Zhukouskaya**, M. Jozanović, M. Kraševac Sakač, N. Sakač, M. Šrajer Gajdošik, L. Vrban, R. Vianello, M. Fizer, D. Marković, D. Vikić-Topić, S. Roca, J. Pánek and M. Hruby	**Ms. Hanna Zhukouskaya**, Institute of Macromolecular Chemistry, **Czech Rep.**
36.	Mass Production of Stretchable Colorimetric Tape for Ammonia Leakage Detection T. N. T. Dang and **Y. S. Kim**	**Prof. Yong Shin Kim**, Hanyang Univervity, **Rep. of Korea**
37.	Preparation, Structural Characterization, and Ethanol Sensing Appli-cations of Phase-Pure WO3 and CuWO4 Thin Films **T. Imrich**, M. Baudys, H. Krýsová, M. Neumann-Spallart and J. Krýsa	**Dr. Tomáš Imrich**, Univ. of Chemistry and Technology, Prague, **Czech Rep.**
38.	Development and Experimental Evaluation of a Four-Channel Chemiresistive Sensor Array for Formic Acid Detection P. Arroyo, **A. Bernal**, E. Pinilla, J. L. Herrero, J. M. Perea, J. A. Fernández, J. I. Suárez and J. Lozano	**Mr. Alejandro Bernal Reina**, University of Extremadura, Badajoz, **Spain**
39.	Structural and Optical Characterization of Hydrothermally Synthe-sized Graphene Quantum Dots **F. Zaleski**, D. Minta, K. Matczyszyn and G. Gryglewicz	**Mr. Franciszek Zaleski**, Wrocław Univ. of Science and Technology, **Poland**
40.	Unconventional Signaling-Off PSA Detection Using Laser-Induced Graphene/ZnO Nanorod Impedimetric Immunosensors S.F. Soares, S.O. Pereira, A. J. S. Fernandes, F. M. Costa and **N.F. Santos**	**Mr. Nuno F. Santos,** Univ. of Aveiro, **Portugal**
41.	Advanced Biological Denitrification Using Graphene Oxide Coated Tubular Ceramic Membranes **Z. Pouramini**, F. E. Stüber and J. Font Capafons	**Ms. Zahra Pouramini,** Univ. Rovira Virgili, **Spain**
42.	PCL Nanofibers Loaded with Antitumor Drugs for the Treatment of Colorectal and Pancreatic Cancer **J. Prados**, C. Melguizo, J. Moreno, I. Fernández, R. Contreras-Cáceres, N. Muñoz-Flores, A. Ortigosa- Palomo and L. Cabeza	**Dr. Jose C. Prados Salazar**, University of Granada, **Spain**
43.	Graphene Oxide-Erlotinib Nanoconjugates Target Tumour Growth and Angiogenesis in Pancreatic Cancer Models **S. Mai**, M. Perez-Lloret, M. Narajczyk, A. M. Olszewska, I. Inkielewicz-Stepniak	**Ms. Shaoshan Mai**, Medical University of Gdansk, Poland

Oral Presentation and Poster terms

For the Oral Presentation:

Duration of each talk type (including 2 to 3 minutes for Questions/Answers):

- Keynote talk: 30 minutes. Oral presentation: 15 minutes.
- We do not impose a template for the oral presentation.
- You need to carry your presentation in USB key or external disk and **use the available presentations laptop** at the conference room.
- **Do not plan to use your own laptop.**

For the Poster:

- Poster dimensions must be within **100cm high X 80cm wide**.
- We do not impose a template for the poster content.
- **Please display your poster at your poster board number as per the conference program**.

SMS 2026 / EGF 2026 / Sensors 2026 / NanoMed 2026 Joint Plenary Session I

Functional Materials: From Self-Cleaning Surfaces to Radiative Cooling Coatings

Ivan P Parkin [1]
[1] Department of Chemistry, University College London (UCL), 20 Gordon Street, London, WC1H 0AJ, UK [2]

Abstract:
The design and scalable synthesis of functional surfaces and smart materials have revolutionized modern engineering, offering profound solutions to global challenges spanning public healthcare, green building efficiency, and environmental sustainability.[1,2] Over the past three decades, the UCL Materials Chemistry Group has pioneered methods to control material architectures at the nanoscale, directly translating laboratory-scale chemical innovations into commercially viable, real-world technologies. This presentation will provide a comprehensive overview of our group's milestones in manipulating wetting behavior, photocatalysis, and smart optical responses through advanced thin-film deposition, polymer composites, and nanoparticle engineering.

A central focus of our research is the optimization of Aerosol-Assisted and Atmospheric Pressure Chemical Vapour Deposition (AACVD / APCVD) techniques, alongside versatile sol-gel pathways. These methodologies allow precise atomic and structural tuning of metal oxides and functionalized nanocomposites. We will explore the fundamental mechanisms of photocatalysis that led to the development and successful commercialization of self-cleaning technologies. By embedding titania (TiO_2) nanoparticles onto glass surfaces, sunlight photo-mineralizes organic dirt while a highly hydrophilic state ensures rainwater sheets uniformly to wash away contaminants.

Transitioning from super-hydrophilic architectures, this talk will highlight our parallel breakthroughs in extreme water-repellent systems, including the fabrication of robust superhydrophobic surfaces and uniquely engineered Wenzel-state "sticky" hydrophobic surfaces. The integration of functionalized nanoparticles—most notably gold and transition metal oxides—extends far beyond wetting properties into healthcare applications. We demonstrate how combining light-activated dye molecules with gold nanoparticles yields highly potent, antimicrobial polymers. These surfaces trigger the release of reactive oxygen species capable of destroying prevalent hospital pathogens, including MRSA, thus serving as a vital countermeasure against antimicrobial resistance.

Furthermore, the presentation will delve deeply into the realm of smart, energy-efficient architectural coatings, highlighting our recent paradigm-shifting work on **passive daytime radiative cooling (PDRC)** surfaces. Operating as an eco-friendly alternative to conventional air conditioning, these smart materials are engineered to achieve high solar reflectance alongside high thermal emittance within the 8–13 micrometer atmospheric transparency window. By utilizing robust polymer-particle composites—such as fluoropolymer matrices embedded with engineered titanium dioxide and barium sulfate nanoparticle blends—we showcase scalable coatings that can lower surface temperatures well below the ambient environment under direct sunlight. We will compare these static cooling systems with our dynamic, thermochromic vanadium dioxide (VO_2) thin films, which undergo a fully reversible, temperature-dependent semiconductor-to-metal phase transition to intelligently modulate infrared solar heat. Work is presented on current trials on London Buses where a 2C reduction in temperature was seen and on test homes in Madrid.

Finally, the talk wraps up with a look into alternative applications of our thin-film materials, highlighting the development of discriminating, zeolite-based gas sensors and photoacoustic ultrasound imaging probes. By bridging fundamental solid-state chemistry with industrial scalability, this body of work illustrates the transformative lifecycle of smart materials—progressing from basic laboratory characterization to impactful market adoption.
optical applications.

Keywords: Coatings, radiative cooling, self cleaning, sensors, industrial applications



Figure 1: Figure Shows two London buses – the front has our new spreay paint formulation and the rear one the “best” current paint.

References:

1. Infrared thermochromic antenna for self adapted thermoregulation, F. Ramariz-Cuevas, I. P. Parkin, I Papakonstantinou* et al Nature Comms, 2024, 15, 9109.
2. All-sat radiative cooling with suoerhydrophobic, fluorine-free polydimethlsiloxand- embedded polyethylene coating; Materials Sustainability, Lingxi Li et al 2025, 31, 10168

High-performance, heteroepitaxial, device layers for wide-ranging electrical and electronic applications

Amit Goyal
State University of New York (SUNY) at Buffalo, USA

Abstract:
For many energy and electronic applications, single-crystal-like materials oder the best performance. However, in almost all cases, fabrication of single-crystal form of the relevant material is too expensive. In addition, for many applications, very long or wide materials are required, a regime not accessible by conventional single-crystal growth. This necessitates the use of artificially fabricated, large-area, single-crystal-like substrates suitable for heteroepitaxial growth of the relevant advanced material for the electronic or energy application in question.
In this talk, details of the fabrication of such substrates will be provided. Heteroepitaxial growth of nanolaminate multilayers and devices on such substrates using a variety of deposition techniques such as pulsed laser ablation, sputtering, e-beam evaporation, MBE, MOCVD, and chemical solution deposition will be reported upon. Application areas that have been demonstrated via the use of such artificial substrates include – oxide high-temperature superconductors, semiconductor materials (Si, Ge, GaAs, CdTe, Cu2O), ferroelectrics (BaTiO3), multiferroics (BiFeO3), etc.
These heteroepitaxial layers have or can be realized via roll-to-roll deposition for scaling-up. In addition, strain-driven self-assembly of second phase nanomaterials at nanoscale spacings has been demonstrated within device layers. Control of heteroepitaxy in lattice-mismatched systems and the edects of strain on self-assembly will be discussed. Such heteroepitaxial device layers on large-area, single-crystal-like artificial substrates are quite promising for a range of electrical and electronic applications.

Ultraclean van der Waals interfaces for novel materials and twistronics

Roman Gorbachev
[1] University of Manchester, UK

Abstract:
Layer-by-layer assembly of van der Waals (vdW) heterostructures underpins new discoveries in solid state physics, material science and chemistry. Majority of current assembly techniques use polymeric supports which limit their cleanliness, ultimate electronic performance, and potential for optoelectronic applications. In the first part of the talk, I will introduce a polymer-free platform for heterostructure assembly using re-usable flexible silicon nitride membranes. This approach enables production of heterostructures with interfaces free from interlayer contamination and correspondingly excellent optoelectronic behaviour. I will then discuss how this new technology affects novel magnetic materials such as VBr3, NiI2, CoI2, Cr2Ge2Te6 and twisted TMDs. Here I will cover their structural properties explored using atomic resolution TEM in conjunction with electronic transport and magnetic studies.

In twisted TMDs I will discuss how the atomic reconstruction can be characterised using multi-slice electron ptychography. We explore this phenomenon works in crystals with multiple layers in order to understand characteristic decay of the interfacial strain into the bulk. In the last, conclusive part I will discuss the importance of nanofabrication in the context of twistronics and offer avenues for future development of nanofabrication pathways.

Coherent propagation of Laser Induced Periodic Surface Structures by doping in ZnO films

Gonzalo Gomez-Munoz[1], Rocio Ariza[1,2], J.F. Ramos-Justicia[3], Fatima Cabello-Pardos[1], Antonio Pablo Perez[1], Jose Gonzalo[1], B. Sotillo[3], Carmen Lopez-Santos[4,5], P. Fernandez[3], Javier Solis[*]

[1]Instituto de Óptica-CSIC (IO-CSIC), c/Serrano 121, ES-28006 Madrid, Spain

[2] Centre of Membrane Separation, Adsorptions, Catalysis and Spectroscopy for Sustainable Solutions – KU Leuven, Celestijnenlaan 200F, BE-3001 Leuven, Belgium

[3]Departamento de Física de Materiales - UCM, Pl. de las Ciencias 1, ES-28040 Madrid, Spain

[4]Instituto de Ciencia de Materiales de Sevilla-US-CSIC (ICMSE-US-CSIC), C/ Américo Vespucio 49, ES-41092 Seville, Spain

[5]Departamento de Física Aplicada I-Escuela Politécnica Superior, Universidad de Sevilla, c/ Virgen de África, ES-41013 Seville, Spain

Abstract:

ZnO is a multifunctional transparent conductive oxide (TCO) with many scientific and technologic uses including applications in biomedicine, photonics, sensing or photocatalysis. Many of them would benefit from the use of large-area, electrically anisotropic surfaces. It has recently been shown that such anisotropies can be induced in other TCO´s (FTO and ITO) by structuring the material surface with fs-laser pulses to induce the formation of coherently propagated low spatial frequency (LSF) Laser Induced Periodic Structures (LIPSS). In this work we have analyzed the role of the carrier density of the material (n_e) in the formation and coherent propagation of LIPSS in ad-hoc doped ZnO films grown by Pulsed Laser Deposition (PLD). As dopant we used small amounts of Yb_2O_3 (below 5 at. %) to induce n-type conductivity due to the role of Yb^{3+} as donor but preserving the functional properties of pure ZnO. For $n_e > 10^{19}$ cm^{-3} coherent propagation of LSF-LIPSS can be successfully achieved upon irradiation with 350 fs and longer pulses at 1030 nm, and a laser scan speed well above 1 m/s. The ablation mechanism (ZnO sublimation at the LIPSS valleys), and the large melting temperature of ZnO, make the thermal conductivity of the substrate, the film thickness and the irradiation pulse duration to play a crucial role in the morphology of the LIPPS propagated over large areas, especially in avoiding film cracking. Processed surfaces can show conductivities along the LIPSS about hundred times larger than transversally. This enables the development large area applications based on LIPSS-structured surfaces, like gas sensing, or electrothermal transparent devices as we will discuss.

Keywords: TCO´s, ZnO, LIPSS, electrical anisotropy, fs-laser processing, large area devices, thermoelectric devices, gas sensing.

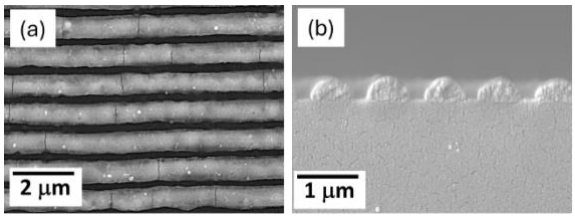


Figure 1: (a) SEM image of a ZnO-film doped with Yb_2O_3 (5.0 wt.%) irradiated with 680 mJ/cm^2 fs-laser pulses at 500 kHz with a d=4μm and v=2.5 m/s for a pulse duration of 350 fs. (b) Cross-sectional image of the sample in (a) showing the morphology of the structure. The fine structure observable in the substrate region is caused by Pt-film deposited to avoid charge effects in the cross image at the SEM.

References:

1. Lopez-Santos, C., et al, Anisotropic Resistivity Surfaces Produced in ITO Films by Laser-Induced Nanoscale Self-Organization. *Adv. Opt. Mater.* **2021**, *9* 202001086 https://doi.org/10.1002/adom.202001086.
2. Gomez-Munoz, G., et al., Formation and Coherent Propagation of Laser Induced Periodic Surface Structures (LIPSS) upon Fs-Laser Irradiation of Fluorine Tin Oxide (FTO): Control, Potential Applications and Challenges. *ACS Appl. Mater. Interfaces*. (under review)

SMS 2026 Session I. A: Multifunctional Materials & Surfaces / Nano-Systems / Adaptive Materials and Structures

Functional thermomechanical properties of NiTi shape memory alloy coatings fabricated by thermal plasma HVAF method

P. Šittner[1], S. Samal[1], S. Joshi[2]
[1] Institute of Physics of the CAS, Na Slovance 1992/2, 18200 Prague, Czech Republic
[2] Department of Engineering Science, University West, 46186, Trollhattan, Sweden

Abstract:
Deposition of various coatings on surface of engineering components with the aim to improve their performance concerning wear, corrosion, friction, and thermal protection is already a standard practice. There are special cases, in which metallic NiTi shape memory alloy coatings may be a viable alternative to the hard ceramic coatings. It is because NiTi coatings offer additional benefits originating from their unique functional thermomechanical properties. However, fabrication of thick NiTi coatings possessing functional thermomechanical properties was not so far successful. Standard electroplating and/or laser cladding methods are not suitable since they melt the NiTi and it does not transform anymore. The plasma spray methods are promising but they tend to produce chemically inhomogeneous coatings that do not transform as well. The cold sprayed NiTi coatings do transform but suffer from poor adhesion to the substrates. In my talk, I will report on HVAF fabrication of thick NiTi coatings (100–300 μm) that display functional thermomechanical properties and simultaneously show very good adherence to the substrate [1]. HVAF method uses high velocity air fuel to fabricate NiTi coatings deposited on mild steel. These coatings contain inhomogeneous nanocrystalline microstructure with voids, oxide particles, high density of dislocation defects and internal stress. Although tensile strength is rather limited, the coatings display thermally and stress induced martensitic transformation. They were found to display thermal actuation in 3-point bending tests and shape memory effects in nanoindentation and scratch tests.

Referebces:

S. Samal, S. Joshi, S. Björklund, M. Chandra, A. Bhardwaj, J. Kopeček, S. Habr, L. Václavek, J. Tomáštík, O. Tyc, O. Molnárová, P. Šittner, HVAF spraying of NiTi coatings: Microstructure, phase transformation and shape memory behavior, Applied Surface Science Advances, 34(2026)101038, https://doi.org/10.1016/j.apsadv.2026.101038 .

Self-stratifying coatings and vitrimers : a path toward multifunctional, repairable and recyclable surface systems

M. Jimenez[1]*, A. Kerrache[1,2], A. Lebeau[1], M. Casetta[1], F. Samyn[1], J.F. Gohy[2]
[1] Univ. Lille, CNRS, INRAE, Centrale Lille, UMR 8207 - UMET, F-59000 Lille, France
[2] Université catholique de Louvain, Louvain-la-Neuve, Belgique

Abstract:
With the growing demand for eco-designed surface technologies, self-stratifying coatings emerge as a sustainable and efficient alternative to conventional multilayer systems. These systems, based on one-pot formulations of incompatible polymers, enable the spontaneous formation of functional multilayer architectures in a single application and curing step, reducing raw material use, energy consumption, and processing complexity [1]. These last years, we designed self-stratifying systems for different applications, such as flame retardancy [2], fouling resistance and aerospace [3]. They were mainly based on oil-based and bio-based epoxies [4] combined with different polymers such as polyurethane, silicone and PVDF. A comparative Life Cycle Assessment (LCA) revealed a significant reduction in environmental impact - up to 30% compared to traditional multilayer systems - due to the simplified processing and bio-based content [5].
Our research now focuses on self-stratifying coatings that incorporate dynamic covalent polymer networks, i.e. vitrimers. Two original self-stratifying coatings were designed, i.e. a bio-based vitrimer expoy/PVDF system [6] (Figure 1) and a bio-based epoxy / vitrimer silicone system [7]. The first one demonstrates robust adhesion to metallic substrates, along with thermally triggered removability, allowing substrate recovery and potential material recyclability. The second shows excellent adhesion to plastics and self-repairing properties at room temperature.
This study paves the way for new generations of coatings combining sustainability, high performance, and smart functionalities, with promising applications in packaging, food processing, electronics, and aerospace sectors.

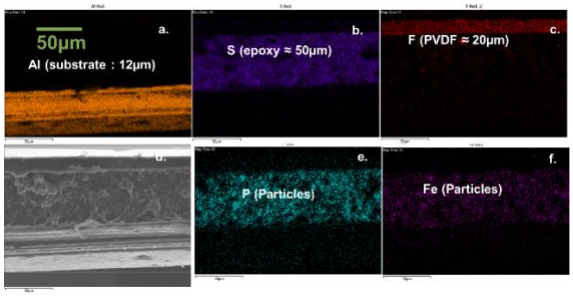


Figure 1: SEM-EDX view of a self-stratifying system. a.: Aluminium as susbtrate. b.: Epoxy layer with a mapping on sulfur from disulfide bond. c.: Fluorine mapping from PVDF layer. d.: SEM view of the bilayer coating. e.: Phosphorus mapping highlighting migration of $LiFePO_4$ particles only on base layer. f.: Iron mapping from $LiFePO_4$ particles

References:

1. A. Beaugendre et al. Self-stratifying coatings: A review, Progress in Organic Coatings 110 210-241 (2017)
2. A. Beaugendre et al. Self-stratifying epoxy/silicone coatings, Progress in Organic Coatings 103 101-110 (2017)
3. A. Beaugendre et al., One pot flame retardant and weathering resistant coatings for plastics: a novel approach, RSC Advances 7 40682-40694 (2017)
4. A. Lebeau et al., Self-stratifying epoxy/thermoplastic polyurethane coatings designed for aerospace applications, Progress in Organic Coatings 109478 (2025)
5. C. Lemesle et al., Self-stratified bio-based coatings: Formulation and elucidation of critical parameters governing stratification, Applied Surface Science 536, 147687 (2021)
6. C. Lemesle et al., Life cycle assessment of multi-step versus one-step coating processes using oil or bio-based resins, Journal of Cleaner Production 242, 118527 (2020),
7. A. Kerrache et al., Self-stratifying epoxy vitrimer/fluoropolymer coatings: Thermally induced detachment for substrate recovery, Progress in Organic Coatings 109593 (2025),
8. F. Samyn al., Eco-efficient, hydrophobic, self-healing and self-stratifying coating for polycarbonate, Progress in Organic Coatings 108732 (2024)

A pre-ceramic sol-gel coating for thermal protection

M. Busquet [1,*], J. Garcia [1]
[1] Institut de Recherche St Exupéry, Toulouse , France

Abstract:
The thermal resistance (temperature, flux and fire) of equipments and structures is a major issue for all industrial sectors, and more particularly for the transport. Meeting these requirements relies on the use of high-perfomances materials (superalloy, refractory materials). However, their production and integration remain costly and challenging: manufacturing, impact on structural weight… Replacing these materials of references with a substrate/coating system that deliver equivalent performances therefore represents a promising strategy for reducing economic and environmental impacts.
To tackle these issues, we have developed a new surface protection coating based on the sol-gel process. This technology offers several advantages, including excellent thermal and chemical properties due to its inorganic nature, even when applied as a thin coating (< 200 µm).[1] It is REACH-compliant, easy to process, and compatible with conventional paint application techniques. Furthermore, with minor adjustments to the formulation and application process, the sol-gel coating can be adapted to a wide range of substrates and a wide range of environments.
The strategy is based on an *in-situ* ceramisation of the pre-ceramic sol-gel layer occurring during thermal exposure, which results in the formation of a protective ceramic layer. This layer demonstrates excellent thermal insulation properties and stability. Finally, it acts as a thermal barrier and insulates the substrate from heat and flames.
This patented sol-gel coating has been evaluated for various use cases.
The first one was the replacement of fireproof titanium part by aluminium. In this case, the sol-gel coting prevents the melting of aluminium substrates when exposed to a 1200 °C gas flame, simulating a kerosene fire. Homemade burn-through tests demonstrated a significant enhancement in fire performance for sol-gel-coated aluminium specimens: they withstood flame exposure for more than 15 minutes, whereas raw aluminium specimens melted in less than 4 minutes (Figure 1).
Following minor formulation optimisation, the sol-gel coating was successfully adapted to oxide ceramic matrix composite (CMC) substrate in order to replace carbide based CMC (C/SiC). The protective sol-gel coating prevents cracking of the O-CMC substrate after multiple exposures to a 1600 °C and 900 kW/m² flame. This solution could be of interest for space application and more specifically for reusable launcher.
For even more demanding high-temperature applications, the sol-gel, when impregnated into mineral fibre insulating material, enabled the fabrication of firewall panels capable of withstanding direct flame exposure at temperatures exceeding 1800 °C for more than 20 minutes.[3]
The sol-gel coating has also demonstrated its ability to be refurbished, a key requirement for industrial applications.

Keywords: surface protection, coating, Sol-gel, thermal protection, fire protection

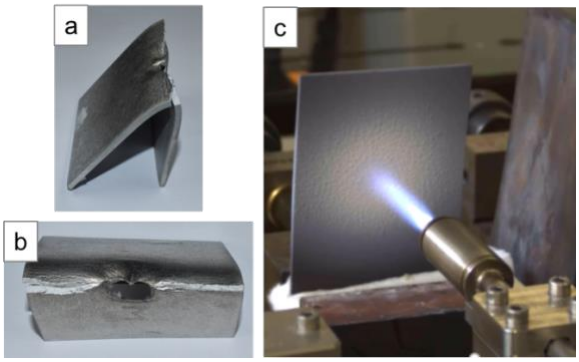


Figure 1: a, b - Uncoated aluminium substrate (120 x 80 x 3 mm) after 3 min of 1200 °C flame exposure ; c- Sol-gel coated aluminium after 15 minutes of 1200 °C flame exposure

References:

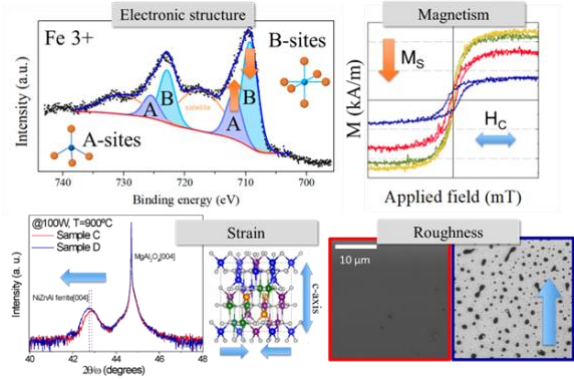
1. Schubert, U., Chemistry and Fundamentals of the Sol–Gel Process, Wiley (2025).
2. WO2023012022A1 - Garcia, J., Escobar, J. & Murat, V. Method for fire protection of a metal substrate. (2022).
3. WO2026068435A1- Garcia, J., Busquet, M. Use of a fire resitant material to protect a substrate (2025).

One-step RF sputtering deposition of strained epitaxial NiZnAl spinel ferrite thin films

Cecilia Granados-Miralles[1], Alicia Gonzalo[2], Jimena Soler-Morala[3], Anna Maria Friedel[4,5], Elisa García-Tabarés[2], Adrián Gudín[6], Juan Rubio-Zuazo[3,7], Paolo Perna[6], Iciar Arnay[2,6]

[1] Instituto de Cerámica y Vidrio, CSIC, Madrid 28049, Spain
[2] Departamento de Física, Universidad Carlos III de Madrid. Campus Leganés, Madrid, SPAIN
[3] Instituto de Ciencia de Materiales de Madrid – CSIC, 28049 Madrid, Spain
[4] Institut Jean Lamour, UMR CNRS 7198, Université de Lorraine, 54000 Nancy, France
[5] Fachbereich Physik and Landesforschungszentrum OPTIMAS, Rheinland-Pfälzische Technische Universität Kaiserslautern-Landau, 67663 Kaiserslautern, Germany
[6] IMDEA Nanociencia, C/Faraday 9, 28049 Madrid, Spain
[7] BM25-SpLine Beamline at the ESRF, 38043 Grenoble, France

Abstract:
Multiferroic material such as Spinel ferrites [1] are increasingly sought-after in spintronics and magnonics allowing for hybrid magneto-acoustic or magneto-electric applications with on-chip functionality control [1, 2]. Hereby, a particular challenge is to find suitable materials for radiofrequency applications, since the hybrid functionality is generally associated with increased magnetic losses damping the high frequency dynamics. Among the different Spinel ferrites, particularly NiZn ferrites are promising candidates for an exploitation to microwave applications: This subgroup presents resonance frequencies in the GHz regime and offers a particularly promising combination of significant magnetostriction with comparably low magnetic losses [3,4]. The addition of Al to the spinel structure promises a significant improvement of magnetic losses combined with an enhancement of the magnetoelastic coupling, for which the optimal stoichiometry $Ni_{0.65}Zn_{0.35}Al_{0.8}Fe_{1.2}O_4$ (NZAFO) is desirable in terms of a maximized ratio of magnetostriction over saturation magnetization and high Curie temperature [5,6]. This work reports on the growth of epitaxial NiZnAl ferrite thin films grown via RF sputtering from sintered targets. Under optimized conditions, commensurate films with large crystallographic domains were obtained on $MgAl_2O_4$ (001) substrates. The films exhibit soft magnetism with magnetization at saturation in the order of 120 kA/m for epitaxial films. Furthermore, adjusting the target-sample distance allows for a tuning of the lattice strain, which significantly impacts the magnetic properties. Our results summarize the effectiveness of this one-step method for preparing complex spinel ferrites, offering high reproducibility, tunability and scalability.



Keywords: spintronics, manonics, ferrites, inverse spinel

Figure 1: Summary of how electronic and structural properties influence the magnetic response of the sputtered films.

References:

1. A. Hao and X. Ning, Frontiers in Materials (2021) 8, 718869.
2. A. V. Chumak et al., IEEE Transactions on Magnetics (2022) 6, 0800172.
3. O. Obi, M. Liu, J. Lou, S. Stoute, X. Xing, N. X. Sun, J. Warzywoda, A. Sacco, Jr, D. E. Oates, G. F. Dionne; J. Appl. Phys. (2011) 109, 07E527.
4. D. Guo, Z. Zhang, M. Lin, X. Fan, G. Chai, Y. Xu and D. Xue; J. Phys. D: Appl. Phys. (2009) 42 125006.
5. Donglin He, Zhibiao Xu, Ke Wang, Peng Wu, Jinghao Cui, Liang Qiao, Tao Wang; J. Magn. Magn. Mater. (2023) 588, 171449.
6. S. Wang, Y. Li, F. Li, M. Qu, Y. Liao, Q. Wen, J. Magn. Magn. Mater. (2023) 576, 170773.

Surface Plasmon Resonance Imaging of Metasurfaces Patterned Via Pyramidial Interference Lithography

Ribal Georges Sabat[1,*]
[1] Department of Physics and Space Science, Royal Military College of Canada, PO Box 17000, STN Forces, Kingston, Ontario, K7K7B4, Canada

Abstract:
Large-area metasurfaces were fabricated using Pyramidal Interference Lithography (PIL) on azobenzene thin films. Azobenzene molecules undergo photoisomerization upon light exposure, which induces molecular mass transport and film surface reorganization, thus enabling the recording of the light interference pattern onto the film surface. This fabrication method, which uses a 488-nm laser, enabled the generation of tunable nano- and micro-scale surface feature periodicities using custom-built 2-face, 3-faced and 4-faced pyramidal prisms. The 2-faced prism produced linear surface relief diffraction gratings, while the 3-faced prism produced triangular lattices and the 4-faced prism produced square lattices. A double inline prism set-up further enabled control over the metasurface feature periodicity, allowing systematic increase of the pattern size. Additional tunability was achieved by placing a prism inline with a lens, allowing precise control over the metasurface feature periodicity. Overall, feature periodicity was tuned and ranged from 682 to 2750 nm. A theoretical model was developed to relate the prism and inscription geometry to the feature periodicity and it was successfully matched to the experimental results. The resulting metasurfaces were subsequently coated with gold and exhibited distinct surface plasmon resonance (SPR), as measured with a spectrometer, and surface plasmon resonance imaging (SPRi) responses, as measured using monochromatic light and camera, thus confirming their functionality. Overall, this work establishes PIL as a cost-effective and highly adaptable metasurface fabrication method for producing customizable periodic metasurfaces for photonic, plasmonic, and sensing applications.

Keywords: Metasurfaces, pyramidal interference lithography, surface plasmon resonance imaging, tunable periodic structures.

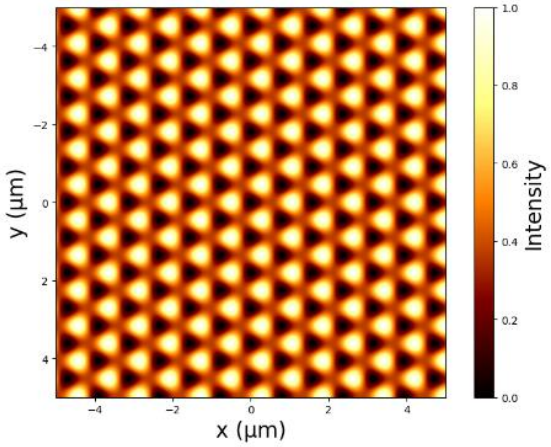


Figure 1: Atomic Force Microscope of a metasurface created with a 3-faced pyramidal prism.

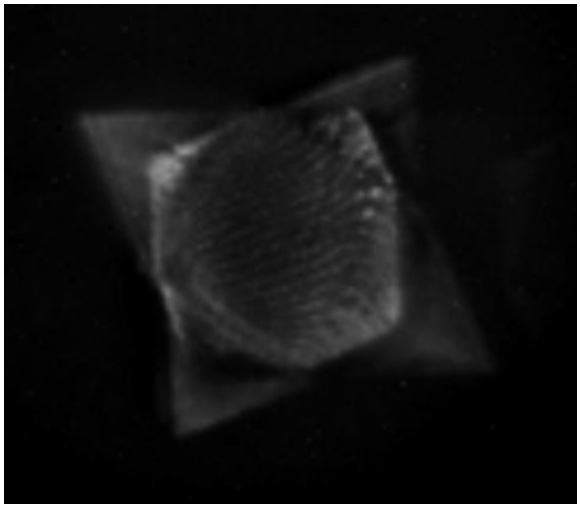


Figure 2: SPR image captured under crossed polarization conditions from metasurfaces fabricated with 4-faced pyramidal prism.

References:

S. Bokhari, Y. Bdour, R.G. Sabat, "*Fabrication and Plasmonic Characterization of Metasurfaces Patterned Via Tunable Pyramidal Interference Lithography*", Micromachines, Vol. 17, Issue 1, 2026.

Generation of structural colors in Ag-based plasmonic nanostructures by direct fs-laser irradiation

A. Philip, A. P. Pérez-Marín, J. Siegel, J. Gonzalo *, M. Garcia-Lechuga
Laser Processing Group, Instituto de Óptica, CSIC, IO– CSIC, Madrid, Spain

Abstract:
Nanostructures containing embedded noble-metal nanoparticles (NPs) constitute an interesting class of materials with distinctive optical properties arising from their plasmonic response. In the case of Ag NPs-based nanocomposites, the strong localized surface plasmon resonance (LSPR), combined with its spectral position in the visible range, makes these systems particularly suitable for visual color applications and optical filtering [1]. This versatility originates from the sensitivity of their optical response to the NP volume concentration, shape, size and size distribution, as well as to the properties of the dielectric matrix. The high degree of control over these parameters opens exciting opportunities for both synthesis and post-processing strategies.

In this work, we focus on tailoring the synthesis of the initial nanocomposite system and developing post-processing strategies to achieve coloration changes spanning the RGB range. Both strategies are based on laser technologies. First sequential pulsed laser deposition (PLD) (λ= 193 nm, τ= 20 ns) allows the synthesis of Ag NPs embedded in amorphous Al_2O_3 layers. Fine tuning of the deposition parameters allows the fabrication of nanocomposites having Ag NPs ranging from dispersed NPs to near-coalescent or semi-continuous Ag layers, exhibiting different spectral responses from narrow to broadband LSPR. Additionally, the control of the top Al_2O_3 layer thickness enables tuning the reflectivity spectrum, thereby enhancing or suppressing specific colors through constructive or destructive interference.

Direct scanning femtosecond laser irradiation (λ= 515 nm, τ= 300 fs) was used for post-synthesis laser processing, which leads to strong and homogeneous coloration changes, as shown in Figure 1 when visualizing the samples in reflection but also probed to show strong coloration in transmission. Furthermore, a strong anisotropic behaviour depending on the polarization of the illumination with respect the laser polarization, allows us to indirectly identify that in addition to localized NP shape and size modification, spatial reorganization of the Ag NPs occurs [2]. Further analysis based both on transmission electron microscopy (TEM) characterization and optical modeling, combining Mie theory and effective medium approximation with the matrix-transfer method, provides the physical origin of this reorganization and its impact on the control of laser-induced nanocomposite coloration.

Keywords: Pulsed laser deposition, laser processing, metal nanoparticles, nanocomposite, Surface plasmon resonance, structural coloration.

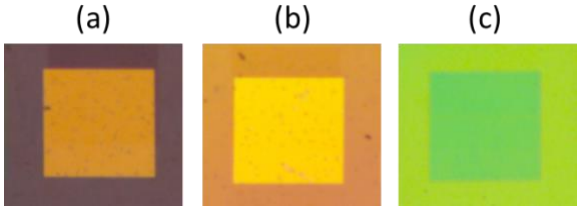


Figure 1: Images in reflection mode (1.5 x 1.5 mm^2) of laser processed Ag NPs:Al_2O_3 nanocomposites having Al_2O_3 cover layers (a) 35 nm, (b) 130 nm and (c) 240 nm thick. The laser energy density was 33 mJ/cm^2 for (a) and 55 mJ/cm^2 for (b) and (c).

References:

1. Wu, B., Zhu, H., Zhang, B., Ren, F., Juodkazis, S., Chen. F. (2023), Plasmon guided assembly of nanoparticles in solids, *Mater Today Nano.,* 21. 100299
2. Doster, J., Baraldi, G., Gonzalo, J., Solis, J., Hernandez-Rueda, J., Siegel J. (2014), Tailoring the surface plasmon resonance of embedded silver nanoparticles by combining nano- and femtosecond laser pulses, *Appl. Phys. Lett.*, 104, 153106.

Hydrophobicity Recovery Mechanisms in Silicone and Epoxy Outdoor Insulating Materials Under Contamination and Corona Stress

A. Milionis [1*], J. Goerlich [2], A. Leal-Ayala [1], P. Meier [1], D. K. Hohl [1], S. Kornhuber [2]
[1] Corporate Research Center, ABB Switzerland Ltd., Baden-Daettwil, Switzerland
[2] Electrical Engineering, University of Applied Science Zittau/Görlitz, Zittau, Germany

Abstract:
Outdoor electrical insulators face multiple environmental challenges including contamination from industrial and natural pollutants as well as corona discharge stress, both of which degrade surface hydrophobicity.[1] Recovery of this property is critical for maintaining long-term electrical performance and preventing leakage currents and flashover events.[2] This study compares hydrophobicity recovery properties of silicone-coated and epoxy-based insulation materials under two complementary and realistic test scenarios: (1) hydrophobicity transfer with thick contaminant deposition (diffusion-limited mechanism, simulating polluted outdoor environments where a contaminant layer acts as a diffusion barrier), and (2) hydrophobicity recovery following corona discharge stress (direct surface recovery in cleaner conditions where surface property changes are captured immediately). Contact angle measurements were performed on both material types following standardized test protocols: static and dynamic contact angles measured on silica powder layers over 6 weeks to simulate contamination recovery, and contact angles measured over 56 days post-corona discharge treatment. Silicone materials exhibited significantly superior hydrophobicity recovery in both tests. In the hydrophobicity transfer scenario, silicone reached contact angles exceeding 120° within one month (surpassing initial values due to roughness-induced hydrophobicity), while epoxy samples showed no recovery (CA=0° throughout). Under corona stress, silicone achieved near-complete recovery in approximately 200 hours, whereas epoxy showed significantly slower and incomplete recovery. The key distinction emerges from the recovery mechanisms: contamination-induced recovery (with intervening contaminant layer) proceeds slower in both materials compared to direct corona-induced recovery in clean conditions, where hydrophobic component diffusion occurs unimpeded. While silicone coatings demonstrate superior hydrophobicity recovery capabilities, epoxy systems remain valuable for applications where structural durability is important.

Keywords: hydrophobicity recovery, silicone coatings, corona discharge, contamination, outdoor insulation, contact angle, epoxy

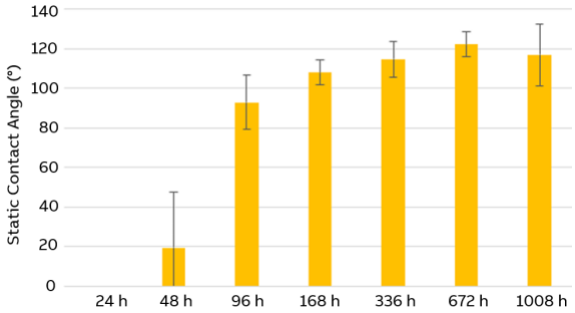


Figure 1: Hydrophobicity transfer test for the silicone coating with contaminant layer deposited. The static contact angle progressively increases, reaching a maximum value after four weeks. Epoxy showed no hydrophobicity recovery with contact angle equal to zero throughout the experiment's duration.

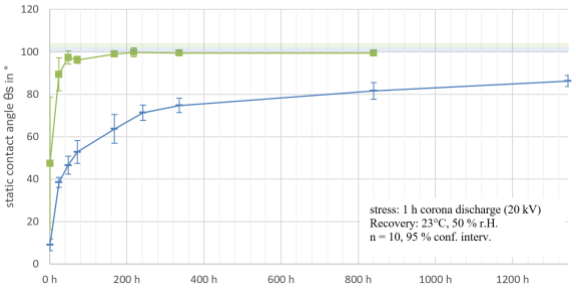


Figure 2: Hydrophobicity recovery on epoxy (blue) and silicone (green) samples after corona pre-stressing, static contact angle in dependence of the recovery time. The faded flat green and blue lines (slightly > 100°) depict the initial contact angle of silicone and epoxy respectively.

References:

1. Milionis, A., Leal-Ayala, A., Meier, P., Hohl, D. K., (2026) A sequential evaluation workflow for early-stage screening of outdoor electrical insulation polymer-based materials: A comparative case study, *Eur. J. Mater.,* 6, 2680755.
2. Hilborg, H. C., (2001), Loss and recovery of hydrophobicity of polydimethylsiloxane

after exposure to electrical discharges, *Royal Institute of Technology, Stockholm*.

Scalable Routes to Functional Materials: Photocatalytic, TCO and Anti-Soiling Coatings

Claire J. Carmalt*
Department of Chemistry, University College London, London, UK

Abstract:
The search for efficient materials for sustainable infrastructure is a key challenge to address the global environmental crisis. Sunlight-activated coatings, particularly those produced from scalable technologies, are sought in the glass industry for applications in self-cleaning windows. Current research involves developing processes towards sustainable and inexpensive functional materials including photocatalysts, anti-soiling coatings, transparent conducting oxides (TCOs) and photoelectrochemical films on glass. These find application as low-emissivity windows, photovoltaics, optoelectronic devices and self-cleaning windows, as well as anti-soiling coatings for solar modules.
Our method uses aerosol assisted chemical vapour deposition (AACVD) to develop scalable coatings. Chemical vapour deposition (CVD) is a film deposition method which involves a series of chemical reactions in the vapour phase. Due to its low cost, scalability and reliability, CVD has been industrially utilized in many optoelectrical fields, particularly glass coating and semiconductors. Compared to conventional CVD, the AACVD method is a solution based process which uses aerosol droplets to transport precursors, with the aid of an inert carrier gases. Therefore, in AACVD volatility is no longer crucial and this allows for a wider choice of precursors being available for use and can lead to high quality films at low cost. AACVD can result in the formation of highly textured coatings which can enhance the functional properties. We have investigated the AACVD of a range functional thin films including perovskites, TCOs, photocatalyst, heterojunctions and low-emissivity coatings.

Keywords: AACVD, photocatalyst, anti-soiling coatings, transparent conducting oxides, heterojunctions.

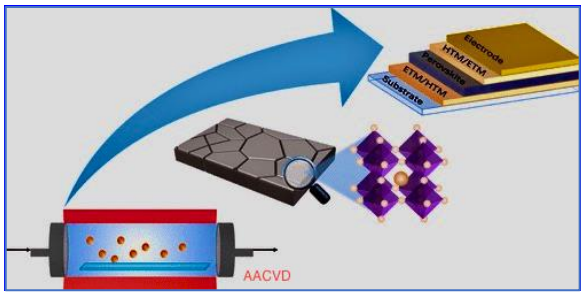


Figure 1: AACVD process for film deposition and device preparation.

References:

1. M. Wang, A. Kafizas, S. Sathasivam, M. O. Blunt, B. Moss, S. Gonzalex-Carrero, C. J. Carmalt. (2023) *Appied. Catalysis B: Environment and Energy*, 331, 122657.
2. M. Wang, R. Quesada-Cabrera, S. Sathasivam, M. O. Blunt, J. Boroweic, C. J. Carmalt. (2023) *ACS Applied Materials & Interfaces*, 15, 49270.
3. H. Li, Z. Lin, F. Guo, S. Li, A. Kafizas, C. S. Blackman, C. J. Carmalt. (2025) *ACS Applied Enery Materials*, 8, 17334.
4. I. Ramzan, M. O. Blunt, I. P. Parkin, C. J. Carmalt. (2026) *ACS Applied Materials & Interfaces*, 18, 19364.
5. I. Ramzan, I. P. Parkin, C. J. Carmalt. (2026) *Advanced Science*, e76476.

The role of casting skin and section thickness in zinc coating formation on cast iron with added Ni

K. Bracka-Kęsek [1,*], J. Marosz [1], M. Górny [1], B. Cygan [2]
[1] Faculty of Foundry Engineering, AGH University of Krakow, Kraków, POLAND
[2] Teksid Iron Poland Sp. z o.o., Skoczów, POLAND

Abstract:
High-quality cast iron is a material widely utilized across numerous industrial sectors due to its unique combination of properties, coupled with relatively low production costs. However, owing to its high susceptibility to corrosion, it is imperative to develop solutions aimed at eliminating this phenomenon or mitigating its impact on material degradation. Zinc coating (galvanizing) constitutes an effective method for addressing this issue in iron-carbon alloys. Nevertheless, the hot-dip galvanizing of cast iron remains a scientifically and practically complex challenge, primarily due to the phase structure heterogeneity of the substrate and the presence of numerous alloying elements. While commercial technological solutions for steel aim to reduce zinc coating thickness through bath additives—predominantly nickel (Ni)—this objective is significantly more challenging for cast iron substrates. This difficulty stems chiefly from the substantial silicon (Si) content in the matrix, which complicates the control of diffusion mechanisms between the liquid zinc bath and the substrate. This study investigates the effect of nickel (Ni) alloying within the cast iron substrate on the formation of the zinc coating, taking into account varying section thicknesses. Furthermore, the differences in coating development between machined and as-cast surfaces are elucidated, highlighting the critical roles played by nodular graphite precipitates and the presence of the casting skin.

Keywords: Hot-Dip Galvanizing, zinc coatings, cast iron, zinc coatings on the cast iron, thin-wall cast iron,

References:

1. Tang N.-Y., (2008) Control of silicion reactivity in general galvanizing, *Journal of Phase Equilibria and Diffusion*, vol. 29, 337-344
2. Bracka-Kęsek, K.Z., Szczęsny, A., Kopyciński, D., Guzik, E. (2023) Evaluation of the Phases Present in the Zinc Coating Obtained on the Ductile Cast Iron Substrate in the Bath with the Addition of Ti*, Archives of Foundry Engineering*, 4, vol. 23
3. Chen, W., Wu, C., Ya, L., Wang, J., Su, X. (2024) Effect of Pre-oxidation Condition on the Microstructure of a Hot-Dip Galvanized Coating on Nodular Cast Iron, *Journal of Materials Engineering and Performance,* vol. 33, 4502-4509
4. N. Pistofidis, G. Vourlias, S. Konidaris, El. Pavlidou, G. Stergioudis, (2007) The combined effect of nickel and bismuth on the structure of hot-dip zinc coatings, *Materials Letters*, vol. 61, Issue 10, 2007-2010

Acknowlegment
This research received European funding no. 101159771 — Project NetCastPL4.0.

Cyclic Behavior of Hybrid SMA-Steel Rings as Smart Dampers and the Effect of Diametric Difference on Interface Interference

Eunsoo Choi[1,*], Seongjun Park[1], Min-Kyung Jang[1]
[1] Department of Civil and Environmental Engineering, Hongik University, Seoul, South Korea

Abstract:
This study investigated the cyclic behavior of hybrid rings as smart dampers composed of a superelastic NiTi shape memory alloy (SMA) ring and stainless steel rings under unidirectional pulling and pushing actions. Five specimens were tested: a pure SMA ring (#0, 80 mm outer diameter, 8 mm thickness) as reference, and four hybrid rings with steel rings placed inside (#1, 2.0 mm), on both sides (#2, 1.0 mm each), outside (#3, 0.6 mm), and on both sides (#4, 0.4 mm each), with diametric differences (δD) of 0.002 mm (#1, #2) or 0.02 mm (#3, #4). The pure SMA ring exhibited stable flag-shaped hysteresis with 96% self-centering capacity up to 12% diametric deformation. The hybrid rings followed nearly identical loading paths to the pure SMA ring, but their unloading paths diverged significantly due to frictional interference at the SMA–steel interface, enhancing energy dissipation while reducing self-centering capacity to below 60% at 12.8 mm displacement. For equal total steel-ring thickness, hysteretic response was independent of ring position. Notably, specimen #3 (0.6 mm, δD = 0.02 mm) produced similar hysteretic behavior to specimen #1 (2.0 mm, δD = 0.002 mm) despite its thickness being approximately one-third that of specimen #1, confirming that diametric difference governs interface interference more decisively than thickness (Figure 1). Local strain analysis revealed that dual steel-ring configurations (#2, #4) preserved the strain pattern of the pure SMA ring, whereas single steel-ring configurations (#1, #3) transformed the lateral response into a pure bending-dominated behavior. These findings demonstrate that the diametric difference, rather than steel-ring thickness or position, is the critical design parameter for tuning the balance between recentering capacity and energy dissipation in hybrid SMA–steel ring smart dampers.

Keywords: shape memory alloy, hybrid rings, interface interference, diametric difference, self-centering, energy dissipation

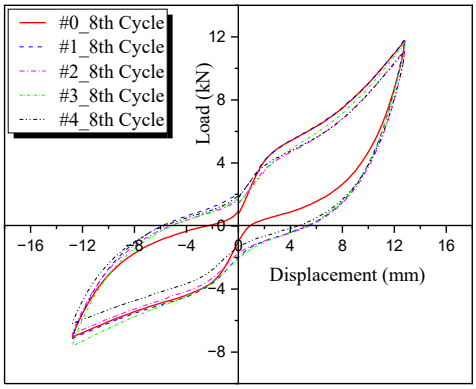


Figure 1: Cyclic force–displacement hysteresis curves of the pure SMA ring and hybrid rings in the 8th loading cycle. Although specimen #1 has a steel-ring thickness (2.0 mm) more than three times that of specimen #3 (0.6 mm), both rings exhibit similar unloading paths and hysteretic areas owing to the tenfold larger diametric difference of #3 (δD = 0.02 mm vs. 0.002 mm), demonstrating that the diametric difference governs the degree of interface interference more decisively than steel-ring thickness.

References:

1. Fang, C. (2022). SMAs for infrastructures in seismic zones: a critical review of latest trends and future needs, *Journal of Building Engineering*, 57: 104918.
2. Gao, N., Jeon, J.-S., Hodgson, D.E. and DesRoches, R. (2016). An innovative seismic bracing system based on a superelastic shape memory alloy ring, *Smart Materials and Structures*, 25: 055030.
3. Choi, E., Nhan, B.T. and Ostadrahimi, A. (2023). On the performance of a smart hybrid damper consisting of shape memory alloy and steel rings, *Engineering Structures*, 291: 116382.

Surface Coating Engineering to Enhance Safety of High-Energy Lithium-Ion Batteries

N. L. Wu*, S, J. Chang
Department of Chemical Engineering, National Taiwan University, Taipei, Taiwan

Abstract:
Ni-rich $Li(Ni,Co,Mn)O_2$ (NCM)-graphite (NCM‖Gr) lithium-ion batteries (LIBs) offer high capacity and energy density but suffer from significant safety issues associated with thermal runaway. Herein, we demonstrate a polymer-based surface-coating strategy for the graphite anode by constructing a protective interphase designed to reduce the severity of thermal runaway. A nanometer-scale (~2 nm) cation selective membrane is employed as an artificial solid electrolyte interphase (A-SEI), leveraging its high lithium-ion conductivity, together with enhanced thermal robustness and low oxygen permeability. In addition to improving the various electrochemical performances of the batteries, calorimetry analyses reveal that the coating significantly reduces heat release associated with reactions involving lithiated graphite and oxygen released during $LiNi_{0.83}Co_{0.12}Mn_{0.05}O_2$ (NCM83) decomposition or present in the environment. Large-scale safety validation using 1 Ah NCM83‖Gr batteries further shows that the surface modified batteries exhibit no ignition during nail-penetration tests, in contrast to the violent combustion observed in cells with bare graphite anodes. We propose a surface-shielding effect of the coating to mitigate oxygen-assisted exothermic reactions at the anode interface, thereby reducing the progression toward catastrophic thermal runaway. This straightforward and scalable polymer surface-shielding strategy provides a practical pathway toward safer, high-energy-density LIBs.

Keywords: Lithium-ion battery, Anodes, Polymer coating, Thermal runaway, Safety.

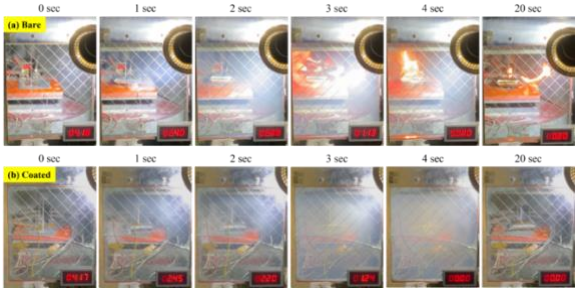


Figure 1: Photographs of 1 Ah(NCM‖Gr lithium-ion batteries during nail penetration tests. (a) Battery with a bare Gr anode, showing severe blazing; (b) Battery with a coated Gr anode, showing no blazing.

References:

Chang, S. J., Wu, N. L. , *et al*., (2026) Polymer Surface Shielding of Graphite Anodes for Mitigating Thermal Runaway in High-Energy Lithium-Ion Batteries, *J. Energy Storage* 180, 124258.

Integrating Safe and Sustainable by Design into the Development of Bio-Based Functional Textile Coatings: The SSbD4CheM Textile Case Study

P.Tovillas
NOVEX, Arnedo, Spain

Abstract:
The transition towards safer and more sustainable chemicals and materials requires moving beyond the assessment of environmental and safety impacts at the end of the development process. Instead, Safe and Sustainable by Design (SSbD) principles should be integrated from the early stages of material selection and formulation, allowing technical performance, safety and sustainability evidence to jointly guide material development. Within the Horizon Europe SSbD4CheM project, the textile case study addresses this challenge through the development of PFAS-free and metal-free functional coatings for apparel textiles using atmospheric pressure plasma (APP). The objective is to replace conventional fluorinated water-repellent treatments and metal-based antimicrobial finishes with alternative coatings derived from renewable organic precursors while maintaining the functional performance required for textile applications. Target functionalities include water repellency, self-cleaning behaviour and antimicrobial activity on polyester-based substrates. A range of bio-based precursors has been investigated for hydrophobic and antimicrobial functionality, while plasma deposition parameters have been systematically adjusted to control coating formation and performance. Atmospheric plasma provides a particularly relevant processing route within an SSbD context, as it enables dry and solvent-free surface functionalization, requires limited amounts of chemicals and produces very thin functional layers without conventional wet-finishing and thermal-curing steps. Importantly, material development within SSbD4CheM is not performed as an isolated optimization of technical performance. Experimental characterization, physicochemical information, hazard assessment, exposure and risk evaluation, environmental fate considerations and life-cycle-based sustainability assessment are progressively integrated into the development process. Evidence generated across these different assessment dimensions provides feedback for precursor selection, formulation refinement and processing decisions. At the same time, coating performance is evaluated through water contact angle measurements, self-cleaning tests, antimicrobial assays and preliminary durability studies, ensuring that improvements in safety and sustainability do not compromise the required functionality. This contribution will present the textile case study as a practical example of evidence-based SSbD implementation, highlighting the interaction between functional material development and the different safety and sustainability assessment methodologies used within SSbD4CheM. Preliminary results demonstrate the potential of plasma-assisted bio-based coatings to provide highly water-repellent, self-cleaning and antimicrobial textile surfaces, while offering a route towards the substitution of conventional PFAS- and metal-based treatments. The case study illustrates both the opportunities and the practical challenges associated with integrating SSbD criteria into an iterative materials-development workflow and provides insights into how multidisciplinary evidence can support decision-making towards safer, more sustainable and technically competitive textile coatings.

Keywords: Safe and Sustainable by Design; SSbD; atmospheric pressure plasma; textile coatings; bio-based coatings; PFAS-free; antimicrobial textiles; sustainability assessment.

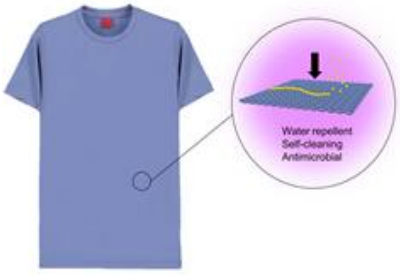


Figure 1: Schematic representation of a functional textile coating providing water-repellent, self-cleaning and antimicrobial properties for apparel applications.

Origami-Inspired Foldable Textile Structures for Programmable Shape Morphing

Danchen Zhang [1*],Cindy Harnett [2], Joana Schulte [3] Cedric Heyen [1] Thomas Gries [1]
[1] Institut für Textiltechnik, RWTH Aachen University, Aachen, Germany
[2] Department of Electrical and Computer Engineering, University of Louisville, Louisville, United States
[3] Digital Additive Production Chair, RWTH Aachen University, Aachen, Germany

Abstract:
Origami-inspired structures provide a promising approach for the development of adaptive materials and smart surfaces due to their ability to undergo large and programmable shape transformations while remaining lightweight and compliant. Combined with textile substrates and additive manufacturing technologies, these concepts enable the realization of foldable textile systems with integrated functionalities.
This work presents the development of origami-inspired textile structures manufactured by fused deposition modeling (FDM) directly onto elastic textile substrates. Shape transformation is achieved through the interaction between the printed reinforcement patterns and the textile material. Three established origami geometries, Miura-Ori, Kresling, and Waterbomb, as well as a bioinspired folding structure derived from the Miura-Ori principle, were investigated with regard to their folding behavior and mechanical response. [1]
Particular attention was given to the influence of manufacturing strategy on structural performance. Two fabrication approaches were compared: single-sided printing and double-sided sandwich printing. The resulting structures were evaluated in terms of foldability, geometric accuracy, hinge formation, interfacial stability, and cyclic performance.
To characterize and validate the folding kinematics, magnetic angle sensing elements were integrated into selected crease regions. The sensing system enables continuous measurement of angular displacement during structural deformation without the need for external optical tracking. Sensor signals were correlated with the folding motion of the structures to assess repeatability and geometry-dependent deformation characteristics.
The results demonstrate the potential of additive manufacturing on textile substrates for the realization of lightweight and programmable folding structures. Furthermore, the combination of origami-based design and integrated magnetic sensing enables quantitative monitoring of structural motion and provides a foundation for future adaptive textile systems with embedded feedback and control capabilities.

Keywords: Adaptive Surfaces, Origami-Inspired Structures,Programmable Structures, Additive Manufacturing, Embedded Sensing

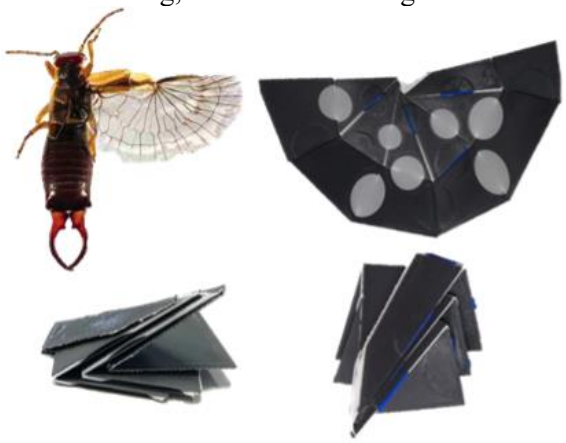


Figure 1: Biological wing-folding mechanism of Dermaptera[1] and its translation into a bioinspired origami textile structure fabricated by 3D printing on textile substrates for compact and programmable folding.

References:

1. Faber, J.A., Arrieta, A.F., Studart, A.R. (2018) Bioinspired spring origami, Science, 359(6382), pp. 1386-1391.

Water Drops Sliding Over Arrays of Janus Micropillars With Hydrophilic Tops: A New Mechanism of Drop Charging

F.Darvish[1,2,*], M.Isaacs[3,4], S.Shumaly[1,2], L. Delance[1,2], H.·Butt[1,2]
[1] Max Planck Institute for Polymer Research (MPI-P), Mainz, Germany
[2] Institute for Condensed Matter Physics, Technische Universität Darmstadt, Darmstadt, Germany
[3]HarwellXPS, Research Complex at Harwell, Rutherford Appleton Lab, Didcot, United Kingdom
[4]Department of Chemistry, University College London, London, United Kingdom

Abstract:
When water drops slide over a flat hydrophobic solid surface, negative charges are spontaneously deposited at the rear ofthe drop, and the drops gain a positive charge. This phenomenon is known as slide electrification. Here, we demonstrate analternative mechanism of spontaneous charge separation in sliding drops. Therefore, arrays of Janus micropillars were fabricatedby photolithography. Each micropillar has a hydrophilic top created by reactive ion etching (RIE) and aminopropyltriethoxysilane(APTES) deposition, while the walls and substrate were hydrophobized by 1H,1H,2H,2H-perfluorooctyltrichlorosilane (PFOTS).Drops on these arrays show high apparent contact angles, remain in the Cassie state, and still contact the hydrophilic top faces.Sliding drops acquire charge, with polarity and magnitude governed by top-surface chemistry, including NH3+/NH4+ formationand PFOTS removal after the RIE plasma exposure, and dense NH 2 groups formation from thermally activated APTES vapordeposition. Unlike flat surfaces, high-speed reflection microscopy reveals tiny satellite droplets left on each pillar that evaporatewithin one second. Consequently, charge separation occurs within the liquid phase between the primary drop and depositedsatellites, rather than directly at the contact line

Keywords: arrays of picoliter-sized droplets, drop charge deposition, Janus micropillar, photolithography, APTES and PFOTS vapor deposition, RIE plasma–surface interactions, XPS imaging

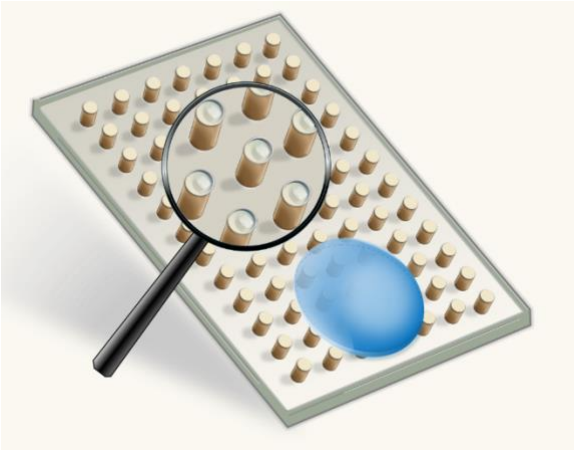


Figure 1: Schematic of a sliding water droplet on fabricated arrays of Janus micropillars—superhydrophobic micropillars with hydrophilic tops fabricated over a large area (7 × 2.5 cm; pillar diameter: 30 μm). On a homogeneous, smooth, hydrophilic surface, the drop would spread; in contrast, it forms a high apparent contact angle on a surface patterned with Janus micropillars.

References:

1. Darvish, F., Isaacs, M., Shumaly, S., Delance, L., Butt, H.-J. (2026), Water Drops Sliding Over Arrays of Janus Micropillars With Hydrophilic Tops: A New Mechanism of Drop Charging, *Small*, 22, e11728.
2. Darvish, F., Shumaly, S., Li, X., Dong, Y., Diaz, D., Khani, M., Vollmer, D., Butt, H.-J. (2024), Control of spontaneous charging of sliding water drops by plasma-surface treatment, *Scientific Reports*, 14, 10640.

Sensors 2026 / EGF 2026- Session I. B: Graphene and 2D Materials / Sensor Materials

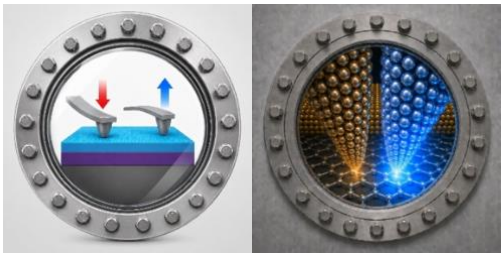
Clean Interfaces in van der Waals Materials: From Adhesion to Transparent Point Contacts

Abstract

Interfaces determine both the mechanical stability and the electrical performance of van der Waals materials, but their intrinsic response is often obscured by adsorbates, water layers and uncontrolled contact conditions. In this talk, I will discuss two examples in which atomic force microscopy under clean-interface conditions provides quantitative access to these interfacial properties. First, I will show how calibrated AFM adhesion measurements in ultra-high vacuum, combined with in situ thermal cleaning and frequency-modulation AFM cross-checks, allow clean-interface Hamaker constants to be extracted for representative layered materials, including few-layer graphene and MoS_2 on SiO_2. These measurements yield benchmark dispersive interaction values and show that even very dry ambient conditions can already enhance adhesion, while higher humidity produces a reversible capillary contribution that helps explain the broad dispersion of reported adhesion values [1].

I will then turn to electrical point contacts on graphite, where self-referenced conductive AFM in ultra-high vacuum is used to separate the response of the metal/graphite junction from changes in the probe. Under these conditions, Pt/graphite contacts reach an unusually high-conductance regime, whereas Au-based/graphite contacts remain around two orders of magnitude less conductive, despite clear mechanical contact and despite forming good metallic contacts on the reference electrode. Load-dependent measurements and first-principles calculations show that the contrast cannot be explained by contact area alone, but reflects metal-dependent electronic coupling at the clean interface [2].

Together, these results show that clean-interface AFM can do more than characterize surfaces: it can isolate the intrinsic mechanical and electronic ingredients that control nanoscale contacts in van der Waals materials. This provides experimentally grounded parameters for adhesion modelling, contact engineering and the interpretation of local transport measurements in low-dimensional materials.



References

1. Gallego-Fuente et al., Hamaker Constants of van der Waals Materials under Clean-Interface Conditions. Adv. Sci. 0:e76609 (2026)
2. Gallego-Fuente et al., Transparent Point Contacts on Graphite. Submitted.

From Process Integration to Functional Graphene Photonic Devices

M. Lukosius[1,*], P. K. Dubey[1], A. I. Raju[1], R. Lukose[1], D. Capista[1], Ch. Wenger [1,2]
[1] IHP– Leibniz-Institut für innovative Mikroelektronik, Im Technologiepark 25, 15236 Frankfurt (Oder), Germany
[2]BTU- Brandenburg Technical University, Platz der Deutschen Einheit 1, 03046 Cottbus, Germany.
[*]lukosius@ihp-microelectronics.com

Abstract:
Graphene is considered as a prominsing material for next-generation photonic devices [1,2]. This study provides a comprehensive investigation into the design, integration and performance of graphene photonic devices that have been integrated with SiN waveguides, which were fabricated on a 200 mm pilot line. Devices employ dual single-layer graphene integrated onto passive SiN waveguides with dielectric gating. This enables the electrical control of the graphene Fermi level and the subsequent modulation of optical absorption via Pauli blocking.
Several key processing steps were identified as critical to achieving reliable device performance when integrating graphene-based components within a 200 mm CMOS-compatible Si platform, including graphene growth, passivation, and electrical contacting. The electrical properties of the graphene devices, particularly sheet and contact resistance, were characterised initially. Electro-optical measurements revealed a a modulation depth of 18.6 dB over 0 to 10 V and, 3 dB bandwidth of 15 GHz for a dual-layer graphene modulator. This confirms the potential of graphene-based photonic devices for use in high-speed optical communication applications.

Keywords: Graphene, CVD, Photonics, Pilot line, modulators

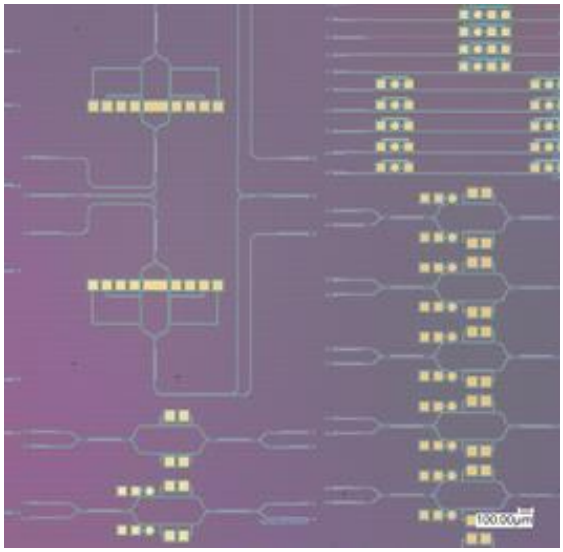


Figure 1: Figure illustrating the fabricated graphene PICs on Si_3N_4 waveguides on 200 mm wafers.

References:

1. M. Tiberi, A. Montanaro, C. Wen, J. Zhang, O. Balci, S. M. Shinde, S. Sharma, A. Meersha, H. Shekhar, J. E. Muench, B. R. Conran, K. B. K. Teo, M. Ebert, X. Yan, Y. Tran, M. Banakar, C. Littlejohns, G. T. Reed, M. Romagnoli, A. Ruocco, V. Sorianello, A. C. Ferrari, Graphene Electro-Absorption Modulators for Energy-Efficient and High-Speed Optical Transceivers https://arxiv.org/abs/2506.03281
2. T. Reep, K. De Bruyn*, C. Wu, J. Jans, J. Van Kerrebrouck, Y. Huang, Y. Guo, D. Yudistira, S. Brems, I. Asselberghs, *2D Mater*. 13, (2026) 025012.

Acknowledgment:
This project has received funding from the European Union's Horizon Europe research and innovation programme under grant agreement No 101120938 (GATEPOST) and under grant agreement 101189797 (2D-PL).

EMI shielding by horizontally- aligned MWCNTs polymer nanocomposites

R. Checchetto [1,2,*], G. Fredi [2,3,4], Brian L. Wardle[4,5]
[1] Department of Physics, University of Trento, Trento, Italy
[2] TIPFA-INFN, Trento, Italy
[3] Department of Industrial Engineering and INSTM research unit, University of Trento, Trento, Italy
[4] Department of Aeronautics and Astronautics, Massachusetts Institute of Technology, Massachusetts, USA
[5] Department of Mechanical Engineering, Massachusetts Institute of Technology, Massachusetts, USA

Abstract:
Microelectronic circuits contain devices such as switches and oscillators, which emit electromagnetic radiation whose intensity can be large enough to cause malfunctioning of nearby electronic systems. The development of innovative materials with enhanced electromagnetic interference (EMI) shielding properties is thus crucial for modern microelectronic devices [1]. Lightweight and high-performance polymer nanocomposites containing carbon- based nanostructures are candidate materials for EMI shielding because they offer the potential to overcome the limitations of commercially used metallic plates, such as high mass density, low flexibility, weak corrosion resistance and difficult integration in miniaturized electronic components [2]. We fabricated laminate composites consisting of 4.6 wt. % horizontally aligned Multiwalled Carbon Nanotubes (MWCNTs) dispersed in a Phase Changing Material (PCM) organic matrix (hex-CNT) and studied their EMI shielding properties in the 8 to 12.4 GHz frequency interval (X-band). Structural analyses show that 250 μm thick 2-ply hex-CNT laminates formed by two stacked laminae of horizontally- aligned MWCNTs with infused hexacosane have microvoid-free structure with the aligned MWCNTs homogeneously distributed forming a 3D network for electron transport having electronic conductivity of 240 S/m. The EMI shielding effectiveness (SE) of the hex-CNT laminate increases from 20 dB for a 2-ply laminate to 40 ÷ 45 dB for a sample formed by three 2-ply laminates with radiation absorption as shielding mechanism. The average specific shielding effectiveness of 0.07 ± 0.01 dB/μm is among the highest reported so far for polymer/CNT nanocomposites when the CNT content is lower than 40 wt. %. The non-infused dry-CNT laminate has thickness ~ 50 μm, exhibit larger electronic conductivity ~ 10^3 S/m and improved shielding effectiveness: SE increases from ~ 40 dB for a 2-ply laminate preform to ~ 50 dB for a 4-ply laminate preform being radiation absorption the dominating shielding mechanism.

Keywords: MWCNT-Polymer Nanocomposites, EMI Shielding, X-band r.f. Frequency, Horizontally Aligned MWCNT Networks.

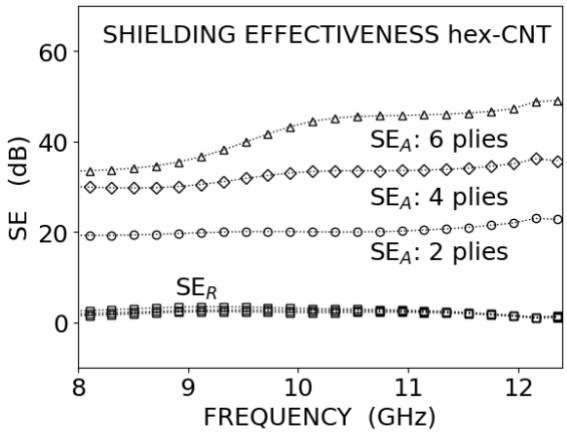


Figure 1: Absorption (SE_A) and reflection (SE_R) shielding effectiveness of hex-CNT nanocomposite samples in the X-band: circles (○), diamonds (◇) and triangles (△) are the SE_A values of the 2-, 4- and 6-plies hex-CNT samples while overlapping squares are their SE_R values.

References:

1. M. S. Hareesh, J. Praveen and G. Sumesh (2025), Electromagnetic interference shileding: a comprehensive review of materials, mechanisms and applications, *Nanoscale Adv.*, 7, 5410-4534.
2. H. Liu, S. Wu, C. You, N. Tian, Y. Li and N. Chopra (2021), Recent progress in morphological engineering of carbon materials for electromagnetic interference shielding, *Carbon* 172, 569-596.

Influence of Directly Deposited Hexagonal Boron Nitride Interlayers on the Interface Properties and Photoresponse of Graphene/Si Heterostructures

Š. Meškinis [1*], A. Vasiliauskas [1], A. Guobienė [1], Š. Jankauskas [1], V. Stankus [1], M. Andrulevičius [1], R. Gudaitis [1]

[1] Institute of Materials Science, Kaunas University of Technology, Kaunas, Lithuania

Abstract:

2D nanomaterials such as graphene and hexagonal boron nitride (h-BN) offer significant advantages for microelectronics, optoelectronics, and various sensor applications. However, both graphene and h-BN are typically fabricated by exfoliation or by transferring the 2D nanolayers grown by chemical vapor deposition (CVD) on catalytic metal foils to target substrates. These technologies are not well suited for standard semiconductor fabrication processes. Notably, exfoliation is not suitable for large-area deposition. In contrast, the transfer process is lengthy and prone to contamination by various adsorbates. Therefore, direct synthesis of these nanomaterials on semiconducting and dielectric substrates would be highly beneficial. In the present research, h-BN films were deposited by reactive high-power impulse magnetron sputtering (HIPIMS) on Si(100). Graphene layers were synthesized directly on silicon, SiO_2, and h-BN substrates via microwave plasma-enhanced CVD. The structure of the 2D nanomaterials was evaluated using Raman spectroscopy, and their morphology was studied using atomic force microscopy (AFM). The composition of the h-BN films was estimated using X-ray photoelectron spectroscopy (XPS). The electrical and optoelectronic properties of graphene/Si and graphene/h-BN/Si heterostructure-based devices were investigated. The insertion of the h-BN interlayer resulted in a significant increase in photocurrent, short-circuit current (I_{SC}), and open-circuit voltage (V_{OC}) compared to the graphene/Si(100) heterojunction. The average ISC and photocurrent nearly doubled, and the average IR-light-excited V_{OC} increased by ~100 mV. Thus, HIPIMS-deposited h-BN interlayers can be used to modify graphene/Si interface properties by reducing graphene self-doping, thereby enhancing photoelectric response and indicating their potential for transfer-free graphene-based optoelectronic structures.

Keywords: graphene, h-BN, direct synthesis, microwave PECVD, HIPIMS, Raman, XPS, AFM, photoelectric properties

Overview of Core-Shell Nanowires with 2D Layered Shell

Boris Polyakov*, Edgards Butanovs, Alexey Kuzmin, Luize Dipane, Sergei Piskunov
Institute of Solid State Physics, University of Latvia, Latvia

Abstract:
Core−shell nanowires (NWs) are modern types of radially heterostructured nanomaterials intensively explored during the last decades. The core−shell approach has several important advantages as compared to conventional two-dimensional (2D) Transition Metal Dichalcogeni-des (TMD) material production technologies: it allows one, for example, to combine materials with lattice mismatch and even to initiate epitaxial growth of shell material on the core tem-plate. As a result, it is possible to significantly modify electrical, mechanical, and optical prop-erties of NWs by proper combination of core and shell materials.

In this work, we synthesized of WS_2, MoS_2, ReS_2, WSe_2, $MoSe_2$, $NbSe_2$, $TaSe_2$ and other layered shells using ZnO, ZnS, GaN or ZnSe nanowires as a core using either one or two-step approach [1-6]. Pulsed laser deposition used as a single step method to deposit MoS_2 and WS_2 around GaN nanowire core [1]. In case of a two-step methods the first step is deposition of a thin safricial layer of TMD precursor (WO_3, MoO_3, ReO_x, Nb, Ta), with following heating in sulfur or selenium atmosphere to initiate chemical reaction in quartz tube [1-4, 6] or sealed quartz ampoule [5] at the second step.

Synthesized core-shell nanowires were characterized by SEM and TEM microscopy, XRD diffraction, XPS and Raman spectroscopies.

Selected core-shell nanostructures were tested as single nanowire photodetectors [2], demonstrating the potential of combining 2D TMDs materials with semiconducting nanowires for optoelectronic applications.

Keywords: core–shell nanowires, transition metal dichalcogenides (TMDs), heterostructures, nanowire arrays; photodetectors, optoelectronic applications.

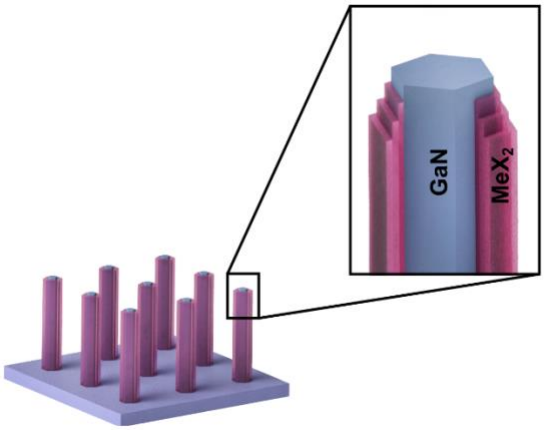


Figure 1: Figure illustrating the schematics of core-shell with single crystal nanwire core and layered TMDs shell.

References:

1. Butanovs E, Kuzmin A, Zolotarjovs A, Vlassov S, Polyakov S. J. Alloys & Compounds. 2022: 918: 165648. DOI: 10.1016/j.jallcom.2022.165648.
2. Butanovs E, Vlassov S, Kuzmin A, Piskunov S, Butikova J, Polyakov B. ACS Appl. Mater. Interfaces. 2018: 10: 13869−13876. DOI: 10.1021/acsami.8b02241.
3. Polyakov B, Kuzmin A, Smits K, Zideluns J, Butanovs E, Butikova J, Vlassov S, Piskunov S, F. Zhukovskii YF. J. Phys. Chem. C. 2016; 120:21451−21459. DOI: 10.1021/acs.jpcc.6b06139.
4. Butanovs E, Kuzmin A, Butikova J, Vlassov S, Polyakov B. J Cryst. Growth. 2017; 459:100–104. DOI: 10.1016/j.jcrysgro.2016.11.106.
5. B.Polyakov , K. Kadiwala, E. Butanovs , L. Dipane, A.Trausa, D. Bocharov, S. Vlassov, ChemEngineering 2024, 8, 25, DOI:10.3390/chemengineering8010025
6. L.Dipane, L.Kotlara , V.Vibornijs , K.Laganovska, A.Zolotarjovs, E.Dipans, J.Gabrusenoks, B.Polyakov, E.Butanovs, Optical Materials 2025: 167, 117360, DOI: 10.1016/j.optmat.2025.117360

Intelligent Actuator(-Sensor) Systems based on Shape Memory Alloys and Dielectric Elastomers

P. Motzki [1,2,*]
[1] Department of Systems Engineering, Department of Material Science and Engineering, Saarland University, Saarbruecken, Germany
[2] CiMS – Center for intelligent Material Systems, SEI – Saarland Engineering Institute, Saarbruecken, Germany

Abstract:
Shape memory alloys enable the realization of compact and light-weight drive systems. Their specific work, namely the ratio of the material's weight or volume in contrast to the work performed, is the highest amongst all actuation technologies [1]. The presented work focuses on using commercially available SMA-wires to design and develop smart actuation systems and use the SMA's "self-sensing" capabilities as a basis for actuator control and condition monitoring [2].
Applications of industrial systems [3], like energy-efficient gripping- and handling systems or end-effectors [4], [5], [6], [7] are being transferred to commercial products and bio-inspired robotic systems like humanoid fingers and hands [8] and soft trunk- or tentacle-inspired continuum robots [9], [10] showcase the generation of embodied or physical AI.
Research focus in the field of SMA actuation has been the realization of increased actuation speeds and actuator efficiencies [11], [12] and the use of data-based approaches for modeling the complex coupling of thermo-mechanical and electrical material behavior [13].
In the field of smart polymers, focus is on silicone-based dielectric elastomer actuators (DEA) and sensors (DE sensors) and their use in soft robotic structures [14] and in higher frequency ranges like switching valves, fluidic pumps [15] and haptic, tactile or acoustic actuation elements integrated into textile structures [16], [17]. To allow efficient operation even at high frequencies, two possible approaches are considered: First, physical vapor deposition (PVD) of metallic nanometer thin films, e.g. nickel or gold, directly to the dielectric PDMS film. Second, application of free-standing laser-structured auxetic micrometer thin films of superelastic Nickel-Titanium to the dielectric PDMS film in a separate assembly step.

Keywords: shape memory alloys, dielectric elastomers, electroactive polymers, SMA, DEA, EAP, artificial muscles, actuator, sensor



Figure 1: From left to right: SMA inspection endoscope robot, SMA humanoid hand, EAP sensing glove, EAP tactile wristband

References:

1. P. Motzki, A. Bucht, K. Pagel, T. Mäder, and S. Seelecke, "Thermische Formgedächtnislegierungen," in Smart Materials - Eigenschaften und Einsatzpotenziale, 1st ed., H. Böse, Ed., Würzburg: Vogel Communications Group, 2023, ch. 4, pp. 89–118. [Online]. Available: https://vogel-fachbuch.de/detail/index/sArticle/1086
2. P. Motzki, "Advanced Design and Control Concepts for Actuators Based on Shape Memory Alloy Wires," Dissertation, Saarland University, 2018. doi: 10.22028/D291-27354.
3. P. Motzki and S. Seelecke, "Industrial Applications for Shape Memory Alloys," in Encyclopedia of Smart Materials, A.-G. Olabi, Ed., Elsevier, 2022, ch. Volume 4, pp. 254–266. doi: 10.1016/B978-0-12-803581-8.11723-0.

4. P. Motzki, F. Khelfa, L. Zimmer, M. Schmidt, and S. Seelecke, “Design and Validation of a Reconfigurable Robotic End-effector Based on Shape Memory Alloys,” IEEE/ASME Transactions on Mechatronics, vol. 24, no. 1, pp. 293–303, 2019, doi: 10.1109/TMECH.2019.2891348.
5. S.-M. Kirsch, F. Welsch, M. Schmidt, P. Motzki, and S. Seelecke, “Bistable SMA Vacuum Suction Cup,” in ACTUATOR 2018 - 16th International Conference and Exhibition on New Actuators and Drive Systems, Conference Proceedings, Bremen, Germany, 2018, pp. 384–387.
6. P. Motzki and S. Seelecke, “BISTABLE ACTUATOR DEVICE HAVING A SHAPE MEMORY ELEMENT,” WO 2017/194591 A1, 2016 [Online]. Available: https://depatisnet.dpma.de/DepatisNet/depatisnet?action=bibdat&docid=WO002017194591A1
7. P. Motzki, B. Holz, F. Simone, and S. Seelecke, “Formgedächtnislegierungen in Applikationen der Greif- und Handhabungstechnologie - Shape Memory Alloys in Applications of Gripping- and Material-Handling-Technology,” in Fachtagung Mechatronik 2015, Dortmund, Germany: VDI/VDE, 2015, pp. 55–60. doi: http://dx.doi.org/10.17877/DE290R-7388.
8. F. Simone, G. Rizzello, S. Seelecke, and P. Motzki, “A Soft Five-Fingered Hand Actuated by Shape Memory Alloy Wires : Design , Manufacturing , and Evaluation,” Front. Robot. AI, vol. 7, no. 608841, 2020, doi: 10.3389/frobt.2020.608841.
9. Y. Goergen, G. Rizzello, and P. Motzki, “Systematic Methodology for an Optimized Design of Shape Memory Alloy-Driven Continuum Robots,” Adv. Eng. Mater., vol. 26, no. 2, p. 2301502, 2024.
10. M. A. Mandolino, Y. Goergen, P. Motzki, and G. Rizzello, “Design and Characterization of a Fully Integrated Continuum Robot Actuated by Shape Memory Alloy Wires,” in 2022 IEEE 17th International Conference on Advanced Motion Control (AMC), 2022, pp. 6–11. doi: 10.1109/AMC51637.2022.9729267.
11. P. Motzki, T. Gorges, M. Kappel, M. Schmidt, G. Rizzello, and S. Seelecke, “High-Speed and High-Efficiency Shape Memory Alloy Actuation,” Smart Mater. Struct., vol. 27, no. 7, p. 075047, Jun. 2018, doi: 10.1088/1361-665X/aac9e1.
12. R. Barakat, S.-M. Kirsch, F. Welsch, and P. Motzki, “Bidirectional rotational antagonistic shape memory alloy actuators for high-frequency artificial muscles,” Sci. Rep., vol. 15, no. 1, p. 9108, 2025, doi: 10.1038/s41598-025-93209-9.
13. K. Koshiya, G. Rizzello, and P. Motzki, “A Neural Network-Based Self-Sensing Embedded Position Control System for Shape Memory Alloy Wire Actuators,” Advanced Intelligent Systems, Jan. 2026, doi: 10.1002/aisy.202501204.
14. D. Herrmann et al., “A mobile tensegrity robot driven by rolled dielectric elastomer actuators,” 2025 IEEE 8th International Conference on Soft Robotics, RoboSoft 2025, 2025, doi: 10.1109/ROBOSOFT63089.2025.11020974.
15. M. Baltes, B. Holz, D. Bruch, and P. Motzki, “Electronic Control System for Optimized Resonance Operation of Dielectric Elastomer Pumps through Self-Sensing,” Adv. Eng. Mater., 2025, doi: 10.1002/adem.202501204.
16. “US12526582B2 - Audio-tactile transducer device based on dielectric electro-active elastomers - Google Patents.” Accessed: Mar. 05, 2026. [Online]. Available: https://patents.google.com/patent/US12526582B2/en
17. S. Gratz-Kelly, D. Philippi, B. Fasolt, S. Nalbach, and P. Motzki, “Gesture and force sensing based on dielectric elastomers for intelligent gloves in the digital production,” Tm-Technisches Messen, vol. 91, no. 3–4, pp. 195–207, 2024.

Wearable Sensors and Flexible Electrodes from Laser-Induced Graphene and MXene

M. Spasenović [1*], T. Vićentić [1], A. Gavran [1], K. Tošić [1], V. Vojnović [1], I. [1]Rašljić-Rafajilović [1], and M.V. Pergal [1]

[1] Center for Microelectronic Technologies, Institute of Chemistry, Technology and Metallurgy, University of Belgrade, Serbia

Abstract:

Wearable devices are a novel technology impacting application domains such as healthcare, sports, and industrial wellbeing. The success of the technology relies on development and implementation of biocompatible, stretchable, flexible material substrates that can be integrated with active components, such as piezoresistors. Nanomaterials integrated into polymer substrates are commonly employed as a solution in this domain (1).

Laser-induced graphene – LIG (2) and MXene are among the materials that are being explored as active, conductive elements for wearable and other flexible devices. LIG is a highly adaptable platform for applications such as physiological sensing, electrode fabrication, gas detection, and biosensing. Traditionally, research has centered on commercial polyimide (PI) tape as the substrate for LIG production. While commercial PI enables the formation of LIG with favorable electronic properties, its poor adhesion, fixed chemical structure, and lack of stretchability pose challenges for applications. To overcome these constraints, we introduce a novel strategy: laser induction of graphene on biocompatible, synthesized cross-linked polymers. These include sodium alginate, PDMS/PEG composites, cross-linked polyurethanes (PUs) derived from ethoxypropyl-terminated PDMS macrodiol, and custom-synthesized polyimides. These materials exhibit desirable mechanical properties, non-cytotoxicity, and biocompatibility, making them promising candidates for versatile sensor platforms, including in wearable technology. We systematically identifiy optimal chemical formulations and laser processing conditions for generating LIG on these substrates for different applications, such as heartbeat monitoring and tracking limb bending. We explore MXene ($Ti_3C_2T_x$) as an alternative active layer for these devices. We use optical, mechanical, biological, and chemical techniques to characterize the different materials. We demonstrate the real-world utility of LIG and MXene-based devices for monitoring vital signs (Figure 1) as well as for electrodes for electrochemistry. These findings lay the groundwork for next-generation, biocompatible, unobtrusive, and cost-effective thin-film sensors for various tailored applications.

This research was supported by the Science Fund of the Republic of Serbia, #4950, Polymer/graphene heterostructures for physiological sensors – Polygraph.

Keywords: graphene, MXene, sensors, polymers, heartbeat, limb motion.

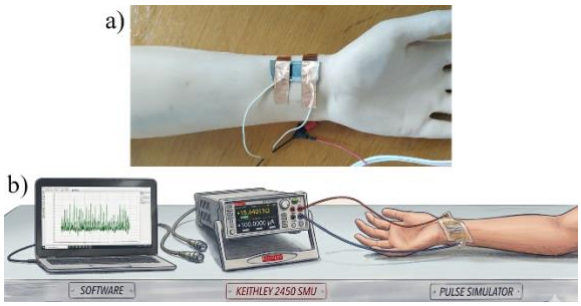


Figure 1: Example use of LIG sensor as heartbeat monitor. (a) Photograph of LIG device attached to the forearm of a pulse simulator. (b) Sketch of measurement setup for acquiring heartbeat data from simulator or human subject.

References:

1. Rodgers, M. M., Pai, V. M., and Conroy, R. S. (2015) Recent Advances in Wearable Sensors for Health Monitoring, *IEEE Sensors Journal*, 15, 3119-3126.
2. Lin, J. et al. (2014) Laser-induced porous graphene films from commercial polymers, *Nature Comm*., 5, 1-5.

Development of printed temperature sensors based on antenna patterns

J. Escobar [1*], F. Bourhim [1], Y. Cervantes [2] , C. Laporte [2]
[1] Material departement, IRT Saint Exupery, Toulouse, France
[2] Orbital vehicles , CNES, Toulouse, France

Abstract:

In the space sector, structural health monitoring is becoming increasingly critical with the rapid growth of satellite constellations and the development of reusable launch vehicles. However, conventional sensing systems often suffer from limited durability under harsh space environments and contribute additional mass, leading to increased launch costs.

With the support of CNES, IRT Saint Exupéry has developed inkjet-printed antenna-based sensors aimed at enabling lightweight, durable, and easily integrable temperature monitoring solutions. These sensors are designed to be directly printed onto complex 3D components without the need for adhesives or wired connections, making them particularly suitable for aerospace applications.

The sensing principle relies on the temperature dependence of antenna material properties, which induces a shift in the resonance frequency. By tracking this frequency, temperature can be accurately determined. Patch antennas were selected due to their ease of fabrication, low cost, compatibility with complex geometries, and strong sensitivity to environmental variations [1]. Silver-based conductive inks were used to fabricate the antenna patterns via inkjet printing (Figure 1).

A key aspect of this work is the influence of the dielectric substrate on sensor performance. Dielectric permittivity was characterized using dielectric spectroscopy over a temperature range of 20 to 150 °C. Antenna performance was then evaluated using a Vector Network Analyzer (VNA) across a wider range from −70 to 150 °C.

The results highlight the critical role of dielectric properties—particularly permittivity and its temperature dependence—in governing the antenna resonance behavior. Appropriate dielectric materials were identified to enhance sensitivity and stability. VNA measurements demonstrated clear and repeatable resonance frequency shifts with temperature, confirming the feasibility of the approach.

These promising results validate the potential of silver-printed antenna sensors combined with tailored dielectric substrates for robust, lightweight, and high-performance temperature sensing in extreme aerospace environments.

Keywords: Printed electronics, Patch antennas, Thermal sensors, Dielectric permittivity, Vector Network Analyzer, space applications.

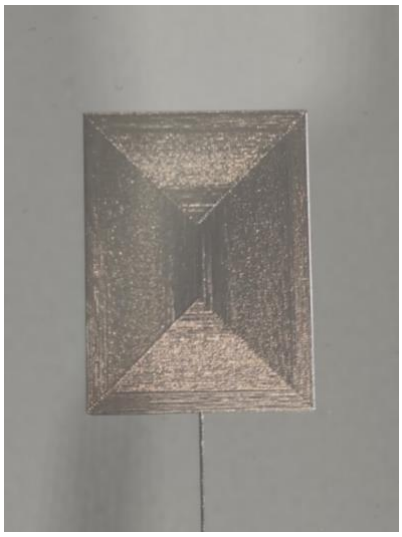


Figure 1: Printed antenna based sensor on aluminium substrate

References:

1. Bhim C. Garg *et al.* Microstrip Antenna Design Handbook. Artech House, 2001.

Flexible Screen-Printed Gold Electrode Arrays as Platforms for Hybrid-Nanomaterial-Enhanced Electrochemical Sensing

Norica Godja[1,2,*], Saied Assadollahi[2], Melanie Hütter[2], Pooyan Mehrabi[2], Narges Khajehmeymandi[2], Thomas Schalkhammer[2] and Florentina-Daniela Munteanu [1,3]
[1] Interdisciplinary School of Doctoral Studies, "Aurel Vlaicu" University of Arad, Romania
[2] Attophotonics Biosciences GmbH, Wiener Neustad, Austria
[3] Faculty of Food Engineering, Tourism and Environmental Protection, "Aurel Vlaicu" University of Arad, Romania

Abstract:
The increasing demand for rapid, portable and multiplexed analytical platforms has driven the development of advanced electrochemical sensors integrating flexible electronics with functional nanomaterials. Hybrid nanomaterials, combining metals, polymers, carbon-based materials and functional nanostructures, enhance sensor sensitivity, selectivity and stability, enabling applications in environmental monitoring, industrial process control and healthcare.
This work presents a flexible screen-printed gold electrode array comprising sixteen individually addressable working electrodes fabricated on polyimide (PI) and polyethylene terephthalate (PET) substrates. The electrodes were produced by scalable screen-printing followed by electroless gold deposition and optional electrochemical gold enhancement, providing excellent electrical conductivity, mechanical flexibility and compatibility with further surface functionalisation. As a proof-of-concept application, the electrochemical behaviour of Ni(II) was investigated in both aqueous sodium sulphite and choline chloride–ethylene glycol deep eutectic solvent (DES) electrolytes. The developed platform demonstrated reliable and reproducible electrochemical responses over concentration ranges relevant to industrial nickel-containing process baths, while achieving micromolar detection capability in DES media. The small electrolyte volume required (100–200 µL) enables low reagent consumption and supports the analysis of minute sample volumes.
Beyond nickel detection, the sixteen-electrode architecture offers significant potential for multiplexed sensing through the selective functionalisation of individual electrodes with hybrid nanomaterials, including metallic nanoparticles, carbon nanomaterials, conductive polymers and biomolecular recognition layers. Such an approach enables the simultaneous detection of multiple analytes within a single device while improving analytical performance and expanding application areas.
The presented platform demonstrates the potential of combining flexible screen-printed electronics with hybrid nanomaterials for the development of next-generation electrochemical sensors suitable for environmental monitoring, industrial process control, food safety and biomedical diagnostics.

Keywords: hybrid nanomaterials; screen-printed gold electrodes; flexible sensors; electrochemical sensing; multiplexed sensing; nickel detection; deep eutectic solvents; environmental monitoring.

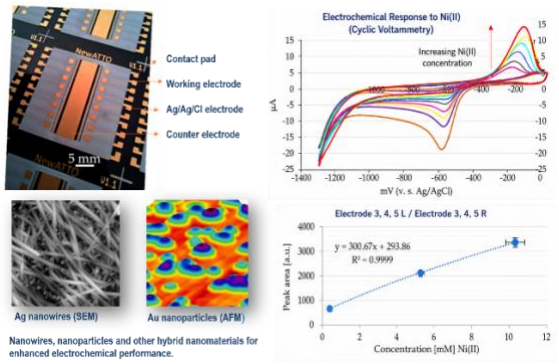


Figure 1: Illustration of a flexible screen-printed gold electrode array for next-generation electrochemical sensing, including the sensor platform, representative cyclic voltammetry responses, the calibration curve for Ni(II) detection, and examples of nanomaterials for potential electrode functionalisation.

References:

1. Godja, N.-C.; Munteanu, F.-D. Hybrid Nanomaterials: A Brief Overview of Versatile Solutions for Sensor Technology in Healthcare and Environmental Applications. Biosensors 2024, 14, 67. https://doi.org/10.3390/bios14020067.
2. Godja, N.-C.; Munteanu, F.-D. Environmentally Friendly Solutions as Potential Alternatives to Chromium-Based Anodization and Chromate Sealing for Aeronautic Applications. Coatings 2025, 15, 439. https://doi.org/10.3390/coatings15040439.

Eco-friendly electrospun PEDOT-based nonwovens for wearable touch sensors

E. A. Slejko [1], G. Carraro [1], D. Cavallo [2], R. Spotorno [2], C. Gambardella [3], V. Piazza [3], M. Pantano [4], M. Smerieri [1, *]

[1] IMEM-CNR, Institute of Materials for Electronics and Magnetism – National Research Council of Italy, Via Dodecaneso 33, 16146 Genova, Italy
[2] Department of Chemistry, University of Genoa, Via Dodecaneso 31, 16146 Genova, Italy
[3] IAS-CNR, Institute for the Study of the Anthropic Impact and Sustainability in the Marine Environment, National Research Council, Via de Marini 16, 16149 Genova, Italy
[4] Department of Civil, Environmental and Mechanical Engineering, University of Trento, Via Mesiano 77, 38123 Trento, Italy

Abstract:
Wearable electronics demand conductive materials that combine flexibility, breathability, mechanical robustness, and environmental sustainability. In this contribution, we present conductive nonwovens developed by electrospinning aqueous blends of poly(3,4-ethylenedioxythiophene):polystyrene sulfonate (PEDOT:PSS) and polyethylene oxide (PEO).
Systematic optimization of solution composition and process parameters yields continuous nanofibers with a controlled diameter (~200 nm). A subsequent thermal treatment under vacuum induces crosslinking between PEO and PSS (via sulfonate-ester bonds) while removing residual unreacted PEO, markedly improving both electrical conductivity and water stability while preserving the nonwoven morphology. Comprehensive electrical, mechanical, and electrochemical characterization demonstrates that the thermally treated mats retain sufficient conductivity and mechanical integrity for soft-sensor applications.
Ecotoxicological assays on representative freshwater and marine organisms (bacteria, algae, and crustaceans) confirm the environmental compatibility of the materials, addressing a critical gap in the assessment of conductive polymers intended for wearable devices.
As a proof of concept, the optimized nonwovens are integrated into a sensorized glove prototype capable of detecting touch and pressure events relevant to rehabilitation monitoring. The results illustrate a multidisciplinary route that links advances in electrospun conductive nanomaterials with practical wearable sensing and responsible material design.

Keywords: electrospinning, nanofibers, thermal treatment, conductive nonwovens, PEDOT:PSS, eco-friendly materials, wearable sensors, flexible electronics, touch sensors, rehabilitation devices

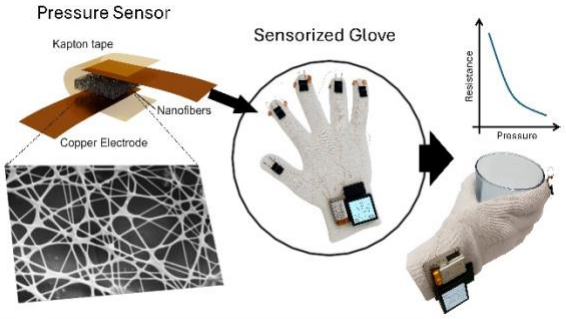


Figure 1: Eco-friendly free-standing conductive PEDOT:PSS/PEO nonwovens prepared by electrospinning, thermally treated to enhance conductivity, and evaluated for electrical, mechanical, and electrochemical performance, aquatic ecotoxicity (freshwater and marine organisms), and application as flexible touch sensors in a wearable rehabilitation glove prototype.

References:

1. Slejko, E.A. et al., Eco-Friendly Free-Standing Conductive PEDOT-based Nonwovens for Wearable and Flexible Touch Sensors, *Adv. Fiber Mater.* 8, 1444–1465 (2026). DOI: 10.1007/s42765-026-00681-7
2. E. A. Slejko, G. Carraro, D. Cavallo, R. Spotorno, and M. Smerieri, "Advanced preparation and characterization of PEDOT-based nonwoven materials for wearable electronics", *Nanocon*, 4992, 278 (2024)
3. E. A. Slejko, G. Carraro, X. Huang, and M. Smerieri, "Advances in the Fabrication, Properties, and Applications of Electrospun PEDOT-Based Conductive Nanofibers", *Polymers*, v. 16, n. 17, p. 2514, 2024, DOI: 10.3390/polym16172514

Design, Electrochemical Characterization, and Analytical Applications of Innovative Bi-Band Microelectrodes

K. Jedlińska*, B. Baś
[1] Department of Analytical Chemistry and Biochemistry, AGH University of Krakow, Krakow, Poland

Abstract:
Band microelectrodes, defined as voltammetric sensors with a working electrode thickness of less than 25 µm and a length spanning several millimeters, uniquely combine the advantages of both micro- and macro-electrodes. While their dimensions and generated current levels resemble those of macro-sensors, they exhibit prominent microelectrode effects, notably the independence of the peak response current from the electrolysis time [1]. Consequently, these sensors ensure exceptional signal repeatability and reproducibility, enabling precise measurements even in highly resistive media. Furthermore, they effectively eliminate the practical constraints typical for conventional microelectrodes, such as the need for Faraday cages, battery-powered amplifiers, or complex signal processing algorithms.

This work introduces the design and fabrication methodology of an original bi-band microelectrode configuration developed by our research group [2,3]. The sensor structure comprises two symmetrically opposed microbands with a thickness of 25 µm and a length of 4.0 mm, positioned along the lateral cylindrical surface of a support body and insulated with a thin layer of epoxy resin (Figure 1). A key feature of this design is its material versatility, allowing for the utilization of various conductive foils and wire substrates tailored to specific analytical needs. The electrochemical behavior of the novel sensor was comprehensively evaluated using a model redox system. Furthermore, versatile voltammetric procedures were established for the determination of both inorganic ions and organic bioactive compounds in synthetic and real matrices, demonstrating the sensor's high sensitivity and broad analytical utility [2,3].

Keywords: bi-band microelectrode, voltammetry, electrochemical sensor, sensor fabrication, microelectrode effect, electroanalysis

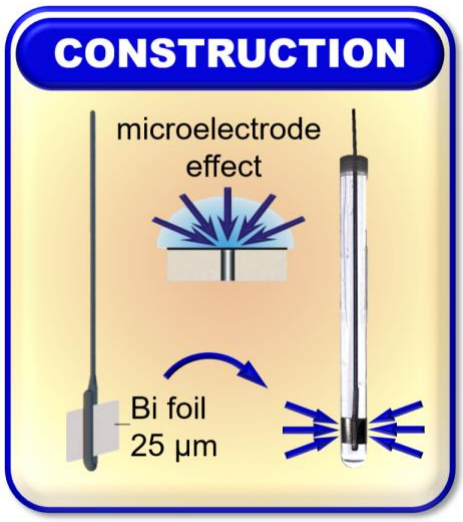


Figure 1: Schematic illustration of the bi-band microelectrode construction and operating principle. From left to right: the inner conductive core assembly showcasing the attachment of the 25 µm metal foil; a conceptual diagram of the microelectrode effect featuring convergent, non-planar mass transport; and a photographic view of the final assembled sensor with arrows indicating the multi-directional diffusion lines toward the symmetrically opposed microbands.

Acknowledgements: Research project supported by program "Excellence Initiative-Research University" for the AGH University of Science and Technology.

References:

1. Li, D., Batchelor-McAuley, C., Chen, L., Compton, R.G. (2019), Nano- and Microbands: High-Speed Electrochemistry, ACS Sensors, 4, 2250–2266.
2. Jedlińska, K., Porada, R., Lipińska, J., Baś, B. (2020), The bi-band silver microelectrode: Fabrication, characterization and analytical study, Sensors and Actuators B: Chemical, 302, 127152.
3. Jedlińska, K., Porada, R., Strus, M., Baś, B. (2022), The bi-band bismuth microelectrode: design, properties and application, Electrochemistry Communications, 134, 107189.

Development of a novel voltammetric sensor based on MWCNT-juglone paste electrode for high sensitive melatonin measurement in pharmaceutical formulations and dietary supplements

Joanna Smajdor-Baran
AGH University of Krakow, Faculty of Materials Science and Ceramics, Krakow, Poland

Abstract:
Melatonin, commonly called the sleep hormone, plays a critical role in the regulation of circadian rhythms of organisms. It is the first-line drug in cases of sleep disorder or to reduce the effects of jet lag. Not only is it responsible for regulating circadian rhythms, but also it expresses major effects on the immune system and acts as an anti-inflammatory and antioxidant agent.
This study presents a novel voltammetric sensor based on a carbon paste electrode modified with functionalised multi-walled carbon nanotubes and juglone for high sensitive determination of melatonin in pharmaceutical formulation and dietary supplements. The aim of the work was to improve the metrological properties and obtain new functionality. In recent years, carbon nanomaterials have gained much attention in this field and found application in various areas, especially in electrochemical sensors. Juglone, used as a paste electrode modifier for the first time, represents a promising candidate for electrode construction. The presence of the naphthoquinone core facilitates rapid electron transfer, which is essential to achieve high sensitivity. Juglone also lowers the overpotential of the oxidation or reduction of analytes, which results in an enhancement of the signal-to-noise ratio. The synergistic effect of the high surface area of MWCNTs and the electrocatalytic properties of juglone significantly improve the sensitivity and selectivity of melatonin detection. The developed sensor offers a wide melatonin linear range (0.002 – 0.22 mg L^{-1}) and a detection limit as low as 2.67 nM (0.62 µg L^{-1}). When hazardous solvents typically used in traditional analysis are replaced with a simple electrochemical setup, the proposed method supports the idea of green and sustainable chemistry and reduces the chemical footprint of clinical laboratories.

Keywords: voltammetry, paste electroche, quinone, MWCNT, juglone, melatonin, biomedical applications.

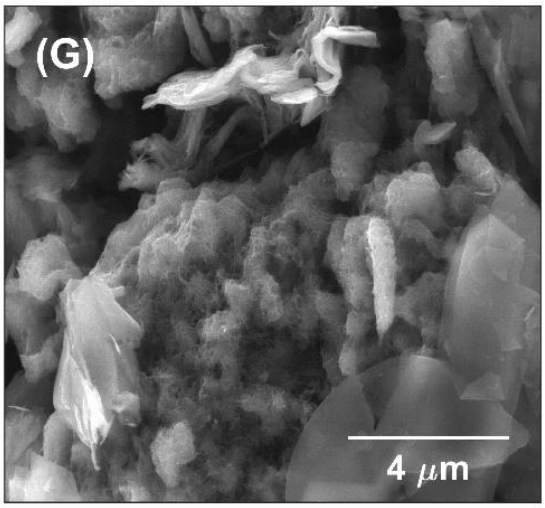


Figure 1: SEM image of JUG-MWCNT-graphite composite mixture.

Funding:
Research project supported by the National Science Centre, Poland (Project No. 2025/09/X/ST4/00422) and by program "Excellence Inititiative-Research University" for the AGH University of Science and Technology.

Effect of Plasma Treatment on Laccase-Based Electrochemical Biointerfaces

S. Baluta [1*], W. Tylus [1], P. Jamróz [1], M. Czok [2], K. Malecha [2], J. Cabaj[1]
[1] Faculty of Chemistry, Wroclaw University of Science and Technology, Wroclaw, Poland
[2] Faculty of Electronics, Photonics and Microsystems, Wroclaw University of Science and Technology, Wroclaw, Poland

Abstract:

The functionality of an electrochemical biointerface depends not only on the amount of immobilized biomolecule but also on the physicochemical environment created at the electrode surface [1,2]. In this work, atmospheric-pressure plasma was used to tailor the surface properties of LTCC-integrated gold electrodes prior to laccase immobilization, providing a simple model for investigating the relationship between surface chemistry, enzyme loading and electrochemical functionality [3,4]. Gold electrodes were treated with plasma for 5, 7.5 and 10 min, followed by laccase immobilization. Surface morphology and chemical composition were investigated using scanning electron microscopy and X-ray photoelectron spectroscopy, while the resulting biointerfaces were evaluated electrochemically using dopamine as a model analyte. Plasma treatment preserved the granular morphology of the gold electrodes while progressively modifying their surface chemistry. XPS analysis after laccase immobilization revealed increasing nitrogen content with increasing plasma treatment time, indicating higher enzyme surface coverage. However, the highest enzyme loading did not correspond to the highest analytical response. The electrode treated for 7.5 min exhibited the most favorable performance, with a linear response from 0.01 to 200 µM, a sensitivity of 2.03 µA μM^{-1} cm^{-2} and a detection limit of 13.8 nM. Prolonged plasma treatment increased enzyme coverage but resulted in a slight decrease in electrochemical response. These findings demonstrate that enzyme loading alone cannot explain biointerface functionality and highlight the importance of surface physicochemistry in determining the functional state of immobilized biomolecules. The presented approach provides a simple strategy for studying and rationally engineering electrochemical biointerfaces.

Keywords: plasma surface modification, electrochemical biointerface, laccase, surface physicochemistry, LTCC, dopamine biosensing

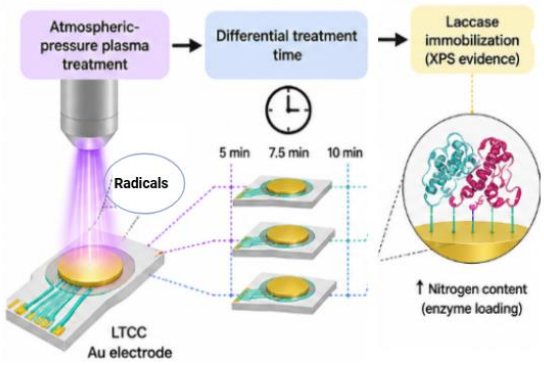


Figure 1: Schematic representation of the experimental approach: atmospheric-pressure plasma treatment of LTCC-integrated gold electrodes for different exposure times, followed by laccase immobilization. Increasing nitrogen content determined by XPS indicates increasing enzyme loading on the plasma-treated electrode surface.

References:

1. Novak, L. M., et al. *Surface property effects in the immobilization of L-lactate oxidase on gold electrodes by self-assembled monolayers.* **Journal of Biotechnology** 413 (2026), 33–41. DOI: 10.1016/j.jbiotec.2026.02.011.
2. Klis, M., et al. *Electroreduction of laccase covalently bound to organothiol monolayers on gold electrodes.* **Electrochimica Acta** 52 (2007), 5591–5598. DOI: 10.1016/j.electacta.2007.02.008
3. Casero E., et al. *Laccase biosensors based on different enzyme immobilization strategies for phenolic compounds determination.* **Talanta** 115 (2013), 401–408. DOI: 10.1016/j.talanta.2013.05.045.
4. Prządka, M. P., et al. *Impact of plasma treatment of Au electrodes on response of EIS biosensors used in aquaculture pathogen detection.* **Surfaces and Interfaces** 54 (2024), 105168. DOI: 10.1016/j.surfin.2024.105168.

SMS 2026 / NanoMed 2026
Session I. C:
Bio-Medical Materials & Living Surfaces/ Bio-Nanofabrication & Engineering

ENGINEERING THE NANO-BIO INTERFACE – From understanding to measuring and controlling biological function.

Pilar Rivera Gil
Integrative Materials and Nanomedicine Lab,
Medicine and Life Science Department,
Universitat Pompeu Fabra
Barcelona, Spain

Abstract:
This talk explores how engineering the nano-bio interface can transform nanomaterials from passive carriers into tools for understanding, measuring, and controlling biological function. It will highlight how cellular uptake, local environment, and spatial distribution shape nanomaterial behavior, and how these interactions can be exploited for quantitative intracellular sensing, molecular targeting, and photothermal therapy.



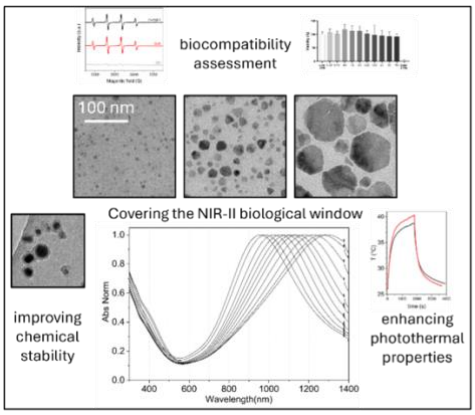
Particular emphasis will be placed on SERS-based nanosensors for pH, H_2O_2, and zinc, linking intracellular chemistry to cancer-related phenotypes. The talk concludes by discussing how these insights could support more predictive design rules for nanomedicine.

Rational Design of Stable and Biocompatible CuS Plasmonic Nanocrystals with Tunable NIR-II Photo-responsive Properties for Biomedical Applications

F. Barbero[1*], S. Shanmugam[1], D. Maccarrone[1], G. Perrone[2], K. Mareschi[3], I. Kokalari[4], A.M. Ferretti[5], I. Fenoglio[1]

[1] Dept. of Chemistry, University of Torino, Italy
[2] Dept. of Electronics and Telecommunications, Politecnico di Torino, Italy
[3] Dept. of Public Health and Pediatric Sciences, University of Torino & R. Margherita Children's Hospital, Italy
[4] Dept. of Biosciences and Engineering, Western Balkans University, Albania
[5] Istituto di Scienze e Tecnologie Chimiche - CNR, Milano, Italy

Abstract:
Covellite (CuS) nanoparticles (NP) are promising materials for biomedical applications due to their localized surface plasmon resonance (LSPR) in the near-infrared (NIR) region. They have been investigated for photothermal therapy, photoacoustic imaging, antimicrobial applications, and SERS sensing[1]. The potential tunability of the CuS plasmonic response across the NIR region is particularly valuable, especially for achieving materials active in the NIR-II biological window (1000–1350 nm), which offers lower scattering, reduced autofluorescence, and deeper tissue penetration compared to NIR-I. Moreover, CuS NPs with different LSPR positions could enable wavelength-selective photothermal activation and multimodal imaging. However, the controlled synthesis of CuS NPs in aqueous media, desirable for greener processing and essential for biomedical applications, remains a significant challenge, as water-based methods typically yield small particles with broad and poorly tunable LSPR absorption mainly in the NIR-I region. We report the development of aqueous synthetic strategies enabling precise modulation of the plasmonic response of CuS NPs across the NIR-II region through control of NP size and phase purity. These results provide deeper knowledge into the synthetic mechanisms and the interplay between CuS NP structural features and their plasmonic properties. In addition, the photothermal conversion efficiency of the obtained CuS NPs was evaluated under NIR irradiation, highlighting the impact of crystal phase purity on light-to-heat conversion. An important limitation hindering the biomedical application of CuS NPs is their poor stability in aqueous environments. To address this issue and improves their applicability, we successfully developed two surface-engineering strategies: the synthesis of CuS@C core–shell nanocomposites[2]; and the functionalization of the CuS surface with thiol-terminated molecules, both strategies enhanced aqueous stability, and lead to superior photothermal performance. Importantly, neither strategy completely suppresses NP degradation, a desirable feature for medical applications that may facilitate body clearance and minimize long-term accumulation, in contrast to widely studied but persistent Au NPs. Following a safety-by-design approach, the developed materials were evaluated for their redox activity by EPR spectroscopy, as well as for in vitro cytotoxicity and hematocompatibility, overall showing good biocompatibility. These findings provide valuable insights into the rational design of CuS NPs, paving the way for their development as biocompatible, stable, and tunable NIR-II plasmonic nanomaterials for advanced biomedical applications.



Keywords: CuS NP, plasmonic NP, photothermal therapy, nanosafety, biocompatibility

References:

1. Y. Liu (2019) *Mol. Pharmaceutics*, *16*(8), 3322-3332
2. S. Shanmugam (2025) *Materials Today Chemistry*, 46, 102765

Adsorption and desorption of bioactive organic molecules in the confined interlayer space of clay minerals for potential drug delivery systems. Experimental and molecular modeling approaches.

C.I. Sainz-Díaz [1,2,*], A. Hernández-Laguna[1], S. Kanwal[1], C. Viseras-Iborra[2,3], A. Borrego-Sánchez[4]
[1] Instituto Andaluz de Ciencias de la Tierra (IACT_CSIC), Av. de las Palmeras, 4, 18100-Armila, Granada, Spain
[2] Raw Materials, Human and Environmental Health, UGR, Associated Unit of the CSIC by the IACT-CSIC, Av. de Las Palmeras 4, 18100, Armilla, Granada, Spain.
[3] Departament of Pharmacy and Pharmaceutical Tecnologhy, University of Granada, Campus de Cartuja s/n 18071, Granada

Abstract:
Adsorption onto natural minerals with confined structures offers a promising approach to protect the bioactive compounds while enabling controlled release. Clay minerals based on Aluminium and Magnesium silicates with lamellar structures, named phyllosilicates, such as, montmorillonite (MNT), provide these confined interlayer space at nanometric scale. In this work, the adsorption of pharmaceutical drugs and essential oils molecules on MNT has been investigated using Fourier Transform Infrared Spectroscopy (FTIR), and X-ray diffraction (XRD) along with molecular modelling approaches. Complementary between experimental and theoretical calculations results will be presented for several surfactants and pharmaceutical drugs in clays. Different theoretical methodologies with force fields based on empirical interatomic potentials and quantum mechanics methods based on Density Functional Theory (DFT) level calculations along with Molecular Dynamics simulations have been used to study the adsorption of organic molecules on models of crystal surfaces of silicates. The results show that the direct adsorption in the intercalation of these organic molecules into the confined interlayer space of MNT was energetically favourable (Figure 1). The adsorption process on the external surface of MNT was also energetically favorable. Molecular dynamics simulations reveal that the diffusion of these molecules within the confined interlayer region is significantly slower than that of water in the same environment enhancing the stability of the drug-MNT materials. Desorption was energetically favourable, particularly for intercalation complexes. A good agreement is observed between theoretical and experimental results: The powder XRD patterns of the adsorption complexes showed a clear shift of the (001) reflection in the clay minerals used confirming the intercalation of the organic molecules into the interlayer space of clay minerals. These properties make phyllosilicates suitable for their use as nanocarriers for controlled release of pharmaceutical drugs.

Keywords: montmorillonite, quantum mechanics, drug release, molecular dynamics

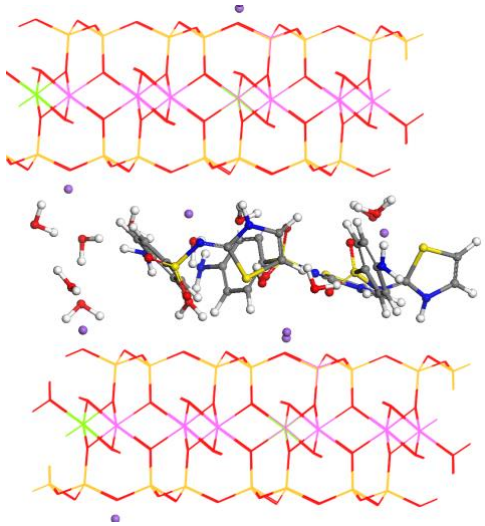


Figure 1: Optimized crystal structure of montmorillonite with sulfathiazole intercalated into the interlayer space of the clay mineral.

References:

1. Moreno-Domínguez, E., Borrego-Sánchez, A., Sánchez-Espejo, R., Viseras, C., Sainz-Díaz C.I. (2023) Experimental and Computational Study for the Design of Sulfathiazole Dosage Form with Clay Mineral. *Pharmaceutics* 15, 575.
2. Kanwal, S., Valarezzo, N., López Galindo, A., Hernández-Laguna, A., García-Villén, F., Viseras-Iborra, C., Sainz-Díaz, C.I. (2026) Adsorption of volatile anti-inflammatory essential oils on phyllosilicate surfaces. Towards montmorillonite-based natural topical drug delivery. *Applied Surface Science*, 744, 167391.

Advanced Synthetic Polymer-Based Blockers: A Superior Pathogen-Free Alternative to BSA for IVD Surface Coating

L. Kostka[1], V. Šubr[1], M. Tůmová[2], P. Dráber[2], J. Plicka[3], T. Etrych [1]
[1] Department of Biomedical Polymers, Institute of Macromolecular Chemistry CAS, Prague, Czechia
[2] Institute of Molecular Genetics CAS, Prague, Czechia
[3] Sophomer Ltd., Prague, Czechia

Abstract:
In vitro diagnostic (IVD) assays are often compromised by non-specific binding (NSB), which increases background noise and reduces sensitivity. Although Bovine Serum Albumin (BSA) remains the industry standard for blocking, it exhibits significant batch-to-batch variability, potential RNase contamination, and risks of animal-derived pathogens—issues that are particularly detrimental to nucleic acid-based diagnostics. We present a solution by developing a versatile library of fully synthetic protein mimetics, based on biocompatible N-(2-hydroxypropyl)methacrylamide (HPMA) or poly(2-oxazoline) (POx). Using RAFT and free radical polymerization (FRP), we engineered these polymers with diverse architectures and hydrophobic anchors, such as dodecyl and aminocyclooctane groups, to enable robust adsorption.

This study highlights new materials designed for high-performance coating of polystyrene (PS) or polypropylene (PP) based surfaces commonly used in IVD platforms. Beyond traditional immunoassays, we addressed the critical challenge of blocking PP surfaces against the non-specific sorption of oligonucleotide aptamers. Unwanted aptamer adsorption to PP walls drastically depletes the available probe concentration, compromising highly sensitive downstream applications. We demonstrate that our synthetic polymers efficiently coat PP surfaces, thoroughly preventing aptamer loss. When these blocked PP substrates were utilized in aptamer-based affinity assays coupled with a highly sensitive Polymerase Chain Reaction (PCR) detection endpoint, we observed a profound reduction in background amplification and significantly improved signal-to-noise ratios.

Furthermore, characterization of human thyroid-stimulating hormone (hTSH) via sandwich ELISA showed that these synthetic blockers provide superior surface coverage compared to BSA. In hTSH assays, the designed polymers fully replaced BSA, achieving comparable or superior calibration responses at 10 to 100-fold lower concentrations. Notably, polymers prepared via FRP with broader dispersity provided enhanced surface "healing" on polystyrene substrates, effectively suppressing NSB while maintaining excellent reproducibility.

These fully synthetic, RNase-free, and pathogen-free macromolecules represent a paradigm shift in IVD surface coating. By outperforming animal proteins at lower concentrations and enabling highly sensitive PCR-based aptamer diagnostics, they offer a scalable, standardized, and safe solution for next-generation diagnostic platforms.**Keywords**: HPMA, non-specific interactions, surface coating, in vitro clinical diagnostics, bovine serum albumin, ELISA, PCR.

Acknowledgment:
Financial support from The Technology Agency of the Czech Republic (project No. FW11020013) is greatly appreciated.

References:

1. V. Subr, L. Kostka, J. Plicka, O. Sedlacek, T. Etrych, Highly Effective Synthetic Polymer-Based Blockers of Non-Specific Interactions in Immunochemical Analyses, Polymers, 16 (2024) 758.
2. www.sophomer.com

HPMA Copolymer–Gemcitabine Conjugates: Impact of Drug Release Kinetics on Antitumor Efficacy

Robert Pola[a,#,*], Kateřina Běhalová[b,c,#], Natálie Adamcová[b], Martin Ivančík[b], Milada Šírová[b], Irfan B. Kilic[b], Petra Procházková[b], Petr Kašpárek[a], Alžběta Bulková[a], Pavol Lukac[b], Luca Vannucci[b], Blanka Říhová[b], Marek Kovář[b] and Tomáš Etrych[a]

[a] Institute of Macromolecular Chemistry of the Czech Academy of Sciences, Heyrovského nám. 1888, Prague 6 - Břevnov 16200, Czech Republic.

[b] Institute of Microbiology of the Czech Academy of Sciences, Vídeňská 1083, Prague 4 - Krč 14220, Czech Republic.

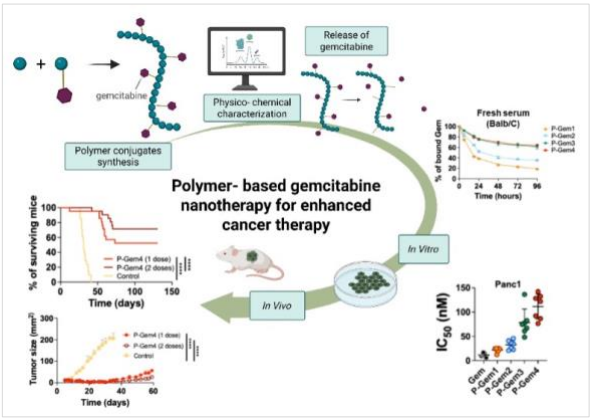
[c] Faculty of Science, Charles University, Viničná 7, Prague 2 - 128 44, Czech Republic.

* pola@imc.cas.cz

Abstract:

Gemcitabine (Gem) is an effective anticancer drug limited by rapid enzymatic degradation, short plasma half-life, and systemic toxicity. We developed N-(2-hydroxypropyl)methacrylamide (HPMA) copolymer–Gem conjugates with different linker structures and release kinetics and evaluated four nanomedicines for pharmacokinetics, antitumor efficacy, and immunomodulatory activity. The optimized conjugates prolonged circulation and enhanced tumor accumulation compared with free Gem. Their cytostatic and pro-apoptotic activity strongly depended on Gem release rate. The slowest-releasing conjugate extended systemic exposure to 96 h versus 2 h for free Gem and showed superior efficacy in several tumor models, including tumor growth inhibition, prolonged survival, complete long-term remissions, and reduced pulmonary metastases. Mechanistic studies revealed sustained pro-apoptotic signaling, transcriptional reprogramming, and modulation of the tumor immune microenvironment. Thus, Gem release kinetics is a critical determinant of HPMA copolymer–Gem nanomedicine performance and a promising route to overcome limitations of conventional Gem therapy.

Keywords: HPMA copolymer, gemcitabine, nanomedicine, drug release, antitumor efficacy, immunomodulation.



Scheme 1. Design, characterization, and biological evaluation of polymer–Gem conjugates for improved anticancer therapy. Created with BioRender.com.

Acknowledgements:

This work was supported by the Technology Agency of the Czech Republic under the National Centres of Competence Program, Project No. TN02000122 (REcombinant TEchnologies for MEDicine – RETEMED).

Tribocorrosion Behaviour of Ti6Al7Nb Orthopaedic Alloy: Comparison Between New and Clinically Retrieved Femoral Stem Surfaces

M. Jenko[1*], B. Kocjančič [2,3], T. Kosec [4], Š. Tadel Kocjančič[5], M. Debeljak [1,6]

1 MD-RI Institute for Materials Research in Medicine, Ljubljana, Slovenia
2 University of Ljubljana, Faculty of Medicine, Ljubljana, Slovenia
3 Department of Orthopaedic Surgery, University Medical Centre Ljubljana, Ljubljana, Slovenia
4 Slovenian National Building and Civil Engineering Institute, Ljubljana, Slovenia
5 University Rehabilitation Institute Republic of Slovenia, Ljubljana, Slovenia
* Corresponding author: Monika Jenko (monica.jenko@gmail.com)

Abstract:
Titanium alloys are widely used in cementless orthopaedic implants due to their favourable mechanical properties, corrosion resistance and biocompatibility. However, their long term clinical performance may be affected by the combined action of mechanical wear and electrochemical degradation in the physiological environment. Tribocorrosion is therefore an important mechanism contributing to surface degradation, particle release, osteolysis and aseptic loosening.

The aim of this study was to evaluate the tribological and tribocorrosion behaviour of Ti6Al7Nb orthopaedic alloy by comparing a new, unused femoral stem sample with a clinically retrieved sample revised due to aseptic loosening. Samples were prepared from femoral stems while preserving the original implant surface. Tribocorrosion tests were performed using a reciprocating tribometer with an Al_2O_3 ball as a counter body in Hank's solution. Open circuit potential was monitored before, during and after sliding, while the coefficient of friction was recorded continuously. Additional dry sliding tests were performed to distinguish the mechanical contribution to total material degradation. Surface morphology and wear tracks were analysed by scanning electron microscopy, energy dispersive X ray spectroscopy and profilometry.

Both samples showed a pronounced decrease in open circuit potential during sliding, indicating disruption of the passive oxide layer. During rubbing, the potential decreased from approximately 0.15 V to about −0.8 V vs. Ag/AgCl and remained low throughout the sliding period. After sliding, repassivation occurred, with the clinically retrieved sample showing faster recovery. The coefficient of friction was slightly higher for the new sample in Hank's solution, approximately 0.34, compared with 0.32 for the retrieved sample. Dry sliding tests showed higher friction values.

Surface analysis revealed differences in oxide distribution and wear track morphology. The retrieved sample showed higher oxygen content outside the wear track, suggesting in vivo modification of the passive surface layer. These unpublished results indicate that Ti6Al7Nb alloy remains relatively corrosion stable in simulated body fluid, while passive layer disruption and repassivation kinetics are important for understanding implant degradation and aseptic loosening.

Keywords: Ti6Al7Nb, tribocorrosion, orthopaedic implants, femoral stem, passive layer, aseptic loosening

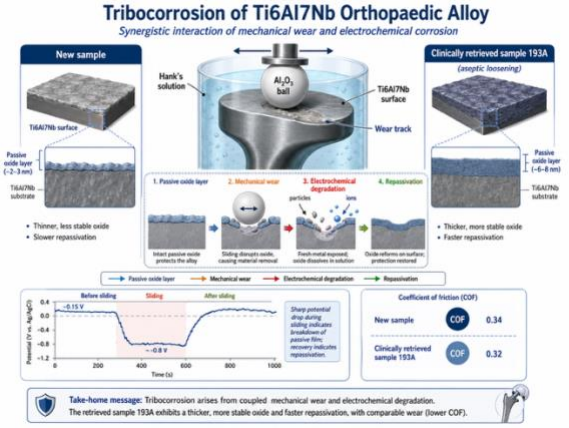


Figure 1. Schematic illustration of Ti6Al7Nb tribocorrosion in Hank's solution, showing passive oxide layer disruption during Al_2O_3 ball sliding, electrochemical degradation, particle and ion release, and subsequent repassivation. The comparison between the new and clinically retrieved 193A samples emphasizes differences in oxide layer stability and repassivation behaviour.

Persistent Micro and Nanoscale Corundum Residues on Grit Blasted Titanium Alloy Hip Implants: Biological and Clinical Implications

B. Kocjančič[1,2] M. Jenko[3]*, M. Debeljak[4]
[1] Department of Orthopaedic Surgery, University Medical Centre Ljubljana, Ljubljana, Slovenia
[2] Faculty of Medicine, University of Ljubljana, Ljubljana, Slovenia
[3] MD RI Institute for Materials Research in Medicine, Ljubljana, Slovenia
[4] University Rehabilitation Institute Republic of Slovenia, Ljubljana, Slovenia
*Corresponding author: monica.jenko@gmail.com

Abstract:
The long term success of cementless total hip arthroplasty depends on mechanical stability and biological integration at the bone implant interface. Surface morphology and chemistry at the micro and nanoscale influence protein adsorption, cellular adhesion, immune activity, and osseointegration. Corundum grit blasting is commonly used to increase the roughness of titanium alloy femoral stems. However, the process can leave embedded alumina particles whose long term biological significance remains insufficiently understood.
This study investigated the persistence, distribution, and potential biological effects of residual corundum on unused and clinically retrieved grit blasted Ti6Al7Nb femoral stems. Surface morphology, elemental composition, nanostructure, and surface chemistry were analysed using scanning electron microscopy, energy dispersive X ray spectroscopy, transmission electron microscopy, X ray photoelectron spectroscopy, and confocal laser fluorescence microscopy. Periprosthetic tissues obtained during revision arthroplasty were examined histopathologically to assess particulate accumulation and inflammatory reactions. Human bone marrow derived mesenchymal stromal cells were used to evaluate short term cytocompatibility and surface dependent cellular responses.
Micro and nanoscale corundum residues were consistently detected on unused and retrieved femoral stems, demonstrating the persistence of embedded blasting particles after clinical implantation. Particulate and metallic debris was also observed in periprosthetic soft tissues. In vitro experiments showed low short term cytotoxicity and no significant increase in cell death. Nevertheless, differences in cell surface interactions indicated that conventional cytotoxicity testing alone may not adequately describe the biological effects of modified implant surfaces. Residual corundum on grit blasted Ti6Al7Nb surfaces was not associated with pronounced acute cytotoxicity under the investigated conditions
However, its persistence and the presence of implant related debris in periprosthetic tissues support further investigation of possible long term inflammatory and osseointegrative effects. Improved control of surface chemistry, blasting particle size, and residual particulate burden may contribute to the development of safer and more predictable precision engineered orthopaedic implants.

Keywords:total hip arthroplasty; Ti6Al7Nb; corundum; grit blasting; nanoscale surface characterization; bone implant interface; particulate debris; cytocompatibility

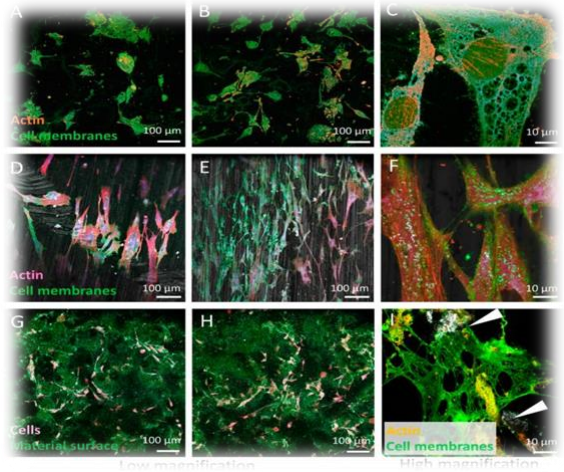


Figure. Confocal fluorescence images of live bone marrow derived mesenchymal stem cells (BMSCs) cultured on Ti6Al7Nb alloy surfaces with different surface finishes. (A–C) On the polished, mirror like surface, BMSCs exhibited randomly oriented growth. (D–F) On the ground surface, the cells showed pronounced directional alignment. (G–I) On the rough surface contaminated with residual Al_2O_3 particles, BMSCs exhibited limited, nonoriented growth and incomplete surface attachment, primarily through discrete anchoring points indicated by arrows. Scale bars: 100 µm in the low magnification images and 10 µm in the high magnification images.

Surface Degradation and Thrombotic Deposition on Blood-Contacting Polymeric Components of ECMO Systems

Š. Tadel Kocjančič[1]*, M. Debeljak[2,3], M. Jenko[2], B. Kocjančič[3,4]
[1]CIM, University Medical Centre Ljubljana, Ljubljana, Slovenia, [2] MD-RI Institute for Materials Research in Medicine, Ljubljana, Slovenia, [3]University Rehabilitation Institute, Republic of Slovenia, Ljubljana, Slovenia, [3]Department for Orthopaedic Surgery, University Medical Centre Ljubljana, Ljubljana, Slovenia, [4]Faculty of Medicine, University of Ljubljana, Slovenia

Abstract:
Extracorporeal membrane oxygenation, ECMO, is an essential life-support therapy for patients with severe respiratory or circulatory failure. However, its prolonged use remains limited by blood–material interactions, thrombotic complications and progressive oxygenator dysfunction. Contact between blood and artificial surfaces initiates rapid plasma-protein adsorption, platelet adhesion and activation, coagulation and inflammatory responses. These processes result not only in macroscopic thrombi but also in the formation of early, thin thrombotic deposits on oxygenator membranes, connectors and tubing. Thrombotic deposits in ECMO systems are complex, heterogeneous structures composed of fibrin, platelets, erythrocytes and leukocyte-derived components. Their formation and spatial distribution depend on material properties, surface chemistry, local flow conditions and the duration of clinical use. Progressive deposition may increase flow resistance, impair gas transfer and contribute to oxygenator failure. Simultaneously, prolonged exposure to blood, mechanical loading and chemical conditions may alter the physicochemical properties of blood-contacting polymers, including their surface chemistry, topography, wettability and the integrity of antithrombogenic coatings. This study aims to investigate the mechanisms of surface degradation and thin thrombotic-layer formation on blood-contacting polymeric components of ECMO systems. New, clinically used and functionally failed ECMO components will be collected and classified according to the duration of use, operating conditions and reason for replacement. Surface morphology, chemical composition, topography and wettability will be analysed using scanning electron microscopy with energy-dispersive X-ray spectroscopy, Fourier-transform infrared spectroscopy, Raman spectroscopy, X-ray photoelectron spectroscopy, profilometry and contact-angle measurements. Deposit composition and thickness will be evaluated and correlated with clinical and operational parameters. In vitro tests will assess protein adsorption, platelet adhesion, coagulation activation and haemolysis. Computational fluid dynamics will be used to identify regions of flow recirculation, low shear stress and other haemodynamically critical conditions associated with thrombotic deposition. The integrated analysis is expected to clarify the relationships among material degradation, surface properties, haemodynamic conditions and oxygenator dysfunction. The results may support the identification of early surface markers of device failure and guide the development of more stable haemocompatible coatings, improved polymeric materials and optimised ECMO component designs. Ultimately, this work will contribute to prolonged oxygenator performance, fewer emergency circuit replacements and safer long-term ECMO therapy. **Keywords**: extracorporeal membrane oxygenation, thrombotic deposition, surface degradation, haemocompatibility, oxygenator failure

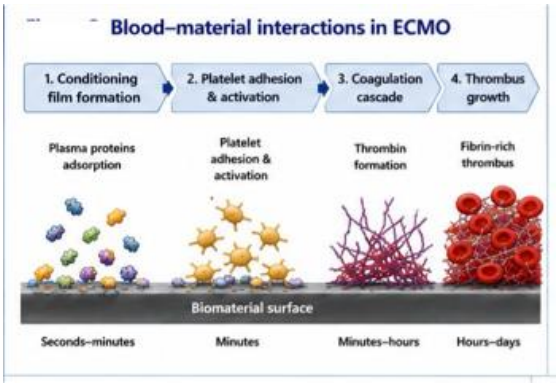


Figure 1: Figure illustrates the blood -material interactions in ECMO

References:

1. Jaffer,I.H., Fredenburgh,J.C., Hirsh, J., Weitz, J.I. *Medical device-induced thrombosis: what causes it and how can we prevent it?* J.Thromb.Haemost., (2015) , 13,S72-S81
2. Combes, A., et al. (2018)*Extracorporeal membrane oxygenation for severe acute respiratory distress syndrome.* N.Engl.J.Med., 378, 1965-1975

Abdominal PP meshes coated with functional biodegradable nanofibers for the simultaneous prevention of postoperative adhesions and infections

Stéphanie Degoutin[*,1], Malo Dufay[1], Maude Jimenez[1], Mathilde Casetta[1], Mickael Maton[2], Frédéric Cazaux[1], Séverine Bellayer[1], Feng Chai[2], Nicolas Blanchemain[2]
[1]Univ. Lille, CNRS, INRAE, Centrale Lille, UMR 8207 - UMET - Unité Matériaux et Transformations, F-59000 Lille, France
[2]Univ. Lille, Inserm, CHU Lille, U1365, Advanced Drug Delivery Systems, F-59000 Lille, France

Abstract:
Abdominal hernia repair is a common surgical procedure, involving in most cases the use of textile meshes in order to consolidate the damaged surrounding tissues and prevent the resurgence of the hernia. However, in more than half cases postoperative complications such as adhesions and infections occur at the surface of the mesh, leading to chronic pain for the patient and a re-intervention to remove the implant. One of the most promising strategies to reduce these risks is to add a physical barrier between the mesh and the abdominal walls. In this study, we developed hernia meshes coated with functional polycaprolactone (PCL) biodegradable nanofibers, confering anticoagulant and antibacterial activities depending on the side of the implant. Two strategies were investigated: the cold plasma induced graft-polymerization of the functional monomers and the formation of core-sheath nanofibers thanks to coaxial electrospinning. Two bioactive polymers were used: polysulfonate (poly(2-acrylamido-2-methylpropane sulfonic acid), PAMPS for anticoagulant activity and (poly((2-tert-butylamino) ethyl methacrylate), PTBAEMA) for antibacterial activity[1,2]. The process parameters were optimized in order to obtain defect-free nanofibrous coatings onto the mesh with improved stability in water. The presence of the functional groups at the surface as well as the core-sheath structure was investigated. The *in vitro* cytocompatibility, anticoagulant activity and antibacterial activity were evaluated and highlighted the high potential of these coatings for the simultaneous prevention of postoperative adhesions and infections.

Keywords: cold plasma induced polymerization, coaxial electrospinning, abdominal hernia treatment, post-operative adhesions, anticoagulant activity, antibacterial activity

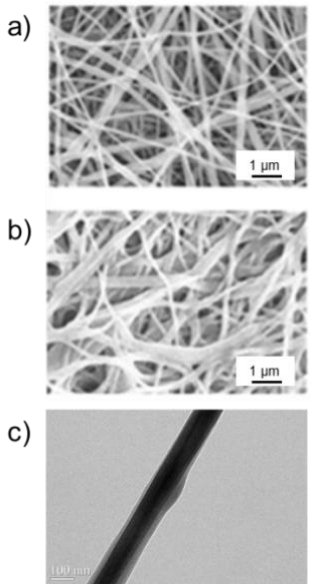


Figure 1: SEM pictures of PCL nanofibers (a), PCL-g-PAMPS nanofibers obtained by cold plasma induced grafting copolymerization (b) and TEM image of core-sheath PCL/PAMPS nanofiber (c).

References:

1. M. Dufay, M. Jimenez, M. Casetta, F. Chai, N. Blanchemain, G. Stoclet, F. Cazaux, S. Bellayer, S. Degoutin, PCL covered PP meshes plasma-grafted by sulfonated monomer for the prevention of postoperative abdominal adhesions, *Materials Today Communications* (2021), 26, 101968.
2. M. Dufay, M. Jimenez, M. Casetta, F. Chai, N. Blanchemain, M. Maton, F. Cazaux, S. Bellayer, S. Degoutin, Abdominal PP meshes coated with functional core-sheath biodegradable nanofibers with anticoagulant and antibacterial properties, *Biomaterials Advances* (2025), 169, 214163.

Evaluation of the Protective Performance and Electrochemical Stability of Nitradine Commercial Formulation

C.A. Freiria de Oliveira [1,*], V.C. Oliveira [1], A.P. Macedo [2], E. Watanabe [3], R. Galo [1], V.O. Pagnano [1]

[1] Department of Dental Materials and Prosthodontics, School of Dentistry of Ribeirão Preto, University of São Paulo (FORP-USP), Ribeirão Preto, SP, Brazil.
[2] Department of Orthopedics and Anesthesiology, Ribeirão Preto Medical School, University of São Paulo (FMRP-USP), Ribeirão Preto, SP, Brazil.
[3] Department of Oral Biology, School of Dentistry of Ribeirão Preto, University of São Paulo (FORP-USP), Ribeirão Preto, SP, Brazil.

Abstract:
The electrochemical stability and surface protection of cobalt-chromium (Co-Cr) alloys are critical factors for ensuring the biocompatibility and longevity of removable partial dentures in the highly corrosive oral environment. This study aims to evaluate the protective performance and corrosion behavior of a Co-Cr alloy exposed to a Nitradine commercial disinfecting formulation compared to a control medium (water) using standard electrochemical techniques. Co-Cr alloy discs (n=5) were positioned as the working electrode in a conventional three-electrode electrochemical cell. The cell was filled with either distilled water (control group) or Nitradine disinfecting solution (experimental group), which served as the test electrolytes. The electrochemical assays were then immediately performed at room temperature. Open Circuit Potential (E_{ocp}), Electrochemical Impedance Spectroscopy (EIS), and Potentiodynamic Polarization curves were recorded across several independent replicates to validate experimental reproducibility. Statistical analysis confirmed that the Eocp dataset followed a normal distribution according to the Shapiro-Wilk test (p=0.41). A paired-sample Student's t-test demonstrated a statistically significant difference (p=0.0076) between the final E_{ocp} values of the control group and the Nitradine solution, highlighting its surface modification capability. For the EIS data at low frequency (0.01 Hz), normality was verified (p=0.90 for water; p=0.38 for Nitradine), and a highly significant statistical difference was revealed (p=0.0017), proving that the Nitradine solution substantially increases interfacial resistance. Furthermore, the polarization parameters showed a significant thermodynamic shift in the corrosion potential (E_{corr}, p=0.03245) along with a strong marginal significance in the kinetic deceleration of the corrosion current density (i_{corr}, p=0.0520), moving the mean values from 1.97×10^{-6} A (water) down to 4.99×10^{-7} A (Nitradine). Taken together, these rigorous statistical assessments mathematically prove that the Nitradine formulation promotes the formation of a highly stable and protective surface barrier.

Keywords: Electrochemical Impedance Spectroscopy, Potentiodynamic Polarization, Open Circuit Potential, Nitradine, Surface Protection.

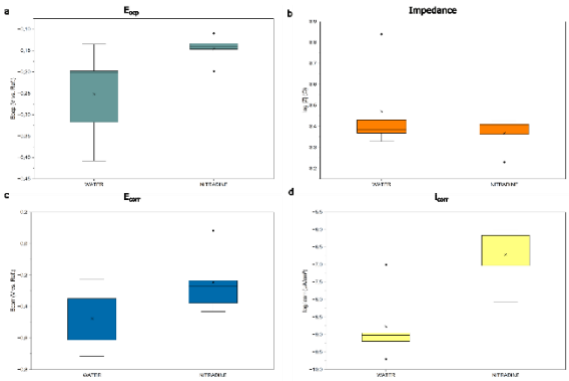


Figure 1: Statistical distribution (Box-and-whisker plots) of the electrochemical and corrosion parameters evaluated for the Co-Cr alloy in control medium (water) and Nitradine disinfection solution: **(a)** Open Circuit Potential (E_{ocp}); **(b)** Low-frequency modulus of impedance ($\log|Z|$ at 0.01 Hz); **(c)** Corrosion potential (E_{corr}); and **(d)** Corrosion current density ($\log i_{corr}$). The boxes represent the interquartile range (25%–75%), horizontal internal lines indicate the median, square/cross symbols represent the mean, and whiskers indicate the data variance, highlighting the surface modifications induced by the commercial formulation.

References:

1. Vasconcelos GLL, et al. Electrochemical Behavior of Cobalt–Chromium Alloy Exposed to Effervescent Denture Cleansers. *Corros Mater Degrad*. 2025;6:23.
2. Pupim D, et al. Electrochemical behavior of Co-Cr alloy in hygienic tablets solution. *Mater Res*. 2022;25:e20210346.

Defect-Engineered Hexagonal Boron Nitride as a Dual-Action Orthopedic Biomaterial for Simultaneous Osteogenesis and Osteosarcoma Therapy

Lucas Souyris[1], Ingrid Charodin[2,3], Fanny Salmeron[1], Zahraa Saleh[2#], Habib Belaid[2,3], David Cornu[2], Pierre-Yves Collart-Dutilleul[3,4], Mikhael Bechelany[2*], Vincent Cavaillès[1*]

[1] Institut de Recherche en Cancérologie de Montpellier, IRCM, U1194, INSERM, Univ Montpellier, ICM, CNRS, 34298 Montpellier, France

[2] Institut Européen des Membranes, IEM, UMR 5635, Univ Montpellier, ENSCM, CNRS, 34090 Montpellier, France

[3] LBN, Univ Montpellier, Montpellier, France

[4] Odontology Department CCMR O-Rares, CHU Montpellier, Montpellier, France

[*] Corresponding authors | [#] Presenter: zahraa.saleh@umontpellier.fr

Abstract:

A paramount challenge in orthopedic oncology is engineering advanced biomaterials that can simultaneously promote bone regeneration and eradicate local malignancies. This presentation introduces a multi-layered therapeutic strategy using hexagonal boron nitride (h-BN) as a mechanically reinforcing agent tailored with intrinsic osteogenic and selective antitumor properties. Through a sequence of high-energy ball milling and high-temperature pyrolysis, we synthesized two modified h-BN variants: h-BND2 (ball-milled) and h-BNG2 (ball-milled and pyrolyzed). Physicochemical profiling via Electron Paramagnetic Resonance (EPR) spectroscopy revealed that while mechanical milling shatters the pristine lattice to generate a high density of unstable paramagnetic defects, subsequent pyrolysis almost completely quenches this radical signal (figure 1). This quenching evidences structural passivation, transforming open defects into oxygen-containing functional groups and boron oxynitride phases. This specific chemical alteration drives enhanced hydrolytic susceptibility, yielding a critical ten-fold increase in controlled boron release. In vitro screenings in human osteoblasts and aggressive osteosarcoma lines (U2OS, SaOS-2) demonstrated that while both variants support healthy bone cell viability and osteogenesis, h-BNG2 exhibits uniquely potent, selective antitumor toxicity. Validated by transcriptomic analyses, this cascade relies on a dual-action model: sustained boric acid flux destabilizes cancer antioxidant defenses, while the oxynitride surface acts as a peroxidase-like nanozyme to convert intracellular hydrogen peroxide into fatal levels of reactive oxygen species (ROS)(1). Ultimately, by balancing chemotherapy-free, highly selective oncology with multi-layered tissue healing capabilities, thermally passivated h-BNG2 emerges as a leading candidate for next-generation 3D porous bone substitute devices.

Keywords: Hexagonal boron nitride (h-BN), Defect engineering, Nanozymes, Osteosarcoma, Bone regeneration, EPR spectroscopy, chemotherapy-free therapeutics.

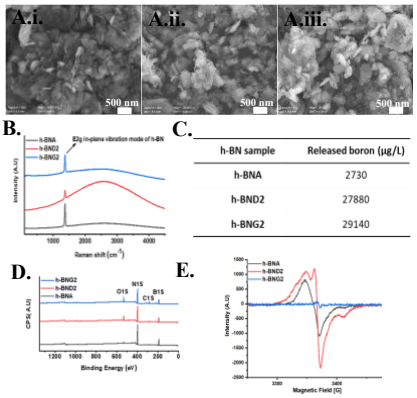


Figure 1. (A) SEM micrographs of (i) h-BNA, (ii) h-BND2, and (iii) h-BNG2. (B) Overlaid Raman spectra. (C) ICP analysis of boron release. (D) Survey XPS spectra. (E) EPR spectra of the h-BN samples.

References:

1. Souyris L, Charodin I, Salmeron F, Saleh Z, Belaid H, Cornu D, et al. Tuning the Oxidation of Boron Nitride for Enhancing its Antitumor Activity. Biomedicine & Pharmacotherapy. 2026.

Nanocellulose as a Cosmetic Ingredient through an SSbD Lens

O. Panák[1],*, U. Novak[1], A. Assis[2], D. Barak[2], D. Kohen[2], A. Blinderman[2], M. Velimirovic Fanfani[3], B. Hardy[4], P. D. Kolokathis5, Y. Kohl[6], W. A. Gebbink[3], F. Pérez Sánchez[7]

[1] National Institute of Chemistry, Hajdrihova 19, 1000 Ljubljana, Slovenia

[2] AHAVA – Dead Sea Laboratories Ltd., Rakefet 1st. P.O.B. 109, Shoham 6083705, Israel

[3] Flemish Institute for Technological Research (VITO), Boeretang 200, Mol 2400, Belgium

[4] Edelweiss Connect GmbH, Technology Park Basel, Hochbergerstrasse 60C, Basel 4057, Switzerland

[5] NovaMechanics MIKE, Piraeus 18545, Greece

[6] Fraunhofer Institute for Biomedical Engineering IBMT, Joseph-von-Fraunhofer-Weg 1, Sulzbach 66280, Germany

[7] Instituto Tecnológico del Embalaje, Transporte y Logística (ITENE), Carrer d'Albert Einstein, 1, Valencia Paterna 46980, Spain

Abstract:

Replacing synthetic rheology modifiers and microplastic-forming polymers with bio-based alternatives is a growing priority for the cosmetics sector, yet new ingredients still need robust evidence of safety and environmental benefit before adoption. Within the Horizon Europe project SSbD4CheM, we are applying a multi-tiered Safe-and-Sustainable-by-Design (SSbD) approach to nanocellulose additives (with varying physico-chemical properties) being evaluated as replacements for conventional thickening and stabilising agents in four Dead Sea-based skincare formulations (Facial Cream, SPF lotion, Facial Mud Mask, Primary Mud). As a first tier, in silico screening of the underlying chemical structures points to a favourable toxicological profile across the modifications assessed so far. Building on this, we are estimating occupational exposure during production and processing, and, in parallel, consumer exposure during product use, drawing on the available toxicological and physicochemical data for these materials. We are now cross-checking these early, largely computational and literature-based assessments against a growing set of New Approach Methodologies, including ex vivo skin, gut, and lung models and a zebrafish embryo assay, to see whether the predicted safety profile holds under more physiologically realistic conditions. Alongside the safety work, a life-cycle assessment of the four formulations is underway to determine where substituting nanocellulose for conventional additives delivers a genuine environmental benefit, and where trade-offs may remain. Taken together, this ongoing case study illustrates how a tiered SSbD assessment can be built alongside product development, rather than retrofitted once a formulation is finalised, and offers a template for how bio-based cosmetic ingredients more broadly might be qualified for market.

Keywords: nanocellulose, Safe-and-Sustainable-by-Design, cosmetic formulation, hazard screening, exposure assessment, New Approach Methodologies, life-cycle assessment, bio-based additives



Figure 1: Figure shows prototypes of cosmetic products containing different types of nanocellulose.

References:

1. Garmendia Aguirre, I., Abbate, E., Bracalente, G., et al. (2025) Safe and Sustainable by Design Chemicals and Materials – Revised Framework, Publications Office of the European Union, JRC143022.
2. European Parliament, Council of the European Union (2009) Regulation (EC) No 1223/2009 on cosmetic products, Off. J. Eur. Union, L342, 59–209.
3. Miao, C., Zhao, M., Hamad, W.Y. (2025) Applications of cellulose nanocrystal (CNC) in cosmetic products – case studies, Colloids Surf. A, 718, 136904.

Multifunctional algae-based treatment combining colouration and antibacterial activity in knitted cotton textiles

Anna Björkquist[1] and Nils-Krister Persson[1]
[1] Swedish School of Textiles, Polymeric E-textiles, Smart Textiles, Science Park Borås, University of Borås. Sweden

Abstract:
Emerging biomaterials derived from marine and aquatic biomass offer new opportunities for advanced functionalisation of textile surfaces. Algae are a promising source of pigments and bioactive compounds that are able to provide textiles with dual properties i.e both colour and additional functional features. One particularly interesting function is antimicrobial activity, as algae-derived extracts have previously been reported to exhibit antimicrobial properties. Combining colouration with such functionality could support the development of multifunctional textile treatments based on renewable biological resources.

This study investigated whether an algae-based textile dye treatment could provide measurable antibacterial activity when applied to cotton single-jersey fabric. The treatment consisted of a water-based formulation containing phycocyanin and tannic acid, followed by a chitosan-based post-treatment. Four treated samples and one untreated reference were prepared (Figure 1). The treatment variants included a) chitosan-based post-treatment alone, b) phycocyanin formulation alone, c) a formulation containing spirulina biomass instead of extracted phycocyanin, and d) the complete treatment combining the phycocyanin formulation with the chitosan-based post-treatment . All samples were prepared using cold pad-batch processing at room temperature. Antibacterial activity against *Staphylococcus aureus* was evaluated according to ISO 20743:2021.

Of the tested variants, the complete treatment (d) was the only one to show significant antibacterial activity. The results demonstrate the potential of algae-derived materials to form part of a textile treatment. However, the results do not clearly show how the individual components or their possible interactions contribute to the observed activity. Further work should therefore investigate how different concentrations and combinations of the treatment components influence colour and antibacterial performance. The retention of the treatment and its antibacterial activity over time during use and repeated laundering should also be evaluated.

Keywords: algae-derived pigments, phycocyanin, chitosan, antibacterial textiles, multifunctional textiles, cold pad-batch dyeing, bio-based materials.

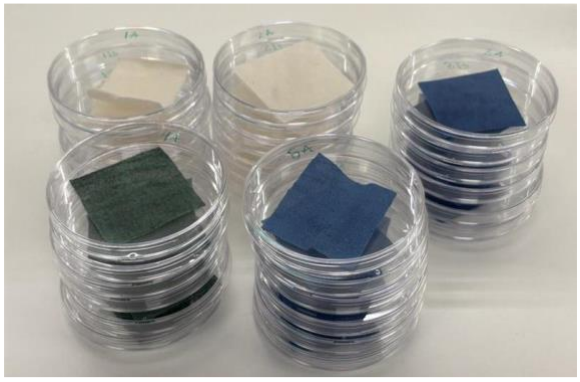


Figure 1: Knitted cotton single-jersey samples after cold pad-batch processing, representing the untreated reference and four treatment variants prepared for antibacterial evaluation. The pigment-based treatments produced a blue colour, whereas the spirulina biomass-based treatment produced a green colour.

References:

1. Janarthanan, M., & Senthil Kumar, M. (2018). The properties of bioactive substances obtained from seaweeds and their applications in textile industries. *Journal of Industrial Textiles*, *48*(1), 361–401. https://doi.org/10.1177/1528083717692596
2. ISO (2021). *ISO 20743:2021 Textiles — Determination of antibacterial activity of textile products.* 3rd ed. Geneva: International Organization for Standardization.

SMS 2026 / EGF 2026 / Sensors 2026 / NanoMed 2026 Joint Plenary Session II

Ultrafast domain wall propagation in amorphous magnetic microwires.

A. Zhukov[1,2]*, P. Corte-Leon,[1,3,4], A. Gonzalez[1,4], P. A. Rodríguez Jiménez[1,4], and V. Zhukova[1,4]
[1] Dept. Appl. Phys., EIG, University of the Basque Country, EHU, 20018, San Sebastian, Spain
[2] IKERBASQUE, Basque Foundation for Science, 48011 Bilbao, Spain
[3] Dept. Mater. Science & Metallurgy, Univ. Cambridge, Cambridge CB3 0FS, UK
[4] Dept. Polym. Adv. Mater, Univ. of the Basque Country, EHU, 20018 San Sebastian, Spain

Abstract:
Fast domain wall (DW) propagation of thin magnetic wires (planar and cylindrical) become a topic of intensive research during the last years owing to promising applications in data storage devices (magnetic random memory devices, logic devices)[1,2]. The Taylor-Ulitovsky method allows preparation of amorphous magnetic microwires with diameters ranging from 0.2 to 100 μm coated by thin, insulating and flexible glass [3]. Fe-rich amorphous microwires with positive magnetostriction constant exhibit spontaneous magnetic bistability and fast DW propagation at relatively low magnetic fields [3]. Additionally, annealing induced magnetic bistability and fast domain wall propagation can be observed in Co-rich amorphous microwires [3]. Therefore, amorphous glass coated microwires are quite interesting material for studies of the single domain wall dynamics. These microwires have composite character. Glass coating surrounding metallic nucleus introduces internal stresses, increasing the magnetoelastic anisotropy of such microwires [3]. Such magnetoelastic anisotropy can be tailored by either tuning of the magnetostriction coefficient or by controllable tuning of the internal stresses [3].
We present our recent studies of DW propagation in Fe-, Fe-Ni-and Co-rich microwires and analyzed observed DW dynamics considering effect of magnetoelastic anisotropy, internal stresses relaxation and induced magnetic anisotropy. We found that annealing allows considerable improvement of DW velocity in Fe-rich microwires (Figure 1). In Fe-Ni- based microwires the DW velocity is considerably lower. Fast magnetic field and current driven single domain wall propagation is observed in Co-rich microwires. Stress-annealing allows achievement of even higher DW velocity and mobility. We attributed these changes to the stress relaxation and induced transverse magnetic anisotropy after appropriate annealing. For interpretation of more complex behavior of Fe-Ni-based microwires we must additionally consider the domain wall stabilzation [3].
Consequently, from experimental dependences we assume that for increasing the DW velocity, *v*, special attention should be paid to minimizing the magnetoelastic energy. In properly processed amorphous microwires the DW velocities up to 4 km/s have been achieved. The routes for tuning DW dynamics are summarized, the correlation of the DW shape with the microwire dimensions and with the magnetic are discussed.

Keywords: Magnetic microwires, magnetic bistability, annealing, internal stresses, domain wall propagation.

References:

1. Allwood, D.A., Xiong, G., Faulkner, C.C., Atkinson, D., Petit, D., Cowburn, R.P. (2005), Magnetic domain-wall logic, *Science,* 309, 1688-1692

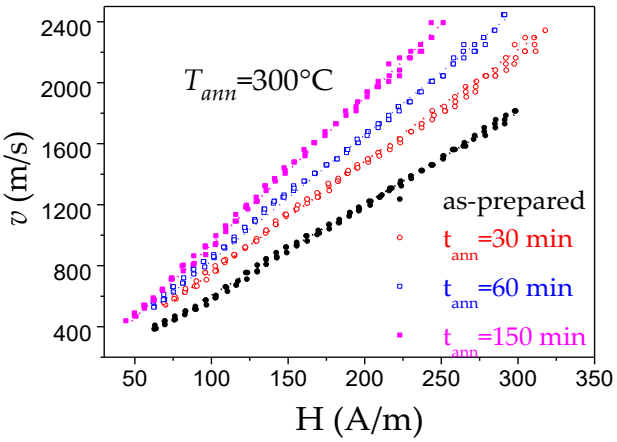


Figure 1. Dependencies of DW velocity, *v*, on magnetic field, *H,* measured in as-prepared and annealed for different annealing time, t_{ann}, $Fe_{74}B_{13}Si_{11}C_2$ microwire.

2. Parkin, S.S.P., Hayashi, M., Thomas, L. (2008), Magnetic domain-wall racetrack memory, *Science*, 320, 190-194
3. Zhukova, V., Corte-Leon, P., González-Legarreta, L., Talaat, A., Blanco, J.M., Ipatov, M., Olivera, J., Zhukov, A. (2020) Review of Domain Wall Dynamics Engineering in Magnetic Microwires, *Nanomaterials,* 10, *2407.*

Crystal Growth and Chemical Engineering of Two-Dimensional Magnets, Semiconductors and Dielectrics

Z. Sofer [1,*]
[1] Department of Inorganic Chemistry, University of Chemistry and Technology Prague, Technicka 5, 166 28 Prague 6, Czech Republic

Abstract:
Progress in two-dimensional materials increasingly depends on the ability to control crystal quality, defect density, composition and surface chemistry during synthesis. This contribution will discuss crystal-growth and chemical-engineering strategies for emerging 2D magnets, semiconductors and dielectrics, with emphasis on scalable preparation of low-defect layered crystals and their subsequent modification. In addition to established transition-metal halides and chalcogenides, mixed halogen-chalcogenide compounds represent a rapidly developing platform combining magnetic order with strong optical and electronic anisotropy. A central example is chromium sulfo-bromide, CrSBr, which adopts an FeOCl-type layered structure and exhibits A-type antiferromagnetic ordering. Its magnetic and optoelectronic properties can be strongly modified by exfoliation, vacancy and defect engineering, strain, substitutional doping and surface functionalization, enabling partial or complete switching toward ferromagnetic behaviour and opening routes toward spintronic and optoelectronic devices. The broader role of crystal growth will also be highlighted for layered semiconductors and dielectrics, including high-*k* 2D dielectric materials and large-scale metal-flux growth of high-quality hexagonal boron nitride. These examples show that controlled synthesis is not only a route to larger crystals, but a key tool for tuning interfacial chemistry, magnetic ground states, excitonic response and device integration. The presentation will therefore connect precursor design, defect control and chemical modification as general principles for next-generation 2D materials.

Keywords: 2D Materials, crystal growth, dielectrics, magnetic 2D, doping.

How to get from nano to active surface in energy storage materials. A long and winding road.

P. Gomez-Romero
[1] ICN2, Catalan Institute of Nanoscience and Nanotechnology, Cerdanyola (Barcelona) Spain.
[2] CSIC, Consejo Superior de Investigaciones Científicas, Spain

Abstract:
Explaining how the surface of a cube material surges as the cube goes from macro to micro to nano is commonplace in conventional nano presentations. But this could lead to the wrong conclusion that nanosize comes automatically with an optimization of active surface area of electroactive materials in energy storage electrodes. Yet things are not so simple.
In this presentation, we will outline our long-term research aimed at harnessing the electroactivity of molecular, nanoclusters and nanosized materials for use in batteries, supercapacitors, and hybrid devices. [1] Our group has gained extensive experience in the design, synthesis, and fabrication of these hybrid materials and devices, working with a wide range of components—from polyoxometalate clusters combined with conducting polymers or nanocarbon materials[2] to electroactive molecular compounds (such as quinones)[3] or nanoscale inorganic phases like LiFePO4 or Prussian Blue.[4] Our research journey has involved tackling numerous challenges and navigating unexpected turns; this experience allows us to discuss the many factors influencing the ultimate performance of nanomaterial-based energy storage devices—factors that go well beyond the fundamental increase in the active surface area of the electrode material.

Keywords: energy storage, hybrid materials, polyoxometalates, nanoclusters, conducting polymers, nanocarbons, quinones, graphene, batteries, supercapacitors, hybrid devices, electrode materials, LiFePO4, Prussian Blue Analogues.

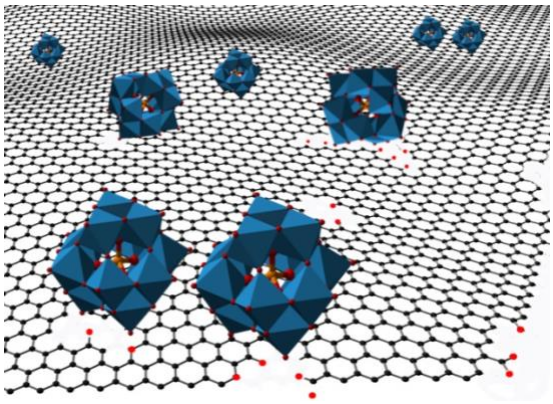


Figure 1: Artistic representation (at approximate scale) of polyoxometalate nanoclusters on the surface of reduced graphene oxide as a conceptual electrode material.

References:

1. Hybrid Energy Storage. The merging of battery and supercapacitor chemistries.D. P. Dubal, O. Ayyad, V. Ruiz, and P. Gomez-Romero. Chemical Society Reviews, 2015, 44, 1777.
2. Polyoxometalates: from Electroactive Clusters to Energy Materials. Michael Horn et al. Energy and Environmental Science, 2021, 14(4), pp. 1652–1700
3. Quinone Quest: Unraveling Electrochemical Performance in Quinone-Anchored 3D Graphene Architectures for High-Energy Supercapacitors. C Karaman, L N Bengoa, R M Gonzalez-Gil, P Gomez-Romero. Electrochimica Acta, 2025, 512, 145414
4. Development of Free-Standing Nanostructured Prussian Blue Electrodes for Zinc-Ion Supercapacitors. RM González-Gil, EM Hamza-Laghizi, L Bengoa, P Gómez-Romero. Proceedings of MATSUS Spring 2026 Conference (MATSUSSpring26)

From Ensemble Binding to Single-Molecule Statistics in pH-conditioned biosensing

Luisa Torsi
[1] Università degli Studi di Bari Aldo Moro, Italy

Abstract:
Plasmonic and potentiometric platforms are well-established label-free approaches for immuno and molecular detections. However, when operated without amplification strategies, their analytical sensitivity has traditionally been limited to the nanomolar concentration range. In this lecture, I will discuss a comprehensive physical and statistical framework showing that biosensing responses over an exceptionally broad dynamic range, from nicromolar down to 10-zeptomolar concentrations, are governed by two distinct sensing regimes.
The study focuses on centimeter-scale sensing interfaces densely functionalized with pH-conditioned recognition layers, where electrostatic and ion-mediated effects play a central role in transducing molecular recognition events. At ultralow analyte concentrations, the sensor response is no longer described by ensemble-averaged affinity interactions. Instead, it is dictated by Poisson statistics associated with stochastic single- and few-molecule capture events occurring on large-area interfaces. In this regime, each binding event can trigger a local pH-conditioned mediated dielectric and electrostatic reorganization of the interfacial layer, producing a measurable plasmonic or potentiometric signal.
This mechanism enables direct, label-free detection at concentrations as low as 10–100 zM with 99% statistical confidence, while keeping false-positive and false-negative rates below 1%. As the analyte concentration increases, the sensing behavior progressively evolves toward a classical Maxwell–Boltzmann regime, characterized by conventional binding isotherms and ensemble-averaged equilibrium affinity.
By explicitly accounting for noise, uncertainty propagation, and statistically robust decision criteria, the full binding curves can be modeled across both regimes, allowing the extraction of equilibrium parameters, including an apparent equilibrium constant specific to the ultra-dilute limit. These results clarify some key aspects of the physical origin of extreme sensitivity in large-area biosensing platforms and highlight the role of electrostatic, ion-mediated interfacial phenomena in the design of next-generation single-molecule sensors operating without labels.
Mechanistically, the two regimes arise from the responsive nature of the pH-conditioned capturing layer. At ultralow antigen concentrations, a single antigen–antibody binding event is proposed to nucleate a localized domain where neighboring antibodies undergo collective dielectric and electrostatic rearrangement, likely involving the cooperative hydrogen-bond networks. This converts a discrete molecular event into a mesoscopic dielectric perturbation detectable by plasmonic or potentiometric transducers. At higher concentrations the formation of a continuous layer of target molecules that are affinity bound to the capturing layer is seen and the response is governed by ensemble-averaged affinity-bindings.

References:

1. M. Catacchio, V. Mongelli, M. Caputo, L. Sarcina, P. Bollella, E. Castrignanò, A. Costantino, C. Di Franco, M. Piscitelli, G. Scamarcio, F. Stellacci, E. Macchia* and L. Torsi* “Coexisting stochastic and ensemble-averaged affinity-binding regimes” submitted
2. E. Macchia, L. Torsi* “Sensing regimes in potentiometric immunoassays” Nature Reviews Materials, 2026, 11, 226-243 - DOI: 10.1038/s41578-025-00863-6
3. E. Macchia, C. Di Franco, C. Scandurra, L. Sarcina, M. Piscitelli, M. Catacchio, M. Caputo, P. Bollella, G. Scamarcio,* L. Torsi* “Plasmonic Single-Molecule Affinity Detection at 10^-20 Molar” Advanced Materials, 2025, 37(9) - DOI: 10.1002/adma.202418610

Clinical Validation of Wearable Piezoelectric Sensor & MicroLEDs for Skin Phototherapy and Cardiovascular Monitoring

Keon Jae Lee
[1] KAIST Endowed Chair Professor, Department of Materials Science and Engineering, Rep. of Korea

Abstract:
This seminar introduces two recent progresses of flexible devices: wearable microLED and self-powered piezoelectric sensors. The first part will introduce the highly efficient a face-fit surface-lighting microLED (FSLED) mask designed for advanced skin anti-aging treatment. Overcoming the limitations of conventional rigid devices, the FSLED utilizes a 3D flexible origami structure to closely conform to complex facial contours, ensuring highly uniform light irradiation. The mask is fabricated via a blister-actuated laser-induced forward transfer technique with an exceptional yield. A built-in light diffusion layer (LDL) maximizes light uniformity, allowing the light to penetrate up to 1.5 mm into the dermis for effective cellular regeneration. In an 8-week clinical trial involving 33 participants, the device significantly improved major aging parameters, notably achieving a 340% greater enhancement in deep skin elasticity in the perioral area compared to conventional LED masks. We also demonstrate red AlGaInP vertical microLEDs for surface-lighting patches for effective melanogenesis inhibition and hair regrowth. In addition, 3D shape-morphing wireless microLEDs provide continuous, targeted light therapy for pancreatic cancer. The device dynamically adapts to tumor size and shape, ensuring conformal contact and stable illumination, leading to effective tumor treatment in an in vivo mouse model. Finally, combining with optogenetic models, flexible microLED stimulates the neurons of motor cortex for manipulating mouse body movements and synchronized electromyogram (EMG) signals.
The second part will discuss the flexible inorganic piezoelectric membrane that can detect the minute vibration of membrane for self-powered acoustic sensor and blood pressure monitor. We reported a machine learning-based acoustic sensor by mimicking the basilar membrane of human cochlear. Highly sensitive self-powered flexible piezoelectric acoustic sensor with a multi-resonant frequency band was employed for voice recognition. Convolutional Neural Network (CNN) were utilized for speaker recognition, resulted in a 97.5% speaker recognition rate with the 75% reduction of error rate compared to that of the reference MEMS microphone. In addition, wearable piezoelectric blood-pressure sensors (WPBPS) were developed for monitoring non-invasive arterial pressure and cardiovascular diseases. WPBPS achieves a high normalized sensitivity (0.062 kPa−1), and fast response time (23 ms). The transfer function of a linear regression model converts flexible piezoelectric pulse signals into blood pressure estimation values. Clinical validation of WPBPS was performed on 35 subjects/175 measurements, that satisfies international standard of blood pressure measuring accuracy (mean error < ±5 mmHg). It overcomes the limitations of conventional PPG-based and rigid sensors, enabling real-time, comfortable, and continuous cardiovascular monitoring.

References:

1. “Wearable Blood Pressure Sensors for Cardiovascular Monitoring and Machine Learning Algorithms for Blood Pressure Estimation” Nature Review Cardiology, 22, 629, 2025
2. "Clinical Validation of Wearable Piezoelectric Blood-Pressure Sensor for Health Monitoring", Adv. Mater., 26, 2301627, 2023
3. "Biomimetic and Flexible Piezoelectric Mobile Acoustic Sensors for Machine Learning Biometrics", Sci. Adv., 7, eabe5683, 2021
4. "Universal selective transfer printing via micro-vacuum force", Nature Comm., 14, 7744, 2023
5. “Deeply Implantable, Shape-Morphing, 3D μLEDs for Pancreatic Cancer Therapy “, Adv. Mater., DOI: 10.1002/adma.202411494
6. “Clinical Validation of Face-Fit Surface-Lighting μLED Mask for Skin Anti-Aging Treatment” Adv. Mater., 36, 2411651, 2024
7. "Simultaneous Emulation of Synaptic and Intrinsic Plasticity using a Memristive Synapse" Nature Comm., 13, 2811, 2022
8. "Progress in Brain-Compatible Interfaces with Soft Nanomaterials", Adv. Mater., 32, 1907522, 2020

SMS 2026 / EGF 2026
joint Session II. A:
Functional Electronics and Energy Materials

Unveiling the Atomic Configuration and Physical Properties of Low-Dimensional (2D) Materials via Advanced TEM

R. Arenal[1,2,3,*]

[1] Instituto de Nanociencia y Materiales de Aragon (INMA), CSIC-U. Zaragoza, 50009 Zaragoza – Spain
[2] Fundacion ARAID, 50018 Zaragoza – Spain
[3] Laboratorio Microscopias Avanzadas, U. Zaragoza, 50018 Zaragoza – Spain

Abstract: Atomic-scale structural and chemical analyses are essential for understanding how nanomaterials influence their properties. Transmission Electron Microscopy (TEM), particularly when combined with spatially resolved Electron Energy Loss Spectroscopy (SR-EELS) in an aberration-corrected instrument, offers an unparalleled approach for obtaining such information. With the capability to focus the electron probe to nearly 1 Ångström, this technique enables direct insight into the atomic configuration of nanomaterials [1–10].

In this communication, I will present a selection of recent works involving all these matters. These works will concern the study of the atomic structure & configuration 2D atomically thin nanostructures (including graphene-like material in pristine and hybrid forms) as well as the opto-electronic properties studies carried out via EELS measurements [1-10]. These works will illustrate the excellent capabilities offered by the use of Cs probe-corrected or image-corrected (S)TEM, combined with the use of a monochromator, to study these properties within a very good spatial resolution. Furthermore, I will also present some recent in-situ TEM-EELS studies showing how powerful this approach can be for allowing the simultaneous measurement of various physical and chemical features of high interest for the study of different phenomena as the reduction of graphene oxide (GO) thin films [1,2].

References

1. M. Pelaez-Fernandez, A. Bermejo Solis, A.M. Benito, W.K. Maser, R. Arenal, Carbon 178, 477 (2021).
2. S. Hettler, D. Sebastian, M. Pelaez, A.M. Benito, W.K. Maser, R. Arenal, 2D Materials 8, 031001 (2021).
3. A. Kagkoura, R. Arenal, N. Tagmatarchis, Advanced Functional Materials 31, 2105287 (2021).
4. A. Cohen, P. K. Mohapatra, S. Hettler, A. Patsha, K.V.L.V. Narayanachari, P. Shekhter, J. Cavin, J.M. Rondinelli, M. Bedzyk, O. Dieguez, R. Arenal, A Ismach, ACS Nano 17, 5399–5411 (2023).
5. R. Canton-Vitoria, T. Scharl, A. Stergiou, A. Cadranel, R. Arenal, D.M Guldi, N. Tagmatarchis, Angewandte (2019).
6. S. Majumder, et al., ACS Applied Nano Materials 8, 9256–9267 (2025).
7. S. Pandey, et al., Advanced Materials 2417669 (2025).
8. M. Downes, et al., Journal of American Chemical Society 146, 31159–31168 (2024).
9. R. Quirós-Ovies, et al., Small 2406030 (2024).
10. R.A. acknowledges financial support from the Spanish Ministry of Science and Innovation MICIU and the Spanish Research Agency AEI (PID2023-151080NB-I00/AEI/10.13039/501100011033, and CEX2023-001286-SMICIU/AEI/10.13039/501100011033), by the MICIU with funding from European Union Next Generation EU (PRTR-C17.I1) promoted by the Government of Aragon (DGA) and from the DGA project E13-26R. These studies have been developed in the Laboratorio de Microscopias Avanzadas (LMA), U. of Zaragoza (Spain).

Ion transportation in organic/inorganic composite electrolyte and its full battery

Yumei Wang [1], Li Lu [1,2]
[1] National University of Singapore Chongqing Research Institute, 401123, China
[2] National University of Singapore, Singapore 117575, Singapore

Abstract:
Organic/inorganic composite electrolytes have emerged as promising materials for advancing sodium-ion batteries (SIBs), offering a synergistic combination of flexibility, ionic conductivity, mechanical strength, and electrochemical stability. By integrating organic polymers with inorganic fillers, these electrolytes combine the processability and good interfacial contact of polymers with the thermal and mechanical stability of inorganic materials. This hybrid approach provides an attractive alternative to conventional liquid electrolytes, while addressing the low ionic conductivity and poor interfacial contact commonly associated with solid electrolytes.

In this study, a full sodium-ion battery was fabricated using $Na_3V_2(PO_4)_3$ (NVP) as the cathode and a newly developed organic/inorganic composite electrolyte. The electrolyte exhibited an ionic conductivity in the range of 10^{-4} S cm^{-1} at room temperature, demonstrating effective Na-ion transport. Solution casting and in-situ polymerization were employed and optimized to achieve a homogeneous microstructure, uniform filler dispersion, and improved electrode–electrolyte contact. The resulting composite electrolyte exhibited an enhanced Na-ion transference number, good electrochemical stability, and improved mechanical integrity.

The full-cell performance demonstrated stable charge–discharge operation and good cycling stability, confirming the compatibility of the composite electrolyte with the NVP cathode. The improved performance is attributed to the synergistic effects of the polymer matrix and inorganic phase, which facilitate Na-ion transport while improving structural and interfacial stability. Key challenges, including filler agglomeration, interfacial resistance, electrolyte thickness, and scalable fabrication, were also considered. Further optimization of electrolyte composition and processing conditions is expected to improve ionic conductivity and reduce interfacial impedance.

Overall, this work demonstrates the potential of organic/inorganic composite electrolytes as a practical platform for safer and high-performance sodium-ion batteries. The findings provide useful insights into electrolyte design, processing, and interface engineering, supporting the future development of scalable solid-state sodium-ion batteries for advanced energy-storage applications.

Building a Coordinated European Ecosystem for Advanced Materials: Lessons from the InnoMatSyn CSA

Ane Irazustabarrena (Tecnalia)

Abstract:
Advanced and innovative materials (AdMa) are essential enablers of Europe's green and digital transitions, industrial competitiveness and strategic resilience. However, the European AdMa landscape remains highly fragmented, with research, innovation and funding initiatives operating across regional, national and European levels with limited coordination. This fragmentation can create gaps between scientific excellence, technology development, infrastructures, industrial uptake and market deployment.

The Horizon Europe Coordination and Support Action **InnoMatSyn – Innovative Materials Ecosystem to Gain Synergies of regional, national and EU Initiatives** addresses this challenge by supporting the development of a more interconnected and coordinated European materials ecosystem. The project brings together 14 organisations from 10 European countries and works across the full innovation ecosystem, involving research organisations, industry, funding bodies, policymakers and other relevant stakeholders.

InnoMatSyn focuses on four complementary areas: **(1)** connecting knowledge and research results through an AI-based materials innovation knowledge repository; **(2)** identifying synergies and complementarities between regional, national and European funding programmes and supporting opportunities for joint funding initiatives; **(3)** strengthening cooperation among the different communities and initiatives involved in advanced materials; and **(4)** developing approaches to assess and mitigate technology leakage risks, contributing to European technological sovereignty.

A particular emphasis is placed on connecting materials research with technology development, manufacturing, testing and Research and Technology Infrastructures (RTIs), as well as on promoting safe and sustainable advanced materials. Recent work within InnoMatSyn includes the mapping and analysis of the European Research and Technology Infrastructure landscape for advanced materials uptake, providing evidence to support future European policies and initiatives.

This contribution presents the **InnoMatSyn approach, its emerging results and the lessons learned from building cross-border and cross-level synergies in the Advanced Materials ecosystem**. Particular attention is given to the mechanisms required to connect regional strengths with European priorities, align funding and innovation strategies, improve access to knowledge and infrastructures, and accelerate the transition from materials research to industrial applications. The experience of InnoMatSyn illustrates how coordination and ecosystem-building can complement technological research and contribute to a more resilient, sustainable and competitive European Advanced Materials landscape.

Keywords: Advanced Materials; Innovation Ecosystems; Research and Technology Infrastructures; European Research and Innovation Policy; Funding Synergies; Industrial Uptake; Scale-up; Safe and Sustainable by Design.

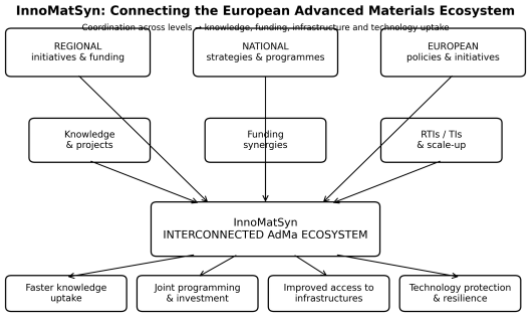


Figure 1: InnoMatSyn conceptual framework for connecting the European Advanced Materials ecosystem.

References:

1. **InnoMatSyn (2026).** *InnoMatSyn – Innovative Materials Ecosystem to Gain Synergies of regional, national and EU Initiatives.* Horizon Europe, Grant Agreement No. 101204218.
2. **InnoMatSyn (2026).** *Mapping & analysing European Research & Technology Infrastructures for Advanced Materials uptake. Independent Experts. European Commission* , September 2026.
3. **European Commission (2025).** *Call for Evidence for an Impact Assessment on the Advanced Materials Act.* Ref. Ares (2025)8964326. The document identifies fragmentation of the AdMa R&I ecosystem and limited access to shared research and technology facilities as barriers to uptake and industrial deployment.

Graphene-based formulations for high-definition capillary printing of electrolyte-gated field-effect transistors

Hassina MAHI[a,b], Marc PASCUAL[b], Nicolas BATTAGLINI[a]
[a] Université Paris Cité, ITODYS, 15 rue Jean-Antoine de Baïf, 75013, Paris
[b] HUMMINK, 5 rue Charlot, 75003 Paris

Abstract:
Several fabrication strategies have been explored for Graphene Field-Effect Transistors (GFET), such as photolithography-based processes on CVD-grown graphene[1]. However, these methods often involve complex processing steps, high fabrication costs, or limited scalability. To address these challenges, this work explores the fabrication of GFETs out of the clean room, using aqueous-based graphene-ink formulations, or exfoliated graphene flakes, and an innovative printing approach, referred to as High-Precision Capillary Printing (HPCAP)[2], enabling rapid, cost-effective, and scalable device manufacturing. HPCAP is inspired by Atomic Force Microscopy (AFM). A feedback-controlled oscillating micropipette (diameter ranging from 1 to 30 µm) maintains a constant resonance frequency shift induced by the formation of a liquid meniscus at the substrate. This controlled meniscus enables uniform and highly accurate printing, compared to conventional ink deposition methods, down to the micrometer scale.
A graphene-based ink compatible with the HPCAP technology was formulated from a suspension of graphene oxide (GO) flakes in deionized water, stabilized with sodium dodecyl sulfate surfactant[3]. The GO ink was successfully integrated onto transistor structures with fully printed gold electrodes obtained from a nanoparticle-based suspension, as well as onto patterned ones by lithography and thermal evaporation. After the printing step, graphene oxide was electrochemically reduced *in situ*, resulting in a significant recovery of graphene's electrical conductivity[4]. Electrical characterization of GFETs operated in the electrolyte-gate configuration reveals very similar behavior for printed and drop-cast graphene channels, with operating voltages below 2V. Moreover, transistors fabricated using printed gold electrodes show a 2.5 times higher on/off ratio than the corresponding photolithographically fabricated device. Finally, our latest investigations lead to the elaboration of fully capillary-printed GFETs with channel length down to the micrometer scale, therefore involving a small amount of graphene flakes. In parallel, we also investigated the use of HPCAP to address single exfoliated graphene flakes as the conductive channel of GFETs.
In conclusion, this work demonstrates the feasibility of fabricating key building blocks of fully printed transistors using HPCAP technology. GO-based inks can be reliably printed and reduced to recover graphene's electrical properties, while gold electrodes can be patterned with micrometric resolution. These results represent an important step toward the realization of fully printed graphene-based electronic devices.

Keywords: graphene field-effect transistor, high precision capillary printing, graphene oxide, electrochemical reduction, printed electronics

References:

1. de Araujo, E. N. D.; Stephan Lacerda de Sousa, T. A.; Guimarães, L. de M.; Plentz, F. Effects of Post-Lithography Cleaning on the Yield and Performance of CVD Graphene-Based Devices. *Beilstein Journal of Nanotechnology* **2019**, *9* (1), 349–355. https://doi.org/10.3762/bjnano.10.34.
2. Canale, L.; Laborieux, A.; Mogane, A. A.; Jubin, L.; Comtet, J.; Lainé, A.; Bocquet, L.; Siria, A.; Niguès, A. MicroMegascope. *Nanotechnology* **2018**, *29* (35). https://doi.org/10.1088/1361-6528/aacbad.
3. Fernández-Merino, M. J.; Paredes, J. I.; Villar-Rodil, S.; Guardia, L.; Solís-Fernández, P.; Salinas-Torres, D.; Cazorla-Amorós, D.; Morallón, E.; Martínez-Alonso, A.; Tascón, J. M. D. Investigating the Influence of Surfactants on the Stabilization of Aqueous Reduced Graphene Oxide Dispersions and the Characteristics of Their Composite Films. *Carbon N. Y.* **2012**, *50* (9), 3184–3194. https://doi.org/10.1016/j.carbon.2011.10.039.
4. Boukraa, R.; Mattana, G.; Battaglini, N.; Piro, B. A Complementary Reduced Graphene Oxide-Based Inverter for Ion Sensing †. *Engineering Proceedings* **2022**, *16* (1). https://doi.org/10.3390/IECB2022-12272.

Modulating The Resonance Response Of Monolayer Graphene Nanodrums: A Molecular Dynamics Study

Javier Varillas[1,2], Martin Kalbáč[1]
[1] Department of Low-Dimensional Systems. Heyrovsky Institute, Czech Academy of Sciences, Dolejškova 2155/3, Prague 8, 182 23, Czech Republic.
[2] Department of Ultrasonic Methods. Institute of Thermomechanics, Czech Academy of Sciences, Dolejškova 1402/5, Prague 8, 182 00, Czech Republic.

Abstract:
Atomically thin graphene resonators are an exceptional candidate for ultra-sensitive sensing applications due to their low mass and high mechanical stiffness. Recent research has shown that these devices exhibit tunable fundamental resonance frequency and quality factor (Q). In this study, we analyze a comprehensive set of molecular dynamics (MD) simulations to investigate oscillation ringdown responses of various monolayer graphene nanodrums under a wide range of pulse-like mechanical excitations, different geometries (namely circular, square, elliptical, hexagonal, and triangular resonators), and boundary conditions (i.e., ideal clamping vs. adhesive substrate support). To describe the C-C interactions in graphene, we use the optimized Tersoff interatomic potential [1], which shows a reasonable balance between realistic mechanical responses and vibrational-mode predictions, critical for reproducing graphene resonance. Our MD results indicate that nonlinear energy dissipation is affected by mechanical excitation parameters, where larger drive amplitudes induce greater mode coupling and faster vibrational decay, generally leading to a decrease in Q. In contrast, the resonance frequency is determined by intrinsic factors, such as the drum's geometry and pretension, remaining relatively stable across low and high-drive ringdowns. Comparing perfectly clamped nanodrums with those with adhesive-supported edges, we find that substrate compliance systematically increases dissipation. In supported graphene nanodrums, clamping losses, dominated by interfacial phonon scattering, generally translate into lower Qs. However, our computational results reveal that graphene-substrate adhesion can effectively tune dissipation, where increasing adhesion levels render higher Qs. These findings offer design insights for optimizing the performance of graphene resonators utilized for sensing.

Keywords: graphene nanodrums, molecular dynamics, nonlinear damping, clamping, ultra-high sensing detectors.

References:

1. L. Lindsay, D. A. Broido, *Phys. Rev. B* 81 (2010) 205441.

Understanding the nanoscale environment in next generation halide perovskite based devices

M. Anaya [1,*]
[1] Institute of Materials Science of Seville, Spanish National Research Council – University of Seville, Seville, Spain

Abstract:
In this talk, I will discuss the importance of nanoscale disorder in halide perovskites and how it governs their optical behaviour. I will show how the development of new strategies to interrogate buried perovskite films in real device configurations is key to modelling, designing and fabricating devices with new functionalities and superior performances.

Unlocking Robust 2D Hybrid Perovskite Optoelectronics

K.J. Riisnaes [1*], R. Mastria [2], A. Bacon [1], I. Lieontis [1], O. Lam [1], L. De Marco [2], M. Craciun [1], S. Russo [1]

[1] Department Physics and Astronomy, University Exeter, Exeter, United Kingdom
[2] Institute of Nanotechnology, Lecce, Italy

Abstract:
The exceptional performance demanded by next-generation optoelectronic systems places stringent requirements on active materials, including ultra-broad bandwidth, sub-nanosecond response times, high sensitivity, and stable operation under ambient conditions. Only a limited number of material systems meet these criteria. 2D organic–inorganic perovskites are emerging as a particularly promising candidate due to their remarkable photophysical properties and excellent charge transport characteristics.[1-5]

Despite these advantages, their broader adoption is hindered by poor environmental stability and high sensitivity to conventional processing solvents. In this talk, I will address these challenges by introducing strategies that enable robust top-down semiconductor processing of high-quality nanoscale structures based on 2D perovskites, alongside encapsulation approaches that significantly enhance their stability and long-term performance. [1-3]

I will then present the extensive characterisation of their optoelectronic properties, demonstrating performance that surpasses state-of-the-art commercial silicon and InGaAs-based devices. [2] In addition, I will provide insight into how intrinsic trap states are leveraged to achieve both ultra-high detectivity and ultrafast response times, effectively reconciling two typically competing performance metrics. [1]

Hence, I will showcase the integration of these materials into demanding real-world applications in both environmental monitoring and in the wearable industry, highlighting their potential to redefine the landscape of high-performance optoelectronics.[3]

Finally, I will briefly present very recent efforts towards wafer-scale fabrication of perovskite devices and the exploration of more sustainable types of 2D pervoskites such as tin-based[5].

Keywords: 2D hybrid perovskites, optoelectronics, ultrafast response, high detectivity, trap-assisted dynamics, environmental stability, top-down processing, nanoscale devices, encapsulation strategies, wearable and sensing applications

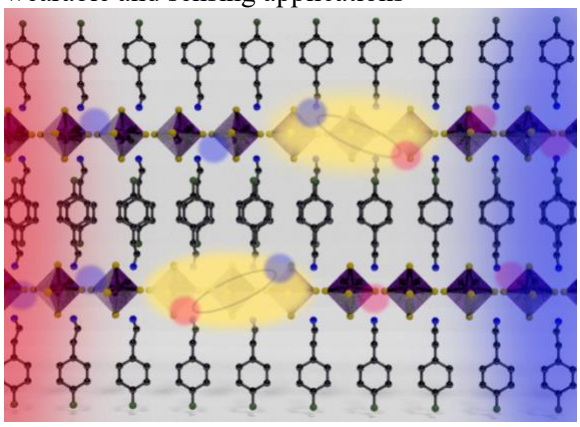


Figure 1: Figure illustrating a 2D perovskite crystal structure, the generation of excitons (yellow) and subsequently how these excitons are effectively split into free charge carriers (blue and red spheres). The figure also shows how these charge carriers are collected by applying an electric field (right, positive in red. Left, negative in blue).

References:

1. Leontis, I et al. 2026. Decoding Trap States in Working 2D Perovskite Multi-Functional Devices. *Advanced Science*, p.e18675.
2. Mastria, R. & Riisnaes, K.J. et al. 2024. Real Time and Highly Sensitive Sub-Wavelength 2D Hybrid Perovskite Photodetectors. *Advanced Functional Materials*, *34*(36), p.2401903.
3. Riisnaes, K.J. et al. 2024. 2D hybrid perovskite sensors for environmental and healthcare monitoring. *ACS Applied Materials & Interfaces*, *16*(24), pp.31399-31406.
4. Mastria, R. et al. 2026. Wafer-Scale Room-Temperature Processing of Lead-Free Perovskites for Optoelectronic Applications. *Advanced Science*, *13*(16), p.e17469.
5. Durante, O. et al. 2026. Trap-Assisted Transport and Neuromorphic Plasticity in Lead-Free 2D Perovskites PEA2SnI4. *Advanced Functional Materials*, *36*(30), p.e26339.

Tailoring structured multifunctional carbon nanotube supported catalysts for the valorization of glycerol to 1,2-propanediol

Dominique Lumpp[1], Mahsa Mohammadi[1], Jakob Albert[1]*
[1] Institute of Technical and Macromolecular Chemistry, University of Hamburg, Bundesstrasse 45, 20146 Hamburg, Germany

Abstract:
A significant challenge within the Collaborative Research Center 1615 “SMART Reactors” is the design of a multifunctional catalyst for the selective hydrogenolysis of glycerol into 1,2-propanediol under mild reaction conditions. To enhance the catalyst's resilience against poisoning, it is essential that the catalyst's properties can be adjusted to the local process conditions, allowing rare noble metals to last longer and be utilized more sustainable. In this context, carbon nanotubes (CNTs) appear to be a promising support material. Identifying the optimal CNT support and the ideal combination of transition and noble metals is a crucial step in the development of the multifunctional catalyst. This lays the foundation for implementing this highly active and selective catalyst in a future SMART reactor for glycerol valorisation. This work supports the sustainable industrial catalytic processes and thus contributes to Sustainable Development Goal 9 "Build resilient infrastructure, promote inclusive and sustainable industrialization, and foster innovation."

Keywords: Glycerol hydrogenolysis, Carbon nanotubes, Heterogeneous catalysis, 1,2-propanediol, Structure-activity-selectivity-relationship.

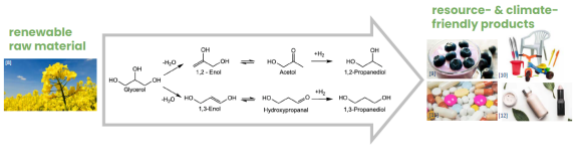


Figure 1: Scheme from renewable glycerol to sustainable 1,2-propanediol for resource and climate-friendly products

References:

1. Sherbi, M., Wesner, A., Wisniewski, V. K., Bukowski, A., Velichkova, H., Fiedler, B., Albert, J., Catalysis Science & Technology 11, 6649 – 6653 (2021), DOI: 10.1039/D1CY01518D.
2. D. Lumpp, S. Shaikh, F. Riebesehl, C. Ruhmlieb, K. Kruber, B. Schroeter, I. Smirnova, M. Ski-borowski, B. Fiedler, J. Albert, „Multifunctional carbon-nanotube supported catalyst for efficient glycerol hydrogenolysis to 1,2-propanediol”, ChemChatChem, 2026, 18, 5, e01748, DOI:10.1002/cctc.202501748.

Sensors 2026 / NanoMed 2026 Joint Session II.B: Nanotechnology in Diagnostics, Imaging & Bio-Sensing / Biomedical sensors

Bioinspired nanobiosensors for portable and wearable diagnostics

Elisa Michelini
Department of Chemistry “Giacomo Ciamician”, Via Gobetti 85 Bologna, 40129-Italy
elisa.michelini8@unibo.it

Abstract:

The development of biosensors that combine sustainability, high analytical performance, and compatibility with smartphone-based readout remains a significant challenge in modern diagnostics. Different biorecognition elements, including enzymes, whole cells, and cell-free transcription-translation systems, can be integrated into sustainable, low-cost supports to produce fit-for-purpose biosensors, including wearable formats such as skin patches and facemask-integrated devices.

This work presents the implementation of multiple strategies and sensing platforms aimed at enhancing the performance of optical biosensors based on bio-chemiluminescent and colorimetric detection, in combination with bioinspired nanomaterials. These approaches address diverse diagnostic challenges, including cystic fibrosis and skin cancer. The integration of bioluminescence with nanomaterials (e.g., metal-organic frameworks and gold nanoparticles) and with paper-based, 3D-printed and facemask-embedded sensors is also reported.[1,2]

Cell-based and cell-free optical biosensors developed using synthetic biology tools and interfaced with smartphone detection are described. Modular biosensing architectures employing orthogonal bioluminescent and colorimetric readouts were designed for multiplexed analysis and embedded into wearable platforms. Facemask-integrated biosensors were developed for monitoring cystic fibrosis biomarkers, specifically nitrate and quorum-sensing molecules associated with *Pseudomonas aeruginosa* infection, in exhaled breath condensate. These devices combine colorimetric detection based on the Griess reaction with bioluminescence to enable multiplexed sensing.

Keywords: biosensor, microneedle, wearable, bioluminescence, diagnostics, point-of-care

References:

1. Cambrea C, Rodriguez Arias RJ, Desiderio R, Nazir F, Calabretta MM, Michelini E (2026). Novel Smartphone Paper Sensor for One Health: Monitoring Free Chlorine in Water and Exhaled Breath Condensate. *Sensors (Basel)*.26,3066.
2. Martínez-Pérez-Cejuela H, Calabretta MM, Michelini E. (2024) Chemiluminescence "Add-and-Measure" Sensing Paper Based on the Prussian Blue/Metal-Organic Framework MIL-101 Nanozyme for Rapid Hydrogen Peroxide Detection. *Anal Chem.* 96:16561-16569.

Matrix-Activated Sensors for Human Serum Analysis

A. Barbaroux [1*], B. Chovelon [1,2], E. Fiore [1], S. Vezirian [1,2], M. Henry [1], M. Zoubeidi [3], M. C. DeRosa [3], C. Ravelet [1], E. Peyrin [1]

[1] DPM UMR 5063, University Grenoble Alpes, Grenoble, France

[2] Biochemistry, Toxicology and Pharmacology Department, Grenoble site Nord CHU– Biology and Pathology Institute, Grenoble, France

[3] Department of Chemistry, Carleton University, Ottawa, Canada

Abstract:

Human serum is one of the most used matrices in blood diagnostics. Several fluorescent aptamer-based assays in solution phase were developed for the detection of small molecules in serum, due to their ease of use. Currently, these assays are developed in buffer solution, before adaptation into matrix. However, the transposition from buffer to serum usually leads to several uncontrolled variations: decrease of aptamer-target affinity[1], partial or complete signal lost[2] or increase of signal background[3]. These effects are called matrix effects. To address these challenges, we propose here an innovative aptamer-based assay considering serum as an integral part of the detection system (Figure 1). When fluorophore-labelled aptamer interacts with most abundant serum proteins, namely albumin and immunoglobulins G, this leads to an increase in fluorescence anisotropy signal (FA). In presence of target, the aptamer displacement from proteins to target induces a decrease in signal. As proof of concept, this assay was at first developed for the recognition of model target, L-tyrosinamide. Variation of L-tyrosinamide concentration for different serum fractions showed an optimal signal between serum 25%-90%. Then, the method was optimised for six biomedical targets detection, at serum 50%. Finally, we used the standard addition method with a logit-log approach[4] to apply the system for quantification. Thus, the developed method enables the direct quantification of small molecules in serum-rich samples, ensuring the robustness to matrix effects. These findings pave the way for advancements in the clinical use of homogeneous aptamer sensors.

Keywords: human serum, aptamer, matrix proteins, small molecule, fluorescent sensor.

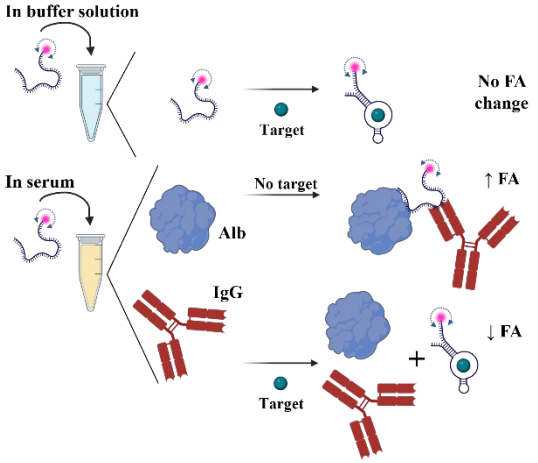


Figure 1: Principle of the developed method. In a buffer solution, the formation of the aptamer-target complex does not result in a sufficient change in mass to cause a variation in fluorescence anisotropy (FA). In the serum, the aptamer interacts with serum proteins in absence of target, leading to a mass-dependent increase in FA. In the presence of the small analyte, these assemblies are competitively prevented by the target binding to the aptamer, which leads to an increased fraction of the non-protein-bound probe and thus a target-dependent reduction in FA.

References:

1. Liu, Y., Zhao, Q. (2017) Direct Fluorescence Anisotropy Assay for Cocaine Using Tetramethylrhodamine-Labeled Aptamer. *Anal Bioanal Chem*, *409* (16), 3993–4000.
2. Gu, L., Zhang, Y., Wang, D., Liu, J. (2024) Light-Up Sensing Citrate Using a Capture-Selected DNA Aptamer. *Advanced Sensor Research*, *3* (6), 2300167.
3. Zhu, Z., Ravelet, C., Perrier, S., Guieu, V., Fiore, E., Peyrin, E. (2012) Single-Stranded DNA Binding Protein-Assisted Fluorescence Polarization Aptamer Assay for Detection of Small Molecules. *Anal. Chem.*, *84* (16), 7203–7211.
4. Conrad, M., Fechner, P., Proll, G., Gauglitz, G. (2023) (R)Evolution of the Standard Addition Procedure for Immunoassays. *Biosensors (Basel)*, *13* (9), 849.

Modulating Agglutination for Quantitative Paper Diagnostics

Anuragmani Tripathi, Rishabh More, Simon Corrie, Gil Garnier*
Bioresource Processing Research Institute of Australia (BioPRIA), Department of Chemical and Biological Engineering, Monash University, Victoria, Australia

Abstract:
Agglutination assays are widely used for many applications such as blood typing and infectious diseases [1, 2]. However, current tests are limited by qualitative or semi-quantitative readout [3]. Paper has emerged as a powerful microfluidic substrate which enables pump-free transport of biomolecules and nanoparticles to detection zones. The integration of agglutination assays with paper-based microfluidic platforms offers a promising approach to engineer low-cost, rapid and even quantitative point-of-need diagnostics. A recent study has demonstrated the feasibility of transport encoded agglutination sensing on paper, enabling instrument-free quantitative analysis [4]. Despite this progress, a fundamental challenge remains: how can the difference in transport behaviour between agglutinated and non-agglutinated particles be amplified to improve sensor sensitivity and signal resolution? Here, we investigate the relationship between particle agglutination, porous paper structure and the resulting distance-based readout. Antibody-functionalised latex particles with controlled physio-chemical properties are used to understand how changes in particle size and agglutinate state interact with the fibrous structure of paper substrate. The influence of key parameters, including paper structure, latex bead size, analyte loading, is quantified to elucidate their role in enhancing signal discrimination. This study aims to identify the bead size and paper structure that maximise the difference in transport distance between agglutinated and non-agglutinated beads. These findings will guide the development of distance-based agglutination sensors with improved signal resolution and sensitivity.

Keywords: agglutination, paper, microfluidics, quantitative sensor, distance-based sensing, point-of-care diagnostics, biomedical sensors.

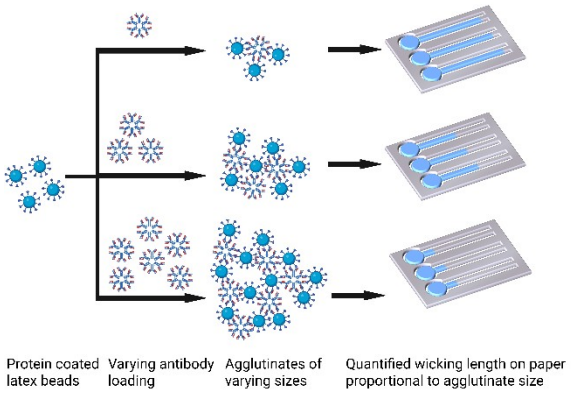


Figure 1: Effect of agglutination on wicking in paper-based microfluidics with coloured latex beads. Analyte concentration is quantified with the wicking lengths of target agglutinates of varying in sizes.

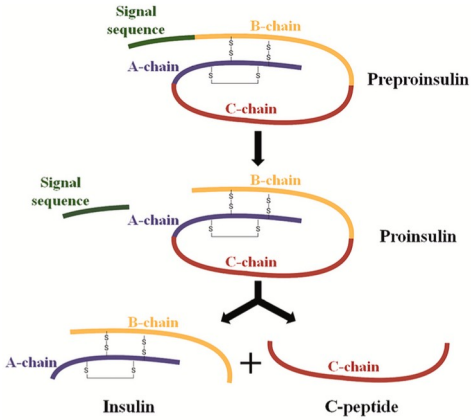
References:

1. M.S. Khan, G. Thouas, W. Shen, G. Whyte, G. Garnier, Paper Diagnostic for Instantaneous Blood Typing, Analytical Chemistry 82(10) (2010) 4158-4164.
2. A. Tripathi, S. Corrie, G. Garnier, Engineering the retention of coloured latex and red blood cells for paper agglutination diagnostics, Journal of Colloid and Interface Science 700 (2025) 138336.
3. S. Esmail, M.J. Knauer, H. Abdoh, C. Voss, B. Chin-Yee, P. Stogios, A. Seitova, A. Hutchinson, F. Yusifov, T. Skarina, E. Evdokimova, S. Ackloo, L. Lowes, B.D. Hedley, V. Bhayana, I. Chin-Yee, S.S.C. Li, Rapid and accurate agglutination-based testing for SARS-CoV-2 antibodies, Cell Reports Methods 1(2) (2021) 100011.
4. B. Kalish, J. Zhang, H. Edema, J. Luong, J. Roper, C. Beaudette, R. Echodu, H. Tsutsui, Distance and Microsphere Aggregation-Based DNA Detection in a Paper-Based Microfluidic Device, SLAS Technology 25(1) (2020) 58-66.

C-peptide Immunosensor as a novel tool for Diabetes Management

Riccarda Antiochia[1], Cristina Tortolini[1], Francesco Dotta[2]
[1]*Dept. of Experimental Medicine, Sapienza University of Rome*
V.le Regina Elena 324, 00166 Rome, Italy
[2]*Dept. of Biomedical Sciences, National Research Council*
Piazz.le Aldo Moro 7, 00185 Rome, Italy
riccarda.antiochia@uniroma1.it; cristina.tortolini@uniroma1.it; francesco.dotta@cnr.it

C-peptide is a critical biomarker for evaluating pancreatic β-cell function and managing diabetes. It is secreted by pancreatic β-cells in equimolar amounts as insulin. They are simultaneously released into the capillary circulation, but C-peptide is not destroyed by the liver and has a longer half-life than insulin [1].



Therefore, C-peptide levels are considered a superior clinical biomarker for β-cell function, and therefore for endogenous insulin secretion. Another practical advantage of C-peptide determination over insulin is that the former can be evaluated in patients undergoing insulin therapy. In addition, circulating C-peptide determination allows to better distinguish between type 1 and type 2 diabetes [2] and may indicate also diabetes-related diseases, such as pancreatic dysfunction and problems related to the kidneys and heart. As a result, several studies have focused on determining C-peptide levels in the body [3]. However, conventional methods, such as enzyme-linked immunosorbent assay (ELISA) and chemiluminescence immunoassay are limited by lengthy processing times and high costs. Biosensors are precise and advanced tools for rapid and low-cost detection of multiple disease-related biomarkers which can help in the early diagnosis of diabetes and related diseases and proper monitoring and treatment. Although significant progress has been made in the development of biosensors in recent years, only a few C-peptide detection biosensors have been designed to date [4].

Here, we describe a novel label-free electrochemical immunosensor for a fast, simple, cheap, sensitive and accurate C-peptide detection, based on iron-oxide magnetic nanoparticles (MNPs), properly modified and immobilized on a graphite screen-printed electrode (SPE). The MNPs, together with the use of a magnetic support for the SPEs, allowed a higher reproducibility of the electrode modification by drop-casting technique, avoiding coffee-ring effect [5]. This aspect plays a key role in the immunosensor development, where the surface stability is one of the main issues to address. Moreover, MNPs amplified current response signals and enhanced sensitivity through their conductive properties and large specific surface areas, showing also excellent biocompatibility with antibodies, and low toxicity. The proposed immunosensor allowed the detection of C-peptide in the nanomolar range in human serum samples collected from healthy people and patients under pharmacological treatment, showing excellent agreement with the results obtained with the conventional ELISA method.

[1] J. Chen, Y. Huang, C. Liu, et al., *Front. Endocrinol*. 14 (2023)
[2] S. Iqbal, A.A. Jayyab, A.M. Alrashdi, et al., *Endocr. Pract*. 29 (2023) 379-387
[3] H. Ahmadirad, F. Teymoori, E. Mokhtari, et al., *Front. Cardiovasc. Med.*, 2023
[4] Z. J. Bahaabadi, P. Kesharwani, A. Sahebkar, *Microchem. J.* 207 (2024) 111922
[5] A. Kaliyaraj, S. Kumar, Y. Zhang, D. Li, R.G. Compton, *Electrochem. Commun*. 121 (2020), 106867

Rapid handheld graphene FET platform for dual acute myocardial infarction biomarker detection

J.P. Ramoso [1*], L. Ranatunge [1], W. Balachandran [1]
[1] Engineering Department, Brunel University of London, London, UK

Abstract:
Rapid rule-out of acute myocardial infarction (AMI) still relies largely on laboratory high-sensitivity cardiac troponin assays with turnaround times of 30–90 minutes, while current quantitative point-of-care (POC) devices typically require 15–30 minutes and the fastest emerging systems report analysis times of about 8–15 minutes. Here we report a portable graphene field-effect transistor (GFET) platform designed to deliver an AMI biomarker result in approximately 5 minutes while maintaining comparable analytical performance. Our device uses commercial CVD graphene transistors functionalised with capture probes for myoglobin (Mb) and cardiac troponin I (cTnI) on separate chips, integrated into a handheld unit incorporating a transimpedance amplifier, microcontroller and custom interface for automated gate-voltage sweeps and on-board Dirac-point analysis. We present preliminary electrical data in buffer demonstrating clear and opposite shifts in the Dirac point upon exposure to each biomarker. For Mb, the transfer characteristics exhibit a leftward shift, with the minimum drain current changing from 0.1469 mA at 0.21 V to 0.1344 mA at 0.12 V (~0.09 V shift). For cTnI, a rightward shift is observed, from 0.1984 mA at 0.45 V to 0.1991 mA at 0.69 V (~0.24 V shift). These results confirm robust, directionally distinct responses for two clinically relevant AMI biomarkers using a unified GFET platform. Ongoing work focuses on establishing calibration curves, analytical sensitivity and selectivity in complex matrices and across devices, to translate this architecture into a clinically deployable handheld AMI triage tool.

Keywords: Graphene, GFET, myoglobin, troponin I.

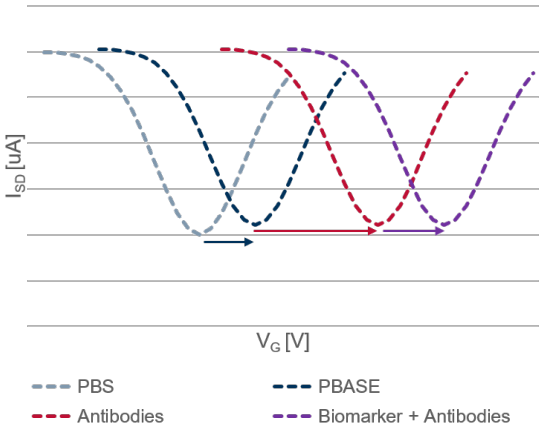


Figure 1: Dirac point shifts in sequential GFET transfer curves measured in PBS, after PBASE functionalisation, after antibody immobilisation and after biomarker binding, confirming successful biofunctionalisation and target recognition.

References:

1. Krsihna, B. V., Gangadhar, A., Ravi, S., Mohan, D., Panigrahy, A. K., Rajeswari, V., & Prakash, M. D. (2022). A Highly Sensitive Graphene-based Field Effect Transistor for the Detection of Myoglobin. *Silicon*, 14(17), 11741–11748. https://doi.org/10.1007/s12633-022-01790-9
2. Lei, Y., Xiao, M., Li, Y., Li, X., Zhang, H., Zhang, Z., Zhang, G., & Zhang, G. (2016). Detection of heart failure-related biomarker in whole blood with graphene field effect transistor biosensor. *Biosensors and Bioelectronics*, 91, 1–7. https://doi.org/10.1016/j.bios.2016.12.018
3. Ramoso, J. P., Rasekh, M., & Balachandran, W. (2025). Graphene-Based Biosensors: Enabling the Next Generation of Diagnostic Technologies—A Review. *Biosensors*, *15*(9), 586. https://doi.org/10.3390/bios15090586

Graphenic DCDR/GERS Platforms for Ultrasensitive and Selective Raman Detection of Human Interleukin-6

Emmanuel de la O-Cuevas[2], José M. Saniger[1]*
[1]Instituto de Ciencias Aplicadas y Tecnología, Universidad Nacional Autónoma de México, Mexico City, Mexico; [2]Universidad Autónoma de Zacatecas, Zacatecas, Mexico. *jose.saniger@icat.unam.mx

Abstract:
Human interleukin-6 (IL-6) is a clinically relevant cytokine whose concentration changes in biological fluids are associated with inflammatory, autoimmune, neurodegenerative, and malignant disorders. Here, we integrate two complementary graphene-based strategies to establish a label-free Raman platform combining ultrasensitive detection with selective molecular recognition. In the first approach, microliter droplets of IL-6 in phosphate-buffered saline were dried on reduced graphene oxide/silicon (rGO/Si) substrates. Drop-coating deposition Raman (DCDR) preconcentration at the coffee-ring, coupled with graphene-enhanced Raman scattering (GERS), enabled reliable identification of IL-6 below 1 pg mL-1, corresponding to an absolute detected mass of approximately 1 fg. Compared with bare silicon, the enhancement factor increased as analyte concentration decreased, while the Raman profile remained well resolved and essentially free from spectral deformation. In the second approach, Langmuir-Blodgett films of graphene oxide and amine-functionalized rGO (rGO-NH2) were functionalized with monoclonal IL-6 antibodies. Raman imaging showed that IL-6 was detected exclusively within the antibody coffee-ring, confirming spatially selective antigen-antibody recognition. The interaction pattern depended strongly on graphene surface chemistry: pristine graphene oxide produced heterogeneous domains, whereas rGO-NH2 promoted a more consistent layered rGO-NH2/antibody/IL-6 architecture. Amination favors antibody anchoring through terminal carboxyl groups while preserving antigen-binding sites, and the larger aromatic domains of rGO support interfacial interactions relevant to GERS. Together, these results demonstrate that control of graphene oxidation, functionalization, and mesoscale deposition can unite sensitivity, selectivity, and spatial readout in a reproducible biosensing platform. This modular concept may be extended to other low-abundance biomarkers and complex biological matrices.

Keywords: graphene-enhanced Raman scattering; reduced graphene oxide; Raman imaging; interleukin-6.

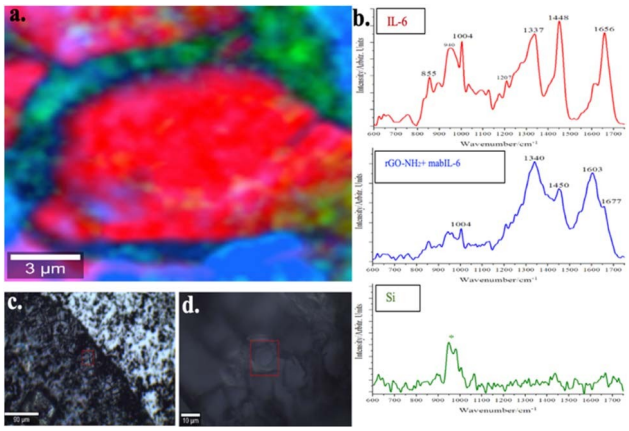


Figure 1. Raman image and representative spectra of the rGO-NH_2/mabIL-6/IL-6 layered array. Reproduced from RSC Advances 13 (2023) 15114-15120, CC BY 3.0.

References

1. E. de la O-Cuevas, I. Badillo-Ramírez, S. R. Islas, C. Araujo-Andrade and J. M. Saniger, “Sensitive Raman detection of human recombinant interleukin-6 mediated by DCDR/GERS hybrid platforms,” RSC Adv. 9 (2019) 12269-12275. https://doi.org/10.1039/C9RA01396B.
2. E. de la O-Cuevas, S. R. Islas, P. Gallegos-Flores, E. L. Esparza-Ibarra, H. Tototzintle-Huitle and J. M. Saniger, “Modulating the interaction of graphenic substrates with human interleukin-6 and its monoclonal antibody: a study by Raman images,” RSC Adv. 13 (2023) 15114-15120. https://doi.org/10.1039/D3RA01627G.

A Novel Lab On-A-Chip For Biomarkers Monitoring On In Vitro Barriers Models

Simone Marasso[1,2], Martina Cicolini[2], Jovana Babic[2], Raquel Cue López[2], Alberto Ballesio[1,2], Matteo Cocuzza[1,2], Francesca Frascella[2], Lucia Napione[2]

[1] IMEM, National Research Council (CNR), Parma, Italy
[2] DISAT, Politecnico di Torino,Torino, Italy

Abstract:
Nowadays, in vitro models lack sensors integration and monitoring tools that are strategic to develop platforms for personalized medicine [1]. Moreover, the detection of specific biomarkers is needed to proper obtain a robust diagnostic output especially to detect the passage through a specific biological barrier i.e. blood brain barrier, gut barrier, endothelial barrier, skin and so on. To face these important issues, in this work **a Lab-on-a-chip (LOC) platform for monitoring barrier models, in particular a skin barrier has been successfully developed**.
The LOC device comprehends two levels of microfluidics with **integrated Organic Electrochemical Transistor** (**OECT**) biosensors for monitoring the conditions of the *in vitro* cellular model and relevant biomarkers [2]. OECT have been selected since they are able to work also in contact with wet environment and humidity for long periods. The first step was the design of the multi-layer microfluidic device in CAD (figure 1), in details: i) a culture chamber with an additional layer for hosting a membrane, ii) two OECT inside a sealing layer to be in contact with the top and with the bottom parts, iii) a filling chamber for the lower part of the central membrane and iv) a microfluidic structure to allow connection between the culture medium and the OECT sensors.
Two versions of the platform were designed to **incorporate two different membranes for cell culture: a PolyCarbonate (PC) and a silk fibroin based**. The two membranes were rispectively (38 ± 3) µm PC one and (210 ± 10) µm for the silk one. The designed platform was made in Polydimethylsiloxane (PDMS) using replica molding technique. **The master molds were obtained by 3D printing** with a PolyJet technology (Stratasys J35), as well as the sealing plugs. The three layers were bonded with plasma embedding the membrane. The OECT chips with the electrodes were fabricated in clean room environment and then completed in the additive manufacturing laboratory by the inkjet deposition of the channel material PEDOT:PSS , with three different values of the drop spacing (80, 100 and 120 µm). The characterization of the fabricated devices included leakage tests (by dyed PBS solution) and electrical measurements of the OECTs.
The platform with PC membrane showed good results in terms of leakage and flow **(**figure 1), while the one with silk membrane requires further optimization to avoid bending and leakages between the two layers. A proof of concept of the biosensing capabilities of the integrated **OECTs was performed by measuring the response of the devices to different concentrations of Ang2 in PBS solution**. Final experiments with cells are ongoing to prove the capability of the chip.

Keywords: Organ on a chip, Biosensors OECTs, PDMS,

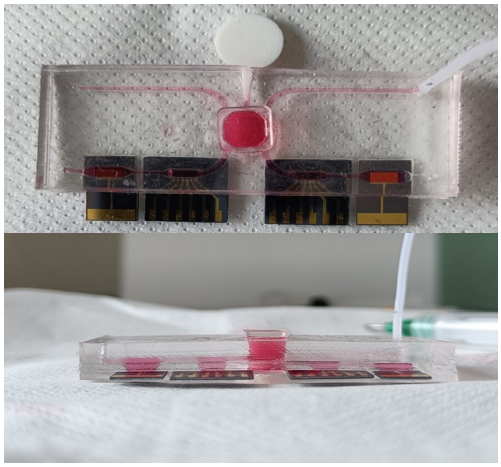


Figure 1: LOC filled with culture medium

REFERENCES

1. Ling S, Xu C, Jiang Y, Xu F, Jin H, Chen H, Chen S, Ding Z, Sun D Toward continuous monitoring systems: emerging trends of on-chip sensors in organ-on-a-chip. *Microsyst Nanoeng*, 2026, **12**,61.
2. Babic J, Ballesio A, Frascella F, Napione L, Pagani M, Parmeggiani M, Marasso SL A contamination-free electrolyte-gated organic transistors platform for high-accuracy tumor biomarker detection. *Sensors and Actuators Reports*, 2025, **9**,100341.

From bilayer to multilayer BGO/ZnO heterostructures for fast-timing ToF-PET detectors

M. Konefał [1,*], N. Babayevska [1], A. Padmanaban [2], I. Yakymenko [2], I. Iatsunskyi [1], M. Jancelewicz [1], O. Sidletskiy [2,3]

[1] NanoBioMedical Centre, Adam Mickiewicz University, Poznań, Poland

[2] Centre of Excellence ENSEMBLE3 Sp. z o.o., Warsaw, Poland

[3] Institute for Scintillation Materials NAS of Ukraine, Kharkiv, Ukraine

Abstract:

Fast and precise tumor detection in modern imaging techniques, such as time-of-flight positron emission tomography (ToF-PET), requires improved detector sensitivity and timing performance [1]. Among the approaches under investigation, heterostructures that combine a dense scintillator with a high γ-ray stopping capability and a fast-emitting component are of particular interest, as energy sharing between the two materials may enhance timing resolution [2]. Here, we combine the widely used scintillator bismuth germanate (BGO) with zinc oxide (ZnO), which has a fast luminescence decay, and present the progression from bilayer to multilayer BGO/ZnO heterostructures. In bilayer systems, ZnO films were deposited on BGO by sol–gel spin-coating, spray-coating, drop-casting, or low-temperature hydrothermal growth, which enabled control of morphology, crystallinity, and luminescence properties. The resulting crystalline ZnO coatings with thicknesses in the range of 2–28 μm reduced the coincidence time resolution (CTR) from 276 ps for pristine BGO to 158-246 ps depending on the deposition method and resulting ZnO layer properties. Subsequently, plate-type multilayer heterostructures of 4 × 4 × 20 mm^3 were assembled from alternating BGO/ZnO layers. The morphology and phase composition of the layers were examined by scanning electron microscopy and X-ray diffraction. The relationships between structure, photoluminescence, and timing performance will be discussed, together with design criteria for multilayer heterostructures as next-generation fast-timing ToF-PET detectors.

Keywords: scintillation heterostructures, BGO, ZnO, ToF-PET, coincidence time resolution, multilayer detectors.

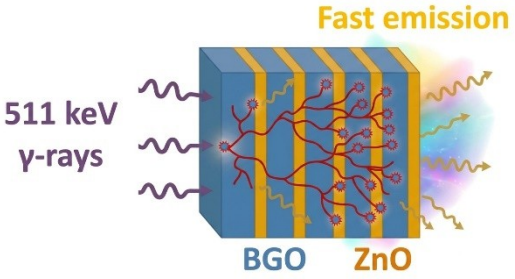


Figure 1: Schematic illustration of the multilayer BGO/ZnO heterostructure.

Acknowledgments: This work was supported by the National Science Centre of Poland (OPUS project DEC- 2022/47/B/ST5/02288).

References:

1. Lecoq, P. et al. (2020) Roadmap toward the 10 ps time-of-flight PET challenge, *Phys. Med. Biol*., 65, 21RM01.
2. Pagano, F. et al. (2022) Advances in heterostructured scintillators: toward a new generation of detectors for TOF-PET, *Phys. Med. Biol.*, 67, 135010.

NanoMed 2026 Session II. C: Nanotechnology in Drug Delivery, Oncology & Theranostics / Safety & Future Frontiers

Nanoengineering the Bone Regenerative Microenvironment

Isabel Izquierdo-Barba
1. Departamento Química en Ciencias Farmacéuticas, Facultad de Farmacia, Universidad Complutense de Madrid, Plaza Ramón y Cajal s/n, 28040 Madrid, Spain.
2. CIBER de Bioingeniería, Biomateriales y Nanomedicina (CIBER-BBN), 28040 Madrid, Spain.

Abstract:
Bone regeneration is a complex process that requires the coordinated interplay of biological, chemical, and physical cues within the local microenvironment. Nanotechnology offers promising opportunities to engineer this microenvironment through the development of multifunctional nanomaterials capable of actively promoting tissue repair [1]. In this context, our research focuses on two complementary nanotechnology-based strategies for bone regeneration: mesoporous bioactive glass nanoparticles (MBGNs) and superparamagnetic iron oxide nanoparticles (SPIONs). MBGNs are being engineered as multifunctional platforms that combine their intrinsic osteogenic potential with the ability to address infection, one of the major challenges in bone tissue regeneration. By integrating regenerative and antimicrobial functionalities within a single nanosystem, these materials offer a promising approach for bone repair in infection-compromised environments [2]. In parallel, SPIONs are being explored as a strategy to promote bone regeneration through magnetically mediated mechanotransduction. Their magnetic responsiveness provides opportunities to deliver physical stimuli to cells and modulate mechanosensitive signaling pathways involved in osteogenic differentiation and tissue regeneration [3]. This keynote will provide an overview of these two research directions, highlighting how the rational design of bioactive and magnetically responsive nanoparticles can contribute to the development of advanced strategies for bone tissue engineering. Although based on distinct mechanisms of action, both approaches share a common objective: to engineer the bone regenerative microenvironment and create favorable conditions for effective tissue repair.

Keywords: Bone regeneration; Mesoporous bioactive glass nanoparticles; Superparamagnetic iron oxide nanoparticles; Osteogenesis; Mechanotransduction; Infection.

References

1. Vallet-Regí, M., Colilla, M., Izquierdo-Barba, I., Vitale-Brovarone, C., & Fiorilli, S. (2022). Achievements in Mesoporous Bioactive Glasses for Biomedical Applications. Pharmaceutics, 14(12), 2636.
2. Polo-Montalvo, A., Gómez-Cerezo, N., Cicuéndez, M., González, B., Izquierdo-Barba, I., & Arcos, D. (2025). Osteogenic and Antibacterial Response of Levofloxacin-Loaded Mesoporous Nanoparticles Functionalized with N-Acetylcysteine. Pharmaceutics, 17(4), 519.
3. Estévez, M., Cicuéndez, M., Colilla, M., Vallet-Regí, M., González, B., & Izquierdo-Barba, I. (2024). Magnetic colloidal nanoformulations to remotely trigger mechanotransduction for osteogenic differentiation. Journal of Colloid and Interface Science, 664, 454–468.

Engineering Nanoemulsions: How Lipid Composition Controls Cellular Outcomes

Dávila Ibáñez AB[1,3,*], Funtes Varela Laura[1,2,3], , Susana Bravo[1,3], Clotilde Costa[1,3] , Antía Cabezas, Rafael López López[1,2,3]

1. Translational Medical Oncology (Oncomet), Health Research Institute of Santiago (IDIS), Santiago de Compostela, Spain
2. Universidade de Santiago de Compostela (USC), Santiago de Compostela, Spain
3. CIBERONC, Centro de Investigación Biomédica en Red Cáncer, Madrid, Spain

Abstract:

Nanoemulsions (NEs) are widely used for the delivery of hydrophobic compounds due to their high solubilization capacity, large interfacial area, and controlled-release properties. Beyond their role as passive carriers, increasing evidence suggests that the intrinsic physicochemical properties of NEs, particularly lipid-core composition, can directly modulate cellular behavior, influencing membrane interactions, intracellular trafficking, metabolic responses, and therapeutic activity. However, the mechanisms by which lipid-core chemistry regulates adaptive versus cytotoxic cellular programs remain poorly understood.

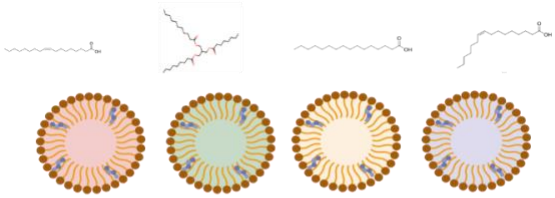
In previous work, we demonstrated that verteporfin-loaded Miglyol®-based nanoemulsions (VP-MG-NEs) exhibited improved physicochemical stability and enhanced photodynamic therapy (PDT) performance compared with oleic acid-based NEs. We also observed that MG-based formulations partially protected cells from verteporfin-associated toxicity before light activation, highlighting the critical role of lipid-core composition in modulating NEs functionality and cell-nanocarrier interactions. Based on these findings, we sought to systematically investigate how different lipid-core formulations intrinsically regulate cellular responses, adaptive programs, and cytotoxicity in SKOV-3 ovarian cancer cells[1].

To address this, we evaluated four lipid-core NEs containing oleic acid (OA), palmitic acid (PA), palmitoleic acid (POA), or medium-chain triglycerides (Miglyol®, MG), which differ in hydrocarbon chain length and degree of saturation, using physicochemical characterization, viability assays, flow cytometry, nanoparticle tracking analysis (NTA), and quantitative proteomics. Despite comparable nanoparticle exposure conditions, each formulation induced markedly distinct cellular responses.

OA- and POA-based NEs (both unsaturated, with different chain lengths) induced an initial transient increase in cellular viability, consistent with a hormetic response, followed by an abrupt, threshold-like collapse in viability. In contrast, PA-based NEs (saturated) induced a more progressive but pronounced cytotoxic effect. Notably, MG-based NEs displayed significantly lower intrinsic toxicity, requiring higher nanoparticle loads to reach IC_{50} values and promoting gradual adaptive remodeling rather than acute cellular collapse.

Proteomic analyses under sub-IC_{50} and IC_{50} conditions revealed formulation-dependent adaptive trajectories involving metabolic rewiring, oxidative stress regulation, membrane remodeling, mitochondrial adaptation, and transcription-associated pathways. Unsaturated lipid formulations preferentially activated oxidative stress, trafficking, and hypoxia-related programs, whereas PA-based NEs induced extensive metabolic and transcriptional reorganization. Notably, MG-NEs elicited comparatively limited stress-associated perturbations despite high nanoparticle exposure.

Furthermore, surviving post-IC_{50} populations displayed protein signatures associated with stress tolerance and survival adaptation, supporting the concept that lipid-core chemistry actively shapes cellular fate under therapeutic pressure. Collectively, our findings demonstrate that lipid composition is not merely a structural component of NEs but a critical regulator of cellular adaptation and therapeutic response, providing mechanistic insights for the rational design of safer and more effective nanocarrier-based therapeutic strategies.



Parameters	OA-NEs	MG-NEs	PA-NEs	POA-NEs
Dynamic Light Scattering (DLS)				
Size (nm)	141 ± 5	106 ± 9	225 ± 16	119 ± 16
PDI	0.20 ± 0.02	0.19 ± 0.01	0.21 ± 0.027	0.25 ± 0.02
Charge (mV)	-34.40 ± 8.30	-14.40 ± 2.88	-36.03 ± 3.19	-34.70 ± 1.49
Nanoparticle Tracking Analysis (NTA)				
N° nanoparticles (nps/mL)	1.07×10^{11}	1.15×10^{11}	6.81×10^{10}	1.41×10^{11}

Figure 1:
Schematic representation of the different nanoemulsions analyzed and their physicochemical properties.

References: *Nanoscale Adv.*, 2025,7, 6972-6986

Biofunctionalized ZnO nanoflowers as a non-viral mechanoporation platform for gene delivery in epidermolysis bullosa

Giacomo **Mandriota**[1,2], Gabriella **Leccese**[1,2,3], Claudia **De Stradis**[1,2,3], Rita Maria **Percoco**[1,2,3], Clara **Baldari**[1,2,3], Simone **Schirinzi**[1,2,4], Stefania **D'Amone**[1,2] Gabriele **Maiorano**[1,2], Giuseppe **Gigli**[1,2,3], Ilaria Elenà **Palamà***[1,2] giacomo.mandriota@cnr.it; *ilariaelena.palama@cnr.it

[1]Institute of Nanotechnology (NANOTEC) - National Research Council (CNR), c/o Campus Ecotekne, Lecce 73100, Italy

[2]Tecnomed Puglia - Tecnopolo per la medicina di precisione (Biotech Lecce Hub), c/o Campus Ecotekne, Lecce 73100, Italy

[3]Department of Experimental Medicine, University of Salento, c/o Campus Ecotekne, Monteroni street, Lecce 73100, Italy

[4]Department of Mathematics and Physics "Ennio De Giorgi", University of Salento, c/o Campus Ecotekne, Lecce 73100, Italy.

Abstract:

Epidermolysis bullosa (EB) is a hereditary blistering disorder caused by mutations in genes that encode structural proteins at the dermal-epidermal junction.[1] Although gene therapy offers a promising treatment approach, delivering nucleic acids safely and efficiently into primary skin cells remains challenging due to issues with viral vectors, including immunogenicity, limited cargo capacity, and manufacturing challenges.[2] This study introduces a non-viral mechanoporation technique using (bio)functionalized zinc oxide nanoflowers (ZnO-NFs) to deliver genes into cells relevant to EB. The ZnO-NFs are produced via a simple alkaline precipitation process and coated with polycations to improve stability and DNA binding. Their flower-like structure, with high-aspect-ratio nanopetals, causes temporary membrane permeabilization upon contact, allowing plasmid entry while preserving high cell viability. Using mechanoporation, a plasmid encoding COL7A1 achieved transfection rates of over 20% in primary keratinocytes and 10% in primary fibroblasts from EB patients. Cell viability remained above 85%, as confirmed by flow cytometry and metabolic assays. The production of type VII collagen was confirmed through immunofluorescence and Western blot analyses. Furthermore, ZnO-NFs exhibited natural antibacterial activity against Staphylococcus epidermidis and Escherichia coli, bacteria commonly associated with EB wound infections. The nanopetals' large surface area disrupts bacterial membranes, helping control infections and potentially promoting wound healing. These findings indicate that (bio)functionalized ZnO nanoflowers are a promising non-viral platform for ex vivo gene correction in EB, offering combined gene delivery and antibacterial properties to address genetic defects and infections. This approach could also be relevant for other genodermatoses.

Keywords: Epidermolysis bullosa; Gene therapy; Mechanoporation; ZnO nanoflowers; Non-viral delivery; COL7A1; Antibacterial activity.

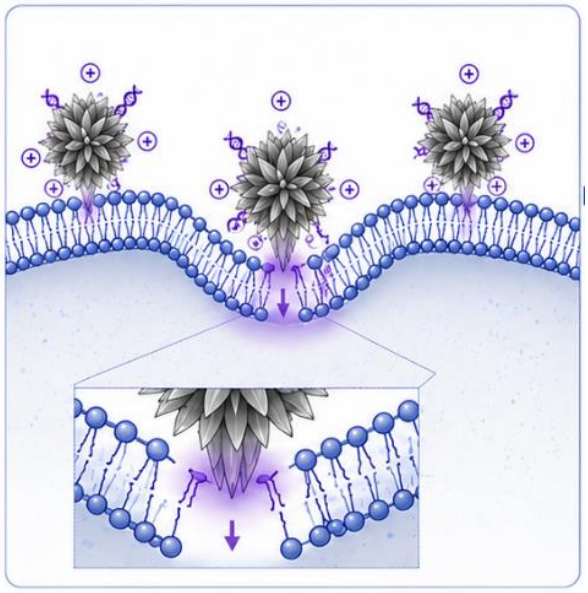


Figure 1: Schematic representation of ZnO nanoflower-mediated mechanoporation. Biofunctionalised ZnO nanopetals create transient micro-fissures in the membrane, enabling delivery of plasmid DNA into the cell and its subsequent release into the cytoplasm.

References:

1. J. Bischof et al, Emerging Gene Therapeutics for Epidermolysis Bullosa under Development, International Journal of Molecular Sciences, 2024, p. 2243.
2. F. Mavilio et al., Correction of junctional epidermolysis bullosa by transplantation of genetically modified epidermal stem cells, Nature Medicine 12(12) (2006) 1397-1402.

Reactivating the STING pathway in PTK7-positive acute leukemia cells using DNA-based theranostic nanodevices

Elisa Ottalagana[1,2], Andrea Marranci[1], Aldo Moscardini[2], Francesco Olimpico[1], Lorena Tedeschi[4], Filomena Rea[1,3], Tiziano Salvatori[1,3], Ivano Squiccimarro[1,2], Pasquale Mastella[1,2], Fabio Beltram[1,2], Stefano Luin[2,#] & Andrea Ghelli Luserna di Rorà[1,#]

[1]Fondazione Pisana per la Scienza Onlus, San Giuliano Terme, Italy[2]NEST, Scuola Normale Superiore and Istituto Nanoscienze-CNR, Pisa, Italy
[3]Department of Biology, University of Pisa, Italy
[4]Institute of Clinical Physiology (IFC), National Research Council (CNR)
[#]Same contribution

Abstract:
In eukaryotic cells, the STING pathway responds to cytosolic dsDNA from pathogens or damaged DNA to promote type-I interferon and pro-inflammatory cytokine production1. In cancer cells, this pathway is often downregulated, allowing tumors to evade immune recognition; thus, its reactivation represents a promising therapeutic strategy. Our project aims to develop and test in vitro an aptamer-based nanodevice (StingApt) designed to selectively activate STING in in PTK7+ acute lymphoblastic (ALL) and myeloid leukemia (AML) models. StingApt contains a single-stranded DNA aptamer targeting the PTK7 receptor and a 90-base dsDNA sequence acting as a STING agonist, ensuring selective function in PTK7$^+$ cells (Figure 1). Basal and activated expression levels of STING components were analyzed by immunoblotting in leukemia cell lines following treatment with the agonist SA-4, or electroporation with StingApt and 90-base dsDNA. PTK7 expression, StingApt binding, and internalization routes were characterized using flow cytometry and confocal microscopy in leukemia cells, evaluating colocalization with endosomal markers. Finally, a StingApt-INF7 conjugate was synthesized, structurally characterized by HPLC, and its biological effects are under investigation.
Activation of the STING pathway was confirmed following treatment with SA-4, StingApt, or 90-base dsDNA, which increased protein levels of downstream mediators. StingApt exhibited markedly higher and more selective binding and internalization efficiency in PTK7$^+$ ALL cells compared to the free dsDNA sequence, with minimal uptake in PTK7 negative leukemia lines. Cellular uptake occurs predominantly through macropinocytosis, as shown by colocalization with dextran. To enhance cytoplasmic release and STING recognition, we are optimizing an endosomal escape strategy by conjugating INF7 to StingApt.
In conclusion, our findings highlight the potential of aptamer-based nanodevices for the selective delivery of STING agonists to PTK7$^+$ leukemia cells. This strategy provides a targeted approach to reactivate the STING pathway in cancer cells, offering a promising platform for immunotherapeutic interventions in leukemia and other PTK7-expressing tumors.

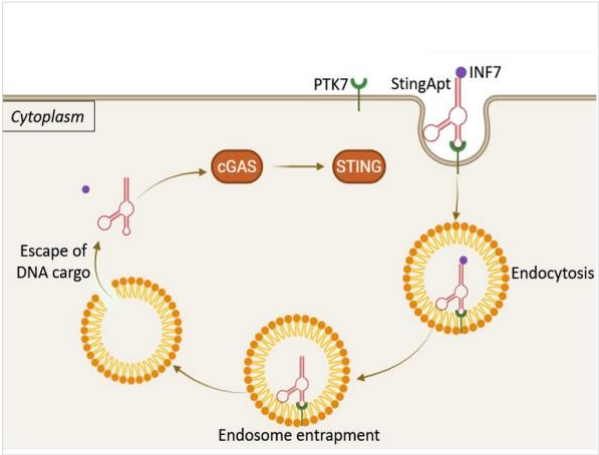


Figure 1: Schematic representation of the StingApt mechanism of action. The aptamer-based nanodevice selectively binds to the PTK7 receptor on the cell membrane, triggering internalization. Following endocytosis, StingApt undergoes endosomal escape (facilitated by the conjugated peptide), releasing the 90-base dsDNA sequence into the cytoplasm.
Once in the cytosolic space, the dsDNA agonist is recognized by cGAS, successfully activating the downstream STING pathway.

References:

Abe T, Harashima A, Xia T, Konno H, Konno K, Morales A et al. Article STING Recognition of Cytoplasmic DNA Instigates Cellular Defense. MOLCEL 2013; : 1–11.

Keywords: STING pathway, aptamer, PTK7 receptor, leukemia immunotherapy, targeted drug delivery, macropinocytosis, nanodevice, endosomal escape.

Magnetic liposomal drug delivery systems in ovarian cancer therapy: new opportunities to overcome drug resistance

J. Nowak-Niedźwiecka[1], A. Mamczur[1], B. Machnicka[1], A. Czogalla[2], M. Cano[3], V. Garcia-Caballero[3], J. J. Giner-Casares[3]
[1] Faculty of Exact and Natural Sciences, Department of Biotechnology, University of Zielona Góra, Zielona Góra, Poland
[2] Faculty of Biotechnology, University of Wrocław, Wrocław, Poland
[3] Department of Physical Chemistry, University of Córdoba, Córdoba, Spain

Abstract:
Ovarian cancer remains one of the most lethal gynecological malignancies due to late-stage diagnosis and the frequent development of resistance to chemotherapeutic agents such as cisplatin and paclitaxel. Consequently, the development of innovative drug delivery systems capable of enhancing therapeutic efficacy and overcoming resistance mechanisms remains a major challenge. Magnetic nanoparticles have attracted considerable attention owing to their ability to facilitate targeted drug delivery, enhance intracellular drug accumulation, generate localized heat under an alternating magnetic field, and act as contrast agents for magnetic resonance imaging (MRI) (Figure 1). These multifunctional properties create opportunities for the development of theranostic platforms integrating diagnosis and therapy. Although nanoparticle toxicity remains an important consideration, iron oxide nanoparticles are generally regarded as biocompatible, and their incorporation into liposomal systems may further improve biological safety by limiting nonspecific interactions and systemic exposure. Here, we report the development of multifunctional liposomal nanocarriers incorporating cisplatin-functionalized iron oxide nanoparticles for ovarian cancer therapy. The developed formulations were characterized with respect to their physicochemical properties, morphology, and biological activity, with particular emphasis on their efficacy against both drug-sensitive and drug-resistant ovarian cancer cell lines. The nanocarriers exhibited facorable physicochemical characteristics and good colloidal stability. Importantly, they demonstrated enhanced anticancer activity compared with free cisplatin, particularly in drug-resistant ovarian cancer cells, highlighting their potential to improve intracellular drug delivery and overcome mechanisms associated with chemotherapeutic resistance. Overall, these findings underscore the potential of magnetic nanoparticle-loaded liposomes as advanced nanocarriers for ovarian cancer therapy and support their further development as multifunctional platforms for the treatment of resistant malignancies.

Keywords: ovarian cancer, magnetic nanoparticles, liposomes, cisplatin, drug resistance, nanocarriers

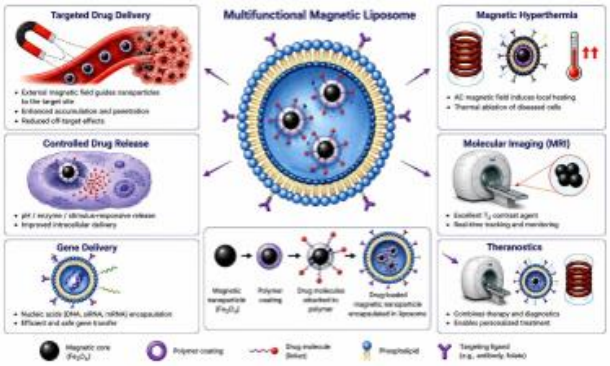


Figure 1: Schematic illustration of multifunctional magnetic liposomes incorporating drug-loaded magnetic nanoparticles. These nanocarriers enable targeted drug delivery, controlled release, magnetic hyperthermia, molecular imaging, and theranostic applications. The integration of therapeutic and diagnostic functions within a single liposomal platform offers a promising strategy for overcoming drug resistance.

References:

1. Patelak, A., Nowak-Niedźwiecka, J., Machnicka, B. (2026) Molecular mechanisms of therapy resistance in ovarian cancer, *Post Biochem*., doi:10.18388/k2p7j927. In press.
2. Nowak-Niedźwiecka, J. (previously Nowak-Jary, J.), Machnicka, B. (2025) Toxicity of Magnetic Nanoparticles in Medicine: Contributing Factors and Modern Assessment Methods, *Int. J. Mol. Sci*., 26(15), 8586.
3. Nowak-Niedźwiecka, J. (previously Nowak-Jary, J.), Machnicka, B. (2024) Comprehensive Analysis of the Potential Toxicity of Magnetic Iron Oxide Nanoparticles for Medical Applications: Cellular Mechanisms and Systemic Effects, *Int J Mol Sci*, 25(22), 1-34.

Harnessing Nature-Driven Nanotechnology: Polyphenol-Based Platforms to Enhance Immune and Cancer Therapy.

Mariafrancesca Cascione[1], Valeria De Matteis[1], Rosaria Rinaldi[2]
[1] Department of Experimental Medicine,University of Salento, Lecce, Italy
[2] Department of Mathematics and
Physics "E. De Giorgi", University of Salento, Lecce, Italy

Abstract:
The development of next-generation therapies for chronic inflammation and cancer increasingly relies on nanotechnology to enhance the stability, bioavailability, and functional impact of bioactive natural compounds. Across different nanoplatforms—protein-based, polysaccharide-based, and green-synthesized metallic systems—polyphenol-loaded nanostructures consistently demonstrate the ability to potentiate anti-inflammatory, antioxidant, and anticancer responses, offering a shared technological strategy for precision medicine.

EGCG-based nanocarriers, whether built on protein (BSA) or polysaccharide matrices (chitosan), markedly amplify the compound's biological activity [1,2]. In immune and cancer cell models, these platforms effectively suppress key inflammatory pathways, reduce NF-κB activation, and modulate cytokine secretion, while also mitigating oxidative stress and preserving cell viability under damaging conditions. Their enhanced intracellular delivery and sustained bioactivity highlight their potential to counteract mechanisms driving chronic inflammation, tumor progression, and therapeutic resistance.

Complementing these soft-matter systems, green-synthesized gold nanoparticles produced with *Laurus nobilis* extract exhibit intrinsic polyphenol functionalization and dual therapeutic behavior. They suppress inflammatory mediator release in dendritic cells and act as efficient radiosensitizers in breast cancer models, increasing radiation-induced cytotoxicity and DNA damage even at reduced irradiation doses [3,4].

Together, these findings reveal a unifying paradigm: nature-derived nanotechnology can transform fragile polyphenols into stable, potent, and multifunctional therapeutic agents. By integrating biocompatible carriers with green metallic nanostructures, these platforms provide versatile tools to modulate immune responses, control oxidative stress, and enhance anticancer treatments. This convergence of natural compounds and engineered nanomaterials paves the way for innovative, selective, and sustainable nanopharmaceuticals tailored for precision anti-inflammatory and oncologic therapy.

Keywords: bioactive natural compounds, BSA NPs, Ch-NPs, inflammation, epigallocatechin-gallate, antioxidant, cancer cell line models, nano-theragnostic, precision delivery, green-synthesized gold nanoparticles**,** radiosensitizers

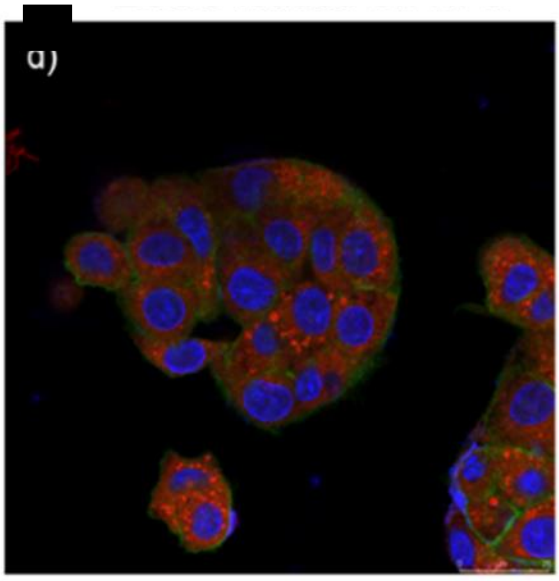


Figure 1: High-resolution confocal fluorescence microscopy images showing the cellular uptake of FITC-labeled EGCG-loaded Ch-NPs by PANC-1 cells, after 6h of incubation. Nuclei are stained with DAPI (blue), and cell membranes are stained with CellMask Plasma Membrane Stain (red).

References:

1. Bianco A. et al., (2026), *ACS Omega*, 11, 29147−29164
2. Martano S, et al., (2025), *Front. Bioeng. Biotechnol*. 13:1666492.
3. De Matteis V., et al., (2024), *Nano Today* 57 102329
4. Tarantino S., et al., (2025), *Discover Nano* 20:10

Novel Cancer NanoMedicines: From Therapy of poorly vascularized tumors to protection from radiotherapy induced damage in the skin

Biana Godin
Houston Methodist Research Institute, USA

Abstract:
Based on their dimensions, nanomedicines can be designed to bridge between processes on molecular and cellular scales in the disease microenvironment. Moreover, novel RNA-based therapies require packaging into nanoparticles to protect the sensitive payload from degradation and enable their efficient delivery. Thus, nanomedicine offers unique and promising advancements in various clinical fields.

This talk will focus on the therapeutic benefits of nanoparticles targeting immune cells in the proximity of poorly vascularized tumor lesions to advance cancer therapy as well as novel mRNA based nanotherapies for wound healing and protection from radiation-induced damage in the skin

Reprogramming the Pancreatic Adenocarcinoma Microenvironment integrating mutSEMA3A mRNA-Lipid Nanoparticles with a Vascularized Organ-on-Chip Model

G.Tomaino[1*], L.Salvioni[1], L.Fiandra[1], E.Giraudo[2], M.Innocenti[1], D.Prosperi[1]
[1] Department of Biotechnology and Biosciences, University of Milan Bicocca, Milan, Italy
[2] Candiolo Cancer Institute, FPO- IRCCS, and Department of Science and Drug Technology, University of Turin, Turin, Italy

Abstract:
Pancreatic ductal adenocarcinoma (PDAC) is a deadly solid tumor characterized by an immunosuppressive tumor microenvironment (TME) and an abnormal vasculature that hampers drug delivery and immune infiltration. Semaphorin 3A (Sema3A) can normalize tumor vasculature and enhance anti-tumor immunity. This project aims to develop lipid nanoparticles (LNPs) encapsulating a mutated constitutively active version of Sema3A mRNA (mut-Sema3A) to inhibit PDAC progression[1].
To evaluate this strategy while reducing in vivo experimentation, we established a vascularized PDAC-on-a-chip model using the Organoplate Graft system[2]. This 3D platform recapitulates the PDAC TME by integrating endothelial cells (ECs), tumor spheroids, and immune components within a collagen matrix, providing a controlled environment to study LNP transcytosis and mut-Sema3A effects.
In vitro validation confirmed high transfection efficiency of mut-Sema3A mRNA and successful protein secretion in PDAC and EC lines. The secreted mut-Sema3A actively reduced EC migration in haptotactic assays, and preliminary results confirmed successful LNP-mediated transfection in both cell lines.
The PDAC-on-a-chip platform will be used to screen and optimize mut-Sema3A mRNA-LNP formulations. Ultimately, these insights will guide future in vivo validation in syngeneic orthotopic mouse models, combining advanced nanotherapy with biomimetic modeling to overcome therapeutic resistance in PDAC.

Keywords: Organ-on-a-chip, 3D in vitro model, Pancreatic ductal adenocarcinoma (PDAC), Tumor microenvironment (TME), Vascular normalization, Semaphorin 3A (Sema3A), Lipid nanoparticles (LNPs), mRNA therapeutics.

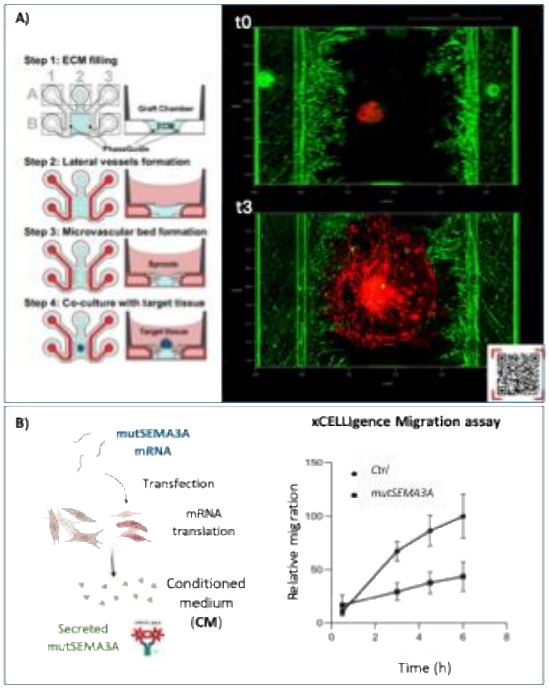


Figure 1: A) Vascularized PDAC-on-*a-chip model*. Left: Experimental workflow using the OrganoPlate Graft: collagen I filling (Step 1), endothelial vessel formation under gravity flow (Step 2), angiogenic sprouting (Step 3), and co-culture with a PDAC spheroid (Step 4). Right: Maximum intensity projection showing MS1 vessels (green) interacting over time with a PDAC spheroid (red). Scan QR code for 3D reconstruction. *B) Functional validation of mutSEMA3A.* Left: Schematic of mRNA transfection and mutSEMA3A protein secretion. Right: xCELLigence assay showing that mutSEMA3A CM significantly inhibits TeloHAEC endothelial cell migration.

References:

1. Gioelli, N., et al., (2018). A rationally designed NRP1-independent superagonist SEMA3A mutant is an effective anticancer agent. *Sci. Transl. Med*. 10 eaah4807
2. Bonanini F., et al., (2022). In vitro grafting of hepatic spheroids and organoids on a microfluidic vascular bed. *Angiogenesis* 25, 455-470.

Dual-Targeting Strategy to Repurpose Cetuximab with HFn Nanoconjugates for Immunotherapy of Triple-Negative Breast Cancer

L. Barbieri[1,*], A. Banfi[1], L. Salvioni[1], M. Innocenti[1], D. Prosperi[1] and L. Fiandra[1]
[1] NanoBioLab, Department of Biotechnology and Bioscience, University of Milano-Bicocca, Piazza della Scienza 2, 20126, Milan, Italy

Abstract:
Immunotherapy has emerged as an effective strategy to treat cancer by re-educating the host immune system to recognize tumor cells as "non-self". Among immunotherapeutic approaches, antibody-based therapies are particularly successful, as monoclonal antibodies (mAbs) induce tumor killing through antibody-dependent cellular cytotoxicity (ADCC) and by directly inhibiting tumor growth. However, their therapeutic efficacy remains limited by poor pharmacokinetics and restricted ability to cross biological barriers. Nanoparticle-based delivery systems represent a promising solution. In this context, H-ferritin (HFn), a recombinant form of human apoferritin, has been extensively studied for its biocompatibility, drug-loading capability, and selective targeting of transferrin receptor 1 (TfR1), which is overexpressed in most solid tumors. Here, we investigated an HFn–Cetuximab (CTX) nanoconjugate as a dual-targeting immunotherapeutic strategy, with a focus on triple-negative breast cancer (TNBC). Building on prior evidence of enhanced mAb delivery across biological barriers,[1] we evaluated the activity of HFn-CTX in 3D spheroid models of TNBC and glioblastoma. The nanoconjugate was optimized in terms of production, conjugation, and biophysical properties, and its activity was assessed through apoptosis assays in the presence of immune cells, uptake studies, and in vivo biodistribution analysis. HFn-CTX significantly enhanced ADCC-mediated apoptosis in TNBC spheroids compared to CTX alone, whereas glioblastoma spheroids showed limited responsiveness. Uptake studies revealed prolonged plasma membrane localization of HFn-CTX in TNBC cells, in contrast to rapid internalization in glioblastoma cells. These differences correlated with higher epidermal growth factor receptor (EGFR) expression in TNBC cells and higher TfR1 levels in glioblastoma cells, indicating that receptor expression profiles critically influence nanoconjugate behavior and immune activation. In vivo imaging confirmed selective accumulation of HFn-CTX in TNBC tumors, with expected liver retention. Overall, these findings demonstrate that HFn-CTX exploits dual EGFR/TfR1 targeting to amplify immune-mediated cytotoxicity and repurpose CTX for refractory EGFR-expressing tumors such as TNBC, supporting its further preclinical development.[2]

Keywords: triple-negative breast cancer, Cetuximab, ferritin, nanoconjugates, epidermal growth factor receptor, transferrin receptor, immunotherapy

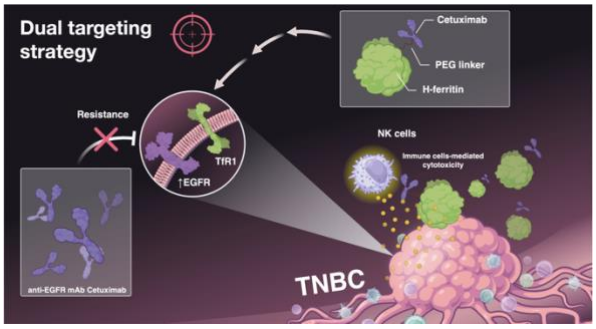


Figure 1: HFn–CTX nanoconjugates simultaneously engage EGFR and transferrin receptor 1 (TfR1) on triple-negative breast cancer cells, prolonging Cetuximab membrane retention and amplifying antibody-dependent cellular cytotoxicity (ADCC) to overcome resistance in CTX-refractory tumors.

References:

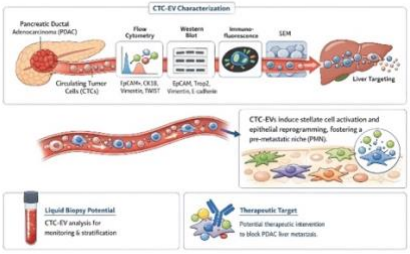
1. Rizzuto, M. A., Dal Magro, R., Barbieri, L., Pandolfi, L., Sguazzini-Viscontini, A., Truffi, M., Salvioni, L., Corsi, F., Colombo, M., Re, F., & Prosperi, D., (2021). H-Ferritin nanoparticle-mediated delivery of antibodies across a BBB in vitro model for treatment of brain malignancies. *Biomaterials science*, 9(6), 2032–2042.
2. Barbieri, L., Salvioni, L., Banfi, A., Garbujo, S., Fiandra, L., Baioni, C., Giustra, M., Morelli, L., Frascotti, G., Colombo, M., Innocenti, M., & Prosperi, D. (2025). Dual-Targeting Strategy to Repurpose Cetuximab with HFn Nanoconjugates for Immunotherapy of Triple-Negative Breast Cancer. *ACS applied materials & interfaces*, 17(23), 33648–33663

Circulating Tumor Cells and Their Secretome Drive Pre-Metastatic Niche Formation in the Liver of Pancreatic Ductal Adenocarcinoma Patients.

Maria Principia Scavo1 , Giorgia Panzetta 1, Rita Palieri 1, Maria De Luca 1, Francesco Balestra 1, Federica Rizzi 2,3, Chiara Perrone 2,3, Nicoletta Depalo 2,3, Gianluigi Giannelli 5.
1 Laboratory of Molecular Medicine, National Institute of Gastroenterology, IRCCS S. de Bellis, Castellana Grotte (Bari), Italy
2 CNR-IPCF, Institute for Chemical and Physical Processes, S.S. Bari, Department of Chemistry, Bari, Italy
3 National Interuniversity Consortium of Materials Science and Technology (INSTM), Bari Research Unit, Bari, Italy
5 Scientific direction, National Institute of Gastroenterology, IRCCS S. de Bellis, Castellana Grotte (Bari), Italy

Abstract
Pancreatic ductal adenocarcinoma (PDAC) remains one of the most aggressive tumour, with limited options for early detection and monitoring[1]. Circulating tumor cells (CTCs) and their secreted extracellular vesicles (EVs) represent promising sources of minimally invasive biomarkers, to follow the progression of disease [2;3]. However, the molecular and functional features of EVs specifically derived from CTCs (CTC-EVs) in PDAC are still poorly understood.
In this study, CTCs were isolated from PDAC patients across disease stages and characterized by cytofluorimetry, Western blot (WB), and immunofluorescence (IF), and SEM (figure 1). Expression of EpCAM and Trop2, alongside EMT marker modulation (e.g., upregulated vimentin, downregulated E-cadherin), correlated with disease stage higher in advanced stages proportional to severity. Comparative analyses were performed with EVs derived from tumor and non-tumor pancreatic cell lines (MIA-PaCa-2, PANC-1).
The aim of this study is to investigates whether PDAC patient-derived CTCs and their secretome fractions reprogram liver cells to establish a pre-metastatic niche (PMN) in the hepatic tissue.
These findings demonstrate that PDAC CTCs and their secretome rapidly induce hepatic stellate cell activation and epithelial reprogramming in a stage-dependent manner, fostering a PMN conducive to metastasis. Targeting stage-stratified CTC-EV signaling (e.g., EpCAM/Trop2 axes) may offer novel therapeutic avenues to prevent PDAC liver dissemination. Flow cytometry confirmed tumor origin of cells (EpCAM+). They displayed a hybrid phenotype, co-expressing epithelial markers (EpCAM, CK18, CK19) and epithelial-to-mesenchymal transition drivers Vimentin and TWIST, indicating marked plasticity and metastatic potential. Preliminary data indicate that CTCs from PDAC patients release a heterogeneous population of EVs with an average size of 100–150 nm. Scanning electron microscopy revealed CTC surface architectures distinct from pancreatic cancer lines (MIA-PaCa-2, PANC-1), suggesting adaptations for haematogenous survival, while EVs exhibited intact, well-defined morphology. CTC-EVs express both general EV markers and tumor-associated proteins.
The present study bridges these gaps through optimized CTC isolation and multi-modal CTC and secretome scrutiny via ddPCR (KRAS mutations, EMT modulation), WB/IF (stemness), and SEM imaging combine the isolation of CTC and their secretome from Serum of PDAC patients, to delineate the role of CTC-EVs crosstalk in tumor progression and metastasis through specific proteins and gene. Further validation in larger cohorts could establish CTC-EVs as a novel liquid biopsy tool for disease monitoring and therapeutic stratification in PDAC.

Keywords: CTC, extracellular vesicles, EVs, PDAC, Secretome



References

1. Sikora et al. (2021). "Circulating tumor cells in pancreatic cancer patients: a systematic review." Pancreatology, 21(4):725-734. [DOI:10.1016/j.pan.2021.02.012]
2. Costa-Silva et al. (2022). "Pancreatic cancer exosomes initiate pre-metastatic niche formation in the liver." Nat Cell Biol, 24(5):668-680. [DOI:10.1038/s41556-022-00892-3]
3. Palamaris K et al. Epithelial to Mesenchymal Transition: Key Regulator of Pancreatic Ductal Adenocarcinoma Progression and Chemoresistance. Cancers (Basel). 2021 Nov 4;13(21):5532. [DOI: 10.3390/cancers13215532]

SMS 2026 / EGF 2026 Session III.A: Environment & Sustainable Materials/Surfaces properties & applications

Solid-State Caloric Cooling: A Clean Path to the Future of Refrigeration

L. Mañosa
Departament de Física de la Matèria Condensada, Universitat de Barcelona, Barcelona, Catalonia.

Abstract:
Cooling is essential for the well-being, health, and prosperity of modern society. Current cooling technologies rely on the compression and expansion of working fluids, typically hydrofluorocarbons (HFCs), which have a significant environmental impact and are expected to be phased out in the near future. At the same time, the global demand for refrigeration and air conditioning is rapidly increasing, making the development of more efficient and sustainable cooling technologies crucial for achieving energy-efficiency and climate goals. In this context, solid-state caloric cooling has emerged as a promising alternative to conventional vapor-compression refrigeration due to its potential for higher efficiency and reduced environmental impact.

Caloric effects are reversible thermal responses, typically quantified through entropy and temperature changes, that occur in materials upon the application and removal of an external stimulus. Depending on the nature of the stimulus, these effects are classified as magnetocaloric, electrocaloric, elastocaloric, and barocaloric when induced by magnetic fields, electric fields, uniaxial stress, and hydrostatic pressure, respectively. Materials exhibiting strong coupling between different degrees of freedom can respond to the simultaneous application of multiple stimuli, giving rise to multicaloric effects.

Although caloric effects are ubiquitous in solids, their thermal response is generally weak and of limited technological relevance. However, these effects can be dramatically enhanced in the vicinity of phase transitions, where large isothermal entropy changes and adiabatic temperature changes occur. Under such conditions, giant or even colossal caloric and multicaloric effects can be obtained, making these materials particularly attractive for solid-state cooling applications.

In this talk, I will first provide a brief overview of the current state of the art in caloric and multicaloric materials and effects. I will then present our recent results on the investigation of several caloric and multicaloric systems, highlighting their fundamental properties and potential for next-generation cooling technologies.

Keywords: Magnetocaloric, Electrocaloric, Barocaloric, Elastocaloric, Multicaloric.

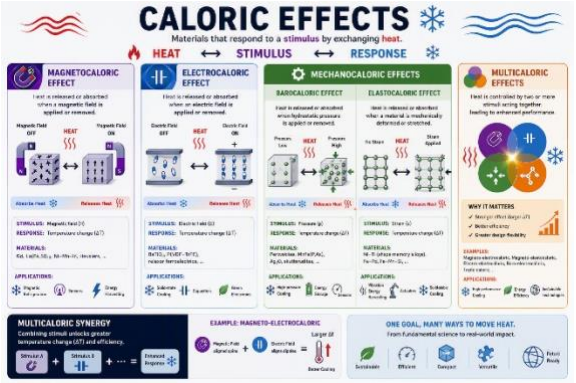


Figure 1: Illustration of the various caloric effects induced by the application and removal of a single external stimulus, and of the multicaloric effect arising from the combined action of two or more stimuli.

References:

1. L. Mañosa, A. Planes, M. Acet, (2013) Advanced materials for solid-state refrigeration *J. Mater. Chem A,* 1, 4925-4936.
2. X. Moya, N.D. Mathur, (2020) Caloric materials for cooling and heating, *Science* 370, 6518.

Low-Carbon 3D Construction Printing: Materials, Modeling and Autonomous Construction

K. M. Liew
City University of Hong Kong

Abstract

This talk presents an integrated strategy that positions 3D concrete printing (3DCP) as a transformative platform for low-carbon and autonomous construction, addressing the urgent need to decarbonize the built environment while enabling resource-efficient infrastructure for extraterrestrial habitats. At its core is a materials-driven innovation, complemented by advanced meshfree computational modeling to optimize printability, structural performance, and durability. We introduce a novel one-part alkali-activated geopolymer formulated entirely from industrial by-products, eliminating Portland cement, as the foundation of a low-carbon 3DCP system. Engineered for additive manufacturing, the material exhibits a distinctive three-stage rheological evolution that provides an exceptionally long printable window, enhancing printability and buildability while reducing mechanical anisotropy. These characteristics are critical for reliable, automated, and large-scale construction with reduced material and energy consumption. To advance 3DCP from empirical mix design toward performance-based and predictive construction, Smoothed Particle Hydrodynamics (SPH) simulates fresh-state extrusion and deposition, while an interface-aware peridynamic framework captures interlayer bonding, fracture initiation, and long-term damage evolution in the hardened geopolymer. Integrating experimental validation with physics-based modeling reduces reliance on trial-and-error and provides a predictive basis for assessing structural performance and life-cycle sustainability. Building on this foundation, the convergence of low-carbon geopolymer binders, autonomous 3DCP, meshfree computational mechanics, and AI-enabled digital twins offers a scalable pathway toward next-generation intelligent construction. This framework supports low-carbon infrastructure on Earth while providing a technological foundation for autonomous, resource-efficient construction in extraterrestrial environments, where minimizing material transport, energy consumption, and human intervention is essential.

Manganese-Modified Co- and Cu- Based Mixed Oxides for Enhanced Catalytic Oxidation of Toluene and CO

C.E. Bounoukta[1], E. Genty[1], C. Poupin[1], F. Cazier[2], G. Leyssens[3], V. Tschamber[3], J.P. Dacquin[4], S. Royer[1,4], Balay[5], F. Robic[5], S. Siffert[1*], R. Cousin[1]

1 : Unité de Chimie Environnementale et Interactions sur le Vivant, Université du Littoral Côté d'Opale, MREI1—145 Avenue Maurice Schumann, 59140 Dunkerque, France.

2 : Centre Commun de Mesures, Université du Littoral Côté d'Opale, 145 Avenue Maurice Schumann, 59140 Dunkerque, France.

3 : Laboratoire de Gestion des Risques et Environnement - Université de Haute-Alsace, 3b rue A. Werner, 68093 Mulhouse Cedex, France.

4 : Univ. Lille, CNRS, Centrale Lille, Univ. Artois, UMR 8181-UCCS-Unité de Catalyse et Chimie du Solide, 59000 Lille, France.

5 : LORFLAM, 4 avenue de kergroise, 56100 LORIENT, France

*Stephane.Siffert@univ-littoral.fr

Abstract:

The biomass sector, and more specifically domestic wood heating, appears today to be a particularly promising alternative. In France, wood and biomass account for around 65% of renewable energy consumption for heat production. Thus, wood heating represents real challenges: energy issues for the environment and for public health. Nevertheless, wood energy is an integral part of the environmental issue. Emissions from wood combustion, both gaseous compounds and fine particles, are undeniably controversial. Among the pollutants produced by wood heating, several families can be distinguished: unburnt gases such as carbon monoxide (CO), Volatile Organic Compounds (VOCs), which include BTEX (Benzene, Toluene, Ethylbenzene and Xylene), and unburnt solid carbonaceous compounds.

Reducing these polluting emissions is crucial and requires the implementation of filtration and treatment technologies. Catalytic oxidation is known as one of the best solutions for reducing CO and VOCs. Total oxidation of CO at low temperature by transition metal oxides is a widely studied subject in heterogeneous catalysis. Specifically, manganese oxides are interesting for toluene oxidation due to its availability and reactivity of surface oxygen species. Transition metal oxides are also being studied as part of the total oxidation of VOCs and are very promising [1-2]. The use of LDH route for the synthesis of mixed oxides allows to develop some interesting properties for pollutants oxidation at low temperature, like high specific surface area and reducibility at low temperature.

To get as close as possible to the real conditions of wood combustion, this work is carried out on the simultaneous elimination of pollutants. Catalytic oxidation is one of the most effective methods for eliminating separately CO and VOCs, this is why it has also been chosen for treating mixtures of pollutants. The simultaneous catalytic oxidation of toluene and CO compounds in mixture has begun to be studied over the last decade, but the number of studies remains fairly limited [2]. In this work, we chose to study the activity of mixed oxides issued from LDH route. The main objective is to evaluate the influence for the association of Mn to Co or Cu-based catalysts for oxidation reactions of pollutants issued from the wood combustion (e.g. CO and toluene).

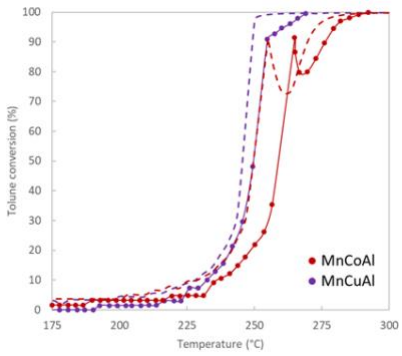


Figure 1: Conversion vs. temperature of toluene in presence (dotted lines) or absence of CO.

References:

1. Santos, V. P., Pereira, M. F. R., Órfão, J. J. M., Figueiredo, J. L. (2010), The role of lattice oxygen on the activity of manganese oxides towards the oxidation of volatile organic compounds, *Appl. Catal. B Environ.*, 99 (1-2), 353-363.

2. Genty, E., Brunet, J., Poupin, C., Ojala, S., Siffert, S., Cousin, R. (2019), Influence of CO addition on the toluene total oxidation over Co based mixed oxide catalysts, *Appl. Catal. B Environ.* 247, 163-172.

Effect of A-Site Substitution on the Catalytic Performance of $LaMnO_3$ Perovskites for Complete Oxidation of pollutants

C.E. Bounoukta[1], E. Genty[1], C. Poupin[1], C. Ciotonea[1], F. Cazier[2], G. Leyssens[3], V. Tschamber[3], J.P. Dacquin[4], S. Royer[1,4], Balay[5], F. Robic[5], S. Siffert[1], R. Cousin[1*]

[1] Unité de Chimie Environnementale et Interactions sur le Vivant, Université du Littoral Côté d'Opale, MREI1—145 Avenue Maurice Schumann, 59140 Dunkerque, France.

[2] Centre Commun de Mesures, Université du Littoral Côté d'Opale, 145 Avenue Maurice Schumann, 59140 Dunkerque, France.

[3] Laboratoire de Gestion des Risques et Environnement - Université de Haute-Alsace, 3b rue A. Werner, 68093 Mulhouse Cedex, France.

[4] Univ. Lille, CNRS, Centrale Lille, Univ. Artois, UMR 8181-UCCS-Unité de Catalyse et Chimie du Solide, 59000 Lille, France.

[5] LORFLAM, 4 avenue de kergroise, 56100 LORIENT, France

*Renaud.Cousin@univ-littoral.fr

Abstract:

The use of biomass as an energy source is considered a promising technological option for achieving carbon neutrality targets [1]. However, emissions generated during biomass combustion may contain gaseous organic pollutants such as volatile organic compounds (VOCs), polycyclic aromatic hydrocarbons (PAHs), as well as CO, NOx, and soot particles. One effective approach to reducing these emissions is their complete catalytic oxidation into CO_2 and H_2O [2]. Mixed metal oxide materials (e.g., Mn-, Co-based oxides) have demonstrated promising performance compared with noble metal catalysts for the complete oxidation of CO and VOCs [3]

Mixed oxides with the ABO_3 perovskite structure have been extensively investigated for total oxidation reaction. These materials exhibit attractive surface properties due to their highly tunable structure, which allows the incorporation of various cations to optimize catalytic performance for targeted chemical reactions. They also possess high chemical stability and favorable redox properties. Furthermore, partial substitution at the A and/or B sites can induce structural defects, leading to the formation of oxygen vacancies. These defects are known to enhance the catalytic properties of perovskite materials [4-5].

The aim of this work was to develop manganese-based perovskite catalysts with the nominal composition $La_{0.8}A'_{0.2}MnO_3$. Part of the lanthanum occupying the A sites was substituted with either alkali metals (A′ = Na^+ or K^+) or alkaline-earth metals (Ca^{2+}, Ba^{2+}, Sr^{2+}, or Mg^{2+}). The synthesized materials were characterized using several physico-chemical tecnics. The catalysts were then evaluated for polutant oxidation (CO, Toluene, Soot). Thus, as represented on Figure 1, substituting La with another element significantly improved the catalytic performance for the CO oxidation. Among the investigated catalysts, Mg substitution results indicate that this formulation could be a efficient catalyst.

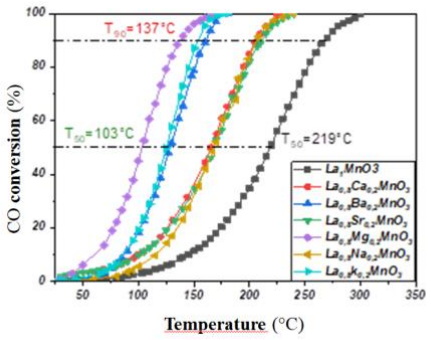


Figure 1: CO conversion as a function of temperature over $La_{0.8}A'_{0.2}MnO_3$ perovskite catalysts.

References:

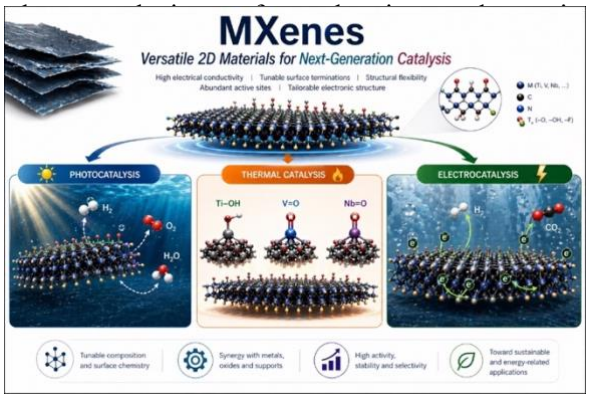
1. Ozgen, S., Cernuschi, S., Caserini S. (2021), An overview of nitrogen oxides emissions from biomass combustion for domestic heat production, *Renewable and Sustainable Energy Reviews,* 135,110113.
2. Maxwell, D., Gudka, B.A., Jones, J.M., Williams, A. (2020), Emissions from the combustion of torrefied and raw biomass fuels in a domestic heating stove, *Fuel Processing Technology*, 199, 106266.
3. Rochard, G., Olivet, L., Tannous, M., Poupin, C., Siffert S., Cousin, R. (2021), Recent Advances in the Catalytic Treatment of Volatile Organic Compounds: A Review Based on the Mixture Effect, *Catalyst* 11(10), 1218.
4. Polo-Garzon, F., Wu, Z. (2018) Acid–base catalysis over perovskites: a review, *J. Mater. Chem. A.* 6 2877–2894.

MXenes as versatile 2D materials for next-generation catalysis

Ana Primo
Instituto de Tecnología Química (CSIC-UPV), Universitat Politècnica de València, Valencia, Spain

Abstract:
MXenes, a rapidly expanding family of two-dimensional transition metal carbides and nitrides, have recently emerged as versatile platforms for catalytic applications due to their unique combination of metallic conductivity, tunable surface chemistry, and structural adaptability. In this contribution, we present a comprehensive study of MXene-based materials across three key catalytic domains: photocatalysis, thermal catalysis, and electrocatalysis.
In photocatalysis[1][2][3][4], we demonstrate that controlling the size and surface terminations of MXenes enables the transition from metallic to semiconducting behavior, allowing their use either as standalone photocatalysts or as cocatalysts in heterojunction systems. Density functional theory (DFT) calculations reveal that both quantum confinement and surface functionalization critically influence the band gap, which can be tailored to match specific redox reactions.
For thermal catalysis[5][6][7], we exploit the intrinsic similarities between MXene surface terminations (–O, –OH, –F) and classical metal oxide active sites (e.g., Ti–OH, Nb=O), while introducing a distinct electronic environment arising from the underlying C/N framework. This duality enables the design of catalytic systems with modified adsorption and activation properties, which we probe through benchmark reactions.
In electrocatalysis[8][9], MXenes exhibit outstanding performance due to their high electrical conductivity, hydrophilic surfaces, and ability to form hybrid structures with metals and porous materials. We highlight the role of MXene-based heterostructures in enhancing charge transfer and catalytic efficiency in reactions such as hydrogen evolution and CO_2 reduction.
Overall, this work establishes MXenes as a unifying platform bridging classical catalysis and emerging nanomaterials, where electronic structure and surface chemistry can be precisely engineered to drive catalytic performance.

Keywords: MXenes, two-dimensional materials, photocatalysis, thermal catalysis,



References:

1. Rubén Ramirez-Grau et al., Small methods, 7 (2023), 2300063
2. Rubén Ramirez-Grau et al., Appl. Catal. B: Environ., 341 (2024), 123316
3. María Cabrero-Antonino et al., Angew. Chem. Int. Ed.,64, (2025), e202503860
4. Dawid D. Kruger et al., Angew. Chem. Int. Ed. (2026), e8425918,
5. Elena Romero-Salicio et al., ACS Appl. Nano Mater.,9, (2026), 2074-2085
6. Aicha Anouar et al., Journal of Catalysis, 450, (2025), 116328
7. Amarajothy Dhakshinamoorthy et al., Chem. Eur. J., 30, (2024), e202400576
8. Dawid D. Kruger et al., npj 2D materials and applications, 10, (2026), 24
9. Dawid D. Kruger et al., J. of Mat. Chem. A, 12, (2024), 25291-25303

Efficient Transformation of Glucose into 5-Hydroxymethylfurfural using PO_4-terminated Nb_2C MXene as Catalyst

A. Raya-Barón [1,*], E. Romero-Salicio [1], L. Tian [1], B. Cojocaru [2], V. Parvulescu [2], A. Primo [1], H. García [1]

[1] Instituto de Tecnología Química, Consejo Superior de Investigaciones Científicas- Universitat Politecnica de Valencia, Valencia, Spain

[2] Department of Organic Chemistry, Biochemistry and Catalysis, University of Bucharest, Bucharest, Romania

Abstract:

In the context of sustainable development and the transition from fossil fuels to renewable feedstocks, the use of biomass as a source of fuels and chemicals is of critical importance. 5-Hydroxymethylfurfural (HMF) has been identified as a platform molecule that can be further derivatized into useful chemicals, such as monomers (2,5-bis-hydroxymethylfuran, 2,5-furandicarboxylic acid) or fuels (dimethylfuran), among others.[1] HMF can be obtained from glucose via a dehydration process, usually in a 2-step reaction that involves fructose as intermediate, and that requires the adequate combination of Brønsted and Lewis acid sites on the catalyst in order to maximise yield and avoid secondary reactions.

In this work, we describe the preparation of phosphate-terminated Nb_2C MXene (Nb_2C-PO_4) as an

heterogenous water-tolerant acid catalyst for the transformation of glucose into HMF.[2] Structural characterization (XRD, HRTEM) of Nb_2C-PO_4 has proven the integrity of the MXene layered structure, and compositional analyses (STEM-EDS, XPS) have demonstrated the presence of phosphate groups on the surface of the material. Additionally, the concentration of acid and basic sites on the catalyst has been determined by NH_3- and CO_2-TPD experiments, respectively, and the type of acid sites (Brønsted or Lewis) has been assessed by pyridine-adsorbed DRIFTS.

In a monophasic THF/water medium, 64% HMF yield can be obtained after 22 hours of reaction using 10 wt% of Nb_2C-PO_4 as catalyst and a concentration of 5% (w/v) of glucose, generating <1% of undesirable humin, and with a turnover frequency (TOF) value of 3077 h^{-1}. The stability of the catalyst has been demonstrated after 5 consecutive recycling experiments, with only small loses in selectivity. The good HMF yield and reusability shown by Nb_2C-PO_4, along with the minimization of side-reactions, while maintaining a low catalyst load and a high glucose concentration, places this catalyst among the most efficient reported to date for the transformation of glucose into HMF in aqueous medium.

Keywords: biomass transformation, MXene, heterogeneous catalysis, water-tolerant Lewis acid, glucose, green chemistry.

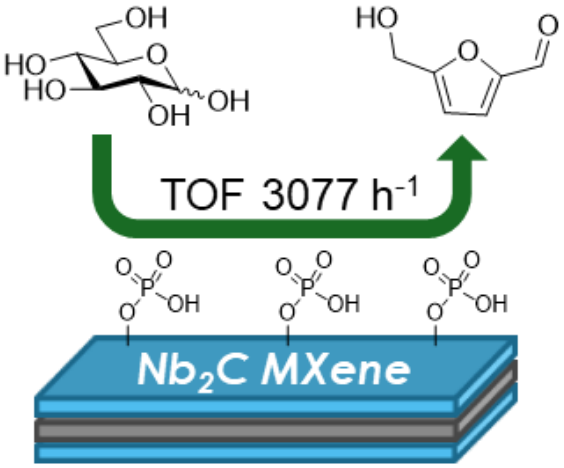


Figure 1: Schematic representation of the dehydration of glucose into HMF catalysed by Nb_2C-PO_4 MXene. Optimal reaction conditions: solvent THF/H_2O (3:1), glucose concentration 5% (w/v), S/C = 10 w/w, 150 ºC.

References:

1. Yao, Y., Chen, S., Zhang, M. (2022), Sustainable Approaches to Selective Conversion of Cellulose into 5-Hydroxymethylfurfural Promoted by Heterogeneous Acid Catalysts: A Review, *Front. Chem*., 10, 880603.
2. Raya-Barón, A., Romero-Salicio, E., Tian, L., Cojocaru, B., Parvulescu, V., Primo, A., García, H. (2026), Phosphate-Terminated Nb_2C MXene as Efficient Catalyst for the Transformation of Glucose Into 5-Hydroxymethylfurfural With 3077 h^{-1} Turnover Frequency, *ChemSusChem*, 19, e70818.

Effect of Graphene on the Consolidation and Tribological Performance of PEEK Composites Processed by Rapid Sinter Pressing

I. C. Vladu[1,*], C. Arévalo[2], E. M. Perez-Soriano[2], A. J. Dudau[1], E. Neubauer[1], I. Montealegre-Meléndez[2]

[1] RHP-Technology GmbH, Forschungs- und Technologiezentrum, 2444 Seibersdorf, Austria

[2] Dpto. Ingeniería y Ciencia de los Materiales y del Transporte, Universidad de Sevilla, Camino de los Descubrimientos s/n, Sevilla, Spain

Abstract:

Poly(ether-ether-ketone) (PEEK) is a high-performance thermoplastic extensively employed in aerospace, automotive and biomedical applications owing to its outstanding mechanical properties, thermal stability and chemical resistance. Graphene has attracted considerable interest as a reinforcing nanofiller due to its exceptional mechanical strength and intrinsic lubricating capability. Nevertheless, achieving an efficient interaction between graphene and the polymer matrix remains one of the main challenges for the development of high-performance PEEK composites.

In this work, the influence of graphene surface modification and processing conditions on the consolidation and tribological behaviour of PEEK composites was investigated. Composites containing three different graphene materials, including plasma-functionalized few-layer graphene, pristine few-layer graphene and a commercial graphene grade were manufactured by Rapid Sinter Pressing (RSP), an advanced powder consolidation technology characterized by short processing cycles and high heating rates. Graphene contents between 1 and 10 vol.% and two sintering temperatures (330 and 350 °C) were evaluated to determine the combined effect of reinforcement characteristics and processing parameters on the final material performance.

Microstructural characterization revealed that graphene incorporation significantly affected composite densification, promoting variations in density and the formation of internal porosity depending on graphene type and concentration. Tribological testing demonstrated that the response of the composites was governed by a complex interaction between filler characteristics, processing temperature and graphene content. While high graphene loadings generally increased friction and wear, low graphene additions exhibited a more favourable behaviour. In particular, the composite reinforced with 1 vol.% G3 graphene displayed the best tribological performance, maintaining a wear rate close to that of neat PEEK while showing only a moderate increase in the coefficient of friction.

The results demonstrate that the tribological performance of PEEK/graphene nanocomposites depends not only on graphene content but also on the surface characteristics of the reinforcement and the optimisation of Rapid Sinter Pressing parameters. These findings provide valuable guidelines for the design of lightweight, wear-resistant polymer composites for advanced engineering applications.

Keywords: PEEK, Graphene, Rapid Sinter Pressing, tribological properties.

Aclnowleadgemnent:

This research was carried out with support from the FFG-funded G4Space project (project number: FO999911933).

Valorization of aggregate-washing sludge and cork residues for porous ceramics with tailored physical and thermal properties

Blanca G. Silva-García[1],*, J. M. Terrones-Saeta[2], L. Segovia-Guerrero[3], N. Baladés[2], D. L. Sales[1]

[1] INNANOMAT Group, Department of Materials Science, Metallurgical Engineering and Inorganic Chemistry, IMEYMAT, Algeciras School of Engineering and Technology, Universidad de Cádiz, Ramón Puyol ave., Algeciras, 11202, Spain.
[2] IEG Group, Department of Industrial Engineering and Civil Engineering, IMEYMAT, Algeciras School of Engineering and Technology, Universidad de Cádiz, Ramón Puyol ave., Algeciras, 11202, Spain.
[3] INNANOMAT Group, Department of Industrial Engineering and Civil Engineering, IMEYMAT, Algeciras School of Engineering and Technology, Universidad de Cádiz, Ramón Puyol ave., Algeciras, 11202, Spain.
*Corresponding author: blanca.silva@uca.es

Abstract:
Aggregate-washing operations generate fine, clay-rich sludge with limited reuse potential, while low-grade cork residues have few value-added applications. Cork has previously been investigated as a lightweight component in building materials [1,2]. This study investigates the combined valorization of both waste streams to produce porous ceramic materials, using ground cork as a sacrificial pore-forming agent. A total of 45 prismatic specimens were manufactured with cork contents of 0, 2.5, 5, 7.5, 10, 15, and 20 wt.%. The mixtures were compacted for 1 min using a hydraulic press operated at a gauge pressure of 100 bar, dried at 100 °C for 24 h, and fired at 950 °C. Dimensional changes, mass loss, geometric density, and water absorption were evaluated. Thermal conductivity was determined using a C-Therm Trident system on representative specimens from each formulated series. Geometric density decreased from 1.88 g·cm^{-3} for the reference ceramic to 1.42 g·cm^{-3} at 10 wt.% cork and 1.25 g·cm^{-3} at 20 wt.%. Cold-water absorption increased from 14.53% for the reference ceramic to 25.89% and 33.53% for specimens containing 10 and 20 wt.% cork, respectively. The available thermal results showed that thermal conductivity decreased from 0.7474 W·m^{-1}·K^{-1} for the cork-free ceramic to 0.6732 W·m^{-1}·K^{-1} at 10 wt.% cork and 0.2926 W·m^{-1}·K^{-1} at 20 wt.% cork. Among the specimens tested to date, the 20 wt.% cork formulation exhibited the greatest reduction in thermal conductivity, reaching 60.8% relative to the reference ceramic. These results support the use of cork residue as a pore-forming agent during firing and demonstrate the potential to transform two waste streams into lightweight ceramic materials with tunable thermal properties.

Keywords: aggregate-washing sludge; cork residue; porous ceramics; pore-forming agent; thermal conductivity; waste valorization; sustainable construction.

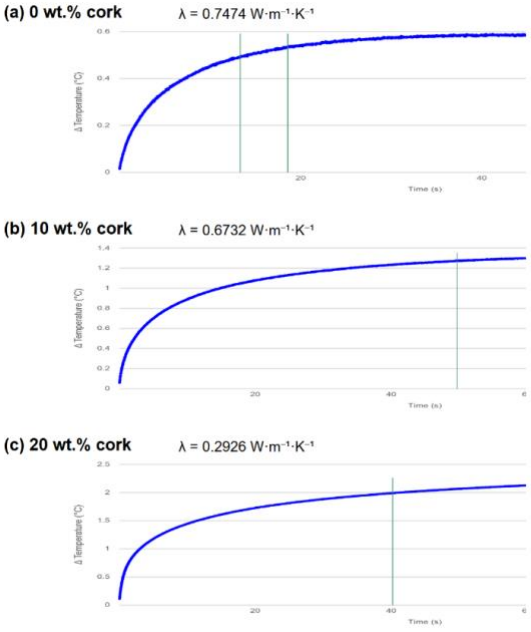


Figure 1: Transient temperature responses recorded using the C-Therm Trident system for fired ceramic specimens prepared with (a) 0, (b) 10, and (c) 20 wt.% cork additions.

References:

1. Mounir, S., Maaloufa, Y., Cherki, A. B., Khabbazi, A. (2014), Thermal properties of the composite material clay/granular cork, Construction and Building Materials, 70, 183-190.
2. Knapic, S., Oliveira, V., Machado, J. S., Pereira, H. (2016), Cork as a building material: a review, European Journal of Wood and Wood Products, 74, 775-791.

NanoMed / Sensors 2026 joint Session III.B: Nanotechnology in Drug Delivery / Environmental Sensors / Smart Sensor Networks

Catalytically propelled Janus pectin micromotors for enhanced tumour penetration and active drug delivery

T. Raj[1*], S. Ariraman[1], S. Chakraborty[2], V. Selvaraj[1], B. Roy[2], H. Kress[3], E. Mani[4], S. Sudhakar[1]

[1] Department of Applied Mechanics and Biomedical Engineering, Indian Institute of Technology Madras, Chennai, India
[2] Department of Physics, Indian Institute of Technology Madras, Chennai, India
[3] Biological Physics, University of Bayreuth, Bayreuth, Germany
[4] Department of Chemical Engineering, Indian Institute of Technology Madras, Chennai, India

Abstract:
Passively diffusing micro/nanocarriers based cancer therapeutics suffer from limited tumour penetration and cellular uptake. While self-propelled micro/nanomotors present as alternatives, their predominant inorganic composition hinders clinical translation. Hence, this study reports the fabrication of self-propelling micromotors derived from pectin polysaccharides, powered by H_2O_2 decomposition by the asymmetric surface platinum coating. Their self-propulsion is characterized through mean-square displacement and optical tweezers based analysis. They exhibit enhanced penetration into extracellular matrix simulant compared to passive counterparts. The 5-fluorouracil-loaded micromotors with H_2O_2 fuel availability (5% w/v) display 25-fold faster drug release than fuel-devoid micromotors. In-vitro assays confirm the micromotors' biocompatibility with human embryonic kidney cells. Contrarily, self-propelling drug-loaded micromotors show superior cytotoxicity against breast cancer cells with 10-fold lesser half-maximal inhibitory concentration than passive microcarriers. Cellular internalization measurements reveal a 21% increase in intracellular platinum content in cancer cells treated with micromotors with H_2O_2 fuel availability, indicating enhanced cellular uptake rates driven by their active motion. Furthermore, the anti-angiogenesis potential of self-propelling drug-loaded micromotors is confirmed by an *ex ovo* chorioallantoic membrane assay. Overall, this work showcases the development of active drug carriers holding tremendous potential to be used in breast cancer therapy.

Keywords: Pectin Micromotors, Self-Propulsion, Active Drug Delivery, Breast Cancer Therapy, Propulsion Force, Optical Tweezers.

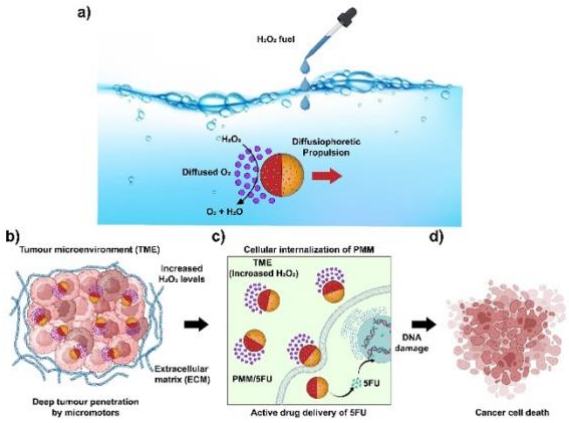


Figure 1: (a) Diffusiophoretic propulsion mechanism of micromotors, Schematics illustrating the (b) enhanced tumour penetration, (c) cellular internalization, and (d) cancer cell death induced by the micromotors.

References:

1. Raj et.al. (2025) Direct measurement of self-diffusiophoretic force generated by active colloids of different patch coverage using optical tweezers, *Journal of Colloid and Interface Science*, 677, 986-996.
2. Yang et.al. (2025) Platinum micromotors for mucosal penetration and colorectal cancer therapy, *International Journal of Pharmaceutics*, 670, 125201.
3. Patino et.al. (2018) Influence of Enzyme Quantity and Distribution on the Self-Propulsion of Non-Janus Urease-Powered Micromotors, *Journal of the American Chemical Society*, 140, 7896-7903.

Functional Materials for Non-Enzymatic Electrochemical Detection of Metabolites

M. Kuznowicz[1,2,*], A. Jędrzak[2], T. Jesionowski[2]
[1]Interdisciplinary Centre for Ecotechnology, Poznan University of Technology, PL–61131 Poznan, Poland
[2]Institute of Chemical Technology and Engineering, Faculty of Chemical Technology,
Poznan University of Technology, Berdychowo 4, PL–61131 Poznan, Poland

Abstract:
Hybrid nanomaterials represent a promising platform for the development of advanced non-enzymatic electrochemical sensors due to their high surface area, tunable surface chemistry, and synergistic combination of individual components. In this work, different hybrid nanostructured materials, including core-shell architectures, were designed and investigated as electroactive sensing platforms for the detection of biologically relevant metabolites, with particular emphasis on nicotinamide adenine dinucleotide (NADH) and glucose [1,2]. The core-shell structure enables the integration of complementary physicochemical properties within a single nanomaterial, improving charge-transfer processes, electroactive surface accessibility, and interactions with target analytes. The developed sensing platforms were systematically characterized and their electrochemical performance was evaluated under optimized experimental conditions. Particular attention was devoted to the comparison of key analytical parameters, including sensitivity, linear detection range, limit of detection, selectivity toward potential interfering species, response time, repeatability, reproducibility, and long-term stability. The influence of nanomaterial composition, surface functionalization, and core-shell architecture on the overall sensing performance was also investigated. The obtained results demonstrate that rational design of hybrid nanostructures can significantly improve the electrochemical recognition and detection of NADH and glucose, providing a versatile approach toward stable, selective, and sensitive enzyme-free sensing platforms for future biomedical and point-of-care applications. enlightened with potential optical applications [3].

Keywords: hybrid nanomaterials; core-shell nanostructures; non-enzymatic sensors; NADH; glucose

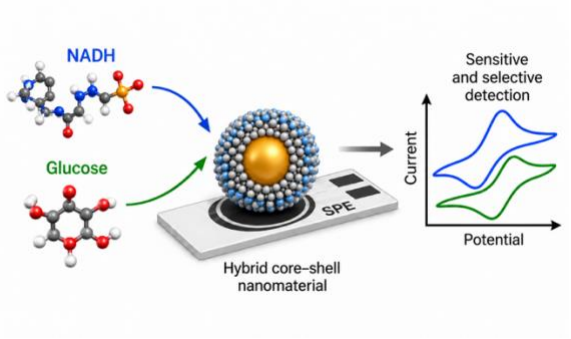


Figure 1: chematic representation of hybrid core–shell nanomaterial-modified SPEs for non-enzymatic electrochemical detection of NADH and glucose.

References:

1. Kuznowicz, M., Rębiś, T., Jędrzak, A., Nowaczyk, G., Szybowicz, M., Jesionowski, T. (2022), Glucose determination using amperometric non-enzymatic sensor based on electroactive poly(caffeic acid)@MWCNT decorated with CuO nanoparticles, Microchim. Acta, 189, 159.
2. Rębiś, T., Kuznowicz, M., Jędrzak, A., Milczarek, G., Jesionowski, T. (2021), Design and fabrication of low potential NADH-sensor based on poly(caffeic acid)@multi-walled carbon nanotubes, Electrochim. Acta, 386, 138384.
3. Jędrzak, A., Kuznowicz, M., Jesionowski, T. (2024), Mobile-assisted diagnostic biosensor for point-of-care glucose detection in real human samples with rapid response and long-life stability, J. Appl. Electrochem., 54, 163–174.

Recent advances in optical materials and smart fibers to combat counterfeiting

Meram S. Abdelrahman[1,*], Zakaria E. Ahmed[2], Yasser A. Attia[2], Claas Falldorf[3], Ralf B. Bergmann[3], Tawfik A. Khattab[1,*]

[1] Dyeing, Printing and Auxiliaries Department, Textile Research and Technology Institute, National Research Centre, Cairo 12622, Egypt;
ms.abdel-rahman@nrc.sci.eg (M.S.A.); ta.khattab@nrc.sci.eg (T.A.K.)

[2] Laser Applications in Metrology, Photochemistry, and Agriculture Department, National Institute of Laser Enhanced Science, Cairo University, Giza 12613, Egypt; zakaria.fm@jp.gov.eg (Z.E.A.); yasserniles@niles.edu.eg (Y.A.A.)

[3] Bremer Institut für Angewandte Strahltechnik, 28359 Bremen, Germany; falldorf@bias.de (C.F.); bergmann@bias.de (R.B.B.)

[*] Correspondence: ta.khattab@nrc.sci.eg

Abstract:
Forgery of official documents, banknotes, and brand protection continues to be a worldwide crisis for government, business, industry, and consumer. Counterfeiting has shown serious security, financial, and health implications. On the other hand, the evolution of fibrous materials has significantly contributed to the improvement of human civilization. Chromic fibers undergo noticeable colorimetric changes upon exposure to external stimuli, such as heat, magnetic field, electricity, moisture, and light. They have been critical for many fields, such as healthcare monitoring, wound monitoring, electronic displays, drug release, and sensory tools. They have also been used to develop protective tools against extreme variations in the surrounding environment, such as high temperatures, radiation, and electric field. This review presents the major classes of chromic agents and their associated processes. The materials and procedures used in the development of chromic fibers are discussed. The sustainability of chromic fibrous materials is explored, demonstrating biodegradability, natural chromic sources, energy-efficient production, and environmental effects. The design strategies for each chromic category are discussed, exploring useful materials, preparation methods, and advanced applications. The challenges and potential improvements of chromic fibers are presented. Recently, the chemical stability and optical characteristics of photochromic and photoluminescent agents result in their extensive usage toward the development of security encoding products. Both aqueous and solvent inks have been reported for anticounterfeiting purposes. In addition, the printing methods of anticounterfeiting ink, including stamping, inkjet printing, labeling, screen printing, and handwriting, onto various surfaces are discussed.
Keywords: Smart fibers; Stimuli-responsive; Anticounterfeiting ink; Security printing.

Acknowledgements

This work was funded by the Deutsche Forschungsgemeinschaft (DFG) within the project "Securing valuable documents using computer generated holograms printed with photochromic inks" (Secret-CGH, project no. 536608072). The authors are thankful for the financial support from the National Research Centre, Egypt.

References:

1. S. D. Al-Qahtani, G. M. Al-Senani, A. A. Al-Wallan. *Journal of Applied Polymer Science* (2026) e71125.
2. M. S. Abdelrahman, T. A. Khattab. *Luminescence* 39 (2024) e4800.
3. Z. E. Ahmed, R. M. Abdelazeem, Y. A. Attia, T. A. Khattab, C. Falldorf, R. B. Bergmann, M. Agour. *Sensors* 25 (2025) 2410.
4. M. H. El-Newehy, H. Y. Kim, T. A. Khattab, M. E. El-Naggar. *Ceramics International* 48 (2022) 3495-3503.
5. M. Gouda, M. F. Abou Taleb. *Cellulose* 32 (2025) 9543-9554.

Humidity-Assisted Machine Learning Calibration of PdAu Resistive Hydrogen Sensors Under Aerobic Conditions

J. Herbeck-Tazibt [1,*], H. I. Turan [1,2], M. A. Djeziri [1], T. Fiorido [1], H. T. Hayvaci [2]
[1] Aix-Marseille Univ, Université de Toulon, CNRS, IM2NP, Marseille, France
[2] College of Engineering and Technology, American University of the Middle East, Egaila, Kuwait
* Corresponding author: jordan.herbeck-tazibt@im2np.fr

Abstract:
Hydrogen concentration estimation using PdAu resistive sensors remains challenging under humid aerobic conditions, where oxygen and water vapor can simultaneously affect the sensitive layer and distort the electrical response. This work presents a humidity-assisted machine learning calibration framework for PdAu resistive hydrogen sensors operating under controlled aerobic conditions. The sensor was characterized over a hydrogen concentration range from 3000 to 30000 ppm under four relative humidity levels: 0 %, 20 %, 40 %, and 80 % RH. Cycle-level descriptors were extracted from resistance and current signals and combined with RH-dependent interaction terms and a humidity-dependent baseline-normalized response. The objective is not to demonstrate an intrinsically humidity-insensitive sensing material, but to compensate humidity-induced distortions by explicitly using relative humidity as an auxiliary input. Several regression models were compared, including Linear Regression, Polynomial Ridge Regression, Support Vector Regression, Random Forest, Gradient Boosting, XGBoost, LightGBM, and a Multi-Layer Perceptron. A leave-one-humidity-out validation protocol was used to evaluate the ability of the models to generalize to unseen humidity conditions. Among the evaluated models, Gradient Boosting provided the best trade-off between prediction accuracy and stability, with a mean relative error of 16.3 % and an average R^2 value of 0.828 when tested on humidity levels excluded from training. The proposed humidity-aware feature set significantly reduced the prediction error compared with a model using only electrical peak descriptors. In addition, statistical analysis and sensitivity tests to RH measurement errors support the relevance of the proposed calibration strategy. These results show that humidity-assisted machine learning can improve hydrogen concentration estimation from PdAu resistive sensors under controlled aerobic conditions.

Keywords: hydrogen sensing, PdAu resistive sensor, humidity compensation, machine learning calibration, Gradient Boosting, relative humidity, aerobic environment.

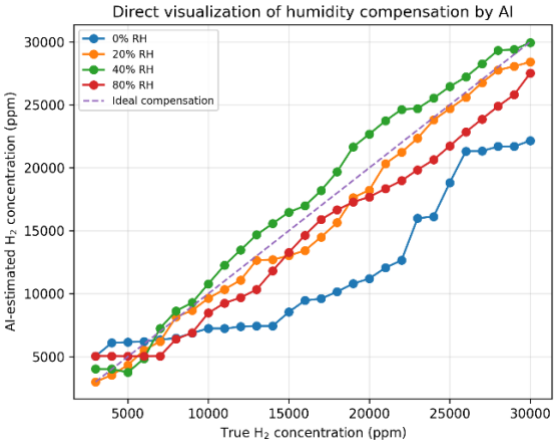


Figure 1: Direct visualization of humidity-assisted machine learning calibration. The true H_2 concentration is compared with the H_2 concentration estimated by the Gradient Boosting model under leave-one-humidity-out validation. The dashed line represents the ideal prediction line.

References:

1. Kim, J. Y.; Kim, J.; Nam, G. B.; Ryu, J.-E.; Park, S. J.; Lee, S. M.; Lee, G.-D.; Kim, J.; Jang, H. W. Highly durable chemoresistive micropatterned PdAu hydrogen sensors: Performance and mechanism. ACS Sensors, 2024, 9, 5363–5373.
2. Yuan, Z.; Luo, X.; Meng, F. Machine Learning-Assisted Research and Development of Chemiresistive Gas Sensors. Advanced Engineering Materials, 2024, 26, 2400782.

Challenges on dual-output rectifier-based power management circuits for triboelectric nanogenerators

F. Reverter, O. López, J. O. Casas, M. Gasulla
Department of Electronic Engineering, Universitat Politècnica de Catalunya—BarcelonaTech, Castelldefels (Barcelona), Spain

Abstract:
In the field of energy harvesting for autonomous sensors, triboelectric nanogenerators (TENGs) have emerged as a promising technology since their introduction in 2012 [1]. TENGs offer several advantages: low cost, light weight, robustness, and flexibility in material selection. However, the design of the ensuing power management circuit (PMC) remains challenging because of the unique properties of the TENG output: low current, high voltage, and high and time-varying internal impedance. Several PMC topologies have been proposed in the literature to manage the power generated by TENGs [2]. Most topologies rely on a rectifier together with a switching stage, thus resulting in the so-called *active rectifier*. Recently, it has been proposed to implement the rectifier by a full-wave rectifier (FWR) with a dual-output (DO): one output capturing energy from the positive half cycle, and the other from the negative [3]. In addition, it has been suggested to complement the FWR-DO with a synchronized switching stage (SSS) [4].
This work evaluates the challenges and limitations of including an SSS in an FWR-DO. The transition from a conventional FWR to an FWR-DO incorporating the SSS is illustrated in Figures 1(a) and (b). The SSS is intended to generate an instantaneous short-circuit across the TENG in synchronization with the maximum and minimum mechanical displacement. In such conditions, the voltage-charge (V-Q) plot can be extended from the representation in Figure 1(c) to that shown in Figure 1(d), where the area highlighted in red corresponds to the energy extracted per cycle. For the in-house fabricated TENG with a vertical contact-separation topology, the theoretical and experimental energy improvement factor was 4 in comparison to the FWR. The next challenge, with respect to [4], is the design of a self-driven, low-power peak detector capable of controlling the SSS while minimizing its loading effect on the TENG.

Keywords: dual-output rectifier, energy harvesting, power management circuit, triboelectric nanogenerator.

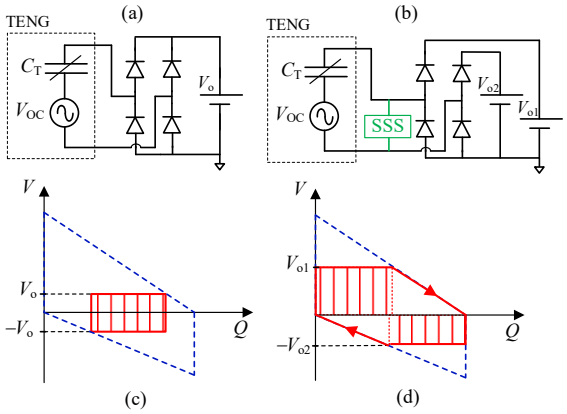


Figure 1: (a) Conventional FWR for a TENG, which is modelled by its equivalent Thévenin circuit that consists of a voltage source equal to the open-circuit voltage (V_{OC}) in series with an inherent variable capacitance (C_T). (b) FWR-DO including an SSS at the input. (c) V-Q plot when using the circuit in Figure 1(a), where V_o is the constant voltage assumed at the output. (d) V-Q plot when applying the circuit in Figure 1(b), where V_{o1} and V_{o2} are the constant voltages assumed at the two outputs of the rectifier.

References:

1. Fan, F.R., Tian, Z.Q., Lin Wang, Z. (2012) Flexible triboelectric generator, *Nano Energy*, 1 (2) 328–334.
2. Reverter, F., Du, S. (2026) Board-level power management circuits for triboelectric nanogenerators: A review, *IEEE Trans. Power Electron.*, 41 (7), 12274-12286.
3. Su, Y., Yanagisawa, M., Shi, Y. (2024) A dual-output rectifier-based self powered interface circuit for triboelectric nanogenerators, *IEEE Trans. Power Electron.*, 39 (6), 6630–6634.
4. Reverter, F., Du, S. (2026) A dual-output full-wave rectifier-based power management circuit with a synchronized input switch for triboelectric nanogenerators, *IEEE Trans. Power Electron.*, 41 (9), 16621-16629.

Acknowledgements: This work was supported by MICIU/AEI/10.13039/501100011033 under Grant PID2022-139505OB-I00.

Self-Powered Non-Contact PP/PVDF Triboelectric Sensor Enhanced by Low-Permittivity Supporting Layers

P. Slobodian[1,2*], Berenika Hausnerova[2,3]
[1]Department of Physics and Materials Engineering, Faculty of Technology, Tomas Bata University in Zlin, Zlin, Czech Republic
[2]Centre of Polymer Systems, University Institute, Tomas Bata University, Zlin, Czech Republic
[3]Department of Production Engineering, Faculty of Technology, Tomas Bata University in Zlin, Zlin, Czech Republic

Abstract:
Self-powered sensors capable of detecting mechanical stimuli without continuous physical contact are of increasing interest for motion monitoring, vibration detection, and flexible sensing platforms [1]. In this work, we present a simple non-contact triboelectric sensor based on commercially available polypropylene (PP) and electrospun polyvinylidene fluoride (PVDF) membranes. The system is first activated by contact electrification between the tribopositive PP and tribonegative PVDF layers, creating an interfacial charge state that remains after separation. Subsequent changes in the distance between the charged layers generate electrical signals by electrostatic induction, enabling sensing in a predominantly non-contact regime [3].
To enhance the sensor response, low-permittivity polymer films were introduced as supporting sublayers beneath the PVDF membrane. Polyvinyl chloride (PVC), biaxially oriented polyethylene terephthalate (BOPET), and low-density polyethylene (LDPE) were investigated as dielectric sublayers affecting the electric-field distribution in the multilayer structure. Rather than acting only as mechanical supports, these layers reduce dielectric screening of the interfacial charge and increase the induced voltage at the electrodes [2].
The electrical output strongly depended on the permittivity of the supporting layer. The reference PP/PVDF device generated an open-circuit voltage of approximately 376 V, while the LDPE-supported configuration reached up to 689 V. Similarly, the maximum power density increased from 2.05 mW cm^{-2} for the reference PP/PVDF device to 5.46 mW cm^{-2} for PP/PVDF+LDPE. The observed performance followed the order LDPE > BOPET > PVC, confirming that the dielectric environment of the tribonegative layer is a key factor controlling the sensor output.
The non-contact sensing function was demonstrated under different mechanical stimuli, including pressure loading, impact, vibration, and ultrasonic excitation. The voltage response reflected changes in the air-gap distance between the charged PP and PVDF layers, showing that the device can transduce mechanical motion into electrical signals without requiring repeated direct contact during operation. In addition to sensing, the generated output was sufficient for energy-harvesting demonstrations, including capacitor charging and intermittent LED operation after rectification.
These results show that PP/PVDF membranes combined with low-permittivity supporting layers provide a low-cost and scalable route toward self-powered non-contact sensors. The proposed approach highlights the importance of dielectric-field engineering in triboelectric sensing systems and offers potential for motion detection, vibration monitoring, touch-responsive interfaces, and mechanical energy harvesting.

Keywords: self-powered sensor, non-contact sensing, triboelectric nanogenerator, dielectric permittivity, vibration detection,

Acknowledgment

This publication was created as part of the implementation of the project Testing laboratory for the implementation of sustainable and resilient technologies, reg. number CZ.02.01.01/00/23_021/0010411, co-financed by the European Union under the OP Jan Amos Comenius.

References:

1. Wang, Z. L., Ren, Z., Dong, K. & Pan, C. (2021). Triboelectric nanogenerator: structure, mechanism, and applications. *ACS Nano* 15, 9600–9633.
2. Fu, X. et al. (2023). Non-contact triboelectric nanogenerator. *Advanced Functional Materials* 33, 2306749.
3. Min, G. et al. (2020). Triboelectric nanogenerator with enhanced performance via an optimized low permittivity substrate. *IEEE Sensors Journal* 20, 6856–6862.

Assessing olive oil adulteration by comparing the discerning performances of nanostructured gas sensors and human olfaction

M. Astolfi [1,2*], M. Masin [1], M. Barbieri [1], I. Donelli [1], L. Montesi [1],S. Gherardi [2], C. Malagù [2,3], A. Pignatelli[1], and G. Rispoli[1]

[1] Department of Neuroscience and Rehabilitation, University of Ferrara, Ferrara, Italy

[2] Scent S.r.l., Via Quadrifoglio 11, 44124, Ferrara (FE), Italy

[3] Department of Physics and Earth Sciences, University of Ferrara, Ferrara, Italy

Abstract:

Olive oil (OO) is a very important food of the Mediterranean diet, characterized by a distinctive flavor, that are clearly recognizable, and well known health-benefits for consumers [1]. Its adulteration (AO) with cheaper oils is a major concern, since it reduces the OO quality and presents concrete risk for consumers, including exposure to undeclared ingredients and or chemical contaminants, presence of allergens, reduced nutritional values, etc. Although effective, current detection methods rely on complex laboratory techniques, requiring long examination times and higly specialized personnel, making them complex and not suitable for field use [2,3]. On this basis, in this study metal-oxide gas sensors, based on semiconductor nanostructures, were employed to discriminate 100% OO samples from 25% (25AO), and 50% (50AO) adultered ones and then compare the sensor's discrimination capabilities with olfaction ones of a sample of 45 randomly selected individuals; indeed olfaction plays a crucial role in the sensory evaluation of foods, including OO, however the ability of untrained individuals to distinguish OO from AO samples is generally considered limited. In order to involve only subjects in normosmic olfactory function, the 45 participants (26 females and 19 males), aged 20–40 years, were preliminarily assessed using Sniffin' Sticks test ODOFIN [4] (Threshold, Discrimination, and Identification): the average score of the participants on the Sniffin' Sticks test was 37 ± 3.6. Since the cutoff score to be classified as normosmic is 30.75, all the selected participants showed normal olfactory performances, alligned with this study constraints. Participants were then asked to discriminate the oil samples by using a triangle test approach [5]: OO vs 50AO, 25AO vs 50AO, and OO vs 25AO. The average scores in discriminating the samples were 1.26/3, 1.10/3, and 0.90/3, respectively, highlighting the limited discriminative performance of the human olfaction in particular between OO and 25AO. Then eight different nanostructured gas sensors were tested on the exhalations of the same oil samples (n=45), and tin and titanium oxide-based sensors (STN and ST10), as well as a tungsten-based sensor (W11), showed the best performance (Fig. 1). These sensors exhibited a progressively decreasing response with increasing levels of adulteration: for STx sensors were observed variations of 12% and 22% by comparing OO sample vs 25AO and 50AO ones, respectively, and these variations were approximately 11% and 25% for W11 sensor. These percentages were obtained by averaging all measurements, while the standard errors were consistently very small and non-overlapping. In conclusion, given the generally poor ability of the human sense of smell to discriminate samples of AO, these findings underline the strong capability of nanostructured gas sensors to outperform human olfaction in detecting olive oil adulteration.

Keywords: Nanosensors, volatile compounds, olive oil, adulteration, response, sniffin'test, olfactory

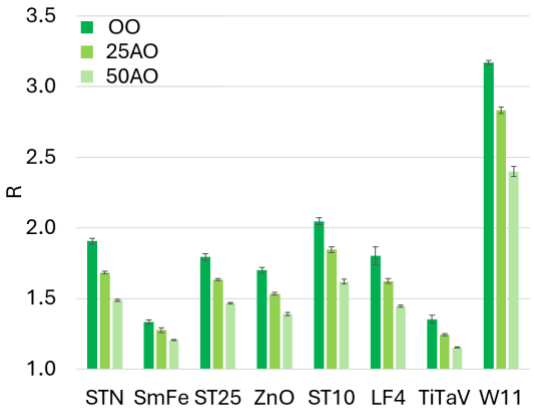


Figure 1: Average sensors responses to OO (dark green bars), and 25AO and 50AO (lighter green bars respectively).

References:

1. Salvo, A.; Tuttolomondo, A. The Role of Olive Oil in Cardiometabolic Risk. Metabolites 2025, 15, 190, doi:10.3390/metabo15030190.
2. Mandal, N.; Moirangthem, R.S. Unveiling Olive Oil Authenticity: A Comprehensive

Study on Adulteration Detection through SPR-Enhanced Ellipsometry. Food Anal. Methods 2025, 18, 442–458, doi:10.1007/s12161-024-02724-4.
3. Alharbi, H.; Kahfi, J.; Dutta, A.; Jaremko, M.; Emwas, A.-H. The Detection of Adulteration of Olive Oil with Various Vegetable Oils – A Case Study Using High-Resolution 700 MHz NMR Spectroscopy Coupled with Multivariate Data Analysis. Food Control 2024, 166, 110679, doi:10.1016/j.foodcont.2024.110679.
4. Sniffin' Sticks Olfactory Test (ODOFIN) Burghart - MediSense. MediSense | Smelltest.eu.
5. Triangle Test. In Discrimination Testing in Sensory Science; Woodhead Publishing, 2017; pp. 153–170.

Damage Detection Sensitivity of Sensor Technologies Under Varying Operational Conditions

M. Dziendzikowski [1,2,*], K. Kowalczyk [1,2], Z. Dworakowski [3]
[1] Airworthiness Division, Air Force Institute of Technology, Warsaw, Poland
[2] Faculty of Materials Science and Engineering, Warsaw University of Technology, Warsaw, Poland
[3] Department of Robotics and Mechatronics, AGH University of Science and Technology, Krakow, Poland

Abstract:
In the presentation we will focus on characterization of resistive crack proapagation sensors, eddy current sensors as well as PZT sensors in terms of their sensitivity to damage, also in varying measurement conditions. For efficiency assessment, a methodology closed to MIL-HDBK-1823A for probability of damage detection will be followed. For PZT sensors, as they are widely used in Structural Health Monitoring (SHM) due to their ability to excite guided waves for damage detection propagating in any type of material, also results of structure evaluation based on guided waves excited by PZT transducers and full wavefield measurements obtained by laser scanning vibrometer will be presented. The measurements were acquired for pristine state of test structure and with introduced damage, therefore it is possible to calculate spatial distribution of various signal characteristics and estimate effective range of PZT sensors for damage detection based on a given damage index. Various parameters affecting the damage detection range will be compared, in particular: extent of damage, type of signal characteristic used, parameters of the excitation signal (e.g. frequency, duration), as well time interval used for damage index calculation. The obtained results may be useful for estimating the efficient range of PZT sensors sensitivity as well as for refining algorithms for sensor placement optimization and damage localization techniques calibration, e.g. based on RAPID imaging algorithm.
For resistance crack gauges, their sensitivity to fatigue crack propagation, both for open and closed-crack condition will be discussed. For eddy current sensors two damage scenarios are considered, i.e.: cracks and material erosion. For PZT sensors, in addition to those types of defects, also sensitivity to impact damage will be presented and discussed as well. Influence of environmental conditions on damage detection capabilities, such as: temperature, humidity or load, will be also discussed.

Keywords: probability of detection, network geometry optimization, Damage Indices sensitivity, laser vibrometer applications

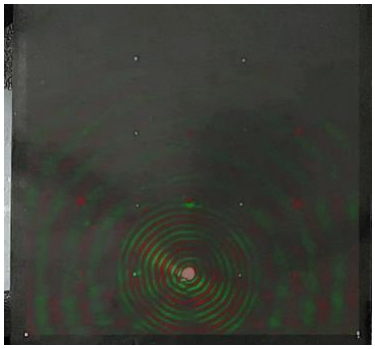


Figure 1: Snapshot of spatial guided waves distribution, excited by a PZT sensor and measured with use of scanning laser vibrometer

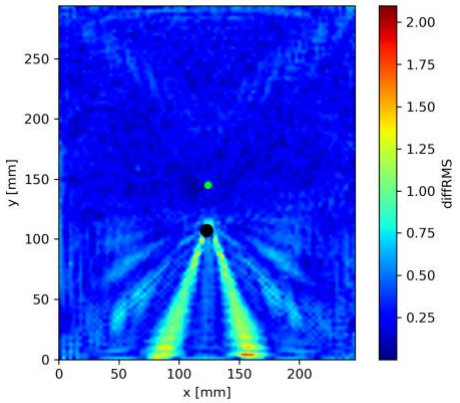


Figure 2: Pattern of Signal Feature distribution after damage introduction, based on full wavefield measurements of guided waves propagation, excited in a plate-like structure by a PZT transducer

References:

1. Dworakowski Z., Kowalczyk K., Dziendzikowski M. (2025) Feature map field fusion of guided wave vibrometer data for increased fault localization capability, *Struct. Health Monit.,* In Press.

Multidirectional Mechanical Stability and Seam Efficiency of Woven Reinforced Laminated Composites

I. Schwarz *
University of Zagreb Faculty of Textile Technology, Zagreb, Croatia

Abstract:
Woven reinforced laminated composites are multilayer textile materials whose mechanical behaviour depends on the interaction between the surface layer, polyurethane foam interlayer and textile reinforcement positioned on the back side of the laminate. In such systems, the reinforcement structure plays a key role in load transfer, directional stability and deformation control. This study investigates the orientation-dependent tensile behaviour, seam efficiency and burst performance of two laminated composites composed of artificial leather, polyurethane foam and cotton woven reinforcement.
The mechanical response of the composites was evaluated through breaking force and elongation at break in six loading directions: 0°, 30°, 60°, 90°, 120° and 150°. The 0° direction corresponded to the weft direction, while the 90° direction represented the warp direction of the woven reinforcement. Based on the tensile results, mechanical anisotropy, directional variability and mean tensile resistance were analysed to assess composite stability under different loading orientations. Seam efficiency and seam-induced weakening were evaluated by comparing seamed and unseamed specimens tested in the principal warp direction. In addition, ball burst force, ball burst elongation and the Burst Performance Index were used to assess resistance to concentrated multidirectional loading.
The results confirmed pronounced anisotropic behaviour in both laminated composites. The highest breaking force was recorded in the warp direction, while lower tensile resistance and greater deformation were observed under off-axis loading. Composite B showed higher maximum, minimum and mean tensile resistance, a lower anisotropy coefficient, reduced directional variability and higher ball burst performance, indicating better overall multidirectional mechanical stability and more balanced load-bearing behaviour. However, Composite A exhibited higher seam efficiency and lower seam-induced weakening, demonstrating better preservation of tensile resistance after stitch formation.
The findings show that superior tensile and burst performance do not necessarily correspond to superior seam-related behaviour. Therefore, the mechanical performance of woven reinforced laminated composites should not be evaluated only through maximum tensile resistance or principal-direction testing. A reliable assessment should include breaking force, elongation at break, off-axis tensile behaviour, anisotropy, seam efficiency, seam-induced weakening and ball burst performance. This distinction is particularly important for laminated materials intended for stitched applications, where high tensile resistance alone does not necessarily ensure good performance after seam formation. This integrated approach provides a clearer understanding of the relationship between reinforcement architecture, directional stability and seam durability in laminated composite material

Keywords: laminated composites, woven reinforcement, tensile properties, mechanical anisotropy, seam efficiency, ball burst performance.

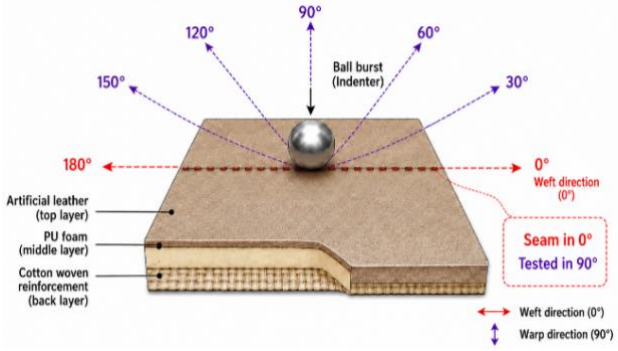


Figure 1. Schematic overview of the testing approach and performance behaviour of the analysed woven reinforced laminated composites.

References:

1. Li, A. et al. (2023). A consistent formulation for yarn re-orientation in shear and off-axis loading of woven composites RVEs. Composite Structures, 324.
2. Vilhanová, A. et al. (2022). The effect of selected factors on the strength of stitches of upholstery faux leather. Materials, 15(19).

Acknowledgment:
The publication of the work is a result of the implementation of the institutional research project "Research and development of sustainable, functional textile components for next-Generation composites ", FUNK-TEX, TTF-IIP-06, funded by the European Union - NextGenerationEU.

Plasmon-Enhanced Photocatalysis in Microflow: Synthesis and Application of surface-modified Au/PDMS nanocomposite

M. Rašljić Rafajilović [1*], M. V. Bošković [1], K. Radulović[1], M. Obradov [1], D. Vasiljević-Radović[1]
[1] Institute for Chemistry, Technology and Metallurgy, Department for Microelectronic Technologies, University of Belgrade, Belgrade, Serbia

Abstract:
Increasing industrialization leads to the generation of wastewater, the combustion of fossil fuels, and the emission of harmful gases, which generally cause many problems, including environmental pollution, energy crisis, greenhouse effect, climate change, and ultimately a global food crisis. Photocatalysis is a promising approach to addressing these issues. To effectively harness photocatalytic reactions and solar energy, it is essential to design a device that optimizes the utilization of solar radiation and photocatalytic processes. The design and fabrication of optofluidic devices, such as optofluidic microreactors with integrated plasmonic materials, is a promising technology that offers several advantages, including controllable microstructures, uniform irradiation, the ability to use a wide range of solar spectra, short molecular diffusion times, large surface-to-volume ratios, precise manipulation of small volumes of fluids, and high reaction efficiency (1). Integration of noble metal nanoparticles at the bottom of the microchannel increases process efficiency by harnessing plasmonic effects to enhance photocatalytic reactions in microreactors. Gold (Au) is among the most effective plasmonic materials (2) while poly(dimethylsiloxane) (PDMS) is a promising material for microreactor fabrication due to its transparency, flexibility, low cost, and non-toxicity (3). In this investigation, we propose synthesizing Au/PDMS nanocomposites on the PDMS surface near the microchannel surface, where the chemical reaction occurs, to maximize the utilization of incident radiation. We used a PDMS layer (Sylgard 184) with a 10:1 mixing ratio as a flexible holder, and an additional thin layer of PDMS 10:3 ratio for nanoparticle synthesis. The curing agent from PDMS, with an aspect ratio of 10:3, served as a reducing agent for the gold precursor (1mM HAuCl4 in ethanol). The Au/PDMS nanocomposite was synthesized via thermally-induced in situ reduction at 60 °C. Three samples were synthesized with varying heat exposure times (30 min, 60 min, 90min). Samples were investigated using UV-VIS, SEM, EDS, and microFTIR. At the end, the photocatalytic performance of all samples was examined by measuring the decomposition of methylene blue (MB) under the solar simulator (ABET LS150) for 30 minutes. The effects of various heat exposure times were used to determine optimal parameters for nanoparticle formation on the PDMS surface for plasmon-enhanced photocatalysis. The goal is to develop a streamlined, cost-effective approach to improve photocatalytic reactions in flexible microfluidic systems.

Keywords: plasmonic, photocatalysis, Au nanoparticles, PDMS, microreactors

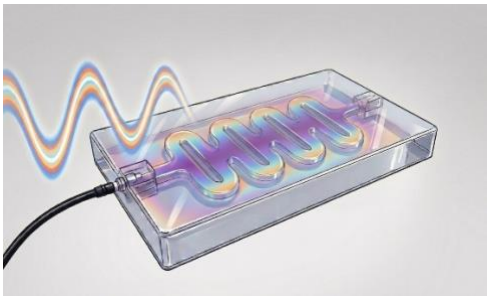


Figure 1: Figure illustrating the fundamental question that we are tempting to solve experimentally: integration of Au nanoparticles in a thin layer of PDMS for continuous-flow plasmonic enhanced photocatalysis. *The figure was AI-generated, Google Gemini*

References:

1. Jensen KF. 2001. Microreaction engineering—is small better? *Chemical Engineering Science* 56:293-303
2. Zhang X, Chen YL, Liu R-S, Tsai DP. 2013. Plasmonic photocatalysis. *Reports on Progress in Physics* 76:046401
3. Miranda I, Souza A, Sousa P, Ribeiro J, Castanheira EMS, et al. 2021. Properties and applications of PDMS for biomedical engineering: A review. *Journal of functional biomaterials* 13:2

Optimization of RF-Sputtered TiO_2 on Dewetted Au Nanoparticles for Plasmonic Photocatalysis

M. V. Bošković[1], O. Živković[1], M. Obradov[1], M. Rašljić Rafajilović[1], D. Vasiljević Radović[1]
[1]Institute of Chemistry, Technology and Metallurgy, Department of Microelectronic Technologies, University of Belgrade, Belgrade, Serbia

Abstract:
Plasmonic photocatalysis is a promising approach to remove organic pollutants from wastewater. It utilizes enhanced light absorption of metal nanoparticles coupled with the photocatalytic activity of certain semiconductors. One of the most used semiconductors for photocatalysis is titanium dioxide, due to its photochemical stability, abundance and cost-effectiveness. When exposed to light, electrons from the TiO_2 valence band are excited to the conduction band. If in contact with water, these electrons can reduce oxygen to form superoxide, while holes can oxidize water, to form hydroxyl radicals. However, it suffers from low activity in the visible spectrum as its bandgap of 3.2eV belongs to the UV part of the spectrum. Another problem with TiO_2 is charge recombination. In order to overcome these issues, TiO_2 is often combined with metal nanoparticles. To be chosen as a material for nanoparticles, metal must fulfil few parameters: It must be stable in electrolyte where catalysis will occur, its nanoparticles must have a plasmonic peak in the visible part of the spectrum, and it must form a Schottky barrier with semiconductor. Typically, nanoparticles are made of gold, silver, and copper or their combinations.
The aim of this study is to investigate the influence of TiO_2 deposition parameters on catalytic activity. We chose radiofrequency (RF) diode sputtering as the deposition method for TiO_2, varying the processing conditions – power and deposition time. RF sputtering allows control over crystal size and morphology, which influence light reflection and scattering, and therefore the amount of light reaching the nanoparticles. As the nanoparticle material, we chose gold prepared by thermal evaporation followed by solid-state thermal dewetting, as a well-known and well-investigated system that allowed us to examine only the influence of the TiO_2 layer. Photodegradation of aqueous solution of methylene blue under solar irradiation was chosen as a benchmark test.

Keywords: plasmonic catalysis, thermal dewetting, heterostructure.

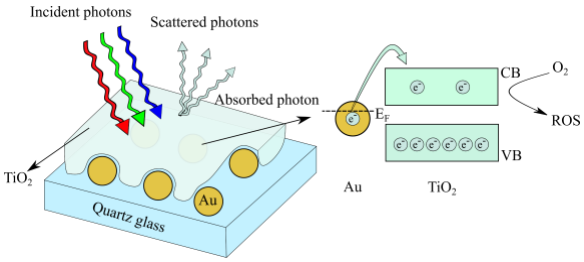


Figure 1. Schematic Illustration of the incident light interaction with TiO_2|Au plasmonic catalyst.

References:

1. Dong, H., Zeng, G., Tang, L., Fan, C.,Zhang, C., He, X., He, Y. (2015) An overview on limitations of TiO2-based particles for photocatalytic degradation of organic pollutants and the corresponding countermeasures, *Water research*, 79, 128-146.
2. Rather, R., Singh, S., and Pal, B. (2017) Photocatalytic Degradation of Methylene Blue by Plasmonic Metal-TiO2 Nanocatalysts Under Visible Light Irradiation, *Journal of Nanoscience and Nanotechnology*, 17, 1210-1216

Safe and Sustainable Bio-Based Functional Coatings for Textiles by Atmospheric Pressure Plasma Polymerization

P.Tovillas, M. Martínez-Falcón. M. Iñiguez, M. Martínez-Vergara
NOVEX, Arnedo, Spain

Abstract:
The textile industry increasingly requires high-performance surface treatments capable of providing water repellency, self-cleaning and antimicrobial properties while reducing the environmental and health concerns associated with conventional fluorinated and metal-based finishing agents. Within the framework of the European SSbD4CheM project, NOVEX is contributing to the development of safer and more sustainable functional coatings for textile applications based on atmospheric pressure plasma (APP) polymerization. Different renewable organic precursors were investigated as alternatives to conventional PFAS-based water-repellent treatments and metal-based antimicrobial coatings. Atmospheric plasma processing parameters, including plasma power, nitrogen and precursor flow rates and number of deposition cycles, were systematically adjusted to promote the formation of homogeneous functional layers on polyester textile substrates. The developed surfaces were characterized in terms of water contact angle, self-cleaning behaviour, antimicrobial activity and preliminary durability against mechanical abrasion and laundering. Plasma treatment transformed intrinsically wettable polyester fabrics into highly water-repellent surfaces, exhibiting excellent droplet roll-off and self-cleaning behaviour against common staining liquids. The optimized coatings retained water contact angles above 140° after a preliminary laundering cycle and maintained their functionality after mechanical abrasion. Furthermore, selected coatings demonstrated strong antibacterial activity against *Staphylococcus aureus*, with the antimicrobial effect being retained after mild laundering. These results demonstrate the potential of atmospheric pressure plasma polymerization as a dry, solvent-free and resource-efficient surface functionalization technology for producing multifunctional textile coatings. The combination of renewable precursors, reduced chemical consumption and functional durability provides a promising route towards replacing conventional PFAS- and metal-based textile finishes while integrating Safe and Sustainable by Design (SSbD) principles from the early stages of material development.

Keywords: Atmospheric pressure plasma; functional coatings; bio-based coatings; hydrophobicity; antimicrobial textiles; PFAS-free; self-cleaning; Safe and Sustainable by Design.

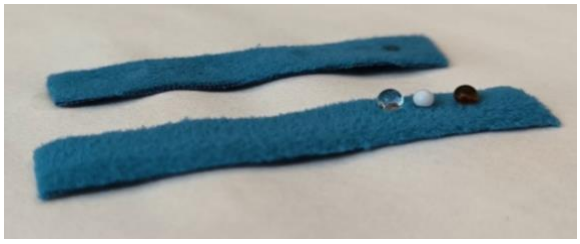


Figure 1: Water-repellent performance of plasma-coated PET textile, showing stable droplets of different liquids on the treated surface without immediate absorption.

Durability assessment of UV-cured functional SiO_xN_y thin films using climate chamber

E. Shmagina [1*], J. Küpersep [1], V.Shirokova [1], S. Bereznev [1, 2]
[1] Virumaa College, Tallinn University of Technology, Kohtla-Järve, Estonia
[2] Department of Materials and Environmental Technology, Tallinn University of Technology, Estonia

Abstract:
Polysilazanes and in particular perhydropolysilazane (PHPS) are currently becoming popular materials for the formation of protective and other functional Si-containing thin ceramic layers, and are also used as a matrix for the formation of various nanocomposites [1]. Particular attention is paid to the study of the transformation (curing) of PHPS into SiO_xN_y under the influence of UV radiation [2], which is compatible with temperature-sensitive technologies. Despite considerable interest and an increasing number of related publications, there remains a lack of knowledge in the area of long-term stability of UV-cured SiO_xN_y films.
In this work, we present the results of accelerated aging of PHPS films using a Memmert HPP110eco climate chamber (Memmert GmbH + Co. KG, Germany) to assess their stability under three-week exposure to moist heat (at various temperature and humidity parameters). A qualitative assessment of the obtained results was performed by using FTIR spectroscopy combined with optical microscopy on a Bruker Lumos II.
FTIR analysis (Figure 1) of the samples shows that the main structural transformations occur during the first week of exposure in the climat chamber and are accompanied by a decrease in the intensity of Si–H and Si–N vibrational bands, an increase in the intensity of Si–O–Si peaks, the formation of hydroxyl groups and the development of a more oxidized Si–O–Si network, which indicates a further transformation of the film material towards SiO_2. As the exposure time increases, the changes in the spectra become significantly less pronounced, indicating that the film structure has reached a steady state. Furthermore, the films demonstrate excellent adhesion to the substrate surfaces (glass and Mo/glass) and show no signs of degradation. The results of this study demonstrate that prolonged exposure to moist heat at various parameters does not lead to degradation of the PHPS-derived SiO_xN_y thin films. Moreover, more deep conversion (self-improving) in direction to SiO_2 was observed.

Keywords: pre-ceramic polymer; UV-curing; protective coating; silicon oxynitride; aging; stability

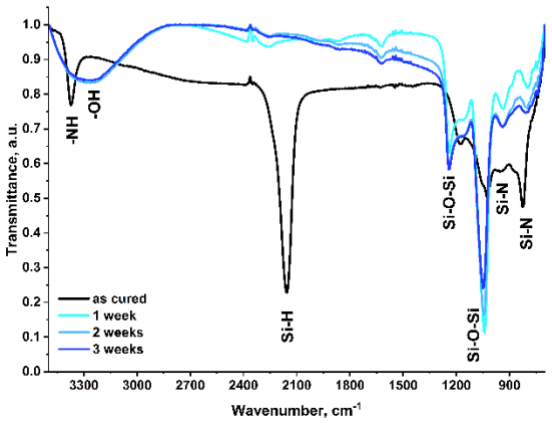


Figure 1: FTIR spectra of the as cured film before exposure in a climatic chamber (black curve) and after 1 week (azure), 2 weeks (light blue) and 3 weeks (blue) of exposure at 70 °C and 55% humidity.

References:

1. A. Chatterjee, S. Sen, D. Ramakanth, S. Singh, P. K. Maji. (2025) Unravelling polysilazanes: Synthesis, structure-property insights and versatile coating applications. *Advances in Colloid and Interface Science*. 342, 103508.
2. E. Shmagina, M. Danilson, V. Mikli, S. Bereznev. (2022) Comparative study of perhydropolysilazane protective films. *Surface Engineering*, 38, 7-9.

Acknowledgement:
This work was supported by the Estonian Ministry of Education and Research [grant number TK210], by the project „Increasing the knowledge intensity of Ida-Viru entrepreneurship “ co-funded by the European Union [in frames of ÕÜF5 project].

Core–Shell Engineering of Ge Quantum Dots for Enhanced Photodetector Response: Experiment and Electromagnetic Simulations

I. Periša[1], T.Car[1], K.V. Kripesh[1], K. Salamon[1], M. Mičetić[1]
[1]Ruđer Bošković Institute, Bijenička cesta 54, 10000 Zagreb, Croatia

Abstract

Core–shell engineering provides a promising approach for tailoring the optical and photoelectrical properties of semiconductor quantum-dot systems. In this work, we investigate the photoresponse of self-assembled Ge-based core–metal shell quantum dots embedded in dielectric matrices by combining experimental external quantum efficiency (EQE) measurements with electromagnetic simulations.

We investigate Ge/Mn and Ge/Al core–shell structures and Ge/Si_3N_4/Al double-shell structures with different Ge core sizes. A quasistatic electromagnetic model is used to calculate the total absorption efficiency, absorption in the inner semiconductor region, and electromagnetic field enhancement relative to bare Ge.

The simulations show that the spectral variations of the measured EQE cannot be explained by total nanoparticle absorption alone. In contrast, the relative electromagnetic field enhancement shows a stronger qualitative correspondence with the experimental photoresponse. Replacing Mn with Al results in pronounced low-energy field enhancement, while introducing an intermediate Si_3N_4 shell further increases and broadens the enhanced-field region, consistent with the experimentally observed increase and spectral broadening of EQE. Changes in Ge core size are also reflected in both the calculated electromagnetic response and the experimental photoresponse.

These results indicate that local electromagnetic field redistribution represents an important optical contribution to the enhanced photoresponse of Ge core–shell quantum-dot photodetectors.

Real-Time Plantar Pressure Monitoring and Personalized Offloading Feedback Using a Graphene/PVDF Fabric Sensor

N. Faramarzi[1], D. Boodaghian Asl[1], N. Pesce[1], H. Cheraghi Bidsorkhi[2], A. G. D'Aloia[1], M. S. Sarto[1]
[1] Department of Electrical and Energy Engineering, Sapienza University of Rome, Rome, Italy
[2] Department of Engineering, University of Sassari, Sassari, Italy

Abstract:
Flexible wearable pressure sensors enable continuous monitoring of plantar loading during daily activities and can provide useful feedback for pressure management, particularly for people with diabetes and reduced protective sensation [1–2]. In this work, we present a flexible graphene/polyvinylidene fluoride (PVDF) fabric-based piezoresistive sensor integrated with a wireless plantar pressure monitoring and feedback system. The sensor combines a graphene/PVDF-coated textile sensing layer with printed silver interdigitated electrodes on a flexible polyimide substrate, separated by an adhesive spacer. Applied pressure produces changes in the electrical resistance of the sensing layer, enabling continuous detection of plantar loading. The flexible, layered architecture is designed for integration into wearable systems and conformability during daily activities. The sensor is integrated with a voltage-divider circuit, a 12-bit nRF52840 Bluetooth Low Energy module, and a customized web application. In a proof-of-concept evaluation involving one healthy participant, sensors positioned at the heel and metatarsal regions detected pressure variations during sitting, standing, and walking and resolved individual gait cycles, demonstrating the feasibility of continuous wireless plantar pressure monitoring (Figure 1(a–c)).
To translate continuous pressure measurements into actionable feedback, the web application incorporates a personalized real-time monitoring and alert approach. It continuously evaluates plantar loading using both Peak Pressure (PP) and Pressure-Time Integral (PTI), representing instantaneous and cumulative mechanical stress, respectively [3]. Since elevated pressure and prolonged loading may both contribute to diabetic foot ulcer development, relying on either parameter alone may not adequately represent tissue loading conditions. Therefore, normalized PP and PTI values are combined into a personalized loading index based on subject-specific baseline measurements collected during normal walking. This calibration accounts for differences in body weight, gait characteristics, foot morphology, and plantar pressure distribution, allowing the loading index and alert thresholds to adapt to each user (Figure 1(d)). When the calculated index exceeds the personalized threshold, the application generates a visual alert prompting pressure redistribution to reduce localized tissue stress.
Demonstrated here in a healthy participant, the system establishes the technical feasibility of personalized real-time monitoring and alert generation and provides a basis for future clinical evaluation of its potential to support offloading in people with diabetes and reduced protective sensation.

Keywords: Graphene, Polyvinylidene fluoride, Pressure sensor, foot ulcer, diabetes.

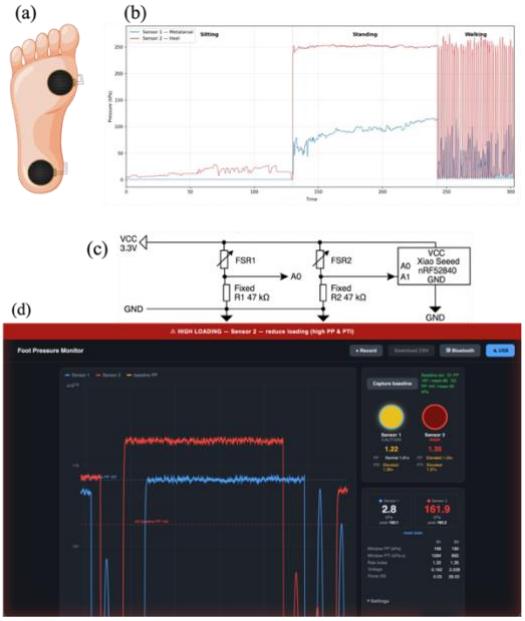


Figure 1. Sensor position under foot(a), real-time application of sensor on healthy volunteer on sitting, standing, and walking (b), electronic diagram (c), Web-based platform providing real-time plantar pressure monitoring and personalized feedback (d)

References:

1. Jodheea-Jutton, Abha, Sandip Hindocha, and Archana BhawLuximon. "Health economics of diabetic foot ulcer and recent trends to accelerate treatment." The Foot 52 (2022): 101909.
2. Fernando, M. E., et al. (2016), Plantar pressures are higher in cases with diabetic foot ulcers compared to controls despite a longer stance phase duration, BMC Endocr. Disord., 16, 51.
3. Bartolo, E., et al. (2023), The pressure time integral: an underused, clinically significant parameter as a determinant of neuropathic ulceration in diabetes, Gait Posture, 100, 210-215.

Atmospheric-Pressure Plasma-Engineered LTCC Gold Electrodes for Dopamine Biosensing

J. Cabaj [1*], W. Tylus [1], P. Jamróz [1], M. Czok [2], K. Malecha [2], S. Baluta[1]
[1] Faculty of Chemistry, Wroclaw University of Science and Technology, Wroclaw, Poland
[2] Faculty of Electronics, Photonics and Microsystems, Wroclaw University of Science and Technology, Wroclaw, Poland

Abstract:

Dopamine determination in biological samples requires sensing platforms combining high sensitivity, selectivity and stability with a simple fabrication procedure [1,2]. In this study, an LTCC-based laccase biosensor was developed using atmospheric-pressure plasma to modify integrated gold electrodes prior to enzyme immobilization [3]. The influence of plasma treatment time on the analytical performance of the resulting biosensors was investigated. Gold electrodes were exposed to plasma for 5, 7.5 and 10 min, followed by laccase immobilization and electrochemical characterization using differential pulse voltammetry. All investigated biosensors showed a concentration-dependent response toward dopamine in the range of 0.01-200 µM. The electrode treated for 7.5 min exhibited the best overall analytical performance, providing a sensitivity of 2.03 µA μM^{-1} cm^{-2} and a detection limit of 13.8 nM. The developed biosensor showed good reproducibility, with an RSD of 2.8%, and retained approximately 97% of its initial response after 14 days of storage. The influence of common electroactive interferents was also limited, with signal changes below 10% in the presence of ascorbic acid, uric acid and tyrosine. When applied to synthetic human serum, the sensor provided a dopamine recovery of 85.45 ± 2.4%. The results demonstrate that atmospheric-pressure plasma offers a simple approach for tailoring LTCC gold electrodes and producing laccase-based biosensors with favorable analytical characteristics without the need for complex nanomaterial-based architectures.

Keywords: dopamine, laccase biosensor, atmospheric-pressure plasma, LTCC, gold electrode, electrochemical detection

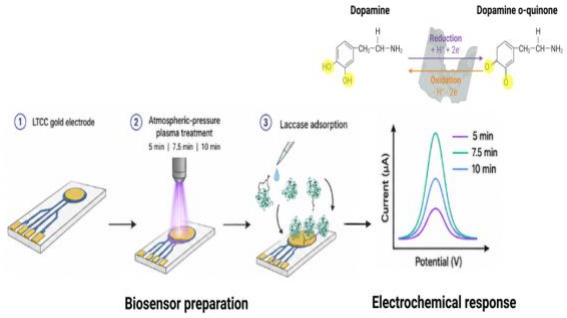


Figure 1: Schematic illustration of biosensor preparation and electrochemical dopamine detection using plasma-treated LTCC gold electrodes.

References:

1. Karimi Shervedani, R.; Amini, A. *Direct electrochemistry of dopamine on gold-Agaricus bisporus laccase enzyme electrode: Characterization and quantitative detection*. **Bioelectrochemistry** 2012, 84, 25–31. **DOI:** 10.1016/j.bioelechem.2011.10.004.

2. Pimpilova, M.; et al. *Biosensing Dopamine and L-Epinephrine with Laccase (Trametes pubescens) Immobilized on a Gold Modified Electrode*. **Biosensors** 2022, 12, 719. **DOI:** 10.3390/bios12090719.

3. Wardak, C.; et al. *Application of cold plasma corona discharge in preparation of laccase-based biosensors for dopamine determination*. **Materials Science and Engineering: C** 2020, 116, 111199. DOI: **10.1016/j.msec.2020.111199**.

Comparative study of the effects of Er:YAG, Cold Plasma and UV treatments on the surface wettability of titanium alloy and zirconium dioxide surfaces: An in vitro study

Zohreh Afradi[1], Brenda Laky[2,3,4], Andreas Moritz[2] , Markus Laky[1,2]and Hassan Ali Shokoohi Tabrizi1[1]

[1]. Core Facility Applied Physics, Laser and CAD / CAM-Technology, University Clinic of Dentistry, Medical University of Vienna, 1090 Vienna, Austria.
[2]. Division of Conservative Dentistry and Periodontology, University Clinic of Dentistry, Medical University of Vienna, 1090 Vienna, Austria.
[3]. Austrian Society of Regenerative Medicine, Vienna, Austria.
[4]. Sigmund Freud University, Faculty of Medicine, Vienna, Austria

Abstract:
Surface wettability plays an important role in the early stages of osseointegration, by influencing protein adsorption, cell adhesion, and tissue integration. The aim of our study was to evaluate the effect of Er:YAG laser (2940nm) on the surface wettability of titanium alloy and zirconium dioxide surfaces in comparison to the ultraviolet (UV) and cold plasma effects on surface treatments. A number of 100 Discs were used in this study, which were divided as follows: A number of 50 discs were used for the main experimental group, in that the contact angle measurements were done immediately after treatments, including 25 titanium alloy discs and 25 zirconium dioxide specimens, which were further divided into 5 subgroups, as follows (n=5 in each subgroup): 1. Control (untreated), 2. Cold plasma treatment, 3. UV treatment, 4. Er:YAG irradiation for 60 seconds, 5. Er:YAG irradiation for 90 seconds. To evaluate the stability of the surface treatment, additional contact angle measurements were performed at 24 and 48 hours post treatment in the selected subgroups. In titanium alloy group, the effects of cold plasma, UV and Er:YAG laser (60 second irradiation) on the surface after 24 and 48 hours were evaluated, with the total number of 30 samples (n=5 in each subgroup). And in zirconium dioxide group, the effect of cold plasma and UV treatments on the surface after 24 and 48 hours post treatment were analysed, with the total number of 20 samples (n=5 in each subgroup). All specimens underwent standardized cleaning procedures before treatment. Surface wettability was assessed by a tensiometer device. Furthermore, the arithmetical mean surface roughness (Ra) of the sample surfaces was measured and presented in tabular form. All data were analysed with ANOVA test to identify the statistically significant differences among treatment groups.Cold plasma and UV treatments significantly decreased the contact angle, which means an increase in surface wettability. Er:YAG laser
irradiation revealed a less decrease in contact angle on titanium alloy discs, in comparison to cold plasma and UV treatments. In contrast, with the Er:YAG surface treatments, no considerable effect could be found on zirconium dioxide discs. Time-dependant analysis demonstrated a gradual increase in contact angle at 24 and 48 hours in all the evaluated groups, which indicated a progressive loss of wettability effect over time, however the Er:YAG treated titanium alloy surfaces showed faster loss of hydrophilicity. The significant surface roughness decrease compared to control was only seen in subgroup 5 (Er:YAG, 90 seconds). Within the limitations of this experimental study, Er:YAG irradiation produces a moderate and transient increase in the hydrophilicity of titanium alloy discs but has no effect on zirconium dioxide. Plasma and UV treatments increase the hydrophilicity of titanium and zirconium dioxide surfaces. Only subgroup 5 (Er:YAG, 90 seconds) exhibited a significant decrease in surface roughness compared with the control.

Keywords: wettability, osseointegration, titanium alloy discs, zirconium dioxide discs, Er:YAG laser, cold plasma, UV, contact angle measurement, scanning electron microscopy, periimplantitis

References:

1. Rupp, F., et al., A review on the wettability of dental implant surfaces I: theoretical and experimental aspects. Acta Biomater, 2014. 10(7): p. 2894-906.
2. Gittens, R.A., et al., A review on the wettability of dental implant surfaces II: Biological and clinical aspects. Acta Biomater, 2014. 10(7): p. 2907-18.

From Catecholamines to Nanohybrids: New Materials for Point-of-Care Biosensing

A. Jędrzak [1,*], M. Kuznowicz [2], T. Jesionowski [1]
[1] Institute of Chemical Technology and Engineering, Faculty of Chemical Technology, Poznan University of Technology, Berdychowo 4, PL-61131 Poznan, Poland
[2] Interdisciplinary Centre for Ecotechnology, Poznan University of Technology, PL-61131 Poznan, Poland, *Corresponding author: artur.jedrzak@put.poznan.pl

Abstract:
The increasing demand for rapid, selective, sensitive, and affordable diagnostic tools has driven the development of point-of-care (POC) technologies. Among these, electrochemical biosensors based on screen-printed electrodes (SPEs) offer several advantages, including low cost, portability, and easy integration into miniaturized analytical systems. However, achieving high sensitivity, selectivity, and long-term stability remains challenging and strongly depends on the properties of the electrode interface.
Catecholamine-derived hybrid nanomaterials provide a promising strategy to address these challenges by integrating the complementary properties of different material classes within a single sensing platform. In this work, bioinspired polymers, including polydopamine and polynorepinephrine, were employed as building blocks for the development of multifunctional hybrid nanomaterial interfaces for electrochemical glucose biosensing.
The study aimed to investigate how the composition and structure of these hybrid materials influence electron transfer, enzyme immobilization, and overall biosensor performance. The developed interfaces were integrated with SPE platforms and systematically evaluated under conditions relevant to point-of-care applications.
The biosensors were characterized in terms of sensitivity, selectivity, limit of detection, linear range, reproducibility, and operational stability. The results demonstrate the potential of catecholamine-derived hybrid nanomaterials as versatile electrode modifiers for the development of robust and high-performance electrochemical glucose biosensors for point-of-care diagnostics.

Keywords: biosensing, POCT sensors, catecholoamines, nanomaterials, nanohybrids

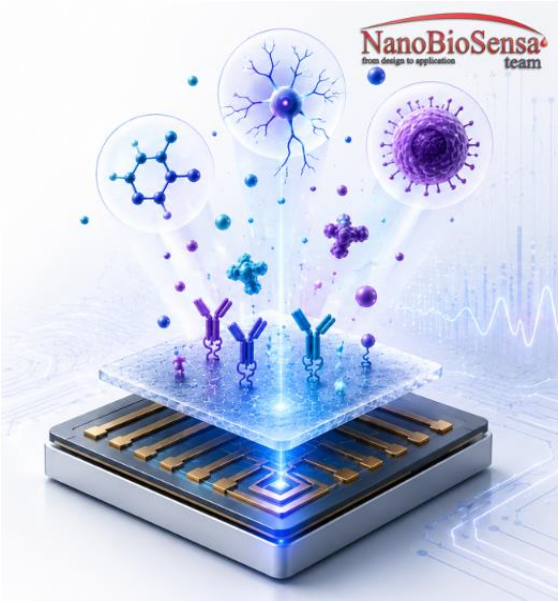


Figure 1: Graphical concept of the biosensor platform based on polycatecholamine materials developed by the NanoBioSensa Group at Poznan University of Technology.

References:

1. Singh S, Wang J, Cinti S. Review An Overview on Recent Progress in Screen-Printed Electroanalytical (Bio)Sensors. ECS Sensors Plus. 1 (2022) 023401. doi:10.1149/2754-2726/ac70e2.
2. A. Jędrzak, M. Kuznowicz, T. Jesionowski, Bioinspired catecholamine- derived AuNPs @polynorepinephrine@MWCNT electroactive nanomaterial for real-time monitoring of glucose dynamics, Microchim. Acta 193 (2026) 479. https://doi.org/10.1007/s00604-026-08201-5.

Acknowledgment:
The work was supported by the Poznan University of Technology under subsidy of Ministry for Science and Higher Education grant no. 0912/SBAD/2606.

Atomic-scale characterization of Ti-based alloy biomaterials for hip and knee endoprostheses

E. A. Gonzalez[1,*], M. G. Sandoval[1], P. V. Jasen[1], M. J. Jiménez[1], G.P. Brizuela[1], A. Hernández-Laguna[2], A. Juan[1], C. I. Sainz-Díaz[2]
[1] IFISUR, Departament of Physics, UNS, CONICET, Bahía Blanca, Argentina
[2] Instituto Andaluz de Ciencias de la Tierra (IACT-CSIC), Granada, Spain

Abstract:
Uncemented titanium implants used in total hip arthroplasty have demonstrated excellent clinical results over decades. However, a percentage of mid- and long-term failures is primarily associated with aseptic loosening and periprosthetic infections. Although experimental evidence demonstrates a correlation between surface contamination and persistent inflammation, the electronic and energetic mechanisms underlying this phenomenon have not yet been described at the atomistic level. In this work, plausible bulk structures of Ti6Al4V and Ti6Al7Nb alloys are developed to computationally simulate either their alpha or beta phases (Figure 1). These geometrical models have been built according to the experimental wt% content of the species reported by Jenko et al. [1]. All supercells have 54 atoms. The Al atoms are considered the alpha stabilizers, while the V and Nb atoms are the beta ones. Atomic-level modeling was performed using Density Functional Theory (DFT), implemented in the VASP code [2] and the CASTEP code within the MaterialsStudio package [3]. For the most energetically stable model of each alloy, the electronic, chemical, and physical properties of the simulated material were characterized. Calculations included densities of states, band structure, charge distribution (via Bader analysis), bond order, bulk and elastic modulus.

Keywords: Ti-based alloy biomaterials, DFT, atomic-scale, endoprostheses, biomedical applications.

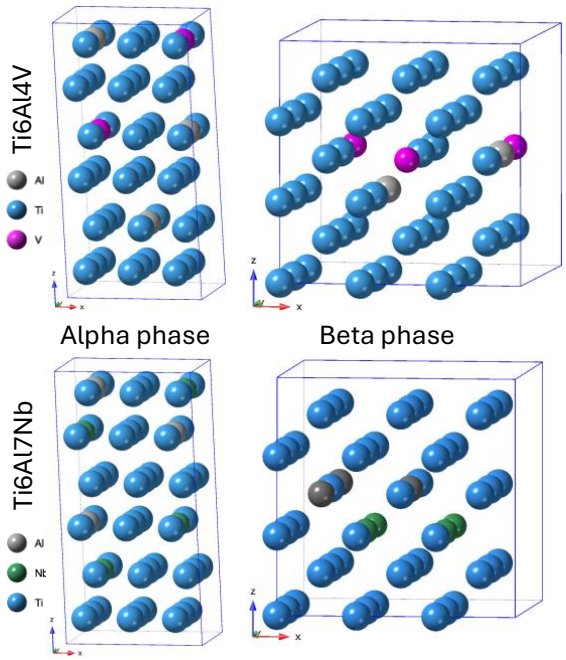


Figure 1: Schematic view of the minimal energy modeled geometry. They are built according to the wt% of the species present in the alloys ([1]).

References:

1. Jenko, M., Gorenšek, M., Godec, M., Hodnik, M., Šetina Batič, B., Donik, C., Grant, J.T., Dolinar, D. (2018) Surface chemistry and microstructure of metallic biomaterials for hipand knee endoprostheses. *Appl. Surf. Sci.*, 427, 584–593.
2. https://vasp.at
3. *BIOVIA Materials Studio*, version 2024; Dassault Systèmes: San Diego, CA, 2024.

Grading of magnetic anisotropy and engineering of domain wall dynamics in Fe-rich microwires by stress- annealing.

A. Zhukov[1,2], P. Corte-Leon,[1,3,4], J. M. Blanco[1], and V. Zhukova[1,4],*
[1] Dept. Appl. Phys., EIG, University of the Basque Country, EHU, 20018, San Sebastian, Spain
[2] IKERBASQUE, Basque Foundation for Science, 48011 Bilbao, Spain
[3] Dept. Mater. Science & Metallurgy, Univ. Cambridge, Cambridge CB3 0FS, UK
[4] Dept. Polym. Adv. Mater, Univ. of the Basque Country, EHU, 20018 San Sebastian, Spain

Abstract:
Magnetic wires present outstanding magnetic properties such as the giant magnetoimpedance (GMI) as well as magnetic bistability and related single domain wall (DW) propagation and hence are quite attractive for a number of technological applications [1,2].The common viewpoint on remagnetization process of magnetic wires presenting magnetic bistability is that under the effect of external magnetic field the depinning and fast propagation of a single DW along the wire takes place [3]. The controllable and reliable DW dynamics is essentially relevant for development of aforementioned applications like racetrack memories. Therefore a few methods, like creation of notches, injection of DW by local field or controllable DW collision are proposed for controllable pinning of DWs [1-3]. The other effective method for local change of the internal magnetic field can be a spatially varying magnetization in a compositionally graded ferromagnets [4]. However, such DW manipulation require use of precise techniques involving nano-manipulation.
We studied magnetic properties and domain wall dynamics in Fe-rich microwires subjected by stress-annealing at variable temperature, T_{ann}. Hysteresis loops of Fe-rich microwires have been considerably affected by stress- annealing. In stress-annealed Fe- rich microwire we obtained drastic decreasing of coercivity and change of character of hysteresis loop from rectangular to linear (see Figure 1a). For stress-annealed at temperature Fe-rich microwires we obtained graded magnetic behavior with local hysteresis loops shape and features (coercivity, remanent magnetization) changing along the sample length (Figure 1b). Observed stress-induced anisotropy must be related to internal stresses relaxation after annealing interplay of compressive "back-stresses" arising after stress annealing and axial internal stresses.

Keywords: Magnetic microwires, magnetic bistability, annealing, internal stresses, graded anisotropy, domain wall propagation, hysteresis loops.

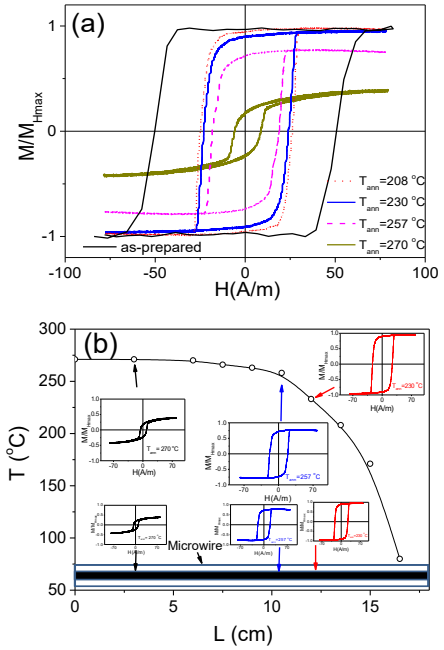


Figure 1. Hysteresis loops of as-prepared and stress-annealed at different T_{ann} $Fe_{75}B_9Si_{12}C_4$ microwires (a) and graded magnetic properties of $Fe_{75}B_9Si_{12}C_4$ microwires annealed at variable T_{ann}.

References:

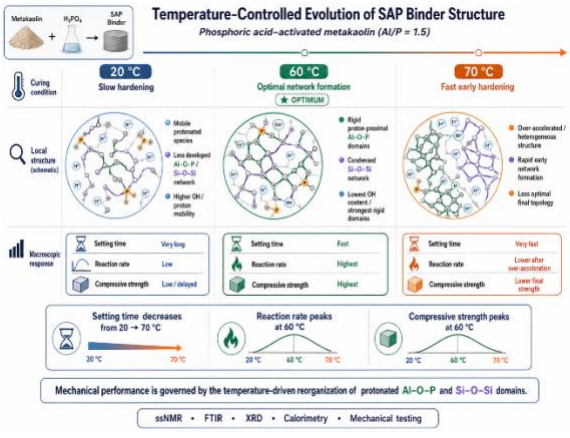
1. Allwood, D.A., Xiong, G., Faulkner, C.C., Atkinson, D., Petit, D., Cowburn, R.P. (2005), Magnetic domain-wall logic, *Science,* 309, 1688-1692
2. Parkin, S.S.P., Hayashi, M., Thomas, L. (2008), Magnetic domain-wall racetrack memory, *Science*, 320, 190-194
3. Zhukova, V., Corte-Leon, P., González-Legarreta, L., Talaat, A., Blanco, J.M., Ipatov, M., Olivera, J., Zhukov, A. (2020) Review of Domain Wall Dynamics Engineering in Magnetic Microwires, *Nanomaterials,* 10*, 2407.*
4. Jin, T. L., Ranjbar, M., He, S. K., Law, W. C., Zhou, T. J., Lew, W. S., Liu, X. X., Piramanayagam, S. N. (2017), Tuning magnetic properties for domain wall pinning via localized metal diffusion, *Sci. Reports*, 7, 16208

Temperature-Guided Formation of Functional Silico-Alumino-Phosphate Binders Revealed by Multinuclear Solid-State NMR

J. Brus[1]*, M. Urbanova[1], I. Sedenkova[1], M. Keppert[2],
[1] Department of Structural Analysis, Institute of Macromolecular Chemistry, Czech Academy of Sciences, Prague, Czech Republic
[2] Faculty of Civil Engineering, Czech Technical University in Prague, Department of Materials Engineering and Chemistry, Prague, Czech Republic
*brus@imc.cas.cz

Abstract:
Silico-alumino-phosphate (SAP) binders prepared by phosphoric acid activation of metakaolin represent a promising class of functional amorphous inorganic materials combining high mechanical performance, chemical resistance and thermal stability. Their macroscopic properties are strongly affected by curing temperature; however, the molecular origin of the temperature-dependent strengthening remains insufficiently understood. In this work, SAP binders with an Al/P molar ratio of 1.5 were cured at temperatures between 20 and 70 °C and investigated using setting-time measurements, isothermal calorimetry, mechanical testing, FTIR spectroscopy, X-ray diffraction, porosimetry and multinuclear solid-state NMR spectroscopy.
Increasing curing temperature strongly accelerated hardening, reducing the final setting time from several hundred hours at room temperature to only a few hours at 70 °C. Nevertheless, the highest calorimetric reaction rate and the highest 28-day compressive strength were obtained for samples cured at 60 °C, whereas curing at 70 °C promoted faster early hardening but led to lower final strength. Since X-ray diffraction and porosimetry indicated predominantly amorphous and similarly compact matrices, the observed mechanical differences cannot be explained by crystallinity or pore structure alone.
Multinuclear solid-state NMR provided direct insight into the local structural processes governing SAP formation. ^{1}H MAS NMR revealed a temperature-dependent transformation of mobile acidic/protonated species into rigid proton-proximal environments. ^{31}P MAS and CP/MAS NMR showed progressive conversion of mobile phosphate-rich species into strongly Al-coordinated P–O–Al domains. ^{27}Al MAS, CP/MAS and 3Q/MAS NMR confirmed extensive acid-induced re-coordination of metakaolin-derived aluminum toward predominantly octahedral AlVI environments associated with hydrated/hydroxylated Al–O–P domains. In parallel, ^{29}Si MAS and CP/MAS NMR evidenced condensation of the silicate network toward Si–O–Si-rich structures and a gradual reduction of protonated silanol environments.
These results demonstrate that the mechanical performance of phosphoric acid–activated metakaolin is governed not only by reaction acceleration, but primarily by temperature-controlled reorganization, dehydration and rigidification of amorphous protonated Al–O–P and Si–O–Si domains. The study highlights multinuclear solid-state NMR as a powerful tool for establishing molecular structure–property relationships and for guiding the rational design of functional SAP binders and related smart inorganic materials.

Keywords: silico-alumino-phosphate binders, acid-activated metakaolin, solid-state NMR, curing temperature, Al–O–P domains, Si–O–Si network, structure property relationships, functional inorganic materials



Acknowledgments:
This work was supported by Czech Science Foundation (Grant No. GA 24-11171S).

Fast-charging Lithium-ions Batteries via Easy Interfacial Modifications

Yu-Ting Weng[1], Nea-Lih Wu[1, 2]
[1]Advanced Research Center for Green Materials Science and Technology, National Taiwan University, Taipei 10617, Taiwan
[2]Department of Chemical Engineering, National Taiwan University, Taipei 10617, Taiwan
e-mail address

Abstract:
With the dramatically improved development of electrochemical storage devices for the 21st century, the increasing requirement of extreme fast-charging (XFC) electric vehicles (EV) is getting widespread attention nowadays. The definition of "fast-charging" depends on the nature of the applications and can be subjective. The U.S. Department of Energy (DOE) has proposed a goal of reducing the charge time (to 80% of full capacity) to 10 minutes (6C-rate) or less. To achieve the goal of practical applications, exploring a novel strategy to obtain the considerable capability of stable and high-lithiation capacity within 10 minutes has become a crucial topic of interest worldwide. This work aims to develop efficient technologies that can substantially improve the interfacial resistances between anode/ cathode materials and electrolytes for the fast-charging capability of state-of-the-art LIBs. To meet an economic and feasible technology for implemental fast-charging LIB commercialization, artificial solid-electrolyte interphase formation via polymeric surface modification is a highly promising strategy, in which Li-ion intercalation into graphite can be sufficiently improved. Meanwhile, for cathode material (NCM811), the polymeric surface modification can be a feasible strategy to mitigate structure degradation, alleviate residual Li-complexes foration, and inhibit the interfacial parasitic reactions with electrolytes on the materials' surfaces. Full cells of modified graphite/ NCM811 are demonstrated to have outstanding cycling stability at 6C-charging for prolonged cycles. In this presentation, the investigation of the effects of organic coatings on fast charging will be reported.

Keywords: Extreme fast-charging lithium-ion batteries, artificial solid-electrolyte interphase, polymeric surface modification, graphite, NCM811.

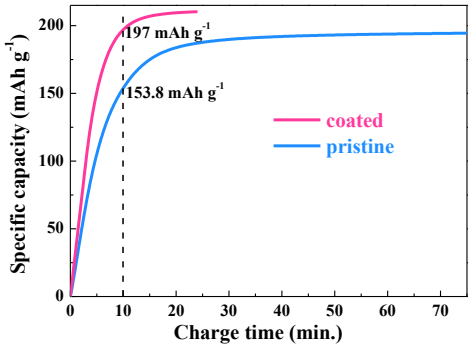


Figure 1: Electrochemical characterizations of NCM811 || Li metal cells: specific charge capacity *vs*. time plots for the 10C charging step.

Recycling Potential of Conductive Ink Printed Substrates

Katarina Itrić Ivanda[1], Marina Vukoje Bezjak[1] Tomislav Cigula[1] Rahela Kulčar
[1]University of Zagreb Faculty of Graphic Arts
Getaldićeva 2, 10000 Zagreb, Croatia, katarina.itric.ivanda@grf.unizg.hr

Abstract
The rapid development of printed electronics has enabled the integration of electronic functionalities into a wide range of paper-based products, including smart packaging, sensors, labels, and disposable electronic devices. Paper is increasingly used as a substrate due to its low cost, flexibility, printability, and renewable origin. However, the growing use of conductive inks in printed electronics raises important questions regarding the end-of-life management and recyclability of such materials. Since paper-based printed electronic products are expected to enter conventional paper recycling streams, it is necessary to evaluate the impact of conductive inks on the recycling process and the quality of the resulting recycled paper. This study investigates the recyclability of paper-based substrate printed with conductive inks using a conventional paper recycling process with the aim of producing recycled paper. The research focuses on the behavior of conductive ink particles during pulping and sheet formation, as well as their influence on the properties of the recycled material. Special attention is given to the retention and distribution of conductive components within the recycled fiber network and their potential effects on paper quality. Experimental work includes the preparation of printed paper based samples, laboratory-scale recycling through fiber disintegration and sheet formation, and characterization of the resulting recycled paper. The results provide insight into the compatibility of conductive ink-printed papers with existing recycling technologies and identify potential challenges associated with their large-scale recycling. The findings contribute to a better understanding of the circularity potential of paper-based printed electronics and support the development of sustainable strategies for managing emerging electronic waste streams. Furthermore, the study provides valuable information for the design of recyclable printed electronic products and for the optimization of recycling processes capable of accommodating novel functional materials while maintaining the quality of recycled paper product.

Keywords: printed electronics, conductive inks, paper-based substate recycling, recycled paper, sustainability, circular economy.

From ceramic powders to 3D printed bio-inspired scaffolds based on baghdadite

Ștefania Caramarin[1,2], Radu-Robert Piticescu[1*], Alexandru Okos[1]
[1]National R&D Institute for Non-Ferrous and Rare Metals, Pantelimon, Romania
[2]Department of Science and Engineering of Oxide Materials and Nanomaterials, Faculty of Chemical Engineering and Biotechnologies, National University of Science and Technology Politehnica Bucharest, Bucharest, Romania

Abstract:
Baghdadite ($Ca_3ZrSi_2O_9$) is a synthetic calcium zirconium silicate bioceramic inspired by the naturally occurring mineral baghdadite, recognized for its promising potential in bone tissue engineering due to its bioactivity and osteoconductive properties [1,2].
This study presents the development of a complete processing route from sol-gel-derived baghdadite powders to porous 3D-printed scaffolds fabricated by robocasting. Ceramic inks were formulated and optimized through rheological characterization to achieve suitable extrusion behavior [3], shape retention, and structural stability during printing. The optimized formulation enabled the successful fabrication of well-defined scaffolds with interconnected porosity and good dimensional fidelity after thermal processing.
These results demonstrate the feasibility of combining sol-gel synthesis, rheological optimization, and direct ink writing to produce customized baghdadite-based ceramic scaffolds with potential for bone tissue engineering.

Keywords: Baghdadite, Sol-gel synthesis, Robocasting, 3D printing, Ceramic scaffolds

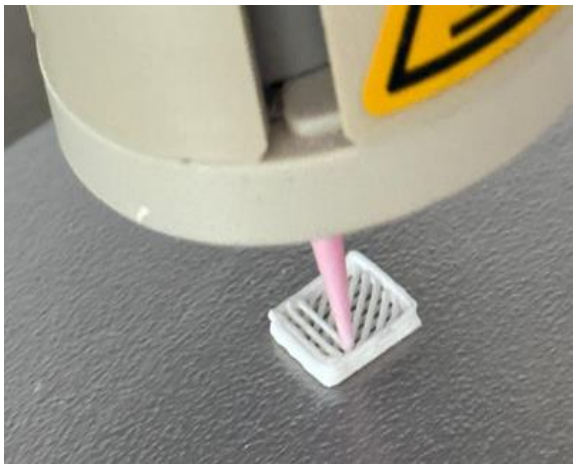


Figure 1: Additive manufacturing of baghdadite scaffolds by robocasting

References:
1. Z.F. Lu, W.J. Zhang, Y.J. No, Y. Lu, S.M. Mirkhalaf Valashani, P. Rollet, L. Jiang, Y. Ramaswamy, C.R. Dunstan, X.Q. Jiang, H. Zreiqat, Baghdadite Ceramics Prevent Senescence in Human Osteoblasts and Promote Bone Regeneration in Aged Rats, ACS Biomater. Sci. Eng. 6 (2020) 6874–6885. https://doi.org/10.1021/acsbiomaterials.0c01120.
2. Z.F. Lu, G.C. Wang, I. Roohani-Esfahani, C.R. Dunstan, H. Zreiqat, Baghdadite ceramics modulate the cross talk between human adipose stem cells and osteoblasts for bone regeneration, Tissue Eng. Part A 20 (2014) 992–1002. https://doi.org/10.1089/ten.tea.2013.0470.
3. J. Bonilla-Cruz, M.A. Ávila-López, F.E.L. Rodríguez, A. Aguilar-Elguezabal, T.E. Lara-Ceniceros, 3D printable ceramic pastes design: Correlating rheology & printability, J. Eur. Ceram. Soc. 42 (2022) 6033–6039. https://doi.org/10.1016/j.jeurceramsoc.2022.06.029.

Acknowledgements:
This work was supported by a grant of the Ministry of Education and Research, CCCDI - UEFISCDI, project number PN-IV-P6-6.1-CoEx-2024-0162, within PNCDI IV.

Green Synthesis of Gold Nanoparticles Using *Silybum marianum* Extracts and Silybin for Future Tissue Regeneration Applications

B. Strojny-Cieślak*, M. Pruchniewski, Z. Nowak, A. Ostrowska
Department of Nanobiotechnology, Warsaw University of Life Sciences, Warsaw, Poland

Abstract:
Milk thistle (*Silybum marianum*) is a medicinal plant widely recognized for its hepatoprotective properties, mainly associated with flavonolignans such as silybin. It is also rich in silychristin, silydianin, as well as flavonoids and phenolic compounds. Plant-derived compounds can also serve as reducing and stabilizing agents in the green synthesis of metallic nanoparticles, offering a sustainable alternative to conventional chemical methods. Bioactive compounds from milk thistle can contribute to the stabilization of the resulting nanoparticles, while also forming a bioactive phytochemical coating on their surface. Gold nanoparticles (AuNPs) are particularly attractive for biomedical applications due to their unique physicochemical properties, biocompatibility, surface functionalization potential, and reported ability to support cellular processes involved in tissue repair and regeneration.
In this study, AuNPs were synthesized under varying reaction conditions using water–alcohol extracts prepared from milk thistle seeds, industrial milk thistle pomace, and pure silybin. The use of pomace further enhances the process's sustainability by valorizing agro-industrial waste and supporting circular economy principles. Successful nanoparticle formation was achieved for all the tested reducing systems. The obtained AuNPs were characterized using transmission electron microscopy, dynamic light scattering, electrophoretic light scattering, and UV–Vis spectroscopy to assess their morphology, size distribution, surface charge, and optical properties. Among the tested synthesis variants, nanoparticles produced using milk thistle seed extracts and the pomace showed the most favorable physicochemical characteristics and the highest potential for biological applications. Importantly, these nanoparticles did not exhibit cytotoxic effects in the investigated *in vitro* models. Future studies will focus on incorporating the selected AuNPs into advanced biomaterials designed to support liver tissue regeneration.

Keywords: milk thistle, gold nanoparticles, green chemistry, green synthesis, tissue regeneration

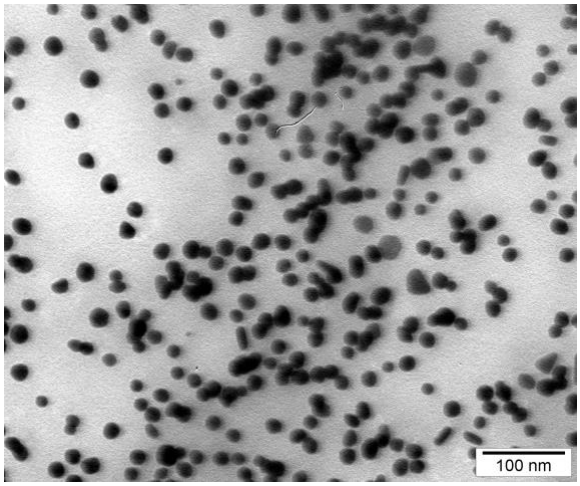


Figure 1: Representative transmission electron microscopy of AuNPs obtained via green synthesis using water–alcohol extracts from Silybum marianum seeds.

References:

1. S. Makouie et al., Compositional Characterization of Milk Thistle (*Silybum marianum*) Seeds and Press Cake with Emphasis on Press Cake Valorization, *Appl. Sci.-Basel*, 16, 11, (2026).
2. M. Pruchniewski, et al. Electrospun poly-(L-lactide) scaffold enriched with GO-AuNPs nanocomposite stimulates skin tissue reconstruction via enhanced cell adhesion and controlled growth factors release. *Mater Des* 251, (2025).

Acknowledgment
The research was supported by the National Science Center (NCN) of Poland, Grant OPUS (grant number 2025/57/B/NZ7/00911).

Advanced Biomaterial Platforms for Tissue Regeneration: Thickness-Tunable PBAT Nanofibrous Scaffolds and Injectable Silk Fibroin Microcarriers

S.O. Akbulut[1], S. Ekicier Acar[1], E. Konuk Tokak[2], D. Çakır[2], A.S. Çakmak[2] T. Gültan[2], M. Gümüşderelioğlu[1,2*]

[1] Bioengineering Division, Hacettepe University, Ankara, Turkiye

[2] Chemical Engineering Department, Hacettepe University, Ankara, Turkiye

Abstract:

Tissue regeneration requires biomaterial platforms tailored to the structural, mechanical, and cellular requirements of target tissues. In this study, two biomaterial strategies were developed for tendon and corneal regeneration: thickness-tunable bilayer poly(butylene adipate-co-terephthalate) (PBAT) nanofibrous scaffolds for supraspinatus (SSP) tendon regeneration and injectable porous silk fibroin-based microcarriers (SF-based MCs) for stem cell delivery to the cornea.

Bilayer PBAT scaffolds, consisting of a random basal layer and an aligned upper layer, were fabricated at different electrospinning durations (4S, 6S, and 8S), resulting in thicknesses of 441–1132 µm. The aligned fibers had an average diameter of 476.8 ± 184.0 nm, with 71.4% oriented within ±20° of the predominant direction. The thinner 4S and 6S scaffolds exhibited higher mechanical performance than the 8S scaffold. During 21 days of culture with rat adipose-derived mesenchymal stem cells (r-AdMSCs), all scaffolds supported cell viability and proliferation, while the aligned architecture promoted cellular orientation. The 4S scaffold showed the most favorable tenogenic response, with enhanced expression of tenomodulin (Tnmd), scleraxis (Scx), and collagen type I (Col1), including approximately eight-fold higher Tnmd expression than 6S on day 21 [1].

For corneal applications, porous SF-based MCs were fabricated using an emulsion-based phase separation method. The microcarriers had an average diameter of 201.5 ± 52.3 µm and interconnected pores of 12.3 ± 4.2 µm. Limbal epithelial stem cells (LESCs) showed favorable attachment, spreading, and viability on the microcarriers. Cell-laden microcarriers also maintained their structural integrity and high cell viability following injection through a 27-gauge needle. Moreover, the SF-based MC/LESC complex increased corneal epithelial cell migration by approximately 36% after 48 h without inducing significant TNF-α or IL-1β expression [2, 3].

Overall, thickness-controlled anisotropic PBAT scaffolds provided structural and mechanical cues supporting tenogenic commitment, whereas porous SF-based microcarriers provided a supportive and injectable environment for LESC delivery while enhancing corneal epithelial cell migration without a significant inflammatory response. Together, these platforms demonstrate how tailoring biomaterial architecture and delivery format can address distinct tissue-specific requirements and provide promising strategies for tendon and corneal regeneration.

Keywords: poly(butylene adipate-co-terephthalate); nanofibrous scaffolds; bilayer scaffolds; adipose-derived mesenchymal stem cells; tenogenic differentiation; supraspinatus tendon; silk fibroin; porous microcarriers; injectable cell delivery; limbal epithelial stem cells; corneal regeneration.

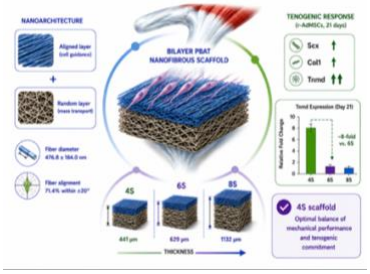


Figure 1: Schematic representation of thickness-tunable bilayer PBAT nanofibrous scaffolds and effects on the tenogenic commitment of r-AdMSCs, highlighting the superior performance of the 4S configuration.

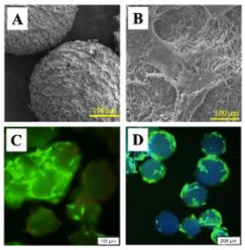


Figure 2. Silk fibroin microcarriers: (A) SEM images of the microcarriers and analysis of limbal epithelial stem cells (LESCs) cultured on the microcarriers by (B) SEM, (C) Live/Dead staining, and (D) F-actin/DAPI staining.

References:

1. Akbulut, S. O., Konuk Tokak, E., Gültan, T., & Gümüşderelioğlu, M. (2026). Thickness-Tunable Bilayer PBAT Nanofibrous Scaffolds for Enhancing r-AdMSCs' Tenogenic Commitment in Supraspinatus Tendon Regeneration. Journal of Functional Biomaterials, 17(7), 310.
2. Jinming, L., Qiaoyu, L., Zhaoxiang, Lu., Wenyu, W., Xiaojun, H., Zhou, Y., Yun, F. (2025) Injectable microcarriers enhance stem cell delivery and promote corneal regeneration for alkali burn, *Chemical Engineering Journal*, 517, 164582.
3. Anton-Sales, I., Koivusalo, L., Skottman, H., Laromaine, A., Roig, A. (2021) Limbal stem cells on bacterial nanocellulose carriers for ocular surface regeneration, *Small*, 17(10), e2003937.

Acknowledgment:
The study was financially supported by The Scientific and Technological Research Council of Türkiye (TÜBİTAK) under Project No. 124M482 and by Hacettepe University Scientific Research Projects (Grant No: FHD-2026-22509).

Biomimetic Poly-(L-lactide) Scaffold Nanostructured with Graphene Oxide and Gold Nanoparticles for Enhanced Skin Regeneration

M. Pruchniewski[1,*], B. Strojny-Cieślak[1], R. Kasprzak[2], P. Nakielski[3], A. Ostrowska[1], E. Sawosz[1]
[1] Department of Nanobiotechnology, Warsaw University of Life Sciences, Warsaw, Poland
[2] Department of Animal Environment Biology, Warsaw University of Life Sciences, Warsaw, Poland
[3] Department of Biosystems and Soft Matter, Institute of Fundamental Technological Research, Polish Academy of Sciences, Warsaw, Poland

Abstract:
The development of multifunctional cellular scaffolds is critical for advancing skin regeneration strategies, necessitating materials capable of modulating cellular and tissue responses to optimize healing outcomes. Biomimetic scaffolds should facilitate cellular proliferation and differentiation while regulating extracellular matrix (ECM) synthesis to prevent fibrosis and hypertrophic scarring. Electrospinning remains a prevalent technique for fabricating biomimetic scaffolds, involving the ejection of a polymer solution under high voltage onto a grounded collector. To enhance bioactivity of polymers, incorporation of nanostructuring agents capable of influencing mechanotransduction pathways is advantageous. In this study, an electrospun poly(L-lactic acid) (PLLA) matrix was functionalized with graphene oxide (GO) nanoflakes and *in situ* hydrothermally deposited gold nanoparticles (AuNPs). The resulting nanocomposite scaffolds were characterized for their physicochemical and mechanical properties, confirming successful integration of nanomaterials and their influence on fiber morphology. Biocompatibility was assessed using human keratinocyte HaCaT cells, demonstrating cytocompatibility and upregulation of maturation markers at the transcriptomic level. *Ex vivo* models utilizing full-thickness human skin explants revealed that PLLA+GO-AuNPs scaffolds significantly accelerated reepithelialization and promoted homogeneous collagen deposition within the wound bed. The synergistic effects of nanostructuring and bioactive nanomaterials confer enhanced regenerative capacity, positioning these scaffolds as promising candidates for advanced skin tissue engineering applications.

Keywords: electrospun cell scaffold; graphene oxide; gold nanoparticles; mechanotransduction; keratinocyte maturation; skin regeneration

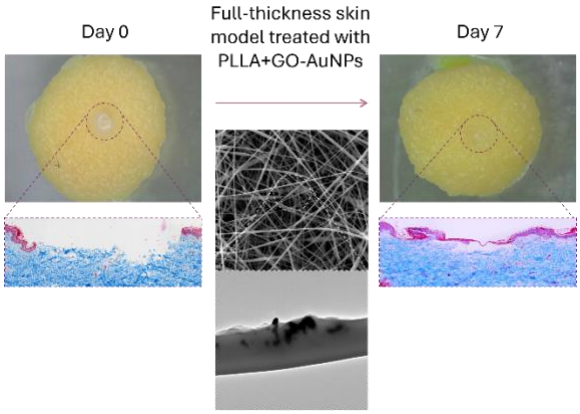


Figure 1: Histological analysis of wounded full-thickness human skin (WoundSkin®; Masson's trichrome staining) prior to and following 7 days of treatment with a PLLA+GO-AuNPs scaffold.

References:

1. Pruchniewski, M., Strojny-Cieślak, B. (2025) Electrospun poly-(L-lactide) scaffold enriched with GO-AuNPs nanocomposite stimulates skin tissue reconstruction via enhanced cell adhesion and controlled growth factors release, *Materials & Design*.

Acknowledgment:
The research was supported by the National Science Center (NCN) of Poland, Grant Opus 29 (2025/57/B/NZ7/00911) and Grant Preludium 22 (2023/49/N/NZ4/02186).

Distinct Thermomechanical Profiles of Conventional and Shape-Memory Polymers for Clear Orthodontic Aligners

Jan Oblak[1,2], Monika Jenko[3], Maja Ovsenik[1,2,4]
[1]Medical Faculty, University of Ljubljana, Slovenia
[2]Orthos Ljubljana, Slovenia
[3]MD-RI Institute of Materials Research in Medicine, Ljubljana, Slovenia
[4]Faculty of Health Sciences, University of Ljubljana, Slovenia

Abstract:
The clinical performance of clear orthodontic aligners depends on the thermomechanical behavior of their constituent polymers. Conventional thermoformed materials and newer directly manufactured shape-memory polymers may respond differently to temperature and intraoral ageing, potentially influencing force delivery and dimensional stability. This study compared the thermal and thermomechanical properties of several conventional clear-aligner polymers and a 3D-printed shape-memory material.

Commercial clear-aligner materials, including Maxflex, Lineup, Orthero, Invisalign, and LuxCreo ActiveMemory™, were investigated. Differential scanning calorimetry (DSC) was used to determine glass-transition temperature (Tg). Thermomechanical analysis (TMA) was additionally performed on Maxflex, Lineup, and Orthero specimens between 22 and 55 °C to evaluate temperature-dependent dimensional behavior and the coefficient of linear thermal expansion. Multiple Orthero aligner phases made from the same material were tested to assess phase-to-phase consistency. For Invisalign, new and clinically used aligners from the same patient were evaluated before and after seven days of wear.

Marked differences in thermal behavior were observed between the investigated polymers. Maxflex exhibited a Tg of 25.7 °C, while Lineup showed a substantially higher Tg of 40.0 °C. Orthero specimens demonstrated closely clustered Tg values between 8.2 and 13.4 °C across different treatment phases, indicating generally consistent thermal characteristics of the material. Maxflex showed a linear thermal expansion coefficient of 153 × 10^{-6}/°C and Lineup 285 × 10^{-6}/°C. Most Orthero phases showed values between approximately 129 and 170 × 10^{-6}/°C, although one specimen exhibited pronounced softening above approximately 40 °C. In the paired Invisalign comparison, Tg changed from 18.8 to 16.3 °C in the upper aligner and from 26.9 to 26.8 °C in the lower aligner after seven days of intraoral use. The LuxCreo ActiveMemory™ shape-memory material showed Tg values of 27.5 and 31.2 °C for the upper and lower aligners, respectively.

Clear-aligner polymers demonstrated distinct thermomechanical profiles, with substantial differences in glass-transition temperature and temperature-dependent dimensional behavior. Orthero showed relatively consistent thermal properties across different treatment phases, whereas short-term intraoral wear produced only limited changes in the tested Invisalign specimens. The LuxCreo ActiveMemory™ material exhibited transition temperatures closer to the intraoral temperature range than several conventional thermoplastics. These findings underline the importance of material-specific thermomechanical characterization when assessing clear-aligner behavior and may contribute to more predictable material selection and orthodontic force delivery.

Keywords: clear aligners; shape-memory polymers; ActiveMemory; thermomechanical properties; glass-transition temperature; orthodontic polymers

In Vitro Cytotoxicity Assessment of Thermoformed and 3D-Printed Clear Aligner Materials: A Pilot Study of Artificial Ageing and Extraction Time

Rok Ovsenik[1,2], Maja Ovsenik[1], Maks Bitenc[3], Monika Jenko[4], Lea Kolenc[1]
[1]Medical Faculty, University of Ljubljana, Slovenia
[2]Orthos Ljubljana, Slovenia
[3]Faculty of Health Sciences, University of Ljubljana, Slovenia
[4]MD-RI Institute of Materials Research in Medicine, Ljubljana, Slovenia

Abstract:
Clear aligner polymers remain in prolonged contact with saliva and oral tissues. Their biological response may be influenced by material composition, ageing and environment of the mouth. This pilot study evaluated the effects of extraction time and artificial ageing of three clear aligner materials on fibroblast and keratinocyte metabolic activity, with particular attention to potential differences between thermoformed and three-dimensionally printed shape-memory polymers.
Three polymeric materials were tested before and after seven days of ageing in artificial saliva: Erkoloc Pro (A) and Maxflex (B), both thermoformed materials, and LuxCreo (C), a three-dimensionally printed shape-memory polymer. Samples were extracted in cell culture medium for 24 or 72 hours using a surface area to extraction medium ratio of approximately 3 cm^2/mL to mimic acute and subacute exposure. Fibroblast and keratinocyte metabolic activity was assessed using a fluorometric resazurin reduction assay (Alamar blue) and normalized to the negative control. The experimental design followed the principles of ISO 7405:2025, ISO 10993-5:2009 and ISO 10993-12:2021. Results were analysed descriptively because of the pilot design and limited number of tehnical replicates. Material A maintained metabolic activity close to the negative control under all tested conditions. Material B also showed generally acceptable responses, although variability between measurements was observed. Material C, the three-dimensionally printed shape-memory polymer, demonstrated the greatest decline in metabolic activity after ageing. In fibroblasts exposed to 72-hour extracts, ageing reduced metabolic activity from 90.20% to 71.92% in the first experiment and from 96.18% to 81.80% in an additional technical repeat. In keratinocytes, ageing reduced metabolic activity from 97.71% to 80.86% following 24-hour extraction and from 93.38% to 78.85% following 72-hour extraction. These findings suggest that artificial ageing may have a greater influence on the metabolic response to material C than extraction duration, particularly in keratinocytes, although this requires confirmation in independent biological replicates. The magnitude of the reduction was therefore similar at both extraction times, with no clear additional effect of prolonged extraction observed in keratinocytes. A clear extraction-time-dependent effect could not be established also due to the variability and unusually high signals observed after 24-hour extraction, particularly in fibroblasts. Several unusually high fluorescence signals were recorded, including 397.07% for nonaged material B in keratinocytes and 159.43% and 136.34% for nonaged and aged material C in fibroblasts after 24-hour extraction. These findings could not be interpreted as increased cell viability because assay interference or other technical artefacts could not be excluded.
Materials A and B showed relatively stable biological responses, whereas material C produced the most consistent reduction in metabolic activity, particularly in fibroblasts after aging. The preliminary findings suggest that artificial ageing in artificial saliva may have a greater biological impact on the three-dimensionally printed shape-memory polymer LuxCreo than on the two thermoformed materials, Erkoloc Pro and Maxflex. Importantly overt citotoxicity was not demonstrated in any of the experiments. However, the present design cannot reveal the effects of material composition and manufacturing technique on the results. The independent contribution of prolonged extraction also remains uncertain. Independent biological replicates are required to confirm the observed effects and clarify whether ageing increases the biological impact of clear aligner polymers especially to a biologically observant extent.

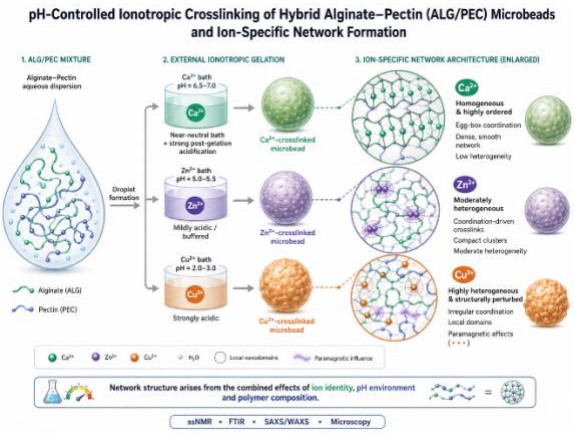
Keywords: clear aligners, polymer ageing, artificial saliva, cytotoxicity, fibroblasts, keratinocytes, alamarBlue, shape-memory polymers;

pH-Controlled Ionotropic Crosslinking of Alginate–Pectin Microbeads: Multiscale NMR Insights into Ion-Specific Network Formation

M. Urbanova[1]*, I. Sedenkova[1], M. Pavelkova[2], K. Kubova[2] and J. Brus[1]
[1] Department of Structural Analysis, Institute of Macromolecular Chemistry, Czech Academy of Sciences, Czech Republic
[2] Department of Pharmaceutical Technology, Faculty of Pharmacy, Masaryk University, Brno, Czech Republic
* urbanova@imc.cas.cz

Abstract:
Alginate- and pectin based hydrogel microbeads represent promising biopolymer platforms for pharmaceutical and biomedical applications due to their biocompatibility, mild gelation conditions and tunable structural properties. Their final architecture, however, is governed not only by polymer composition and the identity of crosslinking ions, but also by the local acid-base environment established during ionotropic gelation. In this work, hybrid alginate/pectin microbeads with systematically varied polymer composition were prepared by external ionic gelation using Ca^{2+}, Zn^{2+} and Cu^{2+} ions. The pH of both polymer dispersions and crosslinking baths was monitored before and after gel formation in order to distinguish the effects of ion-specific coordination chemistry, polysaccharide protonation and polymer ratio.

The resulting materials were characterized across multiple length scales using solid-state NMR spectroscopy, FTIR spectroscopy, SAXS/WAXS and microscopy. The data reveal that Ca^{2+} promotes relatively homogeneous and organized ionic domains, consistent with classical egg-box-type coordination. Zn^{2+} forms more compact but structurally heterogeneous networks, reflecting a broader distribution of local coordination motifs. In contrast, Cu^{2+} induces strongly perturbed, highly heterogeneous hydrogel architectures, where paramagnetic relaxation effects dominate the NMR response and reveal the formation of complex local environments. SAXS analysis further shows that most systems contain characteristic nanoscale structural domains of approximately 35-37 nm, while their spatial organization and hierarchical heterogeneity are strongly ion-dependent.



These results demonstrate that the formation of alginate/pectin microbeads cannot be described by ion identity alone. Instead, their structure emerges from the coupled effects of metal-ion coordination, pH-controlled polysaccharide protonation and polymer composition. Advanced solid-state NMR, supported by complementary structural methods, provides a powerful approach for resolving these relationships and guiding the rational design of polysaccharide-based nanomaterials for pharmaceutical and biomedical technologies.

Keywords: alginate, pectin, hydrogel microbeads, ionotropic gelation, solid-state NMR, metal-ion crosslinking, pH-controlled gelation, polysaccharide nanomaterials

Acknowledgments:
This work was supported by Czech Science Foundation (Grant No. 26-20880S)

Development and Characterization of Curcumin Nanoparticle-Loaded Hydrogel for Skin Regeneration Applications

R.D. Pavaloiu[1], M. Eremia[1], Dana Miu[1], M. Vladu[1], A. Albulescu[1,2], G. Neagu[1], R. Albulescu[1], M. Petrescu[1], F. Shaat[1*]

[1]National Institute for Chemical-Pharmaceutical Research&Development—ICCF, Bucharest, 112, Vitan Av., 31299 Bucharest, Romania

[2]Department of Molecular Virology, Stefan S. Nicolau Institute of Virology, Mihai Bravu Av. nr. 285, 3rd District, 030304 Bucharest, Romania

Abstract:

This study reports the design, characterization, and evaluation of a polymeric nanoparticle-loaded hydrogel for regenerative dermatological applications. Polymeric nanoparticles are increasingly recognized as an effective drug delivery platform, offering improved bioavailability, enhanced stability, and the potential for targeted therapeutic delivery [1, 2]. Polyhydroxyalkanoates (PHAs), biodegradable and biocompatible polymers synthesized via bacterial fermentation, were used to encapsulate curcumin using the nanoprecipitation method. The resulting PHA-curcumin nanoparticles exhibited nanometric size distribution and low polydispersity, with high encapsulation efficiency (>80%), ensuring effective curcumin delivery. Dynamic light scattering (DLS) confirmed size stability over storage, while *in vitro* release studies in phosphate-buffered saline at 7.4 demonstrated sustained curcumin release, indicative of prolonged therapeutic action. Cytotoxicity assays using human astrocytes and fibroblasts confirmed biocompatibility, and EpiDerm™ skin irritation and corrosion tests classified the formulations as non-irritant and non-corrosive, highlighting their safety for topical application. Nanoparticle incorporation was followed by the development of a hydrogel formulation optimized for skin soothing and regenerative properties. Using a Plackett-Burman design, an optimal composition was obtained containing Carbopol 940, vegetable glycerin, propylene glycol, sweet almond and avocado oils, curcumin-loaded nanoparticles, L-menthol, triethanolamine, and vitamin E acetate. Texture analysis using a TX-700 texture analyzer revealed favorable rheological properties: moderate firmness, high cohesiveness, elasticity, low adhesiveness, and rapid structural recovery, critical for patient comfort on sensitive or irradiated skin. The hydrogel displayed a homogeneous, whitish appearance, pleasant odor, immediate cooling sensation upon application, and stable pH (5.74–6.22), ideal for compromised skin. *In vitro* release studies demonstrated sustained curcumin release over 72 hours, supporting prolonged therapeutic activity. This work highlights the successful integration of PHA-curcumin nanoparticles into a hydrogel matrix, producing a biocompatible, non-irritant, and patient-friendly formulation with promising sustained-release properties. The combined physicochemical, textural, and biological assessments suggest that this nanoparticle-loaded hydrogel represents a potential therapeutic platform for skin regeneration and irritation management, including applications in burn care, radiation-induced dermatitis, and general dermatological protection. Future studies should focus on in vivo evaluation and further optimization for clinical translation.

Keywords: polymeric nanoparticles, polyhydroxyalkanoates, curcumin, hydrogel, skin regeneration, sustained release.

References:

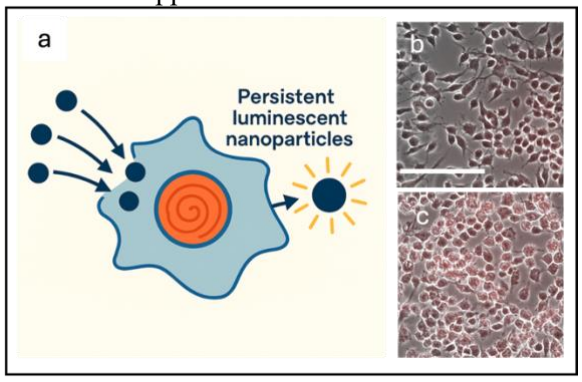
1. Beach, M.A., Nayanathara, U., Gao, Y., Zhang, C., Xiong, Y., Wang, Y., Such, G.K. (2024) Polymeric Nanoparticles for Drug Delivery, *Chem. Rev.,* 124, 5505–5616.
2. Bhardwaj, H., Jangde, R.K. (2023) Current updated review on preparation of polymeric nanoparticles for drug delivery and biomedical applications, *Next Nanotechnol.*, 2, 100013.

Nanoparticle-Based Luminescent Approaches in Biomedical Research: Assesing Cellular Internallization

A.I. Becerro,[1*] E. Arroyo,[1] B. Torres-Herrero,[2] J.M. de la Fuente,[2] M. Ocaña[1]
[1]Instituto de Ciencia de Materiales de Sevilla (ICMS), CSIC-US, Seville, Spain
[2]Instituto de Nanociencia y Materiales de Aragón (INMA), CSIC-UNIZAR, Zaragoza, Spain

Abstract:
Understanding the interaction between biological systems and nanomaterials is essential for the development of optimized nanoparticles (NPs) for nanomedicine applications, both in diagnostics and therapy. The significance of this knowledge lies in the fact that such interactions determine the ultimate fate of nanomaterials within the body, and consequently whether NPs successfully reach the target tissue where they are intended to perform their function.[1,2]
Currently, a variety of qualitative and quantitative techniques are available to study cellular internalization, including spectroscopic methods (such as ICP, a sensitive but destructive technique) and imaging methods (such as TEM and fluorophore-based methods that require the labelling with addition of dyes). Each of these approaches presents specific advantages and limitations, making it necessary to combine the results of two or more complementary techniques in order to accurately determine cellular internalization.[3]
Here, we propose an innovative strategy to quantify cellular internalization of persistent luminescent NPs, an emerging class of probes in bioimaging that improve signal-to-noise ratio by bypassing tissue autofluorescence. The strategy, based on the analysis of their intrinsic luminescent properties, offers significant advantages, improving the reliability of the results and providing a fast and non-destructive approach for assessing cellular internalization of these NPs without additional dyes.

Keywords: persistent luminescence nanoparticles, cellular internalization, biomedical applications.



a) Schematic representation of nanoparticles–cell internalization process. b and c) Luminescence micrographs recorded in a NIKON ECLIPSE Ti microscope (exposure time = 10 ms), 4 min after illumination with a UV lamp for 2 min of Raw 264.7 cells after incubation for 24 h without and with persistent luminescent NPs, respectively, enabling their quantification through intrinsic luminescence. Scale bar = 100 μm

References:

1. Behzadi, S., Serpooshan, V., Tao, W., Hamaly, M., Alkawareek, M, Dreaden, E. C., Brown, D., Alkilany, A., Farokhzad, O.C., Mahmoudi, M. (2017), Cellular uptake of nanoparticles: journey inside the cell, *Chem. Soc. Rev.* 46, 4218-4244.
2. Richards, C. J., Burgers, T. C. Q., Vlijm, R., Roos, W. H., Aberg, C. (2023) Rapid Internalization of Nanoparticles by Human Cells at the Single Particle Level. *ACS Nano* 17, 16517-16529.
3. Drasler, B., Vanhecke, D., Rodríguez-Lorenxo, L., Petri-Fink, A., Rothen-Rutishauser, B. (2017), Quantifying nanoparticle cellular uptake: which method is best?, *Nanomedicine* 12, 1095-1099.

Light-driven organic microrobots as efficient agents for photodynamic treatment of bacterial lung infections.

Lancézeux Allan[1], de Pedro-Jove Roger [2,3], Ratera Imma[1,4], Vila Jordi[1,2,3,5]*, Mayorga-Burrezo Paula[1,4]*

[1]Institute of Materials Science of Barcelona (ICMAB-CSIC), Bellaterra, Spain
[2]Centro de Investigación Biomédica en Red de Enfermedades Infecciosas (CIBERINFEC), Madrid, Spain
[3]Barcelona Institute for Global Health, Hospital Clinic-University of Barcelona, Barcelona, Spain
[4]Centro de Investigación Biomédica en Red: Bioingeniería, Biomateriales y Nanomedicina (CIBER-BBN), Spain
[5]Facultat de Medicina i Ciències de la Salut, Universitat de Barcelona (UB), Barcelona, Spain

Abstract: Respiratory infections represent a major threat among vulnerable populations, including children, older adults, immunocompromised individuals, or patients with pre-existing respiratory conditions. Antimicrobial photodynamic therapy (aPDT) proposes a localized approach as an alternative to the limited effectiveness of current treatments, further complicated by the rise of antimicrobial resistance[1]. Based on the combined use of a photosensitizing agent, a light source, and oxygen to generate reactive oxygen species (ROS), aPDT causes oxidative damage to microbial agents and shows an enhanced ability to penetrate biofilms by bypassing the main biofilm defenses, further expanding its clinical applicability[2]. Therefore, the development of innovative materials for aPDT is a research priority. In this work, we present carbon nitride ($g\text{-}C_3N_4$)-based microrobots with photocatalytic activity to be exploited as dynamic photosensitizing agents for aPDT. A successful microstruturation of this metal-free photocatalytic polymer into donut-like microrobots (1.0 ± 0.1 µm, PDI: 0.23 ± 0.05) has been achieved, showing a substantial surface area. Interestingly, upon visible (blue)-light irradiation (455 nm), the photocatalytic microrobots efficiently generate ROS (mainly holes, $O_2^{\bullet-}$ and OH•), whose asymmetric production drives their self-propulsion, enabling their function as light-driven microrobots. Their intrinsic motion enhances the mass transfer and ROS distribution, ultimately improving the anti-bacterial and anti-biofilm effects[3].

In this sense, antimicrobial assays against *Staphylococcus aureus* (Gram+), *Pseudomonas aeruginosa* (Gram-) and *Acinetobacter baumannii* (Gram-), key bacteria associated with severe respiratory infections, have been carried out. Without the use of any additive (such as H_2O_2), an eradication of 85% of *S. aureus* was observed in 15 minutes, whereas for *P.Aeruginosa* and *A. Baumannii*, 35% and 100%, respectively, in only 5 minutes, validating the performance of the $g\text{-}C_3N_4$ photocatalytic microrobots as antimicrobial platforms.

Keywords: Antimicrobial resistance, antibacterial therapy, photocatalysis, reactive oxygen species, phototaxis.

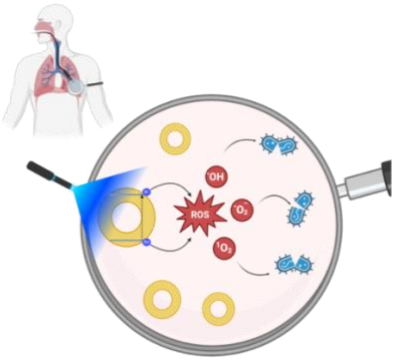


Figure 1: Scheme of the photocatalytic eradication of lung pathogens by $g\text{-}C_3N_4$ microrobots.

References:

1. Soares, J. M.; *et al.* Synergistic in Infection Control: A Review on Photodynamic Therapy as an Adjunctive Strategy to Antibiotics. *ACS Infect. Dis.* **2025**, *11* (10), 2671–2691.
2. Martins Antunes de Melo, W. de C.; Celiešiūtė-Germanienė, R.; Šimonis, P.; Stirkė, A. Antimicrobial Photodynamic Therapy (APDT) for Biofilm Treatments. Possible Synergy between APDT and Pulsed Electric Fields. *Virulence* **2021**, *12* (1), 2247–2272.
3. Zhang, Z.; Wang, L.; Chan, T. K. F.; Chen, Z.; Ip, M.; Chan, P. K. S.; Sung, J. J. Y.; Zhang, L. Micro-/Nanorobots in Antimicrobial Applications: Recent Progress, Challenges, and Opportunities. *Adv. Healthc. Mater.* **2022**, *11* (6), 2101991.

Pancreatic Ductal Adenocarcinoma-Derived Small Extracellular Vesicles Remodel the Hepatic Pre-Metastatic Niche through Hybrid Epithelial–Mesenchymal Transition States

F. Balestra [1], G. Panzetta [1], M. De Luca [1], F. Rizzi [2–3], R. Comparelli [2–3], M. L. Curri [2–3-4], G. Giannelli [5], N. Depalo [2–3], M. P. Scavo [1]

[1] Laboratory of Molecular Medicine, National Institute of Gastroenterology IRCCS S. de Bellis, Castellana Grotte, Italy

[2] Institute for Chemical-Physical Processes, IPCF-CNR, Bari, Italy

[3] National Interuniversity Consortium of Materials Science and Technology (INSTM), Bari, Italy

[4] Department of Chemistry, University of Bari, Bari, Italy;

[5] Scientific Direction, National Institute of Gastroenterology IRCCS S. de Bellis, Castellana Grotte, Italy;

Abstract:

Pancreatic ductal adenocarcinoma (PDAC) is characterized by early liver metastasis; however, the mechanisms underlying hepatic pre-metastatic niche formation, the primary site of dissemination, remain poorly understood (1). Small extracellular vesicles (sEVs) are key mediators of tumour–host communication and may contribute to reprogramming of the liver microenvironment (2). This study investigated the effects of PDAC-derived sEVs on extracellular matrix (ECM) remodelling and epithelial–mesenchymal transition (EMT)-related plasticity in hepatic cells. sEVs were isolated from PDAC cell lines (MIA PaCa-2 and PANC-1) and from the serum of 25 PDAC patients, characterized, and administered to hepatic stellate cells (LX-2), representing the stromal compartment, and hepatocyte-like cells (HEPA-RG), representing the hepatic parenchyma. Cell viability, adhesion, and migration were assessed through functional assays, while SEM evaluated morphological alterations. RT-qPCR, Western blotting, and immunofluorescence analysed gene and protein expression profiles. In LX-2 cells, exposure to sEVs increased metabolic activity, adhesion, and migration, and induced marked morphological changes associated with the modulation of ECM-related proteins, including reduced COL1A1, VIM, and E-CAD expression, consistent with a non-canonical stromal activation state. In HEPA-RG cells, sEV treatment had limited effects on viability but induced pronounced morphological alterations and enhanced migratory capacity, together with reduced E-CAD and VIM expression, supporting an EMT-related plasticity phenotype suggestive of a hybrid EMT state. Patient-derived sEVs induced comparable, although less pronounced, effects. Overall, PDAC-derived sEVs elicited distinct yet convergent responses across hepatic stromal and parenchymal compartments, promoting selective remodelling of the liver microenvironment toward a permissive pre-metastatic niche (Fig. 1). Ongoing analyses suggest that these effects may be mediated, at least in part, through activation of the TGF-β/SMAD signalling pathway. These findings highlight sEVs-mediated tumour–liver crosstalk as a potential therapeutic target for strategies aimed at limiting hepatic metastasis in PDAC.

Keywords: PDAC; small extracellular vesicles; hepatic microenvironment; liver metastasis; pre-metastatic niche.



Figure 1: PDAC-derived sEVs promote hepatic microenvironment remodelling through stromal activation and hybrid EMT-related plasticity. Lower panels show SEM-inspired cartoon representations of CTR and PDAC-sEV-treated cells.

References:

1. Gumberger P, et al. *Cancers (Basel).* 2022;14:3028. doi:10.3390/cancers14123028.
2. Hoshino A, et al. *Nature.* 2015;527:329–335. doi:10.1038/nature15756.

Extracellular Vesicles from Colorectal Cancer Models for Targeted Drug Delivery

Maria De Luca [1], Francesco Balestra [1], Rita Palieri [1],Giorgia Panzetta [1], Federica Rizzi [2,3], Chiara Perrone [2], Maria Lucia Curri [2,3,4], Gianluigi Giannelli [5], Nicoletta Depalo [2,3], Maria Principia Scavo [1]

[1] Laboratory of Molecular Medicine, National Institute of Gastroenterology, IRCCS S. de Bellis, Castellana Grotte (Bari), Italy

[2] CNR-IPCF, Institute for Chemical and Physical Processes, S.S. Bari, Department of Chemistry, Bari, Italy

[3] National Interuniversity Consortium of Materials Science and Technology (INSTM), Bari Research Unit, Bari, Italy

[4]Department of Chemistry, University of Bari, Bari, Italy.

[5] Scientific direction, National Institute of Gastroenterology, IRCCS S. de Bellis, Castellana Grotte (Bari), Italy

Abstract:

Extracellular vesicles (EVs) are emerging as promising nanocarriers for targeted cancer therapy owing to their biocompatibility, nanoscale dimensions, and intrinsic role in intercellular communication. Their lipid bilayer enables efficient encapsulation and protection of therapeutic cargoes, while membrane-associated proteins may enhance selective cellular targeting [1–3].

In this study, EVs were isolated by differential ultracentrifugation from the primary and metastatic colorectal cancer cell lines SW480 and SW620, respectively, and extensively characterized. Dynamic and electrophoretic light scattering analyses confirmed EV size distribution and zeta potential, transmission electron microscopy (TEM) validated vesicle morphology, and western blot analysis verified the expression of canonical EV markers, including CD9, CD81, HSP70, and ALIX.

To evaluate their potential as drug delivery systems, electroporation conditions were optimized for loading the chemotherapeutic agent 5-fluorouracil (5-FU). Under optimized conditions, EVs achieved a loading efficiency of approximately 17% while preserving structural integrity. Immunogold labeling further confirmed the preservation of EV surface markers before and after electroporation, indicating that key membrane-associated proteins were not significantly altered by the loading procedure.

Lipidomic analysis revealed distinct membrane compositions between SW480- and SW620-derived EVs. In particular, SW480 EVs exhibited a markedly higher saturation index compared with SW620 EVs (0.755 vs 0.299), suggesting increased membrane rigidity. These differences may influence membrane permeability and, consequently, affect the efficiency of electroporation-mediated 5-FU loading.

Overall, these findings suggest that colorectal cancer-derived EVs may constitute robust and biologically relevant nanocarriers for drug delivery applications, while highlighting the need for further studies to overcome current limitations and confirm their translational applicability.

Keywords: extracellular vesicles, EVs, drug delivery, colorectal cancer.

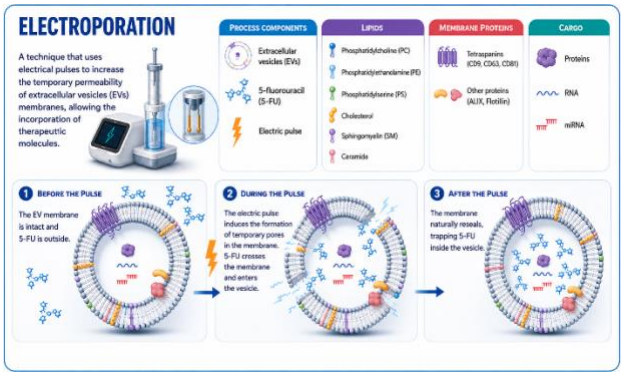


Figure 1: Schematic representation of electroporation-mediated loading of 5-fluoraouracil into extracellular vesicles.

References:

1. Herrmann, I. K., Wood, M. J. A., & Fuhrmann, G. (2021). Extracellular vesicles as a next-generation drug delivery platform. *Nature nanotechnology*, 16(7), 748–759.
2. Dave, K. M., Pinky, P. P., & S Manickam, D. (2025). Molecular engineering of extracellular vesicles for drug delivery: Strategies, challenges, and perspectives. *Journal of controlled release: official journal of the Controlled Release Society*, 386, 114068.
3. Zeng, H.; Guo, S.; Ren, X.; Wu, Z.; Liu, S.; Yao, X. (2023) Current Strategies for Exosome Cargo Loading and Targeting Delivery, *Cells*, 12, 1416.

Verteporfin-loaded nanoemulsions as a promising platform for ovarian cancer photodynamic therapy

L. Fuentes [1,2,3*], A. E. Arias[1], C. Abuín[1], M. Abal[1], C. Costa[1,3], R. López[1,3], A. B. Dávila [1,3]
[1] Translational Medical Oncology (Oncomet), Health Research Institute of Santiago (IDIS), Santiago de Compostela, Spain
[2] Universidade de Santiago de Compostela (USC), Santiago de Compostela, Spain
[3] CIBERONC, Centro de Investigación Biomédica en Red Cáncer, Madrid, Spain

Abstract:
Ovarian cancer (OC) remains one of the most lethal gynecological malignancies due to late-stage diagnosis, high relapse rates, and the limited efficacy of conventional treatments such as surgery and chemotherapy [1]. These therapies are frequently associated with systemic toxicity and the development of chemoresistance, highlighting the urgent need for alternative therapeutic strategies. In this context, photodynamic therapy (PDT) has emerged as a promising minimally invasive approach based on the light activation of photosensitizers to generate reactive oxygen species (ROS), inducing selective tumor cell death while minimizing damage to healthy tissues [2].

Here, we report the development and characterization of biocompatible oil-in-water nanoemulsions (NEs) encapsulating Verteporfin (VP), a clinically approved photosensitizer with recognized anticancer potential but limited by poor aqueous solubility and suboptimal biodistribution [3]. The developed VP-loaded NEs exhibited high encapsulation efficiency, suitable size distribution, and favorable physicochemical stability. In vitro studies using SKOV-3 ovarian cancer cells demonstrated efficient cellular internalization and enhanced photodynamic activity following near-infrared irradiation. Importantly, nanoencapsulation reduced the intrinsic dark toxicity of VP, protecting cells from photosensitizer-induced damage in the absence of light activation.

The therapeutic potential of these nanosystems was further validated in patient-derived organoids and in vivo biodistribution studies, demonstrating antitumoral activity in physiologically relevant 3D tumor models and enhanced peritoneal retention following intraperitoneal administration. Overall, VP-loaded nanoemulsions represent a promising nanomedicine platform to improve PDT efficacy in ovarian cancer and potentially other solid tumors.

Keywords: ovarian cancer, photodynamic therapy, Verteporfin, nanoemulsions, patient-derived-organoids.

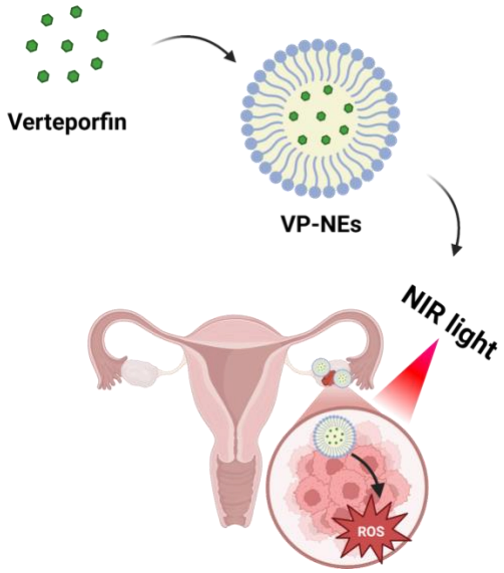


Figure 1: Schematic representation of Verteporfin-loaded nanoemulsions for photodynamic therapy in ovarian cancer. Following cellular internalization, near-infrared (NIR) irradiation activates Verteporfin, promoting reactive oxygen species (ROS) generation and selective tumor cell death.

References:

1. Siegel, R.L., Giaquinto, A.N., Jemal, A. (2024) Cancer statistics, 2024, CA Cancer J. Clin., 74(1), 12–49.
2. Agostinis, P., Berg, K., Cengel, K.A., Foster, T.H., Girotti, A.W., Gollnick, S.O., Hahn, S.M., Hamblin, M.R., Juzeniene, A., Kessel, D., Korbelik, M., Moan, J., Mroz, P., Nowis, D., Piette, J., Wilson, B.C., Golab, J. (2011) Photodynamic therapy of cancer: an update, CA Cancer J. Clin., 61(4), 250–281.
3. Lucky, S.S., Soo, K.C., Zhang, Y. (2015) Nanoparticles in photodynamic therapy, Chem. Rev., 115(4), 1990–2042.

Engineered *Saccharomyces cerevisiae* biosensor for detection of *Candida albicans* virulence-associated pheromone signaling: design, construction, and low-cost smartphone fluorescence readout

L. Gogianu[1,*], M. Simion[1], M. Popescu[1]
[1] Nanobiotechnology Laboratory of the National Institute for Research in Development in Microtechnologies, Bucharest, Romania

Abstract:
Candida albicans is a ubiquitous human commensal, and detecting its mere presence has limited diagnostic value. What distinguishes harmless colonization from invasive disease is the activation of virulence programs, notably biofilm formation, which is linked to mating-type-locus (MTL) homozygosis and white-to-opaque switching.[1] These processes give rise to mating-competent cells that secrete α-pheromone as a signal. Detection of α-pheromone therefore serves as a functional biomarker of active pathogenesis rather than passive carriage, a distinction that culture-based methods and PCR, which report only organism presence, does not make.

We present the design and construction of a two-component *S. cerevisiae* biosensor for *C. albicans* α-pheromone detection, inspired by biosensors that leverage heterologous expression of GPCR receptors for biosensing.[2,3] The sensor is built in a Δ*ste2* background and comprises a monomeric red fluorescent protein (mRFP) reporter under the pheromone-responsive FUS1 promoter, stably integrated at the *his3* locus (pRSII403), and the *C. albicans* Ste2 receptor homolog expressed constitutively from a centromeric plasmid (pRSII415). Upon pheromone binding, the native yeast mating MAPK cascade is activated, inducing mRFP expression.

This architecture places the reporter in the genome and the receptor on an exchangeable plasmid, facilitating the retargeting to other fungal pathogens by a single plasmid transformation into the same universal reporter strain, without new genomic integrations.

For field deployment, we explore encapsulation of the biosensor in alginate hydrogel beads[4,5] and propose a low-cost smartphone fluorescence readout device: a 3D-printed dark enclosure with a green LED (~530 nm) for excitation and an orange-red filter over the phone camera, transmitting only mRFP emission (~607 nm).

Preliminary characterization is ongoing. We report the molecular construction of the platform and discuss its potential as a rapid, equipment-free indicator of virulence-associated signaling in *C. albicans* infections.

Keywords: whole-cell biosensor, *Candida albicans*, pheromone detection, virulence biomarker, GPCR, point-of-care diagnostics, smartphone fluorescence.

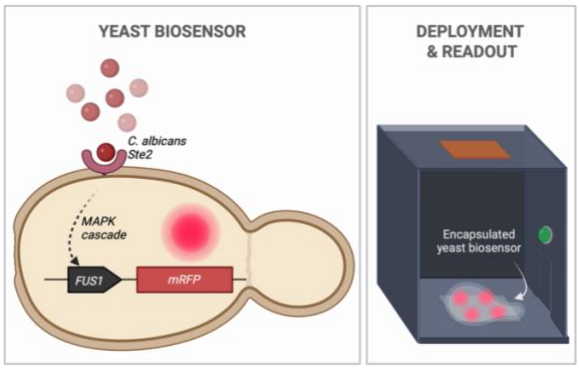


Figure 1: Schematic overview of the biosensor concept Created in https://BioRender.com.

References:

1. Rajendran, R. *et al.* Biofilm formation is a risk factor for mortality in patients with Candida albicans bloodstream infection—Scotland, 2012–2013. *Clin Microbiol Infect* **22**, 87–93 (2016).
2. Ostrov, N. *et al.* A modular yeast biosensor for low-cost point-of-care pathogen detection. *Science Advances* **3**, e1603221 (2017).
3. Lengger, B. & Jensen, M. K. Engineering G protein-coupled receptor signalling in yeast for biotechnological and medical purposes. *FEMS Yeast Res* **20**, foz087 (2020).
4. Li, P., Müller, M., Chang, M. W., Frettlöh, M. & Schönherr, H. Encapsulation of Autoinducer Sensing Reporter Bacteria in Reinforced Alginate-Based Microbeads. *ACS Appl Mater Interfaces* **9**, 22321–22331 (2017).
5. Wahid, E. *et al.* Immobilized Saccharomyces cerevisiae viable cells for electrochemical biosensing of Cu(II). *Sci Rep* **15**, 2678 (2025).

Multilayered BGO@$CsPbBr_3$ Heterostructures as Potential Scintillators for TOF-PET

N. Babayevska[1*], M. Konefał[1], M. Jancelewicz[1], M. Jarek[1], A. Padmanaban[2], I. Yakymenko[2], O. Sidletskiy[2,3]

[1] NanoBioMedical Centre, Adam Mickiewicz University, Poznań, Poland

[2] Centre of Excellence ENSEMBLE3 Sp. z o.o., Warsaw, Poland

[3] Institute for Scintillation Materials NAS of Ukraine, Kharkiv, Ukraine

Abstract:

Positron emission tomography (PET) is a powerful non-invasive imaging technique widely used for tumor detection and functional imaging. Improving the coincidence time resolution (CTR) of time-of-flight PET (TOF-PET) systems is essential for increasing image quality, sensitivity, and the accuracy of event localization [1]. One of the promising strategies for achieving improved timing performance is the development of heterostructured scintillators that combine a high-density, high-Z scintillator for efficient γ-ray absorption with a fast-emitting material capable of rapidly converting the energy of secondary electrons into optical photons [2].

In this context, metal-halide perovskites, particularly $CsPbX_3$ (X = Cl, Br, I), are attractive candidates due to their fast luminescence, high photoluminescence efficiency, and composition-dependent optical and scintillation properties [3]. Their integration with conventional high-density scintillators may therefore provide a route toward improved timing performance in TOF-PET detectors.

The aim of this work was to fabricate and perform the physicochemical characterization of multilayered BGO@$CsPbBr_3$ heterostructures as potential scintillating materials for TOF-PET applications. $Bi_4Ge_3O_{12}$ (BGO) single crystals were grown by the Czochralski method, while $CsPbBr_3$ nanoparticles were synthesized by antisolvent precipitation. Then, the $CsPbBr_3$ NPs were put on BGO by the drop-casting method. Multilayered heterostructures consisting of alternating layers of BGO single-crystal substrate and perovskite nanoparticles were fabricated.

The obtained perovskite nanoparticles exhibited high crystallinity and an average particle size of approximately 5 nm. A homogeneous perovskite-containing layer with a thickness of approximately 13 μm was successfully integrated with the BGO single crystal. The resulting BGO@$CsPbBr_3$ architectures were characterized in terms of optical and scintillation performance.

Keywords: BGO, $CsPbBr_3$ nanoparticles, multilayered heterostructures, crystal structure, scintillator, biomedical applications.

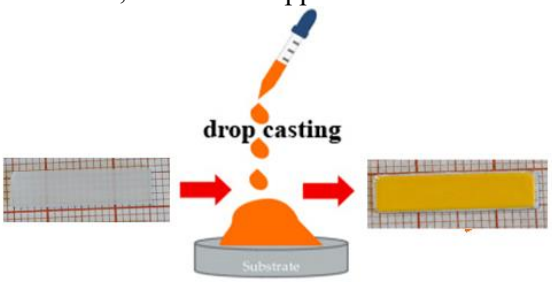


Figure 1: Formation of a CsPbBr3 layer on a BGO substrate by drop-casting.

Acknowledgments: This work was supported by the National Science Centre of Poland (OPUS project DEC- 2022/47/B/ST5/02288).

References:

1. Conti, M., Bendriem, B. (2019) The new opportunities for high time resolution clinical TOF PET, *Clin. Transl. Imaging.,* 7, 139–147.
2. Lecoq, P. et al. (2020) Roadmap toward the 10 ps time-of-flight PET challenge, *Phys. Med. Biol.*, 65, No. 21RM01.
3. Chen, et al. (2018) All-inorganic perovskite nanocrystal scintillators. *Nature*, 561, 88–93.

Treatment of Contaminated Water in Cuba Using Heterogeneous Solar Photocatalysis with Zeolite Minerals

S. Ramírez[1], M. Rodrigo Moya[2], A.R. Ruiz-Salvador[2,3], A. Jimenez[2], I. Canosa[4,5], A. Flores[4,5], L. Riesgo[6], K. Borrego[7], T. Farías[7*], M. Ballesteros[3,4*]

[1] Centro de Estudio de Química Aplicada (CEQA), Universidad Central Marta Abreu de las Villas, Cuba.
[2] Departamento de Sistemas Físicos, Químicos y Naturales, Universidad Pablo de Olavide, Sevilla, España.
[3] Centro de Nanociencia y Tecnologías Sostenibles (CNATS), Universidad Pablo de Olavide, Sevilla, España.
[4] Departamento de Biología Molecular e Ingeniería Bioquímica, Universidad Pablo de Olavide, Sevilla, España.
[5] Centro Andaluz de Biología del Desarrollo, CSIC/Universidad Pablo de Olavide, Sevilla, España.
[6] Departamento de Economía, Métodos Cuantitativos e Historia Económica, Universidad Pablo de Olavide, Sevilla, España.
[7] Instituto de Ciencia y Tecnología de Materiales (IMRE), Universidad de La Habana, La Habana, Cuba.

Abstract:

Access to clean water is a recognized human right that is seriously threatened in Cuba due to recurring droughts, an outdated distribution network, and widespread contamination of water sources. In this context, advanced oxidation processes, particularly heterogeneous photo-Fenton, offer a sustainable, low-cost alternative to conventional treatments. Previous studies have shown that natural clinoptilolite exchanged with iron (NZ-Fe) or copper (NZ-Cu) can completely inactivate *E. coli* (~10^6 CFU/mL) within 2h under visible light and at neutral pH, with no post-treatment bacterial regrowth [1]. NZ-Fe-Cu bimetallic catalyst reduces this time to 60 min. It has also demonstrated efficacy against antibiotic-resistant bacteria (*P. aeruginosa* and *S. aureus*) and in degrading 29 emerging contaminants in real water from the Guadaíra River (Spain). This meets the Class A quality criteria of European Regulation 2020/741 for agricultural reuse [2].

Based on these results, the international cooperation project AACID 2025UI022 was launched [3]. This project is a collaboration between Pablo de Olavide University and the University of Havana. The project's main goal is to improve the quality and availability of water in Cuba. This will be achieved by developing zeolite photocatalytic materials that can degrade organic compounds and pathogenic microorganisms in contaminated water intended for reuse. The research focuses on two strategic locations with distinct water issues: the Varadero tourist resort (Matanzas), where Aguas Varadero is seeking more efficient alternatives to chlorination for reuse in hotel facilities; and the rural settlement of El Palenque (Guantánamo), where discharges from the coffee pulping plant affect the Toa River, a UNESCO Biosphere Reserve.

The project is structured in four phases and aims to achieve the following results: the development of at least four zeolite materials with high photocatalytic activity, validated using actual water samples from Cuba; a comprehensive characterization of the contaminants and pathogens present in these waters; the publication of three open-access scientific articles; four presentations at international conferences; the defense of two doctoral theses and two undergraduate theses under joint supervision by UPO and UH; an economic feasibility report and a patent technology report; and the establishment of agreements with local stakeholders for the production and pilot application of the materials. All knowledge and equipment acquired during the project will be transferred to Cuban institutions, ensuring the continuity of the research line and a sustainable impact on water management in Cuba.

Keywords: natural zeolite, clinoptilolite, heterogeneous photo-Fenton, water treatment, emerging contaminants, solar photocatalysis.

References:

1. Prieto-Laria, P., Fernández-Ibáñez, P., Ruiz-Salvador, A.R., Canosa, I., Flores, A., Salameh, C., Domínguez-Santos, J.E., Núñez, N.O., Ballesteros, M., Farías, T. (2025) Cu or Fe-exchanged natural clinoptilolite as sustainable light-assisted catalyst for water disinfection at near neutral pH. *ChemPlusChem* 90, e202500225.
2. Prieto-Laria, P., Jiménez-Rodríguez, A., Ruiz-Salvador, A.R., Canosa, I., Flores, A., Coll, Y., Borrego, K., Núñez, N.O., Alonso, E., Fernández-Ibáñez, P., Farías, T., Ballesteros, M. (2025) From the lab to the river: Bimetallic clinoptilolite photocatalyst for antibiotic-resistant bacteria and emerging contaminants removal. *J Environ Chem Eng* 13, 116663.

Surface chemistry of Mg–Fe oxide spinels governing selective arsenic and phosphate removal

Simona Delibaltova[1], Biljana Dojčinović[2], Željko Jaćimović[3], Hristo Kolev[1], Iliyana Yordanova[1], Miloš Ognjanović[4], Irena Spasojević[5], Mirjana Milić[4], Vladimír Girman[6,7], Martin Fabián[8], Bratislav Antić[4]*

[1]Institute of Catalysis, Bulgarian Academy of Sciences, Acad. G Bonchev Street, bl. 11, Sofia 1113, Bulgaria
[2]Institute of Chemistry, Technology and Metallurgy, National Institute of the Republic of Serbia, University of Belgrade, Njegoševa 12, 11000 Belgrade, Serbia
[3]Faculty of Metallurgy and Technology, University of Montenegro, Cetinjski put bb, 81000 Podgorica, Montenegro
[4]VINČA Institute of Nuclear Sciences, National Institute of the Republic of Serbia, University of Belgrade, P.O. Box 522, Belgrade, Serbia
[5]Departament de Física, Universitat Autònoma de Barcelona, Bellaterra, Spain
[6]Institute of Physics, Faculty of Science, P. J. Šafárik University in Košice, Park Angelinum 9, 041 54 Košice, Slovakia
[7]Institute of Materials Research, Slovak Academy of Sciences, Watsonova 47, 040 01 Košice, Slovakia
[8]Institute of Geotechnics, Slovak Academy of Sciences v.v.i., Watsonova 45, 04 01 Košice, Slovakia

Abstract:
Elevated concentrations of arsenic in groundwater present serious health concerns for the population. Removing it is complicated due to the presence of other dissolved species competing for the same adsorption sites. Iron oxide spinels have been investigated as selective adsorbents for arsenic. In this study, magnesium was introduced to the spinel structures to see its effects on adsorption. XPS was used to determine the surface properties of the materials, and relate them to the adsorption mechanisms [1]. Seven samples were prepared through co-precipitation, with increasing Mg content. ICP-OES measurements were performed to give insight into bulk compositions. The results show incomplete incorporation of Mg into the structures. Only 32-52% of the nominal Mg content was reached. XPS measurements were performed before and after adsorption. However, the surface As concentration after adsorption remained below the XPS detection limit, therefore the analysis is focused on the fresh materials. The fresh materials were measured at Fe2p, O1s and Mg1s regions. The Fe2p narrow scan shows a mix of Fe2+ and Fe3+ for all samples. In the samples with the highest Mg content (6 & 7), there is a slight increase in the 2+ oxidation state [2]. The O1s region shows lattice and non-lattice components. The non-lattice components can be attributed to hydroxyl groups [3]. This component increases with higher Mg content. This can also be tied to the lower binding energy peaks in Mg1s for samples 5, 6 and 7. Mg is in the 2+ state, but the higher Mg samples show a lower binding energy shoulder. This component can be attributed to Mg(OH)2-like surface species [4]. Mg is also much higher in concentration compared to the bulk ICP-OES results. This indicates a Mg-rich hydroxylated surface, guiding the adsorption kinetics of the materials. The incorporation of Mg changes the surface. Magnesium is not uniformly dispersed into the bulk, but is enriched at the surface and aids hydroxylation, which is beneficial for arsenic adsorption. Therefore, Mg-Fe spinels are promising materials for arsenic removal from groundwater.

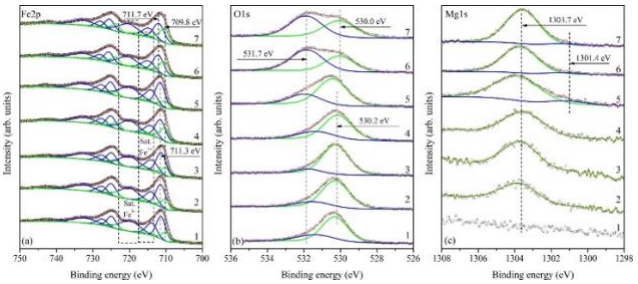


Fig. 1: XPS spectra of the Fe2p, O1s and Mg1s regions for all seven samples.

References:

1. Dojčinović, B., Jaćimović, Ž., Kolev, H., Yordanova, I., Ognjanović, M., Spasojević, I., Milić, M., Girman, V., Antić, B. (2026), Engineering defect-rich Mg–Fe oxide spinels via composition–structure–surface relationships for selective removal of arsenic and phosphate from natural groundwater, J. Alloys Compd., 1065, 188024.
2. Radu, T., Iacovita, C., Benea, D., Turcu, R. (2017), X-ray photoelectron spectroscopic characterization of iron oxide nanoparticles, Appl. Surf. Sci., 405, 337-343.

3. Porodko, O., Kavan, L., Fabián, M., Pitňa Lásková, B., Šepelák, V., Kolev, H., Da Silva, K.L., Lisnichuk, M., Zukalová, M. (2025), Preparation of novel lithiated high-entropy spinel-type oxyhalides and their electrochemical performance in Li-ion batteries, Nanoscale, 17, 3739-3751.
4. Lu, J., Wei, X., Chang, Y., Tian, S., Xiong, Y. (2016), Role of Mg in mesoporous $MgFe_2O_4$ for efficient catalytic ozonation of Acid Orange II, J. Chem. Technol. Biotechnol., 91, 985-993.

Effect of Mg Incorporation on the Structure and Groundwater Purification Performance of Mg–Fe Oxide Spinels

Anna Vasileva[1], Biljana Dojčinović[2], Željko Jaćimović[3], Hristo Kolev[1], Iliyana Yordanova[1], Miloš Ognjanović[4], Irena Spasojević[5], Mirjana Milić[4], Vladimír Girman[6,7], Martin Fabián[8], Bratislav Antić[4]*

[1]Institute of Catalysis, Bulgarian Academy of Sciences, Acad. G Bonchev Street, bl. 11, Sofia 1113, Bulgaria

[2]Institute of Chemistry, Technology and Metallurgy, National Institute of the Republic of Serbia, University of Belgrade, Njegoševa 12, 11000 Belgrade, Serbia

[3]Faculty of Metallurgy and Technology, University of Montenegro, Cetinjski put bb, 81000 Podgorica, Montenegro

[4]VINČA Institute of Nuclear Sciences, National Institute of the Republic of Serbia, University of Belgrade, P.O. Box 522, Belgrade, Serbia

[5]Departament de Física, Universitat Autònoma de Barcelona, Bellaterra, Spain

[6]Institute of Physics, Faculty of Science, P. J. Šafárik University in Košice, Park Angelinum 9, 041 54 Košice, Slovakia

[7]Institute of Materials Research, Slovak Academy of Sciences, Watsonova 47, 040 01 Košice, Slovakia

[8]Institute of Geotechnics, Slovak Academy of Sciences v.v.i., Watsonova 45, 04 01 Košice, Slovakia

Abstract:

Arsenic in water is a serious health concern that requires the development of new materials that can remove it efficiently. Iron spinels are known to provide good adsorption with selectivity towards arsenic, rather than other species. Magnesium is a relatively cheap metal, which raises interest in Mg-Fe spinels and how magnesium incorporation changes the structure and adsorption kinetics. This study gives insight into their efficacy for removing arsenic and phosphates from groundwater [1]. The spinels were prepared through co-precipitation followed by microwave-assisted hydrothermal treatment. Seven samples were created with varying Mg concentrations. The prepared samples were characterized and tested for their adsorption capacity. ICP-OES measurements were performed on both the spinels and the groundwater. This gave the bulk composition of the material and served as a measure of the adsorption of arsenic and phosphates. The materials were also characterized through XPS for the surface composition of the spinels, XRPD to uncover crystalline phases, degree of structural order and crystallite size, and BET to calculate the available surface area. ICP-OES measurements show incomplete incorporation of Mg into the lattice. The data show between 32-52% of the nominal content. XRPD and BET analysis were also performed. The results link increasing Mg concentration to lower degree of crystallinity, smaller crystallite size, but higher surface area. The surface area for the sample with highest Mg-concentration showed an almost six-fold rise in surface area compared to the sample with least Mg, increasing from 55 to 298 m^2/g. Specifically, the two most Mg-rich samples showed significant increase in available surface area compared to the rest of the samples, and also correspond to the smallest crystallite size. XRPD measurements give an average size of below 3 nm, while the pristine sample averaged at 20 nm. The adsorption kinetics were tested, and higher Mg content was linked to more efficient adsorption. Magnesium incorpotation increases the structural disorder and reduces the crystallite size, increasing surface area for arsenic and phosphate. The final concentrations measured by ICP-OES from the groundwater samples show efficient removal of the contaminant. Especially for the two samples with highest Mg content, the arsenic levels were reduced to well below 10µg/L - the guideline value, defined by the World Health Organization [2]. This study shows Mg incorporation in ferric spinels is a promising solution to arsenic adsorption from groundwaters. Excess amounts of Mg are necessary due to incomplete incorporation via this synthesis method, while higher contents reduce crystallite size, providing more adsorption sites for arsenic and phosphorus. This improves adsorption

kinetics and makes the material a promising adsorbent.

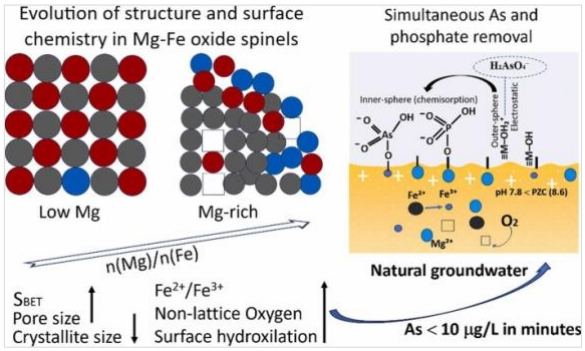


Fig. 1: Illustration of the effects of Mg-incorporation to the spinel structure and its effect on arsenic and phosphate removal [1]

References:

1. Dojčinović, B., Jaćimović, Ž., Kolev, H., Yordanova, I., Ognjanović, M., Spasojević, I., Milić, M., Girman, V., Antić, B. (2026), Engineering defect-rich Mg–Fe oxide spinels via composition–structure–surface relationships for selective removal of arsenic and phosphate from natural groundwater, J. Alloys Compd., 1065, 188024.
2. Frisbie, S.H., Mitchell, E.J. (2022), Arsenic in drinking water: An analysis of global drinking water regulations and recommendations for updates to protect public health, PLoS ONE, 17, e0263505.

Synergy in contact electrification mechanisms of polyvinyl acetate nanogenerators

Berenika Hausnerova[1,3,*], P. Slobodian[2,3]
[1]Department of Production Engineering, Faculty of Technology, Tomas Bata University in Zlin, Zlin, Czech Republic
[2]Department of Physics and Materials Engineering, Tomas Bata University in Zlin, Zlin, Czech Republic
[3]Centre of Polymer Systems, University Institute, Tomas Bata University, Zlin, Czech Republic

Abstract:
Polyvinyl acetate (PVAc) is a highly polar, fluoropolymer-free adhesive that combines strong interfacial adhesion with good processability and broad availability, yet it has rarely been explored as an active dielectric layer in mechanoelectric energy harvesters and pressure sensors[1]. Owing to its ability to form good contact with metallic surfaces, PVAc is particularly attractive for triboelectric systems in which efficient interfacial coupling is essential for charge generation. In this work, the contact electrification behavior of PVAc was investigated in a nanogenerator assembly operated in three configurations: vertical contact-separation, static-contact pre-pressure, and air-gap induction.

In the contact-separation mode, the PVAc/Cu device generated open-circuit voltages exceeding 160 V and reaching up to 350 V at 10 Hz, together with short-circuit current densities of 1.8 $A \cdot cm^{-2}$ and power densities of 0.07 $mWcm^{-2}$ at a maximum power point of 4.4 MΩ. In static-contact pre-pressure mode, where macroscopic separation of the tribo-pair is suppressed, the system still delivered up to 120 V, 2.6 Acm^{-2}, and a comparable maximum power density at 2.2 MΩ, while maintaining stable output over 10^4 loading cycles.

The data support the coexistence of triboelectric charge transfer, electrostatic induction associated with residual polarization or trapped charges, and deformation-mediated interfacial polarization. The output voltage in static-contact mode decreased markedly with increasing pre-pressure, while thinner PVAc layers produced substantially stronger responses in both operating regimes, with the thickness effect being especially pronounced under preloaded contact conditions. Likewise, the voltage measured in the air-gap configuration decayed strongly with increasing separation distance, consistent with an induction-controlled contribution originating from polarized or partially charge-retaining interfaces.

These trends indicate that the PVAc/Cu system should be understood as a multimodal mechanoelectric interface in which interfacial contact mechanics, local deformation, and electric-field redistribution act together rather than as an idealized single-mechanism triboelectric generator.

The rough and mechanically rigid copper counter-electrode can locally indent much softer PVAc layer, creating highly non-uniform deformation fields near the interface.

The fact that the static-contact response remains measurable without macroscopic approach-separation, and that it is strongly suppressed by increasing pre-pressure and film thickness, is nevertheless consistent with a significant role of strain-gradient-mediated interfacial polarization. This interpretation is particularly relevant for flexible sensing applications, because it suggests that PVAc-based devices may respond not only to repeated impact and contact cycling, but also to subtle pressure-modulated interfacial changes, making them promising for low-frequency mechanical energy harvesting, touch-responsive interfaces, and wearable pressure-sensing platforms.

Keywords: polyvinyl acetate, triboelectric nanogenerator, contact electrification, flexoelectricity, wearable sensors, fluoropolymer-free materials

Funding: This publication was created as part of the implementation of the project Testing laboratory for the implementation of sustainable and resilient technologies, reg. number CZ.02.01.01/00/23_021/0010411, co-financed by the European Union under the OP Jan Amos Comenius.

References:

Verners, O., Lapčinskis, L., Ģermane, L., Kasikov, A., Timusk, M., Pudzs, K., Ellis, A. V., Sherrell, P., Šutka, A. (2022). Smooth polymers charge negatively: Controlling contact electrification polarity in polymers. *Nano Energy* 104, 107914.

Potentiometric determination of anionic and cationic surfactants using an imidazolium–tetrakis(perfluorophenyl)borate ion-pair sensor

H. Zhukouskaya[1,2,*], M. Jozanović[3], M. Kraševac Sakač[4], N. Sakač[4], M. Šrajer Gajdošik[3], L. Vrban[5], R. Vianello[5], M. Fizer[6], D. Marković[7], D. Vikić-Topić[8], S. Roca[9], J. Pánek[1], M. Hrubý[1]

[1] Department of Supramolecular Polymer Systems, Institute of Macromolecular Chemistry, Czech Academy of Sciences, Prague, Czech Republic

[2] Department of Physical and Macromolecular Chemistry, Charles University, Prague, Czech Republic

[3] Department of Chemistry, Josip Juraj Strossmayer University of Osijek, Osijek, Croatia

[4] Faculty of Geotechnical Engineering, University of Zagreb, Varaždin, Croatia

[5] Laboratory for the Computational Design and Synthesis of Functional Materials, Division of Organic Chemistry and Biochemistry, Ruđer Bošković Institute, Zagreb, Croatia

[6] Department of Glycochemistry, Institute of Chemistry, Slovak Academy of Sciences, Bratislava, Slovakia

[7] Faculty of Biotechnology and Drug Development, University of Rijeka, Rijeka, Croatia

[8] Department of Natural and Health Sciences, Juraj Dobrila University of Pula, Pula, Croatia

[9] NMR Centre, Ruđer Bošković Institute, Zagreb, Croatia

Abstract:

Ionic surfactants are widely used in detergents, disinfectants, and personal-care formulations and therefore require reliable analytical methods for quality control and environmental monitoring. Conventional procedures for their determination are usually time-consuming, may involve hazardous organic solvents, and are often complicated by complex sample matrices. These limitations highlight the need for stable and versatile sensing platforms suitable for the determination of both anionic and cationic surfactants. Here, we demonstrate that 1,3-didecyl-2-methylimidazolium tetrakis(perfluorophenyl)borate (DDMIm–TPFPhB), incorporated into a plasticized poly(vinyl chloride) membrane, provides a common sensing platform for both anionic and cationic surfactants[1,2]. The resulting sensor was evaluated by direct potentiometry and potentiometric titration for the determination of the anionic surfactants sodium dodecyl sulfate (SDS) and sodium dodecylbenzenesulfonate (DBS), as well as the cationic surfactants cetylpyridinium chloride (CPC), cetyltrimethylammonium bromide (CTAB), and Hyamine 1622. The response characteristics were determined by incrementally adding the analytes to deionized water and were described by the modified Nernst relationship. For all five surfactants, the sensor showed near-Nernstian slope magnitudes of 56.8–59.1 mV decade^{-1}, high linearity (R^2 = 0.9914–0.9997), limits of detection ranging from 8.1×10^{-8} to 2.2×10^{-6} M, and response times of 1–5 s. The sensor also exhibited low signal drift and stable operation over a broad pH range. It was successfully applied to commercial detergent products, mouthwashes, hospital disinfectants, and eye drops, showing good agreement with standard two-phase titration for anionic surfactants and with a commercial ion-selective electrode for cationic surfactants.

Keywords: environmental analysis; surfactant determination; potentiometric sensor; ionic surfactants; hydrophobic ion-pair ionophore; ion-selective PVC membrane.

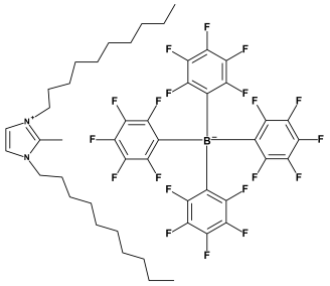


Figure 1: Chemical structure of the DDMIm–TPFPhB ion pair.

References:

1. Zhukouskaya, H., Vrban, L., Vianello, R., Jozanović, M., Hrubý, M., Pánek, J., Kraševac Sakač, M., Marković, D., Vikić-Topić, D., Roca, S., Šrajer Gajdošik, M., Sakač, N. (2026), Imidazolium–perfluorophenylborate ion-pair as a high-performance surfactant ionophore, *J. Electroanal. Chem.*, 1009, 120012.
2. Kraševac Sakač, M., Fizer, M., Zhukouskaya, H., Hrubý, M., Pánek, J., Suljagić, J., Marković, D., Drenjančević, D., Sakač, N., Šrajer Gajdošik, M., Jozanović, M. (2026), Rational design of a hydrophobic ion-pair sensor for potentiometric determination of cationic surfactants in disinfectants: Combined experimental and DFT study, *Chemosensors*, 14, 150.

Mass Production of Stretchable Colorimetric Tape for Ammonia Leakage Detection

T.-N. T. Dang [1], Y. S. Kim [1,2,*]
[1] Graduate School of Applied Chemistry, Hanyang University, Ansan 15588, Republic of Korea
[2] Department of Energy and Bio Sciences, Hanyang University, Ansan 15588, Republic of Korea

Abstract:
Ammonia is widely used in industrial processes and is emerging as a promising carbon-free energy carrier. Nevertheless, its toxicity and occupational exposure limit of 25 ppm necessitate the development of sensitive and reliable sensors for early leak detection. In this study, a stretchable silicone-based colorimetric tape was produced by the conventional roll-to-roll coating process in mass quantity. Its colorimetric ammonia detection and tensile properties were successfully evaluated. Based on these results, the fabricated detection tape has confirmed its applicability in on-site ammonia leakage detection application.

The optimized tape, with a thickness of approximately 200 μm, exhibited good mechanical flexibility, with a tensile strength above 3.0 MPa and an elongation at break of about 1000%, enabling conformal attachment to curved and irregular surfaces. Upon exposure to 25 ppm NH_3, the sensor produced a visible color change from yellow-orange to dark blue within 1 min, accompanied by a shift in the UV–Vis reflectance maximum from 423 to 623 nm. Furthermore, it demonstrated high detection selectivity toward ammonia and other basic volatile amines, with negligible responses to common volatile organic compounds (VOCs). These sensing properties were also evaluated over a broad range of humidity and temperature conditions.

Keywords: ammonia detection tape, colorimetric sensor, leakage detection, stretchable silicon tape, roll-to-roll fabrication.

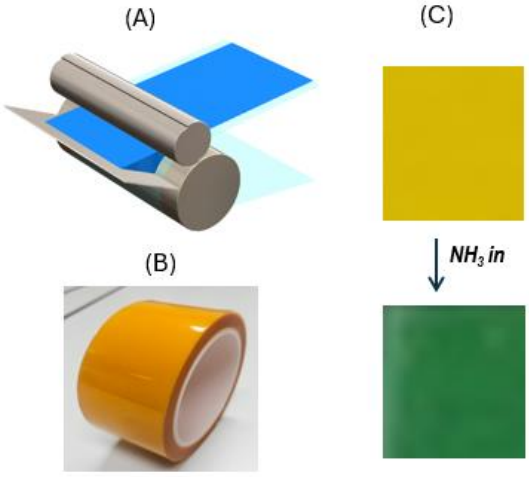


Figure 1: (A) Schematic illustration of the roll-to-roll coating process, (B) fabricated ammonia detection tape (width = 50 mm and length = 10 m), and its colorimetric detection performance.

References:

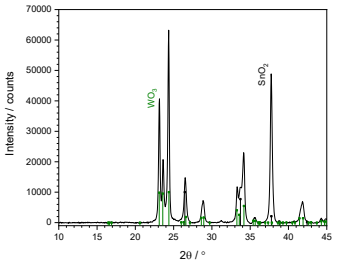
1. Hoang, A. T., Cho, Y. B., Park, J.-S., Yang, Y., Kim Y.S. (2016) Sensitive naked-eye detection of gaseous ammonia based on dye-impregnated nanoporous polyacrylonitrile mats, *Sens. Actuators B Chem.*, 230, 250–257.
2. Mao, Y., Zhang, D., Zhang, H., Chen, Y., An, W., Niu, C., Shao, J. (2025) Flexible wearable/stickable ammonia colorimetric sensors with assistance of deep learning for ammonia leakage monitoring and early warning, *Chem. Eng. J.*, 515, 163809.

Preparation, Structural Characterization, and Ethanol Sensing Applications of Phase-Pure WO_3 and $CuWO_4$ Thin Films

T. Imrich [1,*], M. Baudys [1], H. Krýsová [1,2], M. Neumann-Spallart [1], J. Krýsa [1]
[1] Department of Inorganic Technology, University of Chemistry and Technology, Prague, Technická 1905/5, 166 28 Prague 6, Czech Republic
[2] Heyrovský Institute of the Czech Academy of Sciences, Dolejškova 2155/3, 182 23 Prague 8, Czech Republic

Abstract:
Gas sensors play an indispensable role in monitoring and assessing air quality across various indoor and outdoor environments. Among the wide array of sensing materials, metal oxide semiconductors have emerged as particularly promising candidates due to their low cost, ease of fabrication, high sensitivity, and long-term stability. Within this group, tungsten trioxide (WO_3) has garnered significant research interest owing to its excellent chemoresistive response toward diverse gaseous species. Recently, the integration of transition metals to form ternary metal oxides, such as copper tungstate ($CuWO_4$), has shown great potential in overcoming the limitations of binary oxides, offering enhanced selectivity and lower operating temperatures.
In this work, WO_3 and $CuWO_4$ thin films were successfully deposited on fluorine-doped tin oxide (FTO)-coated glass substrates. The structural properties of the prepared layers were systematically evaluated using X-ray diffraction (XRD), confirming high crystallinity and the absence of unreacted secondary phases, as shown in Figure 1.

(a)



(b)

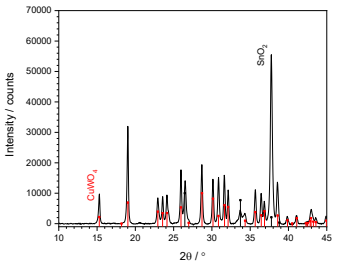


Figure 1: XRD patterns of (a) WO_3 and (b) $CuWO_4$ thin films deposited on FTO/glass substrates at 250 °C and annealed at 550 °C for 2 h in air. Layer thickness 4 µm.

Furthermore, the synthesized phase-pure thin films were applied for chemoresistive gas sensing testing, focusing specifically on ethanol vapor detection. In general, chemoresistive sensors rely on surface interactions between target gas molecules and pre-adsorbed oxygen ions (O^-, O_2^-). When exposed to a reducing agent such as ethanol (C_2H_5OH), the gas molecules react with oxygen species, releasing trapped electrons back into the conduction band of the metal oxide and causing a measurable reduction in electrical resistance. The performance evaluation presented in this study demonstrates the feasibility and functional applicability of both FTO/WO_3 and FTO/$CuWO_4$ thin film structures for practical alcohol vapor sensing systems.

Keywords: gas sensors, metal oxides, tungsten trioxide, copper tungstate, ethanol sensing, phase purity, thin films

Acknowledgement:
This work was supported by the project "Sensors and Detectors for Future Information Society – SENDISO reg. n. CZ.02.01.01/00/22_008/0004596" by the Programme Johannes Amos Comenius, call "Excellent Research".

References:

1. Li, X., Fu, L., Karimi-Maleh, H., Chen, F., Zhao, S. (2024), Innovations in WO_3 gas sensors: Nanostructure engineering, functionalization, and future perspectives, *Heliyon*, 10, e27740.
2. Kumar, N., Kumar, A., Čapek, J., Comini, E., Haviar, S. (2025), WO_3/$CuWO_4$ nanocomposite thin films for humidity resilient acetone gas sensing, *Appl. Surf. Sci. Adv.*, 30, 100894.

Development and Experimental Evaluation of a Four-Channel Chemiresistive Sensor Array for Formic Acid Detection

P. Arroyo [1*], A. Bernal [1], E. Pinilla [2], J. L. Herrero [3], J. M. Perea [3], J. A. Fernández [1], J. I. Suárez [1], J. Lozano [1]

[1] Dept. of Electrical, Electronic and Automation Engineering, University of Extremadura, Badajoz, Spain

[2] Dept. of Analytical Chemistry, University of Extremadura, Badajoz, Spain

[3] Dept. of Computer Systems and Telematics Engineering, University of Extremadura, Badajoz, Spain

Abstract:

Formic acid is a major volatile contaminant in cultural heritage settings, as it commonly accumulates inside display cases and storage areas, thereby contributing to the degradation of sensitive materials [1]. Therefore, sensor systems capable of detecting low HCOOH concentrations could support preventive conservation strategies. This work presents the development and preliminary experimental evaluation of a four-channel chemiresistive sensor array for sub-ppm formic acid detection. The sensitive layers combine graphene with metal oxides and Pt or Pd, an approach previously studied to enhance the gas-sensing properties of conventional metal oxide devices [2]. Four formulations were evaluated: ITO/Pt/graphene, ITO/Pd/graphene, SnO_2/Pd/graphene and WO_3/Pt/graphene. The layers were deposited by drop-casting on top of gold interdigitated electrodes with a finger width and spacing of 10 µm. The substrate on which the materials have been deposited includes the four electrodes on top and the heaters on the bottom. Channel resistance was sequentially measured using a Keithley DMM 2700 controlled through an automated LabVIEW acquisition system. The array was evaluated by static headspace generation, using water headspace as the reference atmosphere and estimated gas-phase HCOOH concentrations of 70, 200 and 700 ppb. All channels exhibited an increasing relative resistance change with increasing concentration. Under the evaluated fabrication and operating conditions, the WO_3/Pt/graphene channel showed the highest response, reaching 4.83% at 200 ppb and 17.64% at 700 ppb. At 700 ppb, the ITO/Pt/graphene, ITO/Pd/graphene and SnO_2/Pd/graphene channels showed responses of 4.45%, 6.20% and 8.69%, respectively.

Keywords: formic acid, chemiresistive sensor, graphene, metal oxide, gas sensing, preventive conservation.

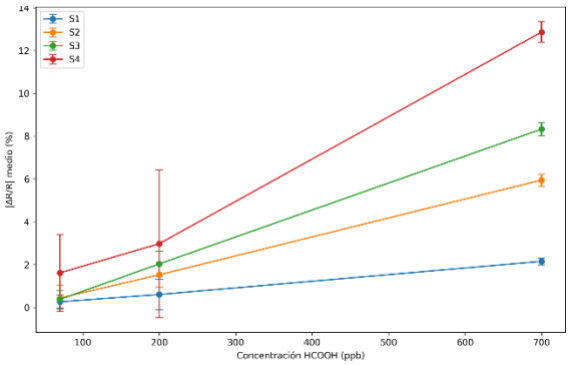


Figure 1: Relative resistance change of the four sensing channels as a function of the estimated HCOOH concentration: S1, ITO/Pt/graphene; S2, ITO/Pd/graphene; S3, SnO_2/Pd/graphene; and S4, WO_3/Pt/graphene.

References:

1. Chiantore, O.; Poli, T. (2021), Indoor air quality in museum display cases: Volatile emissions, materials contributions, impacts, Atmosphere, 12, 364. https://doi.org/10.3390/atmos12030364
2. Sun, D.; Luo, Y.; Debliquy, M.; Zhang, C. (2018), Graphene-enhanced metal oxide gas sensors at room temperature: a review, Beilstein J. Nanotechnol., 9, 2832–2844. https://doi.org/10.3762/bjnano.9.264

Structural and Optical Characterization of Hydrothermally Synthesized Graphene Quantum Dots

F. Zaleski [1*], D. Minta [1], K. Matczyszyn [2], G. Gryglewicz [1]
[1] Department of Process Engineering and Technology of Polymer and carbon Materials, Wrocław University of Science and Technology, Wrocław, Poland
[2] Institute of Advanced Materials, Wrocław University of Science and Technology, Wrocław, Poland

Abstract:
Carbon dots, and in particular graphene quantum dots (GQDs), are attracting enormous interest thanks to their unique optical properties, high biocompatibility and solubility in water and other polar solvents, and represent a promising basis for applications in fields such as optoelectronics, sensor technology and bioimaging. The optical properties of GQDs, in addition to their nanometre dimensions and disc-like shape and the quantum confinement effect resulting from these characteristics are determined by the surface chemistry of the dots, specifically by the presence of numerous functional groups located on the surface and at the edges of the dots. It is therefore very important to select specific precursors and an appropriate synthesis method in order to obtain dots with the desired properties. In this work, graphene quantum dots were synthesized via an one-pot green hydrothermal method using graphene oxide as the carbon precursor and hydrogen peroxide as an oxidizing and cutting agent. The obtained dispersions were purified by dialysis and subsequently isolated as solid material by lyophilization. The nanoparticles obtained after dispersion in water, when irradiated with a UV lamp at a wavelength of 380 nm, exhibit intense green emission. For more detailed optical analysis, UV-Vis absorption spectroscopy and photoluminescence spectroscopy were employed. Using transmission electron microscopy (TEM), the morphologies and size distributions of GQDs were investigated, and it was shown that the majority of the nanoparticles had a diameter of approximately 4 nm. Raman spectroscopy analysis revealed an I_D/I_G ratio of 0.95, confirming a partially ordered graphitic structure with the presence of defects and numerous edges. XPS analysis, in turn, confirmed the presence of numerous oxygen-containing functional groups on the surface of the GQDs, with a particularly high proportion of carboxyl groups. This gives the material of great potential for further post-synthesis modification. The GQDs obtained represent a promising material for further research, and the next stage of the work will involve their purification and fractionation using size-exclusion chromatography (SEC).

Keywords: GQDs, hydrothermal synthesis, photoluminescence, functionalization, emission.

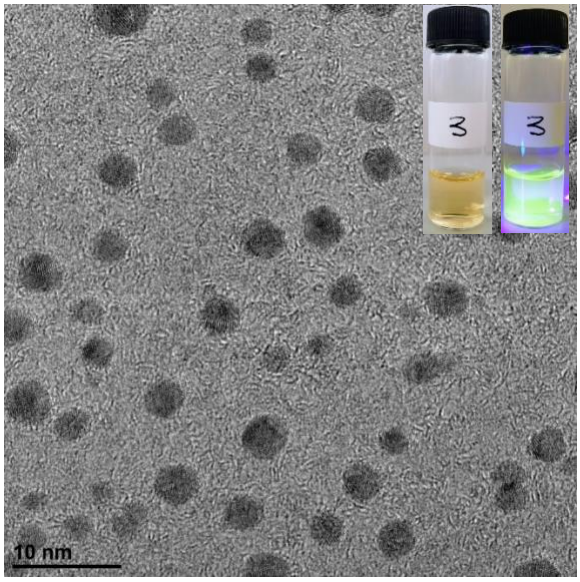


Figure 1: An image of the dots from TEM and a view of the GQDs dispersed in water, before and after illumination with a UV torch at a wavelength of 380 nm.

References:

1. Đorđević, L., Arcudi, F., Cacioppo, M., Prato, M. (2022), A multifunctional chemical toolbox to engineer carbon dots for biomedical and energy applications, Nat. Nanotechnol., 17, 112-130.
2. Halder, A., Godoy-Gallardo, M., Ashley, J., Feng, X., Zhou, T., Hosta-Rigau, L., Sun, Y. (2018), One-pot green synthesis of biocompatible graphene quantum dots and their cell uptake studies, ACS Appl. Bio Mater., 1, 452-461.

Unconventional Signaling-Off PSA Detection Using Laser-Induced Graphene/ZnO Nanorod Impedimetric Immunosensors

Simone F. Soares, Sónia O. Pereira, António J. S. Fernandes, Florinda M. Costa, Nuno F. Santos
i3N and Physics Department, University of Aveiro, Campus Universitário de Santiago, 3810-193 Aveiro, Portugal

Abstract:
Laser-induced graphene (LIG) provides a scalable route to porous, electrically conductive carbon architectures that can be directly patterned into electrochemical devices. However, the biofunctionalization of LIG-based immunosensors remains non-trivial because charge-transfer kinetics are governed not only by biomolecular recognition, but also by surface morphology, defect density, interfacial chemistry and local electrostatics. Here, we report a label-free impedimetric immunosensor for prostate-specific antigen (PSA) based on LIG decorated with electrodeposited ZnO nanorods. The concept exploits the hierarchical porosity and electroactivity of LIG together with the high isoelectric point and large surface area of ZnO nanorods to promote antibody immobilization and modulate faradaic charge transfer at the sensor/electrolyte interface.

LIG electrodes were patterned on polyimide by CO_2 laser irradiation and subsequently modified by pulsed electrodeposition of ZnO nanorods. Two anti-PSA immobilization strategies were compared: covalent coupling through APTES/EDC-NHS chemistry and direct antibody adsorption onto ZnO. Faradaic electrochemical impedance spectroscopy, using the ferro/ferricyanide redox probe, revealed that the adsorption-based architecture provided the analytically relevant response, enabling PSA detection in PBS within the clinically meaningful range of 0.1–10 ng mL^{-1} and yielding a detection limit of 81 ± 19 pg mL^{-1}. The sensor also showed specificity against the non-target glycoprotein hCG, supporting the role of selective anti-PSA/PSA recognition in the measured response.

Most importantly, the adsorption-based LIG/ZnO immunosensor exhibited an unconventional "signaling-off" impedance behavior: the charge-transfer resistance decreased with increasing PSA concentration. This trend contrasts with the commonly assumed blocking mechanism of faradaic impedimetric immunosensors, where antigen binding usually hinders access of the redox probe to the electrode. XPS follow-up of the functionalization and sensing steps suggests that PSA binding may induce antibody or immunocomplex reorganization/desorption, while ZnO surface-charge effects may further modulate electron-transfer accessibility at the n-type semiconductor/electrolyte interface. These findings show that nanostructured graphene/semiconductor transducers cannot be interpreted using oversimplified impedance-blocking models. Instead, their sensing response emerges from the coupled effects of biomolecular recognition, interfacial charge, surface isoelectric point and protein coverage.

This work highlights LIG/ZnO nanorod composites as low-cost, scalable transducers for decentralized biosensing, while also emphasizing the need for mechanistic impedance analysis when designing label-free electrochemical immunosensors.

Keywords: laser-induced graphene; ZnO nanorods; electrochemical impedance spectroscopy; PSA; label-free immunosensor; charge-transfer resistance; biointerfaces.

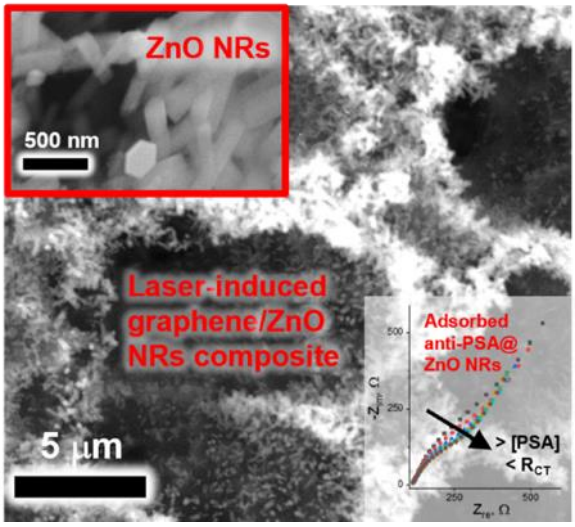


Figure 1: Laser-induced graphene decorated with ZnO nanorods (NRs) enables label-free impedimetric PSA detection. Direct anti-PSA adsorption on ZnO produces a concentration-dependent decrease in charge-transfer resistance, revealing an unconventional signaling-off response governed by the LIG/ZnO biointerface.

References:

M. S.Soares, S. O.Pereira, A. J. S.Fernandes, F. M.Costa, and N. F.Santos, "Label-Free Detection of PSA Using Laser-Induced Graphene/ZnO Nanorod-Based Impedimetric Immunosensors." Advanced Sensor Research5, no. 3 (2026): e00151. https://doi.org/10.1002/adsr.202500151

Advanced Biological Denitrification Using Graphene Oxide Coated Tubular Ceramic Membranes

Zahra Pouramini[1], Frank E. Stüber[1], José Font Capafons[1]
[1] Departament d'Enginyeria Química, Universitat Rovira i Virgili, Tarragona, Spain

Abstract:
Biological denitrification is one of the most efficient and widely used methods for nitrate removal from contaminated water, owing to its ability to convert nitrate into harmless nitrogen gas. To fully exploit bacterial capabilities in environmental biotechnology, stable and well-functioning microbial communities are essential. Advanced biofilm-based systems offer a promising platform for leveraging diverse microbial functions in nitrate removal. Figure 1 illustrates the configuration developed in this project, which enables the attachment of a high density of denitrifying microorganisms. This study investigates a novel integrated technology that combines a graphene oxide-coated tubular membrane with a membrane bioreactor configuration for biological nitrate removal using an anaerobic mixed microbial culture. The graphene oxide layer will serve as a structural support for biofilm development, an environmentally friendly electron shuttle, a favorable surface functionality, and mechanical stability, which are critical properties for long-term operational reliability. The membrane functions simultaneously as a biofilm support and a filtration layer, thereby enhancing overall system performance. Nitrate removal was evaluated in long-term experiments across a range of concentrations under a stable permeate flux of 0.1 L/m²·h. Experiments were conducted at a COD/N ratio of 6 and operating temperatures of 25°C and 35°C, to assess the influence of thermal conditions on denitrification performance. Results demonstrated that this novel approach achieved approximately 90% nitrate removal even at high nitrate concentrations of up to 1000 mg/L.

Keywords: biological denitrification, graphene oxide, attached growth system, wastewater treatment

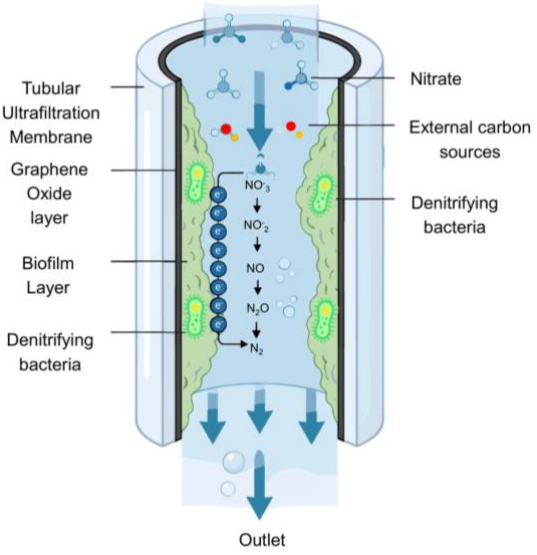


Figure 1: Schematic illustration of the graphene oxide-coated tubular membrane bioreactor used for biological nitrate removal. The graphene oxide layer promotes biofilm development and facilitates electron transfer, while denitrifying bacteria convert nitrate (NO_3^-) to nitrogen gas (N_2), enhancing nitrate removal efficiency.

References:

1. Mohseni-Bandpi, A., Elliott, D. J., & Zazouli, M. A. (2013). Biological nitrate removal processes from drinking water supply-a review. Journal of environmental health science and engineering, 11(1), 35.
2. Wu, L., Wei, W., Xu, J., Chen, X., Liu, Y., Peng, L., ... & Ni, B. J. (2021). Denitrifying biofilm processes for wastewater treatment: developments and perspectives. Environmental Science: Water Research & Technology, 7(1), 40-67.

PCL Nanofibers Loaded with Antitumor Drugs for the Treatment of Colorectal and Pancreatic Cancer

N J. Prados[1,2,3], C. Melguizo[1,2,3], J. Moreno[1,2,3,] I. Fernández[,4] R. Contreras-Cáceres[,4] N. Muñoz-Flores,[4] A. Ortigosa- Palomo[1,2,3], L. Cabeza[1,2,3],

[1] [1]Institute of Biopathology and Regenerative Medicine (IBIMER), Center of Biomedical Research (CIBM), University of Granada, 18100 Granada, Spain

[2]Biosanitary Institute of Granada (ibs.GRANADA), 18014 Granada, Spain

[3] Department of Anatomy and Embryology, Faculty of Medicine, University of Granada, 18071 Granada, Spain

[4] Department of Chemistry and Physics, Research Centre CIAIMBITAL, University of Almería, Almería 04120, Spain

Abstract:

Polymeric nanofibers fabricated by electrospinning provide a nanoplatform for the localized, continuous, and sustained delivery of chemotherapeutic agents, in contrast to conventional oral and implantable drug-delivery approaches, while potentially reducing undesirable side effects in healthy tissues. In the present study, polycaprolactone (PCL) nanofibers fabricated by electrospinning and loaded with the antitumor agents 5-fluorouracil (5-FU), either alone or in combination with calcitriol (the active form of vitamin D), and gemcitabine (GCB), were evaluated as potential therapeutic platforms for colorectal and pancreatic cancer. Drug-loaded and drug-free nanofibers, the latter used as controls, were evaluated by cell proliferation assays in the human colorectal cancer cell lines T84 and SW480 and the human pancreatic cancer cell line Panc-1. Cell proliferation was assessed using the sulforhodamine B (SRB) colorimetric assay. The results showed a time-dependent reduction in cell proliferation in both colorectal and pancreatic cancer cell lines, with approximately 50% cell death being achieved in most cases after 6 h of treatment. The antiproliferative effect was comparable between the free drugs and the corresponding drug-loaded nanofibers. Notably, only the GCB-loaded nanofibers produced a greater reduction in cell proliferation than free GCB, reaching an additional reduction of up to 14.58%. The optimal synergistic ratio between 5-FU and calcitriol was established at 1:20. Drug-free nanofibers showed no cytotoxic effects in any of the cell lines tested. Treatment with 5-FU/calcitriol-loaded nanofibers at the 1:20 ratio produced an effect comparable to, or even greater than, that observed with the corresponding free-drug combination, with reductions in cell proliferation of up to 12.86% at concentrations of 1 and 20 µM of 5-FU and calcitriol, respectively, compared with the free drugs. Overall, these findings indicate that electrospun nanofibers represent a promising platform for the localized treatment of solid tumors, preserving and potentially enhancing the cytotoxic activity of antitumor agents while enabling the local administration of high concentrations of poorly soluble molecules such as vitamin D. This approach may overcome the limitations associated with systemic and oral vitamin D administration, which are restricted by the risk of hypercalcemia.

Keywords: Polymeric nanofibers, electrospinning, cancer

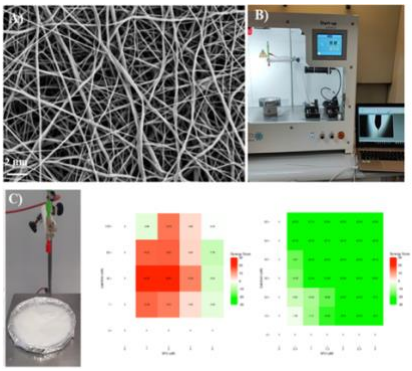


Figure 1: Figure 1. A) Scanning electron microscopy (SEM) image of PCL nanofibers, together with an image of the electrospinning apparatus and the nanofibers obtained during the electrospinning process. B) Electrospinning setup. C) Nanofiber membranes and synergy analysis..

References:

1. Bingol Ozakpinar O, et al Composite Aerogels Loaded with Vitamin D: The Cytotoxic and Apoptotic Effects on Colon Cancer Cells. Gels. 2023 Jul 10;9(7):561. doi: 10.3390/gels9070561. PMID: 37504440; PMCID: PMC10379131.
2. Suner SC, et al Electrospun PLA: Gelatin core-shell nanofibers for dual delivery of docetaxel and heparin with enhanced in vitro antiproliferative activity. Eur J Pharm Biopharm. 2026 Oct;227:115212. doi: 10.1016/j.ejpb.2026.115212. Epub 2026 Aug 7. PMID: 42567422.

Graphene Oxide-Erlotinib Nanoconjugates Target Tumour Growth and Angiogenesis in Pancreatic Cancer Models

Shaoshan Mai[1], Marta Perez-Lloret[2], Magdalena Narajczyk[3], Anna M. Olszewska[4], Iwona Inkielewicz-Stepniak[1]
[1] Department of Pharmaceutical Pathophysiology, Faculty of Pharmacy, Medical University of Gdansk, Poland
[2] School of Biological and Chemical Sciences, University of Galway, Ireland
[3] Laboratory of Electron Microscopy, Faculty of Biology, University of Gdansk, Poland
[4] Department of Histology, Medical University of Gdansk, Poland

Abstract:
Pancreatic ductal adenocarcinoma (PDAC) remains poorly responsive to EGFR-targeted therapy, partly because dense stromal and vascular barriers limit intratumoural drug delivery. Graphene oxide (GO) offers a high-surface-area, chemically versatile platform for the delivery of small-molecule inhibitors. Here, we developed nano-GO-erlotinib (nGO-Erlo) by covalently conjugating erlotinib to size-reduced GO and evaluated its antitumour and anti-angiogenic activity in PDAC models. Two solvent-defined formulations (ethanol- and DMSO-based) were character-ised by NanoSight and dynamic light scattering, scanning transmission electron microscopy-energy-dispersive X-ray spectroscopy, and UV calibration. Antitumour activity was assessed in MIA PaCa-2, PANC-1 and AsPC-1 cells using CCK-8 assays and in patient-derived PDAC organoids using CellTiter 3D. To model tumour-vascular crosstalk, organoids were co-cultured with human umbilical vein endothelial cells and analysed by tube-formation metrics; intracellular localisation in organoids was examined by transmission electron microscopy. nGO-Erlo reduced via-bility in all PDAC cell lines and patient-derived organoids in a dose-dependent manner. At equivalent nominal drug doses, its activity matched or exceeded that of free erlo-tinib and GO controls. In organoid-endothelial co-cultures, nGO-Erlo decreased tube-formation parameters, support-ing suppression of pro-angiogenic phenotypes in a tumour-relevant microenvironment. Transmission electron mi-croscopy confirmed intracellular nGO-Erlo in organoid cells, consistent with efficient uptake and retention. To-gether, these findings identify nGO-Erlo as a dual-function nanotherapeutic that couples EGFR-targeted activity with anti-angiogenic effects in clinically relevant PDAC mod-els. Further in vivo studies should define its biodistribution, pharmacology and safety.

Keywords: graphene oxide; erlotinib; pancreatic ductal adenocarcinoma; patient-derived organoids; angiogenesis; nanomedicine

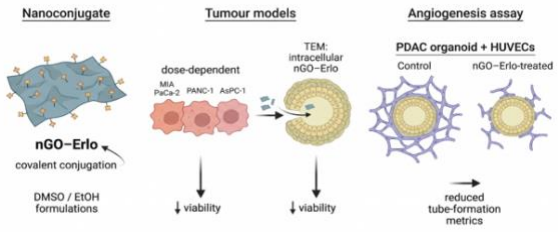


Figure 1: Graphical summary of nano-graphene oxide–erlotinib (nGO–Erlo) evaluation in pancreatic ductal adenocarcinoma (PDAC) models. Nano-graphene oxide was covalently conjugated to erlotinib using DMSO- and ethanol-based formulations. nGO–Erlo reduced viability dose-dependently in MIA PaCa-2, PANC-1 and AsPC-1 cells and in patient-derived PDAC organoids; transmission electron microscopy (TEM) showed intracellular nGO–Erlo in organoids. In organoid–human umbilical vein endothelial cell (HUVEC) co-culture, nGO–Erlo reduced tube-formation metrics relative to control.

SETCOR
Conferences & Exhibitions

www.setcor.org

SCIENCE · TECHNOLOGY · ENGINEERING

SMS 2026 · NanoMed 2026 · Sensors 2026 · EGF 2026
21 – 23 October 2026 · Seville, Spain